The Role of MicroRNAs in *Chlamydia* Infection

Die Rolle von MicroRNAs in der Chlamydien-Infektion

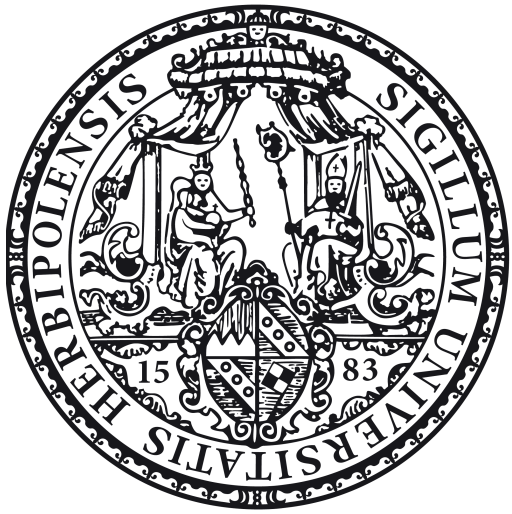

Dissertation

for

Doctoral degree at the Graduate School of Life Sciences

Julius-Maximilians-Universität Würzburg

Infection and Immunity

Authored by:

Suvagata Roy Chowdhury

from

Calcutta, India / Glasgow, United Kingdom

Würzburg, 2017

The Role of MicroRNAs in *Chlamydia* Infection

Die Rolle von MicroRNAs in der Chlamydien-Infektion

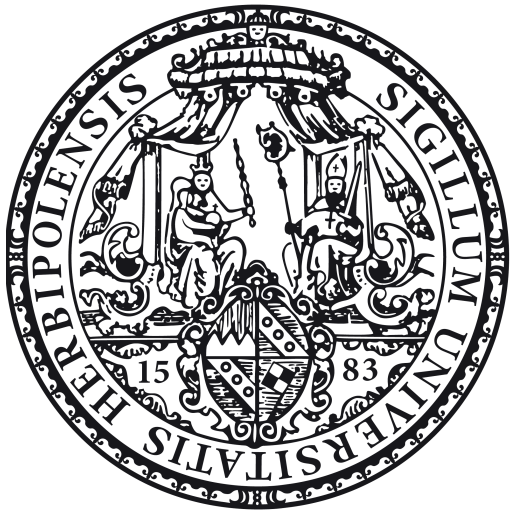

Dissertation

for

Doctoral degree at the Graduate School of Life Sciences

Julius-Maximilians-Universität Würzburg

Infection and Immunity

Authored by:

Suvagata Roy Chowdhury

from

Calcutta, India / Glasgow, United Kingdom

Würzburg, 2017

Submitted on:

Members of the *Promotionskomitee*:

Chairperson	**Prof. Dr. Thomas Dandekar** Chair of Bioinformatics, Biozentrum, Julius-Maximilians- Universität Würzburg, Germany
Primary supervisor	**Prof. Dr. Thomas Rudel** Chair of Microbiology, Biozentrum, Julius-Maximilians- Universität Würzburg, Germany
Supervisor (second)	**Dr. Ana Eulalio,** Institut für Molekulare Infektionsbiologie, Julius-Maximilians- Universität Würzburg, Germany
Supervisor (third)	**Prof. Dr. rer. nat. Jörg Wischhusen** Sektion für Experimentelle Tumorimmunologie, Frauenklinik and Ployklinik, Julius-Maximilians- Universität Würzburg, Germany

Date of Public Defence:

Date of Receipt of Certificates:

Zusammenfassung

Das Gram-negative Humanpathogen *Chlamydia trachomatis* versursacht das Trachom, eine ansteckende follikuläre Bindehautentzündung, die letztlich zur Erblindung Infizierter führt, sowie sexuell übertragbare Entzündungen im Urogenitaltrakt. *C. trachomatis* ist ein obligat intrazelluläres Bakterium mit einem biphasischen Lebenszyklus, der in einer spezialisierten Vakuole innerhalb des Wirtszellzytoplasmas durchlaufen wird, der sogenannten Chlamydien-Inklusion. *C. trachomatis* ist daher davon abhängig, dass die infizierte Wirtszelle überlebt, bis die Entwicklung des Erregers abgeschlossen ist und moduliert dazu das apoptotische Signalnetzwerk der Wirtszelle. Dieses besteht aus mehreren fein aufeinander abgestimmten regulatorischen Kaskaden aus pro- und anti-apoptotischen Proteinen, die normalerweise auf Veränderungen in der zellulären Homöostase reagieren und als Folge den programmierten Zelltod einleiten können. Es ist jedoch bekannt, dass *Chlamydia* die Apoptose der Wirtszelle durch Stabilisierung mehrerer anti-apoptotischer Wirtsproteine wie cIAP2 und Mcl-1 inhibiert. Während pro- und anti-apoptotische Proteine Hauptregulatoren des Apoptosesignalnetzwerks darstellen, wurde kürzlich eine neue Ebene der Apoptose-Regulation identifiziert, die durch kleine, nicht-kodierende microRNAs (miRNAs) gesteuert wird.

In der vorliegenden Arbeit untersuchte ich die Veränderungen in dem miRNA Expressionsprofil von Wirtszellen nach einer Chlamydieninfektion. Mittels miRNA *deep sequencing* wurden dabei mehrere miRNAs identifiziert, die abhängig von der Infektion mit *Chlamydia* differentiell in menschlichen Endothelzellen exprimiert werden und deren Funktion mit der Modulation der Apoptose-Signalwege assoziiert sind. Dabei war miR-30c-5p von besonderem Interesse, da deren molekulares *target* das Tumorsuppressorprotein p53 ist. Unter anderem durch unser Labor wurde dabei bereits gezeigt, dass *Chlamydia* den Proteasom-vermittelten Abbau von p53 fördert und somit die Menge des Proteins in der Wirtszelle depletieren kann. In der hier vorliegenden Arbeit zeige ich darüberhinaus, dass eine Chlamydia-Infektion die p53 Mengen in den Wirtszellen senkt, indem miR-30c-5p verstärkt produziert wird, während das intrazelluläre Wachstum von *C. trachomatis* durch den Verlust von miR-30c-5p inhibiert wird.

Zusammen mit den apoptotischen Regulationskaskaden entscheiden auch die Integrität der Mitochondrien sowie die Dynamik des mitochondrialen Netzwerks über das Schicksal der Zelle. Eine Dysregulation dieser Funktionen führt zur Einleitung

des Zelltods und bildet die Grundlage der Pathogenese mehrerer Krankheiten. Zu den wesentlichen Aufgaben des mitochondrialen Netzwerkes gehören, neben zahlreichen anderen, die Synthese von ATP, die Detoxifizierung von reaktiven Sauerstoff-Spezies sowie die Kalziumhomöostase. Die funktionelle Integrität des mitochondrialen Netzwerks ist dabei stark von Teilungs- und Fusionsraten mitochondrialer Fragmente abhängig und diese mitochondriale Dynamik ist wiederum eng mit der Apoptose verknüpft; so sind etwa viele Proteine, welche die mitochondriale Dynamik regulieren, auch an der apoptotischen Signalgebung beteiligt. Zum Beispiel wird die Transkription des an der Mitochondrienteilung beteiligten Proteins Drp1 durch p53 reguliert und eine miR-30c-vermittelte Inhibition von p53 senkt daher die Menge an Drp1 in der Zelle.

In der hier vorliegenden Arbeit demonstriere ich die signifikante Veränderung der mitochondrialen Dynamik in menschlichen Zellen nach einer Chlamydieninfektion. Die entstehende hyperkondensierte Architektur des mitochondrialen Netzwerks ist dabei auf den Verlust von Drp1 zurückzuführen, welcher durch die miR-30c-5p-induzierte Depletion von p53 vermittelt wird. Während die Abhängigkeit des intrazellulären Wachstums von *Chlamydia* vom Stoffwechsel der Wirtszelle weitgegen akzeptiert ist, wurde die Rolle der Mitochondrien und die Dynamik des mitochondrialen Netzwerks in infizierten Zellen bisher vernachlässigt. Innerhalb der vorliegenden Arbeit wurde zum ersten Mal die Abhängigkeit von *Chlamydia* auf miR-30c-5p induzierte Veränderungen in der mitochondrialen Architektur illustriert.

Abstract

The obligate intracellular pathogen *Chlamydia trachomatis* is the causative agent of trachoma related blindness and the sexually transmitted pelvic inflammatory disease. Being an obligate intracellular pathogen, *C. trachomatis* has an intricate dependency on the survival of the host cell. This relationship is indispensible owing to the fact that the pathogen spends a considerable fraction of its biphasic lifecycle within a cytoplasmic vacuole inside the host cell, the so-called chlamydial inclusion. The cellular apoptotic-signalling network is governed by several finely tuned regulatory cascades composed of pro- and anti-apoptotic proteins that respond to changes in the cellular homeostasis. In order to facilitate its intracellular survival, *Chlamydia* has been known to inhibit the premature apoptosis of the host cell via the stabilization of several host anti-apoptotic proteins such as cIAP2 and Mcl-1. While the pro- and anti-apoptotic proteins are the major regulators of the host apoptotic signalling network, a class of the small non-coding RNAs called microRNAs (miRNAs) has increasingly gained focus as a new level of regulatory control over apoptosis.

This work investigates the changes in the host miRNA expression profile post *Chlamydia* infection using a high throughput miRNA deep sequencing approach. Several miRNAs previously associated with the modulation for apoptotic signalling were differentially expressed upon *Chlamydia* infection in human endothelial cells. Of the differentially regulated miRNAs, miR-30c-5p was of particular interest since it had been previously shown to target the tumor suppressor protein p53. Our lab and others have previously demonstrated that Chlamydia can downregulate the levels of p53 by promoting its proteasomal degradation. This work demonstrates that *Chlamydia* infection promotes p53 downregulation by increasing the abundance of miR-30c-5p and a successful infection cycle is hindered by a loss of miR-30c-5p.

Over the last decade, dedicated research aimed towards a better understanding of apoptotic stimuli has greatly improved our grasp on the subject. While extrinsic stress, deprivation of survival signals and DNA damage are regarded as major proponents of apoptotic induction, a significant responsibility lies with the mitochondrial network of the cell. Mitochondrial function and dynamics are crucial to cell fate determination and dysregulation of either is decisive for cell survival and pathogenesis of several diseases. The ability of the mitochondrial network to perform its essential tasks that include ATP synthesis, anti-oxidant defense, and calcium homeostasis amongst numerous other processes critical to cellular equilibrium is tied closely to the fission and fusion of individual mitochondrial fragments. It is, thus,

unsurprising that mitochondrial dynamics is closely linked to apoptosis. In fact, many of the proteins involved regulation of mitochondrial dynamics are also involved in apoptotic signalling. The mitochondrial fission regulator, Drp1 has previously been shown to be transcriptionally regulated by p53 and is negatively affected by a miR-30c mediated inhibition of p53. Our investigation reveals a significant alteration in the mitochondrial dynamics of *Chlamydia* infected cells affected by the loss of Drp1. We show that loss of Drp1 upon chlamydial infection is mediated by the miR-30c-5p induced depletion of p53 and results in a hyper-fused architecture of the mitochondrial network.

While it is widely accepted that *Chlamydia* depends on the host cell metabolism for its intracellular growth and development, the role of mitochondria in an infected cell, particularly with respect to its dynamic nature, has not been thoroughly investigated. This work attempts to illustrate the dependence of *Chlamydia* on miR-30c-5p induced changes in the mitochondrial architecture and highlight the importance of these modulations for chlamydial growth and development.

Table of Contents

“ Daß ich erkenne was die Welt

Im Innersten zusammenhält,

Schau’ alle Wirkenskraft und Samen,

Und thu' nicht mehr in Worten kramen ”

“ Wo fass’ ich dich, unendliche Natur? ”

- Johann Wolfgang von Goethe

(Faust. Eine Tragödie)

“ Forty-two ”

- Douglas Adams

(Hitchhiker’s guide to the galaxy)

Chapter 1. Introduction

1.1 *Chlamydia*

1.1.1 A Brief History of *Chlamydia*

The cytoplasmic inclusion bodies of *Chlamydia trachomatis* were first described in 1907 by the German radiologist Ludwig Halberstädter and the Czech parasitologist Stanislaus Josef Mathias von Prowazek (Halberstadter and von Prowazek, 1907b). Halberstädter and Prowazek went on to show that scrapings of particles from the eyes of patients suffering from trachoma gave rise to conjunctival infection in the eyes of Orangutans. They also documented the similarity between the inclusions found in the cervical regions of the mother and those found in the conjunctiva of infants borne by the infected mothers.

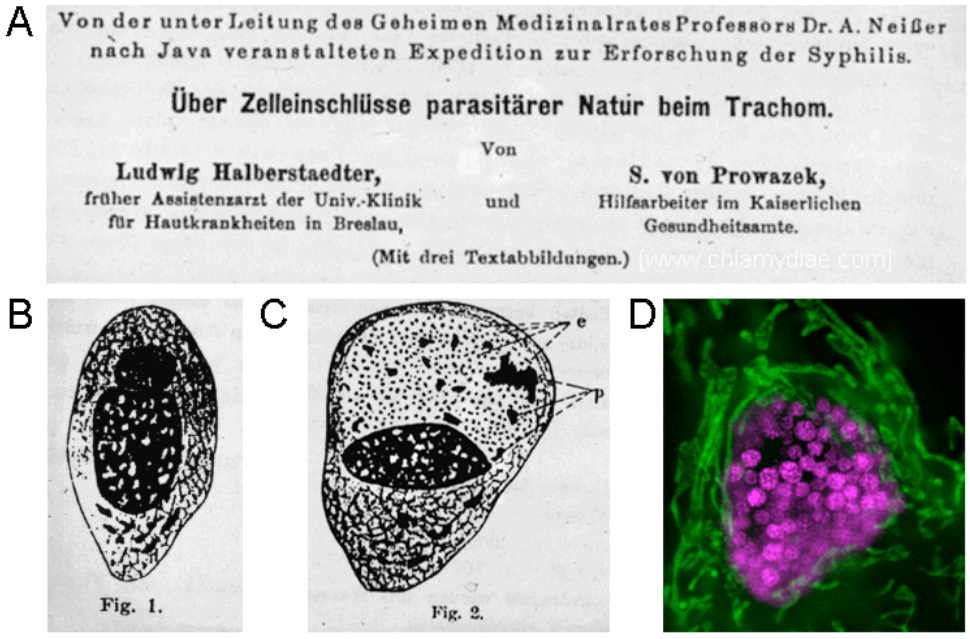

Fig 1.1.1: The Beginning of *Chlamydia* research. (A) Title of the original paper from 1907 describing the nature of *Chlamydia* infection. (B and C) Illustrations by Halberstaedter and von Prowazek describing the difference between a normal and *Chlamydia* infected conjunctival epithelial cell. Reproduced from www.chlamydiae.com. (D) A *Chlamydia* inclusion filled with chlamydial particles (magenta) surrounded by mitochondria (green) as seen under structured illumination microscope.

They also found similar inclusion bodies in the urethral scrapings of men suffering from non-gonococcal urethritis (Halberstadter and von Prowazek, 1907a). However the general consensus at the time was that the microorganisms under observation

were a class of “protozoans with a mantle”. Hence, the name “*Chlamydozoa*” from the greek word for mantel (“Chlamys or Khlamus”) was designated to define this unique infectious agent (Collier, 1990).

In 1930, Phillip Thygeson, an American ophthalmologist and his associates performed what is now known as “The Phillips Thygeson Experiment in Trachoma” to illustrate the infectious nature of the “elementary bodies” from the Halberstädter-Prowazek inclusion and their ability to cause trachoma. The group used an ultrafiltrate of elementary bodies to inoculate Clarence Brown, a terminal patient suffering from advanced conjunctival epidermoid carcinoma. As a result, Brown developed a classic case of trachoma that responded to a treatment with copper sulphate (Thygeson, 1958). In 1935, Miyagawa et al. succeeded in culturing *Chlamydiae* in the chorioallantoic membrane of embryonated hen’s eggs which was later improved upon by T’ang et al. who used the yolk sac of embryonated hen’s eggs for culturing *Chlamydiae* (Miyagawa, 1935; Tang et al., 1957).

In the early days of its discovery, *Chlamydiae* were categorized as an intermediate stage between bacteria and viruses on the account of its size and the fact that the microbe needed a host for replication and survival. It was not until late 1960s that *Chlamydiae* were properly classified as bacteria when James W. Moulder, made a thorough study of the organism. He showed, via electron microscopy, that these organisms exhibit cellular structure reminiscent of bacteria including a cell wall of gram-negative origin whereas molecular studies showed that *Chlamydiae* possess ribosomal particles and DNA-RNA metabolism pathways exclusive to bacteria (Moulder, 1966).

1.1.2 *Chlamydia* In The Grand Scheme Of Things: A Taxonomic Overview

"**A big virus is a virus. A small bacteria is a bacterium**"

- **A. Lwoff**

At the time of discovery, as previously mentioned, *Chlamydia* was classified as a mantle-bearing protozoan, a big virus and eventually as an intermediate stage between bacteria and viruses. However, if the latter classification was accurate, as Moulder pointed out, there would exist or have existed organisms that exhibit properties common to both bacteria and viruses. Careful examination of chlamydial characteristics, both physical and molecular established the fact that Chlamydiae are obligate intracellular pathogens of a gram-negative bacterial origin.

Decades of modifications and lack of molecular techniques that are taken for granted in current phylogenetic analysis greatly hampered accurate classification of Chlamydiae. However, once it was established that the Chlamydiae indeed were of bacterial origin and are obligate intracellular bacteria, the bacterial order Chlamydiales was created to encompass the family Chlamydiaceae and the genus *Chlamydia* (Johannes and Page, 1971). Based on the phenotypic differences and inclusion morphology of diverse chlamydial strains genus was sub-divided house two species, *Chlamydia trachomatis* for the strains isolated from human sources and *Chlamydia psittaci* for those isolated from a variety of animal sources (Page, 1968)

With the advent of state-of-the-art genomic studies, next generation sequencing and advanced diagnostic techniques the number of chlamydial species has widened considerably. *Simkania negevensis* and *Parachlamydia acanthamoebae* were both identified in late 1990s (Amann et al., 1997; Kahane et al., 1998). While S. *negevensis* and *P. acanthamoebae* are quite different from each other in terms of host specificity and morphology both of them were found to have almost 75-87% ribosomal RNA gene sequence similarity with other bacteria form the Chlamydia genus (Everett et al., 1999).

In 1999, Everett et. al. identified differential clustering of the 16SrRNA by defining "Signature sequence" segments within the chlamydial 16SrRNA and partial 23sRNA. Based on these findings it was proposed that the family Chlamydiaceae be divided into two genera, *Chlamydia* and *Chlamydophila* which would, in turn, host nine separate species (based on 16SrRNA clustering) or eleven species (based on 23SrRNA clustering). This classification also illustrated the presence of four separate groups at the family (Chlamydiales) node comprising Chlamydiaceae, Parachlamydiaceae, Simkaniaceae and Waddliaceae (Everett et al., 1999).

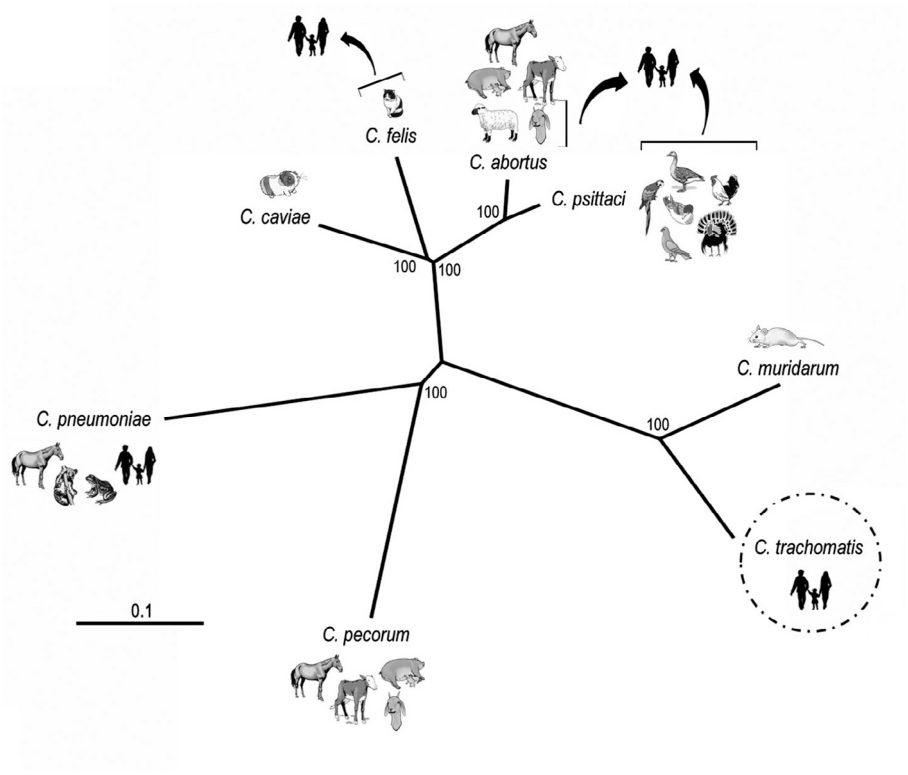

Fig. 1.1.2: Phylogenetic representation of the *Chlamydia* genus: This graphic illustrates the natural host for every species of the pathogen. Black arrows demonstrate the zoonotic potential of *C. abortus* and *C. psittaci* (Illustration adapted from Nunes and Gomes, 2014).

However, in light of current knowledge of molecular markers and cutting edge sequencing data, the two-genera classification has now been refuted (Stephens et al., 2009). Instead, a united genus *Chlamydia* was created to encompass nine species with some very singular and highly conserved biological features (*Chlamydia abortus, Chlamydia caviae, Chlamydia felis, Chlamydia muridarum, C. psittaci, Chlamydia pecorum, Chlamydia pneumoniae, Chlamydia suis* and *C. trachomatis*) (Greub, 2010).

The classification system for any organism is a detailed and intricate method that follows pathways that are created by the influx of new evidence and data. Categorization of *Chlamydia* has passed through morphological, phenotypical, serological genetic and molecular classifications to give rise to an approximate phylogenetic tree that closely resembles its lineage based on the data available. This, however, is likely to change since it is inevitable that new strains and species will continue to be discovered.

1.1.3 Medical Relevance of *Chlamydia*

In terms of host species preference and range, the genus *Chlamydia* exhibits a variety of species, which differ not only in host selection but also in disease pathology and tissue tropism. Of the nine species in the *Chlamydia* genus, *Chlamydia trachomatis* has gained substantial notoriety owing to its exclusive choice of the human host leading to urethritis in men and cervical infections in women, a fact known since the early 1970s (Schachter, 1999). *Chlamydia* had already been implicated as the causative agent of ocular trachoma and molecular studies pinpointed the involvement of *C. trachomatis* as the human specific pathogen. Serological classifications indicated that the chronic inflammatory ocular trachoma was caused by serovars A to C while serovars D to K are involved in one of the most common sexually transmitted bacterial diseases affecting the ano-urogenital regions of both men and women (Wang and Grayston, 1970).

Chlamydial infections result in cervicitis in women, which may lead to Pelvic Inflammatory Disease, a major risk for infertility and ectopic pregnancy (Schachter et al., 1976). It has also been pointed out that infection of the genital tract in women might have possible links to cancer development (Meijer et al., 1989; Ness et al., 2003; Zhu et al., 2016). In men, the infection presents itself as urethritis and upon progression to upper genital tract might lead to epididymitis and eventually infertility. Other serovars of *C. trachomatis* namely L1 to L3 are the causative agents of Lymphogranuloma Venereum (LGV) also known as the Durand-Nicolas–Favre disease (Durieux, 1945; Harrop et al., 1940). The microbe may enter the lymphatic system via skin lesions after crossing epithelial layers of the mucous membrane and multiplies within mononuclear phagocytes in uro-genital lymph nodes. LGV is a systemic disease that presents itself as a painless genital ulcer but eventually leads to obstruction of lymph flow and chronic swelling of genital tissues (Stoner and Cohen, 2015).

Another species that has been known to cause several pathological conditions in humans is *C. pneumoniae* (Grayston et al., 1990). However, unlike *C. trachomatis, C. pneumoniae* is able to infect marsupials, horses and frogs (Myers et al., 2009). Infection by *C. pneumoniae* has been associated with a diverse range of chronic upper body pathologies including but not limited to obstructive pulmonary disorder, reactive arthritis and asthma (Elkind et al., 2006; Hahn et al., 1991). In certain instances *C. pneumoniae* has also been implicated in atherosclerosis, coronary heart disease, multiple sclerosis and lung cancer (Belland et al., 2004; Chaturvedi et al., 2010; Fainardi et al., 2008; Joshi et al., 2013).

Amongst other species of Chlamydia, *C. psittaci* and *C. abortus* are known to affect humans through zoonotic transmission (Sachse and Grossmann, 2002). *C. psittaci* is responsible for endemic chlamydiosis in birds and respiratory psittacosis is humans which presents itself with symptoms akin to flu but eventually develops into life-threatening pneumonia (Chau et al., 2015; Hutchison et al., 1930). The typical host of choice for *C. abortus* is ruminants and is responsible for enzootic abortions in horses, rabbits, guinea pigs, mice and pigs. It has been shown that *C. abortus* can infect humans resulting in pre-term labor and abortion (Longbottom and Livingstone, 2006; Thomson et al., 2005).

1.1.4 Life and times of *C. trachomatis*: The Chlamydial Life-cycle

Similar to other obligate intracellular pathogens such as *Coxiella* and *Rickettsia,* all *Chlamydiaceae* are consummate parasites. In other words, they are dependent, solely, on the resources of the host for their development and transmission. The fact that these pathogens do not multiply outside the nutrient rich environment of the host cell lead to the emergence of the theory that *Chlamydia* was a form of an intermediate organism between bacteria and virus. That theory being disproved led to several important studies that elucidated the biphasic developmental life cycle common to all members of the *Chlamydiaceae* family.

Bedson et al. discovered that *Chlamydia* undergoes a series of developmental changes that during its life cycle by studying infected tissues (Bedson and Gostling, 1954). With the development of the electron microscope and microtome techniques two morphologically distinct forms of the developing *Chlamydia* were identified (Bedson, 1955; Bedson and Gostling, 1954). The elementary bodies (EB) and the reticulate bodies (RB) are distinguishable from each other not just morphologically, but functionally as well (Moulder, 1991). While the EBs are responsible for attachment to and infection of the host cell, upon internalization it transforms into the pleomorphic and larger RB. The RB is metabolically active, capable of replication and non infectious. A typical cycle of infection by *C.trachomatis* consists of attachment of EB to the host, transformation into RB, which then multiplies within the so-called “chlamydial inclusion”, asynchronous transition of RBs into infectious EBs and finally, the release of progeny EB by cell lysis. This cycle lasts approximately 46-48 hours however the time frame varies between serovars and host cell type.

The EBs are spore like particles encapsulated in a cell wall that is reinforced with proteins crosslinked by disulphide bonds. This cell wall functions to protect the EB

and allows it to survive the unforgiving environment outside the cell while stabilizing the cell against physical and osmotic stress (Nelson, 2012). It was well accepted that the EBs function as the infectious particle that attaches itself to the host cell and is internalized by receptor mediated endocytosis but are metabolically and transcriptionally inert (Iliffe-Lee and McClarty, 1999). Recent data generated by Omsland et al., however, has shown that EBs are metabolically active when cultivated in an axenic media and supplemented with d-glucose-6-phosphate (Omsland et al., 2012).

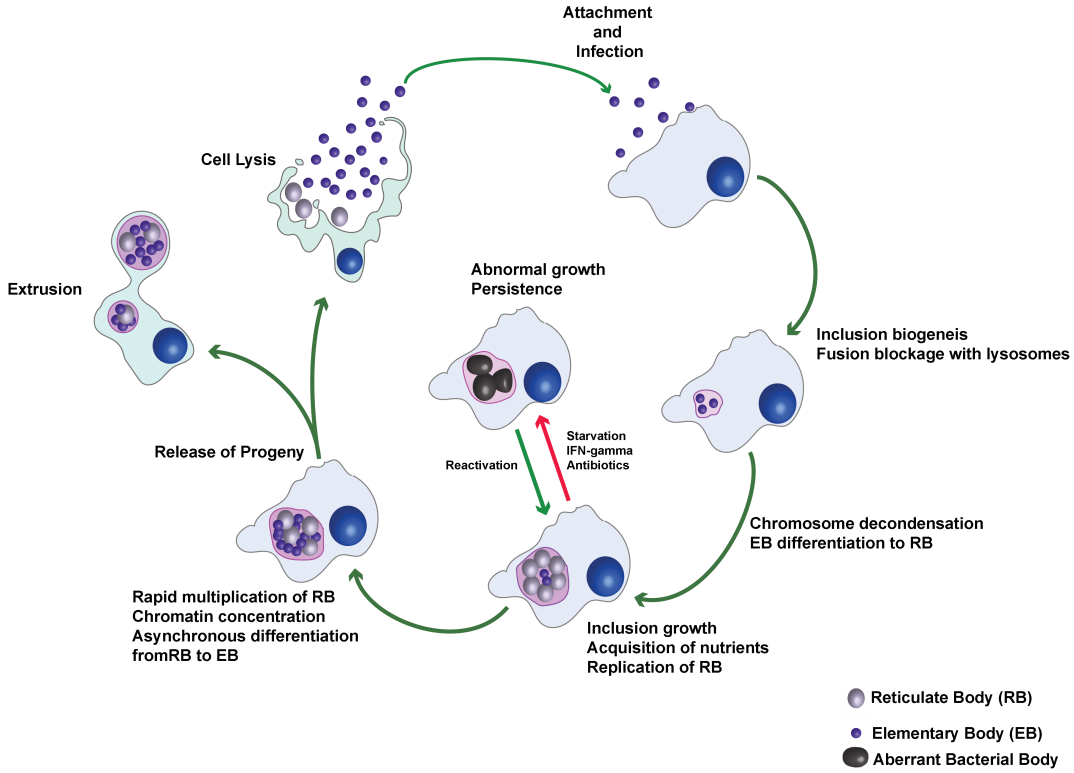

Fig. 1.1.3 Chlamydial life cycle: The small elementary bodies (EBs) bind to the host cell via interactions of bacterial and host factors and are internalized to create the so-called chlamydial inclusion. Within the inclusion the EBs differentiate into the transcriptionally and metabolically active reticulate bodies (RB). The RBs replicate within the inclusion, which also increases in volume over the progression of the infection. Presence of cytokines like interferon-γ, antibiotics or nutrient starvation leads to disruption of the normal progression of chlamydial life cycle creating morphologically aberrant RBs. This effect is reversible upon availability of normal growth conditions. At the end of the lifecycle, the RBs undergo asynchronous transition into EBs and are released from the cell either by extrusion of parts of the inclusion of by lysis of the host cell.

Over the years several studies have built upon the idea that the binding of chlamydial EBs are dependent on a diverse array of host and bacterial surface factors which determine the choice of host and the tissue tropism for the pathogen. In case of *C. trachomatis* and *C. pneumoniae*, initial attachment is believed to be the result of an interaction between chlamydial outer membrane proteins and heparan sulfate proteoglycans (HSPGs) (Hegemann and Moelleken, 2012). However other adhesion

molecules have also been implicated, especially in case of *C. trachomatis* such as LPS, which could bind to the cystic fibrosis transmembrane conductance regulator (CFTR) and CT017, which targets the β1 integrin (Ajonuma et al., 2010; Hegemann and Moelleken, 2012; Stallmann and Hegemann, 2016). It is possible that such a variety of adhesion strategies are responsible for the tissue tropism shown by the different serovars of *C. trachomatis.*

Chlamydia induced actin-remodeling assists the internalization of the pathogen into the host cytoplasm. The process of internalization is assisted by RHO family of GTPases, which recruit actin regulators necessary for the rearrangement of actin (Bastidas et al., 2013; Nans et al., 2014). Several host cell factors like caveolin and clathrin are involved in the post-rearrangement actin polymerization (Bastidas et al., 2013; Korhonen et al., 2012). Other studies have also implicated that EB internalization might occur via a clathrin-independent mechanism or might involve lipid rafts (Jutras et al., 2003; Stuart et al., 2003). *C. trachomatis,* being a gram-negative bacterial species, possesses a needle-like machinery termed typed 3 secretion system (T3SS) by means of which it injects effector proteins into the host cytoplasm (Hackstadt, 2012; Moore and Ouellette, 2014). These injected effectors are responsible for the induction of necessary cytoskeletal rearrangement required for successful invasion and subsequent redirection of the host signaling pathways (Dai and Li, 2014). One of the T3SS injected protein critical to the actin re-polymerization followed by internalization is Tarp (**T**ranslocated **a**ctin **r**ecruiting **p**rotein) also known as CT456. Tarp has been shown to possess globular (G-) and filamentous (F-) actin domains by the means of which it nucleates and bundles the host actin. (Hackstadt, 2012; Jiwani et al., 2013). Furthermore, phosphorylation of Tarp by the host tyrosine kinases such as Src family kinases allows it to interact with SHC-1, PI3K and ARP2/3 complexes (Hackstadt, 2012; Mehlitz et al., 2010). It is believed that Tarp activates the host cell ARP2/3 complexes in a GTPase dependent manner while its interaction with SHC-1 alters host-signaling pathways that promote cell survival during chlamydial development (Jiwani et al., 2012). It has been shown that the Tarp - ARP2/3 complex interaction enhances the rates of actin polymerization. This is accompanied with an increase in the levels of branched actin filaments (Jewett et al., 2006). All of these events are necessary and responsible for the internalization of bacteria in non-phagocytic cells. Upon internalization the EBs are restricted to a membrane bound non-lysosomal vesicle called the chlamydial inclusion (Bedson and Gostling, 1954; Moulder, 1991).

The chlamydial inclusion is not tagged with any markers of the endocytic or lysosomal pathway and is able to intercept sphingomyelin and cholesterol from a

Golgi-dependent exocytic pathway (Carabeo et al., 2003; Hackstadt et al., 1996). It is reported that after the initial modification of the inclusion to allow fusion with the vesicles containing sphingomyelin, the chlamydial inclusion is completely segregated from the endocytic pathway allowing the creation of a secluded niche for the growth and development of *Chlamydia* within the host cell. Interestingly, lysosomal fusion with the chlamydial inclusion is prevented possibly by recruitment or restriction of proteins involved in the host endocytic or exocytic vesicular trafficking pathways (Delevoye et al., 2008; Paumet et al., 2009). Syntaxin 6 (a member of the SNARE family of proteins) and selective members of the Rab family of GTPases responsible for vesicle targeting, tagging and fusion present on the chlamydial inclusion membrane possibly, to assist in selective fusion with nutrient containing vesicles form the host cell (Kabeiseman et al., 2013; Rzomp et al., 2003). Annexins III, IV, and V, which have been implicated in the regulation of vesicle trafficking and membrane dynamics of fusogenic endosomal vesicles, have also been detected in close to chlamydial inclusion (Majeed et al., 1994). The inclusion, while immune to lysosomal degradation, is fragile and need reinforcements provided by F-actin and intermediate filaments. The localized cytoskeletal matrix forms a sort of dynamic scaffolding that provides structural endurance and limits the bacteria to the inclusion (Kumar and Valdivia, 2008). Furthermore, a gross reorganization of the microtubule to create a superstructure is observed around the inclusion that provides an additional backbone to the inclusion (Al-Zeer et al., 2014).

The seclusion that the inclusion bound *Chlamydia* face is substantial but not absolute. Indeed, the chlamydial inclusion has been shown to interact with the host organelles such as the smooth endoplasmic reticulum (S-ER) via contact sites, which are often found in close proximity to ER – Golgi or ER – plasma membrane contact sites (Agaisse and Derre, 2015; Derre, 2015). Interestingly, the lumen of the chlamydial inclusion has been found contain lipid droplets and peroxisome, though it is not understood how the peroxisome might translocate into the inclusion (Boncompain et al., 2014). Finally, the mitochondrial network is closely juxtaposed to the inclusion. A study by Matsumoto et al. demonstrated that while *C. psittaci* inclusions had close associations with the mitochondria, this association was not observed in with *C.trachomatis* or *C. pneumoniae* inclusions (Matsumoto et al., 1991). Recently, it has been shown that C.trachomatis infection is hampered upon depletion of the mitochondrial TIM-TOM complex (Kokes and Valdivia, 2012). The exact reason for such an interaction or its consequences are not fully understood but it can be speculated that *Chlamydia* may scavenge energy metabolites and inhibit

apoptotic signaling via such interactions. Indeed, recent studies have revealed the presence of NAD(P)H on and within the chlamydial inclusion (Szaszak et al., 2011). Within the protective environment of the inclusion the chlamydial EBs transits into the RB and initiates the transcription of the early genes (6 – 9 hours post infection). The exact events that underlie the transition of the EB to RB (early) and RB to EB (late) are not fully understood but transcriptional studies have elucidated several gene sets which are transcribed at specific developmental stages (Nicholson et al., 2003). The RBs have a large de-condensed chromatin core compared to the EBs owing to their metabolically and transcriptionally active nature. The transition from the metabolic and transcriptional silent nature of the EB to that of the active RB is attributed to the release of the histone H1 homologues, Hc1 and Hc2 from the chlamydial DNA during the early stages of EB to RB transition. 2-C-methyl-d-erythritol 2,4-cyclodiphosphate (MEC), a small metabolite in the methylerythritol 4-phosphate pathway of isoprenoid biosynthesis has been shown to be responsible for the separation of Hc1 from the chlamydial DNA and while a *Chlamydia* – encoded small RNA named IhtA acts as the negative regulation of Hc1 during the exponential growth phase of the RB. (Grieshaber et al., 2006a; Grieshaber et al., 2006b). The binary fission of the RB results in the expansion of the chlamydial population within the inclusion. Until recently the expansion of the chlamydial inclusion has been closely linked to chlamydial replication and the increase in the size of the inclusion has been used as a marker for chlamydial replication and growth. However recent data has shown that expansion of the chlamydial inclusion can happen in absence of chlamydial replication as well (Engstrom et al., 2015). The later transition of RB to EB can gain be attributed to the Hc1 and Hc2 induced “switch-off” the transcription of several genes (Grieshaber et al., 2006b). The proteomic composition of RB has been shown to change from being primed with proteins necessary for mRNA transcription, nutrient transporters proteins (amino acid, sugar and oligopeptides), ATPase subunits to ones needed for protein synthesis and ATP accumulation as they progress from replicative phase to the final transition to EB (Saka et al., 2011). The transition of RB to EB is largely asynchronous and, to some extent, believed to be triggered by the detachment of the EB from the inner wall of the inclusion membrane (Fields, 2012). The fine tuned developmental cycle of *Chlamydia* can be disrupted and reversibly arrested by antibiotic induced, immune factor induced, environmental or nutrition deprivation induced stress. Introduction of such stress factors leads to a transition to a persistent form of *Chlamydia* called aberrant bodies, which remain viable but are reproductively impaired. Manire and Matsumoto observed enlarged and morphologically aberrant RBs when *C. psittaci* infected L929 cells were treated

with penicillin (Matsumoto and Manire, 1970). However, these effects are largely reversible upon removal of the penicillin and after a period of lag, the RBs returned to normal size and re-initiated replication and matured into infection EBs. Persistence can also be induced exposing the infected cells to cytokines such as Interferon γ which leads to the decrease in the intracellular availability of tryptophan, iron deprivation and interestingly, herpes virus infection (Al-Younes et al., 2001; Carlin and Weller, 1995; Vanover et al., 2008). In absence of such persistence inducing conditions the release of *C. trachomatis* from infected cells occurs around 48 hours post infection in culture.

Two well described methods of EB release have been documented in several studies: Release of EB by lysis of the host cell and the packaged extrusion by a process reminiscent of exocytosis (Hybiske and Stephens, 2007). The lytic exit of *Chlamydia* invariably leads to the death of the host cell. It is understood that several chlamydial proteases including the Chlamydia protease-like activity factor (CPAF) is responsible for the degradation of several important host cell proteins prior to inclusion membrane permeabilization (Snavely et al., 2014). The lytic release of *Chlamydia* also necessitates the permeabilization of the nuclear membrane, along with a permeabilization of several other organelles and a calcium dependent permeabilization of the plasma membrane (Hybiske and Stephens, 2007). In contrast, the extrusion mechanism of *Chlamydia* exit from host cells leaves the host cells intact and viable and is a much slower process, which might result in the extrusion of the entire chlamydial load from the cell or retention of chlamydial particles within the host. Additionally, the extrusion pathway requires the modifications of the host cell cytoskeletal network, primarily actin-myosin interactions, depolymerization of microtubules. The one of the final step for extrusion of chlamydial inclusion is a pinching event similar to what happens during cytokinesis and involves myosin II and RhoA dependent formation of a contractile ring (Hybiske and Stephens, 2007).

1.1.5 *Chlamydia* and its Dependence On The Host Cell

For years *Chlamydia* has been branded as an energy parasite due to the presumed metabolic inactivity of the EBs outside the host cell. Study of chlamydial biochemistry and genomics provided no evidence towards any capability of generating their own ATP and no evidence was available to show that they possessed any component of the electron transport chain necessary for oxidative phosphorylation (Moulder, 1991).

Indeed, studies showed that *Chlamydia* infected cells showed an increase in rates of glycolysis as a response to infection (Moulder, 1970). Interestingly *Chlamydia* was also shown to grow in cell lines with mitochondria lacking ATP synthesis capabilities illustrating *Chlamydia* scavenged ATP from glycolysis as well as from respiratory generation (Tipples and McClarty, 1993). Detailed dissection of the chlamydial genome has revealed that, while *Chlamydia* are probably unable to synthesize its own amino acids, purine and pyrimidine nucleotides and possesses well defined (ADP)/ATP translocases, the chlamydial genome encodes the complete set of genes required for the glycolytic pathways barring the gene for fructose-1, 6-diphosphate aldolase. Furthermore, *Chlamydia* also appears to be capable of utilizing its own pentose phosphate pathway and the tricarboxylic cycle if supplied with exogenous glutamate or 2-oxoglutarate (Hatch et al., 1982; Stephens et al., 1998). Recently, with the development of a cell free (axenic) medium, it has been shown that EBs and RBs are not entirely inactive in terms of metabolic function outside the host cell even though they have separate preferences for energy sources. While RBs are partial to ATP, reflecting its natural source within the cell, EBs prefer Glucose-6-Phosphate (G6P). In presence of G6P in *Chlamydia* intracellular phosphate-1 (CIP-1) medium, EBs have been shown to be able to produce ATP, initiate transcription of specific gene sets and synthesize proteins from de-novo synthesized mRNA and from mRNA carried over from a previous developmental cycle (Omsland et al., 2012). In the light of the current findings it is evident that while *Chlamydia* depends on the host cell for most of its metabolites it is also capable of synthesizing the bare minimum necessary for survival, inside or outside the cell if provided with the appropriate substrates. However cell-free replication of *Chlamydia* has not been observed as of yet and thus survival of the host cell during the chlamydial intracellular lifecycle remains as important as ever. Several groups and multiple studies have provided evidence that illustrate that *Chlamydia* can block pro-apoptotic pathways and prevent premature host cell death (Fan et al., 1998; Fischer et al., 2004). Bacterial pathogens, such as *Shigella* and *Salmonella,* which utilize apoptosis as a defensive mechanism while others, such as *Listeria* spp., and *Staphylococcous* induce apoptosis due to bacterial toxin induced stress (Barsig and Kaufmann, 1997; Esen et al., 2001; Monack et al., 1996; Nonaka et al., 2003). Obligate intracellular pathogens such as *Coxiella* and *Chlamydia* inhibit premature cell death and confer protection to the host cell against intrinsic and extrinsic pro-apoptotic stress (Voth et al., 2007; Ying et al., 2007). To carry out such a feat, *Chlamydia* hijacks several well-known cell-signaling pathways such as MEK-ERK and phophoinositide 3-kinase (PI3K) pathways, which are responsible for promoting cell survival (Du et al., 2011; Sarkar et al., 2015).

Furthermore, to prevent cell death from intrinsic stress *Chlamydia* has been shown to induce proteasomal degradation of the tumour suppressor protein p53 and inhibition the activity of BCL-2 associated agonist of cell death (BAD) by 14-3-3β-binding Inc protein dependent sequestration to the inclusion membrane (Siegl et al., 2014; Verbeke et al., 2006). *Chlamydia* also provides an encompassing protection to the host cell from pro-apoptotic extrinsic stressors by a cFLIP-mediated blockage of caspases 8 activities (Bohme et al., 2010). In light of such well-developed mechanisms employed by *Chlamydia* to prevent host cell death it is quite evident that, metabolic dependencies aside, the pathogen presence inside the host cell has much far reaching consequences than just being a vessel for its replication.

1.2 MicroRNAs

1.2.1 A Big Family of Small Regulators: The MicroRNAs

Ever since the human genome was sequenced, it became increasingly evident that a considerable segment of the genes and the RNA transcribed from them do not code for proteins. These non-coding RNAs (ncRNAs) form a complex regulatory network whose function range from being transcriptional or translational switches to gene regulation and even genome defense (Mihailescu, 2015; Moazed, 2009; Simonelig, 2011; Taylor et al., 2015; Valencia-Sanchez et al., 2006). Indeed, with the advent of next generation sequencing and increasingly fine tuned methodologies under the umbrella of "experimental RNAomics", the field of ncRNAs is enriched incessantly by hundreds of studies every year (Huttenhofer et al., 2004). To attempt a brief description of the entire spectrum of ncRNAs involved in any cellular process would do a gross injustice to the subject and thus this chapter will focus on one of the more illustrious member of the ncRNA family: the microRNA.

The *lin-4* RNA was the first miRNA identified by the Rosalind Lee and Victor Ambros along with 15 other regulatory miRNAs in the *Caenohabiditis elegans* genome. They showed that in place of producing a regulatory protein the *lin-4* gene produced a small 22-nucleotide RNA that targeted the 3' UTR of the *lin-14* mRNA and exerted control over the expression of the corresponding LIN-14 protein (Lee et al., 1993). In 2000, seven years after the identification of *lin-4,* the group of Gary Ruvkun described another small RNA called *let-7* that regulated the developmental transition of *C. elegans* by targeting *lin-41*(Reinhart et al., 2000; Slack et al., 2000). Additionally, Ruvkun and his group also demonstrated the presence of the *let-7* RNA in several other species leading to the speculation that these small RNAs may act as temporal regulators of development in a variety of species, including humans (Pasquinelli et al., 2000). While the Ruvkun group worked extensively to elucidate the regulatory mechanisms of these novel RNAs, Thomas Tuschl, David Bartel and Victor Ambros independently demonstrated that lin-4 and let-7 belonged to an exhaustive class of small RNAs in drosophila, humans and *C. elegans*. However, it was observed that the expression of most of the members of this group did not coincide with the developmental timings, which hinted at the possibility that individual members, now classified as microRNAs, may have roles in the regulation in other cellular pathways as well. The original studies on LIN-14 showed that in order to be regulated by the *lin-4* RNA it was essential that the LIN-14 mRNA carry an intact 3'

UTR sequence and following molecular studies demonstrated the need of a direct but largely imprecise base-paring between the *lin-4/LIN-14* and *let-7/lin-41* RNA molecules for the regulation to take effect (Didiano and Hobert, 2008; Vella et al., 2004; Wightman et al., 1993). Characterization of these salient properties involved in the regulation of gene expression by these newly discovered class of RNA molecules heralded an in depth analysis of the biogenesis, modes of regulation and the scope of effect of miRNAs in human physiology and pathogenesis.

1.2.2 Nomenclature of miRNA and miRNA genes

While next-gen sequencing and in silico tools along with direct cloning increased the numbers of miRNAs in humans and other species by leaps and bounds, a slight inconsistency is observed in the nomenclature of the miRNAs. The miRNA genes discovered in the earliest of studies were named after the genes or phenotypes they affected (let-7, lin-4 and lys-6) and miRNAs discovered from cloning or sequencing screens were assigned numerical identifiers such as mir-30 (Ambros et al., 2003). If there were more than one miRNA in the so-called miRNA "family", lettered suffix was used to differentiate between miRNA sisters such as mir-30c and mir-30d. It is possible that the same mature miRNA might be transcribed from a different or multiple genomic loci, in which case an additional numeric identifier is added to the gene name such as mir-30c-1 and mir-30c-2 (Ambros et al., 2003; Griffiths-Jones et al., 2006). With the accumulation of miRNA research, evidence gathered to show that the hairpin duplex that harboured the mature miRNA was processed by Dicer to produce a duplex made of the mature miRNA and a "passenger strand" (Hu et al., 2009; Mah et al., 2010). For example, the human mir-30c-2 has 2 mature products hsa-miR-30c-2 and hsa-miR-30c-2* where the "hsa" is the identifier for a human miRNA, the upper-case "R" in miR- indicates that this is a mature product as opposed to "mir-" in precursor miRNAs and the "*" indicates that this is the passenger strand or the minor product (Ambros et al., 2003). However, there are increasing number of studies that show that this is not the case and many of these "minor" or "*" miRNAs are functional and it is possible that in certain cases this "*" is accumulated and becomes the major miRNA (Yang et al., 2011). Thus this form of nomenclature was replaced with the "-5p" or "-3p" identifiers representing the "arm" of the hairpin from which the miRNA is generated. Currently, the nomenclature of the mature miRNA-30c would be represented as hsa-miR-30c-2-5p or hsa-miR-30c-2-3p (Budak et al., 2016).

1.2.3 Biogenesis of miRNA

Over the years, on going discovery of new miRNAs has made it one of the most abundant families of ncRNA. The latest release of miRBase, miRBase21, lists 1881 precursors and 2588 mature miRNAs in humans (Kozomara and Griffith-Jones, 2014). While the function and the regulatory circuits of many of these miRNAs are still unresolved, the sheer enormity of the number of mature miRNA indicates the level of complexity that miRNAs add to the over-all mechanism of gene regulation. miRNA genes are found in to be widely distributed in plants, animal and according to recent findings, viruses (Zhang, B et al., 2008; Meshesha et al., 2012; Tsai et al., 2017). Molecular phylogenetics and next-gen small RNA sequencing data indicates that certain miRNA based regulatory circuits are evolutionarily conserved and miRNA played an important role in the evolutionary process of animals. Several clusters of miRNAs are shared between eumetazoans with addition of more clusters at the bilaterian lineage (Grimson et al., 2008; Peterson et al., 2009; Christodoulou et al., 2010). Additional miRNA clusters are observed as one progresses though the vertebrates towards placental mammals and it is understood that conserved clusters of microRNAs or individual miRNAs are retained in descendant lineages (Sempere et al., 2006; Lee et al., 2007; Chen and Rajewsky, 2007; Heimberg et al., 2008; Heimberg et al., 2010).

Owing to the low rates of loss in miRNA clusters and addition of new ones during evolution massively increased the repertoire of miRNAs in higher mammals and this increase in the number of miRNAs seems to be a key driving force in the development of complex organisms (Sempere et al., 2006). Apart from evolutionary pressure that fueled the development of novel miRNAs, there are other genomic sources for the emergence of novel miRNAs as well. One of the sources for the novel miRNAs would be the intronic region of protein coding genes. A significant population of miRNAs is transcribed from the intronic regions of “host-genes” (Rodriguez et al., 2004). Furthermore, these intronic regions are found to be particularly suitable for the development of novel miRNAs since they provide the right conditions for the evolution of a novel hairpin form a pre-transcribed hairpin and have no need for a promoter (Campo-Paysaa et al., 2011). However, it is increasingly evident that intronic miRNAs might possess promoter regions within the intron itself (Monteys et al., 2010). Gene duplication might also have promoted the emergence of novel miRNAs especially since most human miRNA can be grouped into specific families based on sequence homology and seed sequence the mature miRNA use to target their complimentary mRNA (Ambros et al., 2003). Several such duplication

events that might have given rise to novel microRNAs followed by acquisition of novel function or distribution of the original function can be traced back in the vertebrate lineage (Gu et al., 2009; Ruby et al., 2007).

Irrespective of the source of the miRNA, the transcription miRNAs are driven by RNA polymerase II (Pol II) to produce a long transcript with a hairpin structure called the primary miRNA (pri-miRNA) (Denli et al., 2004). While, several human miRNAs were shown to be transcribed by RNA polymerase III (Pol III) especially ones derived from Alu elements or tRNA genes, recent studies with CHIP-seq has since refuted the involvement of Pol III in the transcription of many of these miRNAs except in the cases of certain Alu element derived miRNAs and viral miRNAs (Borchert et al., 2006; Diebel et al., 2010). Though the transcription of miRNAs are largely governed by Pol II-associated transcription factors and epigenetic modifications, the transcriptional control of the majority of miRNAs are not well understood (Cai et al., 2004; Lee et al., 2004). This surprising discrepancy in our current knowledge about the control of miRNA gene expression can be, in part, be attributed to lack of better characterization of promoter sequences. However, on going studies have successfully pointed the many miRNA genes have their unique transcription initiation regions irrespective of their location within intronic regions or in DNA spans between gene clusters existing as stand-alone genes (Chien et al., 2011; Monteys et al., 2010). Advancements in characterizing chromatin signatures (especially modification of histones by methylation or acetylation) which mark promoter sites in humans have contributed toward the transcriptional initiation regions and putative upstream regulatory regions of several miRNAs (Ozsolak et al., 2008; Santos-Rosa et al., 2002; Schneider et al., 2004). This process is augmented by the study of relevant transcription factors that bind on the nucleosome-free transcriptional start sites proximal to a miRNA. Subsequently, several of these studies have revealed that transcription factors such as MYC, p53, PTEN and CREB have been shown to regulate the transcription of specifc miRNAs and even whole clusters of miRNAs (Chang et al., 2011; Krol et al., 2010; O'Donnell et al., 2005; Schulte et al., 2008; Vo et al., 2005).

1.2.4 Nuclear Processing of MicroRNAs

Primary miRNAs under go processing inside the nucleus to generate the precursor miRNAs (pre-miRNAs), which are then exported to the cytoplasm where they undergo further processing to generate the mature miRNA (Lee et al., 2002). The

nuclear processing of primary miRNAs, which might be several Kb long, involve the Microprocessor complex composed of the RNase III enzyme Drosha and its essential cofactor called DGCR8 (Denli et al., 2004; Lee et al., 2003). Drosha generates the hairpin shaped pre-miRNA by cropping the long pri-miRNA at a site approximately 11 bps away from the "basal" junction point between the dsRNA and ssRNA. This point is approximately 22bps away from the "apical junction" that links the rest of the structure to the terminal loop and, along with the basal junction, serves as an important reference point for determination of cleavage cite and accurate processing of the pri-miRNA (Auyeung et al., 2013; Han et al., 2006).

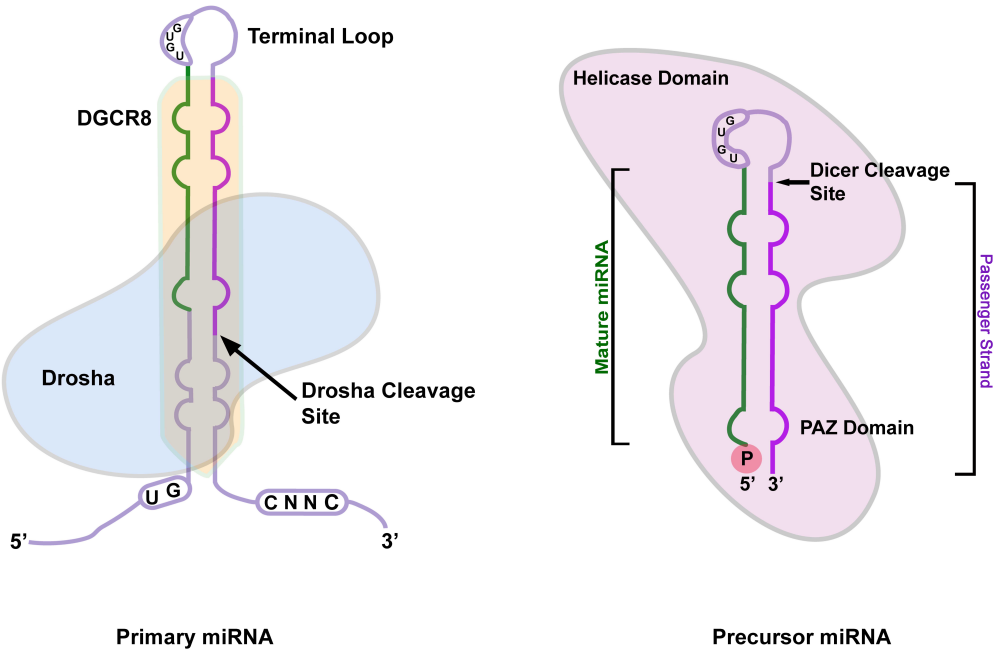

Fig.1.2.4. Primary and Precursor miRNAs: The primary miRNA is found exclusively in the nucleus where it is processed by the microprocessor complex composed of Drosha and DGCR8. Appropriate processing of the primary transcript by the microprocessor complex creates the precursor miRNA, which is then exported to the cytoplasm. Once exported to the cytoplasm, the precursor miRNA is further processed by the cytoplasmic Dicer to produce the mature miRNA (Illustration adapted after Ha and Kim, 2014).

Drosha mediated cleavage of intronic miRNA occurs simultaneously with the transcription of the host pre-mRNA and precedes splicing events (Kataoka et al., 2009; Kim and Kim, 2007). Efficient processing of the pri-miRNA by the Microprocessor complex is essential for promoting the abundance of a specific miRNA. The functions of the Microprocessor complex can be modulated by the auto-regulation that exists between DGCR8 and Drosha since protein-protein interactions between them stabilizes Drosha (Yeom et al., 2006). Conversely, Drosha is capable

of downregulating DGCR8 by processing a hairpin from the DGCR8 mRNA (Kadener et al., 2009). Drosha is also a substrate of several post-translational modifications, which modulate its nuclear localization and protein stability and thus altering the effectivity of the Microprocessor complex (Herbert et al., 2013; Tang et al., 2010; Wada et al., 2012). Alternatively, other RNA binding proteins that interact directly with Drosha or with the pri-miRNA also control pri-miRNA processing. While most of such interactions have been shown to promote either the effectiveness of the Microprocessor complex (SMAD1-3, SMAD5, p53) or by increasing the stability of Drosha (TDP43), other proteins like Lin28 binds to the pre-let-7 molecule and prevents processing by Drosha (Di Carlo et al., 2013; Nam et al., 2011; Suzuki et al., 2009). The maturation of the Drosha processed pre-miRNA carries on in the cytoplasm following the exportin 5 mediated nuclear export (Wang et al., 2011c). Exportin 5 is member of the karyopherin group of proteins that exports cargo from the nucleus in a GTP dependent manner. The binding of nuclear cargo, such as a double stranded pre-miRNA molecule, to the exportin 5 necessitates the association of exportin 5 with a GTP bound form of the Ran GTPase. The hydrolysis of the GTP by the Ran GTPase in the cytoplasm leads to the release of cargo (Yi et al., 2003). There are evidences that point towards regulation of pre-miRNA export leading to the modulation of miRNA availability in the cytoplasm. Exportin 5 has been shown to be positively regulated by the PI3K during cell cycle entry and in an ATM dependent manner during DNA damage (Iwasaki et al., 2013; Wan et al., 2013).

1.2.5 Cytoplasmic Processing of MicroRNAs

Cytoplasmic processing of the pre-miRNA depends on the endoribonuclease Dicer. The Dicer protein is highly conserved across species and contains two RNase III domains along with a helicase and an ATP binding domain (Bernstein et al., 2001). The interaction between the pre-miRNA and Dicer depends on the Drosha-generated 3’ overhang on the pre-miRNA. Dicer binds to the 3’ overhang as well as the 5’ end of the pre-miRNA via its PIWI– AGO–ZWILLE (PAZ) domain and cleaves 21-22 nucleotides into the stem using the RNase III domain (Ma et al., 2004; Macrae et al., 2006; Park et al., 2011). The specificity and effectivity of Dicer depends on the sequence and the structure of the end loop structure of the pre-miRNA (Vermeulen et al., 2005).

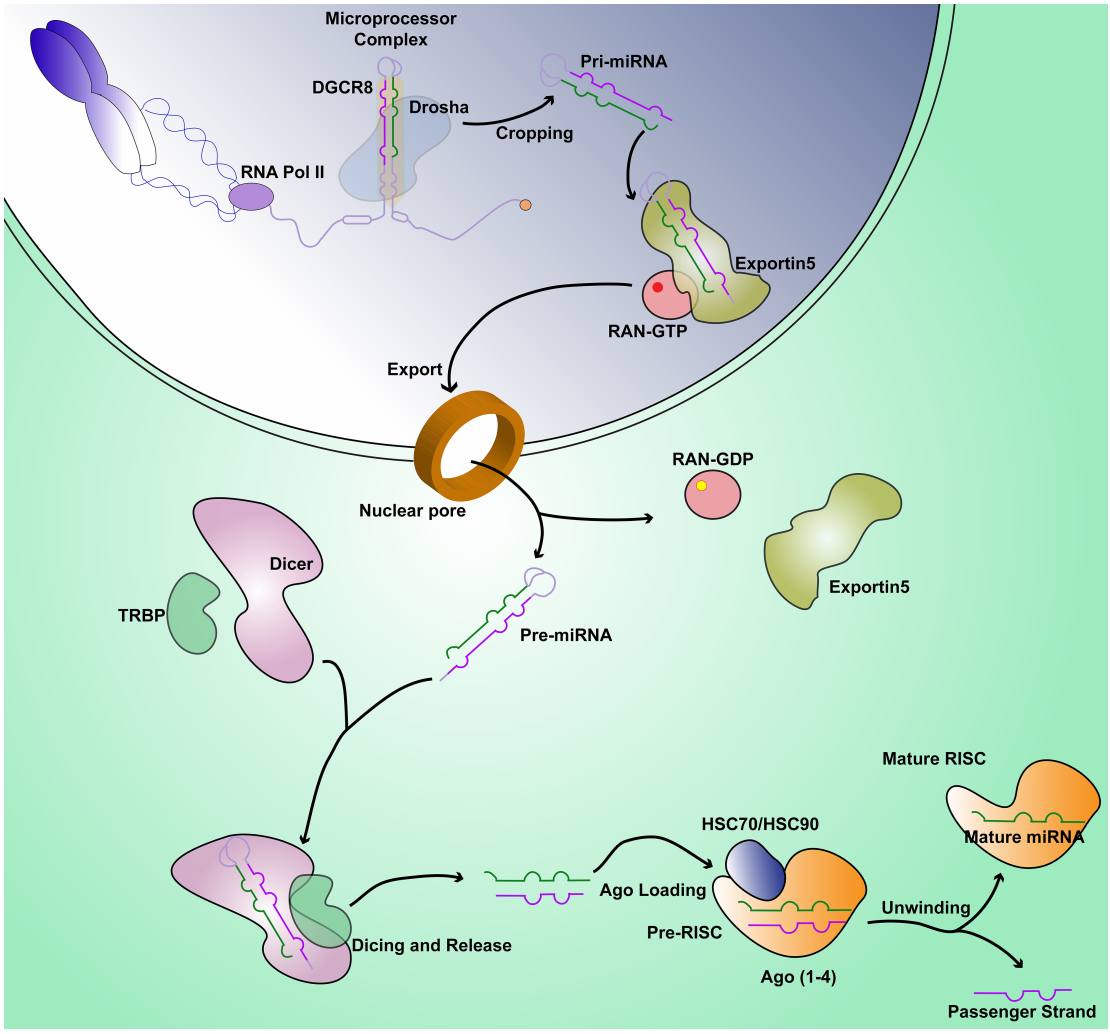

Fig.1.2.5. Biogenesis of miRNAs: miRNAs are transcribed as primary miRNAs in the nucleus by the RNA polymerase II and processed by the Microprocessor complex to produce the precursor miRNA. The precursor miRNA is exported to the cytoplasm by the exportin 5-RGNA-GTP complex in GTP dependent manner via the nuclear pore. In the cytoplasm the precursor miRNA undergoes cleavages at specific sequences by the RNase endonuclease Dicer to produce the mature miRNA duplex. Dicer interacts with the pre-RNA induced silencing complex (RISC) to promote the loading of the miRNA duplex into the RISC where it undergoes unwinding. The passenger strand of the miRNA duplex is discarded or functions as an independent miRNA depending on cell type.

Like other RNase III proteins, Dicer interacts with several other dsRNA binding proteins, which serve to regulate its activity and efficiency (Nicholson, 2014). The *trans*-activation response (TAR) RNA-binding protein (TRBP) and the dsRNA binding cofactor PACT both associate with the Dicer in humans (Lee et al., 2013). TRBP affects the processing efficiency of Dicer for specific pre-miRNAs and regulates mature miRNA length (Fukunaga et al., 2012; Wilson et al., 2015). The exact function of PACT in the miRNA-processing pathway is not fully understood though loss of PACT in HeLa cells leads to a decrease in the abundance of the mature miRNAs (Lee et al., 2006). Interestingly, TRBP is subject to phosphorylation by the mitogen activated protein kinase (MAPK) Erk, which results in a selective promotion of growth enhancing miRNA profile, while inhibiting the expression of the anti-tumorigenic

miRNA let-7 (Paroo et al., 2009). TRBP itself is also known to negatively affect the dsRNA dependent protein kinase R (PKR) although the exact role of PKR-TRBP interaction in miRNA processing pathway is not known (Emde and Hornstein, 2014; Haase et al., 2005). Finally, Dicer itself has been shown to be a subject of a feedback loop enforced by the mature miRNAs generated by the miRNA-processing pathway. The Dicer mRNA possesses binding sites for the let-7 miRNA and expression of let-7 leads to an establishment of a negative feedback loop causing a downregulation of Dicer and consequently, of let-7 itself. Enforced overexpression of let-7 also leads to a depletion of other miRNAs (Tokumaru et al., 2008). Alternatively, the tumour suppressor miRNA miR-375 can positively enhance the transcription of Dicer by downregulating its target mRNA, the HPV E6 oncoprotein (Lu et al., 2016).

1.2.6 The RNA Induced Silencing Complex

The miRNA produced following the processing of the pre-miRNA by Dicer is double-stranded and was previously termed as the miRNA-miRNA* duplex identifying the two strands of the duplex (Kim et al., 2009). The nomenclature as the miRNA-miRNA* duplex has now been scrapped (see: Nomenclature of miRNA and miRNA genes) and is simply called the miRNA dsRNA duplex. The major miRNA in the duplex is referred to as the guide strand of the duplex and the minor as the passenger strand (Ghildiyal and Zamore, 2009). The association of the miRNA to its target mRNA within the RNA Induced Silencing Complex (RISC) necessitates the unwinding of the duplex and removal of the minor miRNA strand in order to create a functional RISC. The RISC assembly can be viewed as a two-step process that involves Step 1. miRNA duplex loading and Step 2. Unwinding of the duplex (Kawamata and Tomari, 2010; Maniataki and Mourelatos, 2005; Wang et al., 2009).
The most well studied components of the RISCs are the members of the Argonaute (Ago) family of proteins. The Ago proteins are critical for the eventual target recognition and silencing function of the miRNA associated RISC (Hutvagner and Simard, 2008; Steiner and Plasterk, 2006). The Ago family can be broadly classified into three subclades, which comprises the Ago (responsible for binding to si- and miRNAs), Piwi (necessary for binding piRNAs) and the worm-specific Ago proteins (WAGO) (Hock and Meister, 2008; Swarts et al., 2014). Structural analysis of Ago reveals as bilobed, duck-shaped molecule consisting of a N-terminal lobe, a PAZ domain followed by a C-terminal lobe containing a middle (MID) domain and a P-element Induced WImpy testis (PIWI) domain (Elkayam et al., 2012; Song et al.,

2004). During the process of ATP driven miRNA duplex loading, the MID and the PIWI domains together form a 5' -phosphate-binding pocket that grips the 5' –monophosphate end of the guide RNA in the miRNA duplex (Schirle and MacRae, 2012). This binding is directed by a nucleotide specificity loop that prefers a uridine or adenine nucleotide at the 5' end of the guide strand (Frank et al., 2010). The 3' end of the guide strand associates with the PAZ domain of the Ago protein with two nucleotides at the end associated with a cleft in the PAZ domain (Elkayam et al., 2012; Schirle and MacRae, 2012). The key feature that allows the mature miRNA to recognize its target is a 5' end "seed" sequence complimentary to a binding sit in the 3' UTR of the target mRNA. This seed sequence in the guide strand forms an A-form helix within the Ago protein along the MID-PIWI lobe to allow effective scanning of the target mRNA for complimentary binding sequences (Frank et al., 2010; Hibio et al., 2012). In most species, including flies, the RNA duplexes are selectively loaded into separate Ago proteins (Ago1 for miRNAs and Ago2 for siRNAs) guided by the mismatches in and the structure of the RNA duplex (Okamura et al., 2004; Tomari et al., 2007). However, in humans no such preference has been observed and the four different Ago proteins (Ago1 through Ago4) are loaded non-selectively with near-identical sets of miRNAs. There are no specialized Ago proteins dedicated to si- or miRNAs since all four Ago proteins can be loaded and function with either form of RNA duplex (Azuma-Mukai et al., 2008; Dueck et al., 2012).

Association of the miRNA duplex with the RISC leads to the formation of a "pre-RISC" which matures into the "holo-RISC" by ejection of the passenger strand (Kim et al., 2007). The determination of the guide strand is strongly guided by thermodynamic properties of the miRNA duplex, which in turn governs the stability of either end of the miRNA duplex (Hu et al., 2009; Khvorova et al., 2003). The Ago2 protein in humans possess what is termed as "slicing" ability by means of which it is able to cleave the passenger strand if the central sequence in the duplex is perfectly matched as is the case in siRNAs. However incase of miRNAs, mismatches between the guide and passenger stands at positions 2-8 and 12-15 facilitate the ATP dependent unwinding of the rather rigid dsRNA duplex. Another protein complex associated with the RISC is the HSC70-HSP90 chaperone complex that promotes the ATP driven conformational change of Ago proteins to facilitate the unwinding of the passenger strand.

General consensus suggests that the strand with a weaker or unstable 5' terminus and a U nucleotide at position 1 is typically selected to be the guide strand by Ago proteins (Hu et al., 2009; Noland and Doudna, 2013; Okamura et al., 2009). This selection is, however, quite variable. While in majority of the cases the passenger

strand undergoes rapid degradation following ejection, these minor miRNA also have active silencing properties (Guo and Lu, 2010; Yang et al., 2011; Yang et al., 2013). Recent studies have also exemplified tissue specific alternate selection of the guide and passenger strand of the similar duplex (termed as “arm switching”). Most studies, amongst other mechanisms, attribute arm switching to alternate processing by Drosha that affects the thermodynamic properties of the pre-miRNA in different tissues (Griffiths-Jones et al., 2011; Guo et al., 2015; Li et al., 2012b; Yang et al., 2013).

1.2.7 Post-translational Regulation by MicroRNAs

MicroRNAs along with other micro-ribonucleoprotein (miRNPs), such as GW182 proteins and its interacting partners, are the critical components of the functional miRISC and form the basis of a complex regulatory network that governs gene expression (Fabian and Sonenberg, 2012). A single miRNA species can target several hundred genes and alternatively a single gene can be targeted by several different miRNAs (Bonci et al., 2008; Wu et al., 2010). Efficient downregulation of a gene by a miRNA is not only dependent on the binding of the miRNA to the 3’ UTR of the target via its seed sequence but also on the abundance and stability of the miRNA, interaction between the members of the miRISC complex and the stability of the target mRNA, all of which is governed by the cellular conditions. Depending on these factors several outcome of a miRNA-mRNA interactions can be expected which range from mild downregulation of the gene to loss of the protein product over time.

Although targeting ability of the miRISC is most certainly dependent on the sequence of the core miRNA, the ability of the miRISC to carry out the actual silencing of the target mRNA is conferred by its protein components. Apart from one of the four Ago proteins previously described as a part of the RISC, an Ago-bound GW182 protein supplements the miRISC (Eulalio et al., 2009b).

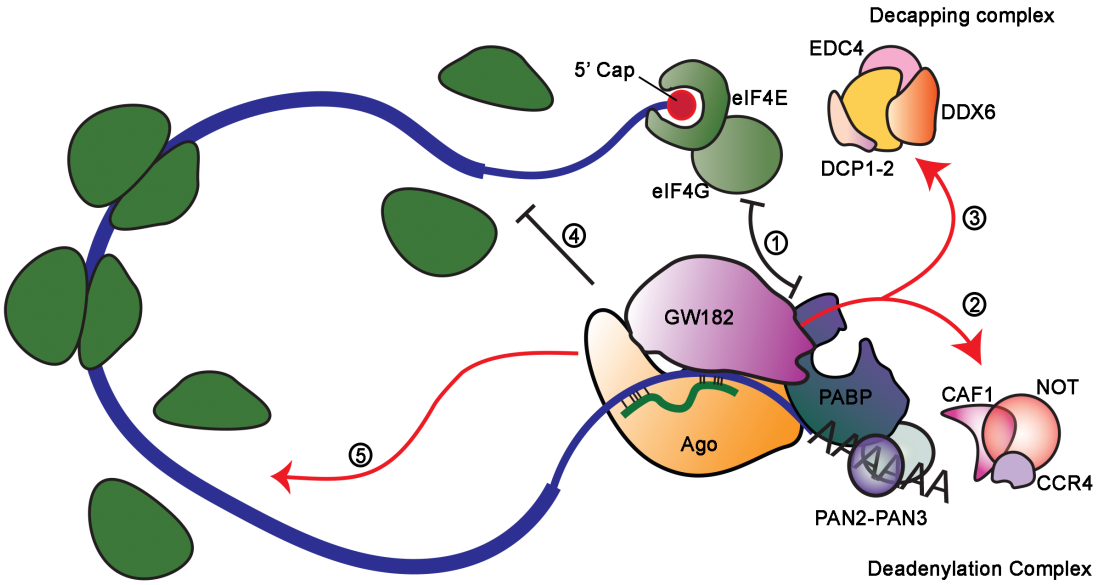

Fig.1.2.7.1 MicroRNAs in action: The mature miRNA at the heart of the RISC is the key element that potentiates the targeting ability of the silencing complex. However, the Ago associated GW182 protein recruits other mediators that carry out the silencing actions of the RISC. Some of the major strategies of miRNA mediated post-translational silencing are represented here: 1) GW182 association with PABP inhibits its interaction with the eIF4E and eIF4G preventing the assembly of the translational initiation complex. 2.) GW182 association with PABP also promotes the recruitment of the components of the deadenylation complex. CCR4–NOT and PAN2–PAN3 deadenylation complex decreases the stability of the target mRNA by removing the poly(A) tail. 3.) The tryptophan repeats of GW182 associated with the Ago promotes the recruitment of the 5' decapping complexes. The DDX6 decapping complex can act independently of GW182 to promote 5' decapping and prevent translation initiation. Finally, the RISC complex can effectively inhibit mRNA translation by preventing the 4.) ribosome assembly by interfering with the eIF6 and 5.) elongation of the nascent peptide by promoting ribosome drop-off (Illustration modelled after Braun et al., 2013 and Jonas and Izaurralde, 2015)

The GW182, named after its glycine and tryptophan repeats and its molecular weight, forms distinct cytoplasmic loci called GW bodies (GWB). It was later discovered that GW182 colocalises with mRNA processing proteins and mRNAs within these GWBs (Eystathioy et al., 2002; Eystathioy et al., 2003). Humans and other vertebrates express three GW182 paralogs called termed trinucleotide repeat-containing protein (TNRC) 6A, B and C (Behm-Ansmant et al., 2006). All of the three paralogs are found to interact non-specifically with all four human Ago proteins via their N-terminal GW, WG or GWG repeats (Behm-Ansmant et al., 2006; El-Shami et al., 2007; Landthaler et al., 2008; Lian et al., 2009; Takimoto et al., 2009; Yao et al., 2011). It has been shown that while Ago proteins have a single GW protein-binding domain, a single GW protein can simultaneously interact and stabilize multiple Ago proteins in separate miRISCs (Eulalio et al., 2009b; Takimoto et al., 2009). Deletion of GW182 in *Drosophila melanogaster* leads to a partial loss of miRNA silencing function without affecting the abundance of miRNA suggesting that GW protein are essential effectors of miRNA function but not required for their biogenesis or processing (Behm-Ansmant et al., 2006; Eulalio et al., 2008). The silencing function

of GW proteins is limited to its C-terminus and is composed of a RNA-recognition motif (RRM) and a middle domain (Eulalio et al., 2009a). The C-terminal silencing domain of human GW protein also contains a poly(A) binding protein (PABP)-interacting motif called the PAM2 domain (Huntzinger et al., 2010; Zipprich et al., 2009). Finally, the N-terminal effector domain (NED) of GW proteins have also been shown to interact with the CCR4–NOT deadenylase complex (Chekulaeva et al., 2011; Chekulaeva et al., 2010). It appears that while Ago proteins serve to unwind the miRNA duplex and position the guide miRNA for proper targeting of the mRNA, GW proteins along with its effector proteins such as poly (A) binding protein, CCR4–NOT and PAN2–PAN3 deadenylase complexes and the ubiquitin E3 ligase EDD are responsible for silencing the target mRNA (Huntzinger et al., 2013; Inada and Makino, 2014; Su et al., 2011).

Multiple mechanisms are proposed for the actual silencing event that occurs upon the association of a miRISC complex to the target mRNA via the interaction of the miRNA seed sequence and the binding site on the 3' UTR of the target mRNA. In plants the miRNA-mRNA interactions are almost siRNA like and exhibit near-complete complementarity resulting in endonucleolytic cleavage of the target mRNA (Tang et al., 2003). Even though certain mammalian miRNAs are known to cleave their target mRNAs, such events are rare and the complementarity is usually limited to the 5' end seed sequence (Lai, 2004; Majoros and Ohler, 2007). The lack of extensive complementarity between mammalian miRNA and their target mRNA leads to a translational block in place of endonucleolytic cleavage of the target. However, it has been shown that incase that the target is cleaved the degradation occurs via pathway independent of RNA-directed endonucleolytic cleavage (Olsen and Ambros, 1999). Mammalian microRNA act upon their target mRNA in process analogous to the functioning of a rheostat as explained by David Bartel in one of his opinion pieces about miRNA function. Briefly, the 3' UTR carry binding sites for several miRNA but with different degrees of complementarity to its corresponding miRNAs varying from very high to weak complimentarily. Some of these miRNAs are highly expressed in the cells at all times, some moderately and some of the miRNAs are expressed weakly. The translation of the mRNA in question is dependent on which miRNA is bound to the binding site, the degree of complementarity between that miRNA and the binding site and finally, other miRNAs that can bind to the mRNA simultaneously. All of the factors thus fine-tune the protein expression from this mRNA. At the same time, this delicate modulation of mRNA regulation, in different cell types and under different cellular conditions, is governed by the combined action of all the miRNAs

that can bind to the mRNA and are expressed in under the conditions in question (Bartel and Chen, 2004).

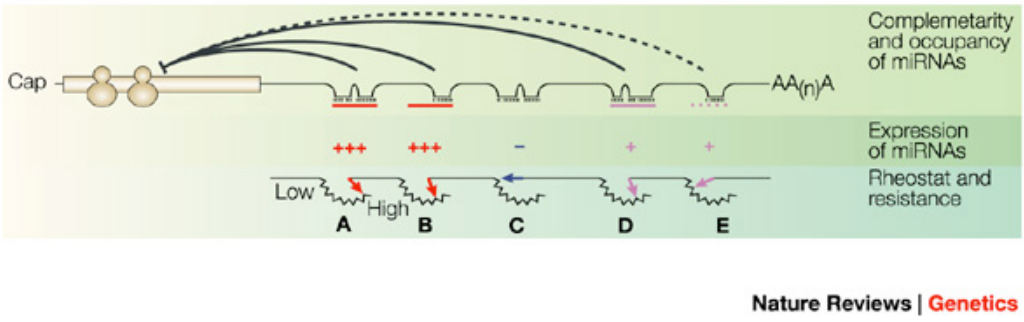

Fig.1.2.7.2. The rheostat model of miRNA function as described by Bartel and Chen, 2004. The model proposes that every miRNA binding site within the 3'UTR of acts as an adjustable resistor (the jagged line indicate a resistor whereas the arrows indicate the adjustment). Rheostats A, B, C, D, and E act together to dampen the translation of the mRNA to fine tune the expression of the protein for the particular cell type. Reprinted with permission from Macmillan Publishers Ltd: [Nature Reviews Genetics] (Micromanagers of gene expression: the potentially widespread influence of metazoan microRNAs; D. Bartel and CZ. Chen), copyright (2004).

The effect of miRNA binding is not only determined by the degree of complementarity but also by the components of the miRISCs. The GW associated protein PABP can induce protein translation via interactions with PABP-interacting protein 1 and eIF4G (Derry et al., 2006). However, it is proposed that interaction of GW proteins with PABP can inhibit translation by preventing PABP-eIF4G interaction and hindering mRNA circularization (Fabian et al., 2009; Zekri et al., 2009). Since binding of PABP to the transducer of ERBB2 (Tob) or the poly(A) nuclease (PAN) complex are associated to regulation of mRNA deadenylation and decay, it is also speculated that association of GW proteins with PABP could promote mRNA deadenylation by positioning miRISC associated deadenylation complexes in close proximity to the poly (A) tail (Fabian et al., 2009; Mauxion et al., 2009; Siddiqui et al., 2007). The process of miRNA mediated deadenylation of target mRNA requires the association of the CCR4–NOT and PAN2–PAN3 deadenylase complexes to the miRISC associated GW proteins which can also act as a deadenylation coactivator (Braun et al., 2011; Chekulaeva et al., 2011; Fabian et al., 2011; Kuzuoglu-Ozturk et al., 2012). Finally, the E3 ubiquitin ligase, EDD, which also directly binds to miRISC associated GW proteins has been shown to promote mRNA decapping and repress cap dependent translation via interactions with the miRISC associated DEADbox helicase RCK/p45 (Chu and Rana, 2006; Coller and Parker, 2005; Su et al., 2011). It is suggested that mRNAs that experience translational repression due to miRNA binding accumulate in the cytoplasm as GWB, also known as P-bodies (Liu et al., 2005; Pillai et al., 2005). There are also indications that miRNA mediated repression

can occur after translation initiation (post-initiation repression) by promoting ribosome drop off or facilitation of nascent proteins degradation by miRISC associated proteases. However no such proteases have yet been identified (Nottrott et al., 2006; Petersen et al., 2006; Seggerson et al., 2002).

1.2.8 MicroRNAs in Infection

Beginning with the association of *mir15* and *mir16* gene deletion in chronic lymphocytic leukemia, research in the field of disease-related miRNA regulation has broadened exponentially (Calin et al., 2002; Li and Kowdley, 2012). This is hardly surprising given the wide spectrum of gene regulatory networks that are modulated just by the fraction of miRNA whose targets are validated. This is just the tip of the proverbial iceberg since of the 2,588 mature miRNAs now available within the miRBASE 21 collection, targets of many of the miRNAs have not been experimentally verified and, in many cases, have never been studied (Kozomara and Griffiths-Jones, 2011). Under such conditions, it is quite challenging to draw up a regulatory network via which one could possibly predict the effect of miRNAs on the human physiology as a whole. Of recent, mathematical modeling has been used to understand the network dynamics of miRNA based gene regulation (Hsu et al., 2015; Lai et al., 2013; Lai et al., 2016). However, such efforts are hampered by the ability of miRNAs to target unconventional mRNAs under very specific cellular condition, multiple modes of miRNA biogenesis and processing control and the sub-cellular availability of the miRNA.

These factors have, however, not hindered the progress of disease based miRNA research since, as of 2014, there are ~10000 experimentally supported miRNA–disease association entries in the 2nd version of the Human miRNA Disease Database (HMDD) with more being discovered with increasing regularity (Li et al., 2014). To gauge an estimate regarding the possible roles of miRNA in human diseases one only has to regard the number of key biological processes whose modulation via miRNAs have been experimentally validated. These processes include, but are not limited to, cellular dynamics, innate and adaptive immunity, inter and intracellular signalling, metabolism pathways, developmental signalling, cell survival and death pathways and cell cycle (Dang et al., 2013; Fordham et al., 2015; Jung and Suh, 2014; Liston et al., 2012; Meng et al., 2007; Sakha et al., 2016; Song et al., 2009; Turchinovich et al., 2011; Zhu et al., 2015).

Under such conditions it is not hard to imagine that mammalian miRNAs might have valid roles in augmenting or inhibiting bacterial infection and most interestingly, be regulated by viral and bacterial infections. Over the last few years, a number of studies have focused on the role and effect of miRNAs in viral infection. Furthermore, in case of Epstein-Barr virus (EBV, γ-herpesvirus), Human Cytomegalovirus (HCMV, β-herpesvirus) and Herpes Simplex Virus Type 1 (HSV-1, α-herpesvirus), the presence of virally encoded miRNAs in the host cells has generated much interest (Meshesha et al., 2012; Suen et al., 2008; Tsai et al., 2017). While viruses with an RNA genome, such as the retro- and flaviviruses, seem to lack miRNAs, the Human Immunodeficiency Virus (HIV) has been shown to encode a small 59 bp TAR RNA which forms a hairpin loop structure that resembles endogenous pre-miRNAs (Klase et al., 2007). Many of these virally encoded miRNAs, identified primarily from the Herpesviruses, target the ORFs in the viral genome to regulate development. There is also a growing vein of evidence showing that some of these miRNAs might also target specific host genes to promote viral gene expression and assist viral development (Roberts et al., 2011; Skalsky and Cullen, 2010). One of the major functions of the virally encoded miRNAs appear to be the establishment of and/or maintenance of latency by targeting viral immediate early genes or proteins necessary for lytic exit (Grey et al., 2007; Tang et al., 2009). The Kaposi's Sarcoma-Associated Herpes Virus (KSHV) encoded miRNA miR-K12-11 shares its seed sequence with the host miR-155 and targets several mRNAs that regulate TLR3 Expression, B-cell function and innate immunity (Boss et al., 2011; Skalsky et al., 2007). Taking into account the profound effect that viral infection have in regards to the host immune response and the role of cellular miRNAs in the regulation of immune response, it is not surprising that several cellular miRNA have been shown to be modulated by the onset of a viral infection. Time and again, the host miR-155 has been shown to be intricately involved in the regulation of the host immune response especially in lymphocyte immune function and modulating interferon signalling (Banerjee et al., 2010; Liu et al., 2016b). In context of viral infection, EBV infected lymphocytes exhibit high levels of miR-155 and is reported to affect the expression of several genes involved in transcriptional regulation including NF-KappaB (Lu et al., 2008; Yin et al., 2008). The E6 and E7 proteins encoded by the oncogenic human papillomavirus regulate several miRNA by inhibiting the p53 and Rb (Retinoblastoma) tumour suppressor proteins (Fujii et al., 2016). As a result, E6 expression leads to a downregulation of the p53 dependent miR-34a, which eventually promotes oncogenic growth (Ribeiro et al., 2015; Ribeiro and Sousa, 2014; Sun et al., 2008). Additionally, E6 expressing cells also exhibit downregulation

of miR-218, which enhances tumorigenicity due to the dysregulated levels of laminin 5 β3 (Martinez et al., 2008).

While prokaryotes are not known to express miRNAs, several bacterial species, such as *Salmonella enterica*, *Shigella flexineri*, *Chlamydia trachomatis* amongst others, have been shown to express small, non-coding RNAs (sRNAs) that modulates and shape their transcriptional profile (Frohlich et al., 2016; Grieshaber et al., 2006a; Wang et al., 2016). Most of these bacteria, with the exception of *Chlamydia* and certain other bacterial species, depend on the Hfq chaperone for efficient base pairing between a sRNA and its target mRNA (De Lay et al., 2013; Wroblewska and Olejniczak, 2016). Of recent, bioinformatics studies have predicted the existence of pre-miRNA like secondary structures in multiple bacterial genomes and several of these putative miRNAs are capable of targeting host genes (Shmaryahu et al., 2014). As in the case of viral infection, the regulation of the immune response by host miRNAs is also affected by bacterial infection. One of the earliest evidence of host miRNA regulation by bacterial infection was observed in *Arabidopsis thaliana* in context of *Pseudomonas* infection. Infection of *Arabidopsis thaliana* with *P. syringae* leads to an upregulation of miR-393a, a host miRNA that modulates Auxin receptors and regulates the plant's immunological defense (Navarro et al., 2006). The evidence towards the existence of a profile for miRNA expression in mammalian cells as a response to bacterial infection came from a study that stimulated human monocytes (THP-1) using bacterial cell wall components such as lipopolysaccharide (LPS). It was shown that stimulation of the Toll-like receptor (TLR) family of the THP-1 cells by pathogen-associated molecular patterns (PAMPs), such as those of LPS, leads to the changes in the expression patterns of miRNAs under the control of TLR4 and IL-1 receptor associated kinase (IRAK1) (Taganov et al., 2006). TLR4 and IRAK1 promote the expression of immune-responsive genes governed by the NF-KappaB and AP-1 dependent transcription pathways (Akira and Takeda, 2004). It was observed that LPS stimulation induced the abundance of several mature miRNAs, which affects different aspects and branches of the mammalian immune response (Taganov et al., 2006). Given the possible chances of faulty and accidental activation of TLR signalling, several negative regulators of above discussed pathways exist, which act as fail safe mechanisms by modulating the upstream mediators (Liew et al., 2005). During this study, a significant elevation was observed in the expression of miR-146a and miR-146b in an NF-KappaB dependent manner (Taganov et al., 2006). Previously, it was reported that both miR-146a and miR-146b are involved in the determination of lymphocyte cell face owing to their elevated levels in T helper1 cells (Monticelli et al., 2005). It has now been shown that miR-146 upregulation upon

LPS stimulation (and in case of NF-KappaB driven T-cell resolution) counteracts IRAK1 and TNF receptor associated factor-6 (TRAF6), both of which are important mediators of NF-KappaB/AP-1 dependent TLR activity activity establishing a feedback loop (Dai et al., 2016; Ramkaran et al., 2014; Taganov et al., 2006; Yang et al., 2012). It has now been shown that mycobacteria infection induced upregulation of miR-146a and prolongs survival of the pathogen. miR-146a suppresses inducible nitric oxide synthase (iNOS)-mediated generation of nitric oxide in macrophages by targeting TRAF6 and impairing signalling via NF-KappaB, p38 MAPk and JNK pathways (Li et al., 2016). Another miRNA, which was reported to be upregulated upon LSP stimulation, was miR-155 (Doxaki et al., 2015; Taganov et al., 2006; Tili et al., 2007). Several studies have shown miR-155 to be closely tied to immunological responses. Additionally, infections with multiple bacterial pathogens exhibit upregulation of miR-155. This is not surprising given the fact that mediators of inflammation such as LPS, polyriboinosinic–polyribocytidylic acid (poly-IC), TNF-α and IFN-γ can induce miR-155 expression (O'Connell et al., 2007; Taganov et al., 2006; Tili et al., 2007). Furthermore, studies show that deletion of *mir-155* gene severely compromises T-cell dependent antibody response, cytokine production, IL-2 and IFN-γ production in mice (Rodriguez et al., 2007; Thai et al., 2007). Several cell types infected with *Helicobacter pylori* exhibit high abundance of miR-155 and its induction is attributed to the virulence factors VacA, GGT and the LPS expressed by *H. plyori* (Fassi Fehri et al., 2010). While in gastric epithelial cells *H. plyori* induced miR-155 expression suppresses cytokine (IL-8 and GRO-α) production by targeting mRNAs of IKK-ε, SMAD2, and FADD, in *H. plyori* infected macrophages, miR-155 upregulation leads to enhanced activation and/or apoptosis of the infected macrophages (Xiao et al., 2009; Yao et al., 2015). Amongst miRNAs affected by *H. plyori,* miR-21 stands out due to its illustrious nature. Being one of the most frequently studied miRNA, it has been associated with numerous diseases, ranging from psoriasis to neurodegeneration (Meisgen et al., 2012; Yelamanchili et al., 2010). Both, *H. plyori* infected gastric mucosa and human gastric cancer tissues exhibit elevated levels of miR-21 (Belair et al., 2011; Zhang et al., 2008). Given the role of *H. plyori* in promotion of gastric cancer and the oncogenic potential of miR-21, this correlation generated considerable enthusiasm in further studies towards bacterial regulation of host miRNA profiles. Interestingly, Salmonella infection also induced mir-21 and miR-155 expression in mouse macrophages along with miR-146a, all of which are regulated by the NF-KappaB pathway. Additionally, *Salmonella* infected macrophages and epithelial cells both exhibit a repression of the let-7 family of miRNAs as a mechanism for IL-6 and IL-10 expression (Schulte et al., 2011).

Intercellular pathogens such as *Coxiella* and *Leishmania,* both of which reside within a parasitophorous vacuole within the host cytoplasm, have also been shown to modulate certain miRNAs. Interestingly, majority of the regulated miRNAs by either pathogen appear to have roles in the host cell apoptotic pathways. In case of *Coxiella,* anti-apoptotic miRNA genes, such as *mir-181d, mir-28 and miR-362* were found to be upregulated while *Leishmania* infection led to a downregulation of the anti-apoptotic *mir-221* gene and enhanced the expression of pro-apoptotic miRNAs (miR-15b and miR-29b) (Geraci et al., 2015; Millar et al., 2015). While *Salmonella* infection can downregulate the pro-apoptotic miR-15 via an E2F1 dependent transcriptional block, *Shigella* infection is enhanced upon overexpression of miR-15 (Maudet et al., 2014). This alternative preference of a specific miRNA or miRNA family is seen between several pathogens, some of which might even be closely related in terms of niche preference. However it appears that bacterial modulation of host miRNAs are strictly governed by the physiological, biochemical and mechanistic aspects of the infection process. The fine-tuned nature of regulation affected by miRNAs is evidently quite a helpful repertoire for the bacterial pathogens to establish infection and even promote their growth development and survival within the host cell.

1.3 Mitochondria

"**Over the long term, symbiosis is more useful than parasitism. More fun, too. Ask any mitochondria**."

- **Larry Wall**

1.3.1 A Lot More Than Just a Kitchen: The Mitochondria

The mitochondrion is one of the most well studied and influential cellular organelles that comprise two well-defined membranes, an inter-membrane space, and the mitochondrial matrix. The mitochondrion is unique in being the only eukaryotic organelle known to possess its own extra-nuclear DNA (Nass and Nass, 1963; Schatz et al., 1964). Apart from being the site of ATP synthesis, the cellular mitochondrial network is a highly dynamic structure that plays significant roles in numerous physiological processes. Mitochondrial function and dynamics is crucial to cell fate determination and dysregulation of either is decisive for the pathogenesis of several diseases. The ability of the mitochondrial network to perform it's essential tasks that include ATP synthesis, production of free radicals, calcium homeostasis amongst numerous other processes critical to the well being of the cell is closely ties to the fission and fusion of individual mitochondrial fragments.

Studies reporting the presence of intracellular structure resembling mitochondria started surfacing as early as the 1840s following the discovery of the nucleus (Aubert, 1852; Kolliker, 1856; Retzius, 1890). The German histopathologist Richard Altmann noted the ubiquitous presence of the described structures in his samples. Altmann used the term "Bioblast" to describe what he understood to be "Elementarorganismen" or elementary organisms living within eukaryotic cells and carrying out vital functions (Altmann, 1890). However, Altmann's theory of the mitochondria being related to bacteria was severely criticized and ignored similar to those of the Russian biologist Konstantin Mereschkowski, which is ironic in the light of our current knowledge about the organelle (Mereschkowski, 1905; Sagan, 1967). Carl Benda proposed the name "mitochondria" in 1898 due to the heterogeneous nature of the organelle.

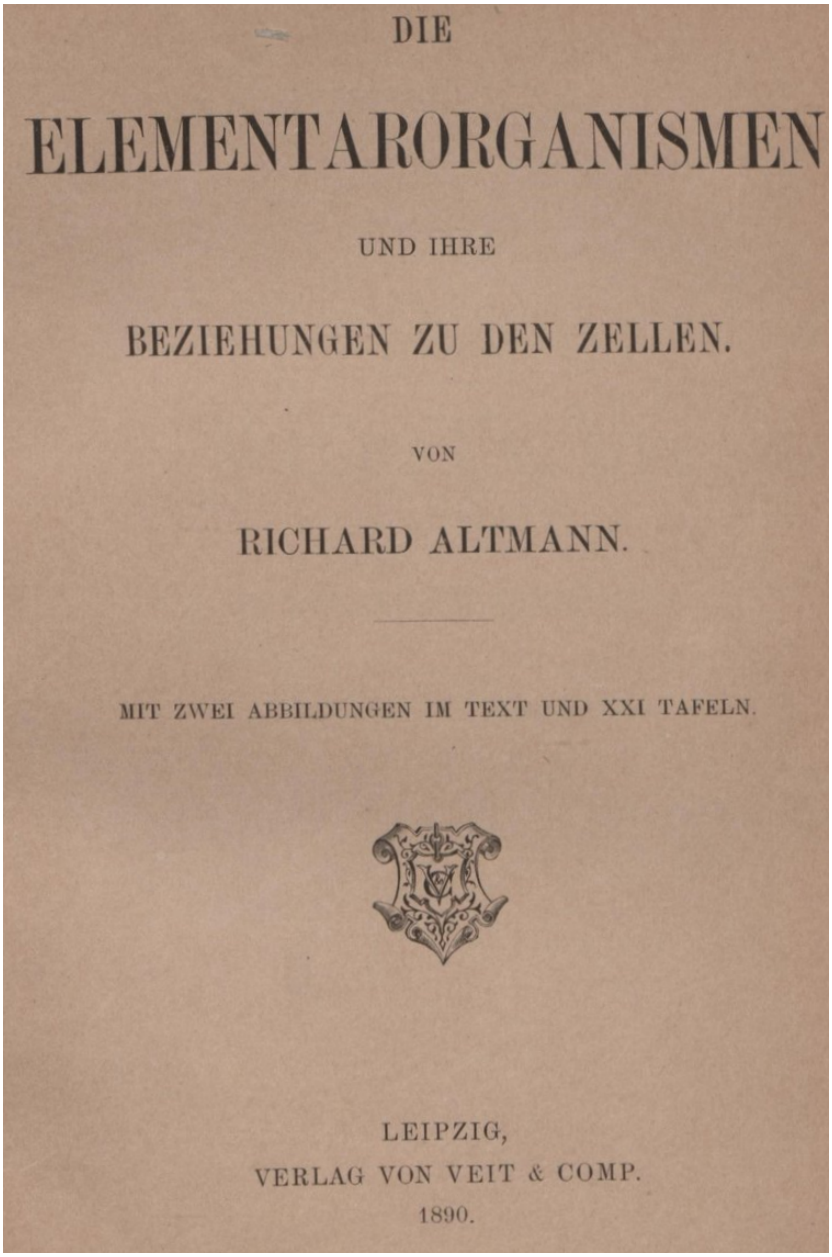

DIE

ELEMENTARORGANISMEN

UND IHRE

BEZIEHUNGEN ZU DEN ZELLEN.

VON

RICHARD ALTMANN.

MIT ZWEI ABBILDUNGEN IM TEXT UND XXI TAFELN.

LEIPZIG,
VERLAG VON VEIT & COMP.
1890.

Fig. 1.3.1. Reproduction of the title page of Richard Altmann's original report of "Die Elementarorganismen" or the elementary organism, ca. 1890. Reproduced from www.deutschestextarchiv.de

Using crystal violet for staining the mitochondrial granules, he observed that the presentation of the organelle varied between "ball-shaped" and "thread-like" which justified the name mitochondria from the Greek word "mitos" (for thread) and Khondrion (for little granule) (Sapp, 2007). The interchangeable nature of mitochondrial morphology was expanded upon by Lewis and Lewis' observations of mitochondria in endothelial, mesenchymal and cardiac tissues. They described the constant movement of mitochondrial particles in live cells and gave flight to the study of mitochondrial motility and dynamics (Lewis and Lewis, 1914).

Role of the mitochondrion in respiratory control and oxidative phosphorylation were recognized in the late 1950s. In retrospective, one of the first evidences towards a possible involvement of mitochondria in cellular respiration was its property of being specifically stained with the reduced form of the Janus Green B dye as demonstrated by Michaelis (Michaelis, 1900). Michaelis, however, did not attribute this property to any biochemical function of the mitochondrial particles. Kingsbury made one of the first proposals towards a possible connection between mitochondria and cellular biochemistry and suggested that the mitochondria might be phospholipid complexes that assist in cellular respiration (MacCardle, 1964). As early as 1910, it was believed that most biological oxidations occurred within insoluble cellular components and the particulate nature of cellular respiration was thoroughly studied and supported by Warburg, Wieland and Keilin. However, in absence of reliable methods for cell fractionation it was not possible to gather concrete evidence toward understanding the role of mitochondria in cellular respiration (Brand, 2010; Dixon, 1929; Warburg, 1928; Wieland, 1922). During this period considerable advances were made towards understanding the biochemical aspects of cellular respiration albeit without much focus on the mitochondria it self. While, both Wieland and Warburg both agreed on the particulate nature of the respiratory complexes, they differed in their views of the chemistry: Wieland proposed the transfer of hydrogen whereas Warburg proposed a transfer of oxygen (Warburg, 1928; Wieland, 1922). Late 1930s saw a great deal of advancement towards the understanding the energetics, reaction mechanisms and pathways involved in aerobic respiration with the elucidation of Kreb's cycle, and Kalckar's studies of aerobic phosphorylation (Kalckar, 1991; Krebs and Johnson, 1937). While several groups were toiling on the production of "washed tissue particles" and fine-tuning the process of cellular fractionation, Ochoa demonstrated the production of 3 moles of organically bound phosphate from the aerobic oxidation of pyruvate as well as the process of glycolysis in heart tissues (Ochoa, 1938; Ochoa, 1939).

Significant breakthrough in the cell fractionation and eventually, separation of fractionates containing mitochondrial particles, was achieved due to the efforts of Albert Claude and George Palade (Claude, 1943; Palade, 1943; Palade, 1953). Claude's studies revealed a startling correlation between the morphological characteristics and the biochemical properties of the isolated mitochondrial particles. These brilliant observations contributed enormously to advance the understanding of the cellular respiration and were quickly and, at times, simultaneously followed studies that determined the presence of the cytochrome oxidase, enzymes involved in the citric acid cycle, fatty acid oxidation and oxidative phosphorylation within the

mitochondria (Chance and Williams, 1952; Friedkin and Lehninger, 1948; Kennedy and Lehninger, 1948; Kreb, 1937).

Hand in hand with the advancements in the understanding of the mitochondrial biochemistry, the interest in the structural aspects of the mitochondria was being explored. With the advent of critical developments in electron microscopy and sample preparation, high-resolution micrographs of intracellular structures were being published quite rapidly. During this period Palade introduced the osmium-fixation technique for various animal tissues (Palade, 1952). Palade and Sjostrand, separately, determined the double membraned nature of the mitochondria and demonstrated the presence of the folded cristae structure of the inner membrane (Palade, 1953; Sjostrand 1953; Sjostrand, 1954). In 1966, the neurobiologist V. P. Whittaker offered a brilliant line of reasoning for the folded nature of the mitochondrial inner membrane, which he associated with the increase in surface area similar to the invaginations found in the adrenal cortex of the brain (Whittaker, 1966). This association was in line with the Palade's observation that an abundance of cristae are associated with high respiratory. While, recent developments in the area of Electron microscopy assisted tomography and super-resolution confocal microscopy has enhanced the study of the mitochondrial architecture and function to a nanometer scale, the original double membraned-cristae structure of the mitochondria has survived the test of time and is widely regarded as the standard model (Jakobs, 2014; Lewis, 2016; Youle, 2012).

1.3.2 Dance to live, live to dance: Mitochondrial Dynamics

The idea that mitochondria were motile and actively changed shape and structure was put forward by the observations of Lewis and Lewis in 1914. They observed that the mitochondrial particles changed shape, size and even divided in several fragments and that such changed were governed, at times, by the composition of the suspension solution (Lewis and Lewis, 1914). Considering the rudimentary nature of microscopy at that time, their observation regarding the dynamic nature of mitochondria were ground breaking and brilliantly accurate.

Advancements in the areas live cell microscopy has resulted in a renewed invigoration in the field of mitochondrial dynamics beginning with vital dye staining followed by phase contrast microscopy and later, live cell confocal microscopy of fluorescent and photo-switchable proteins targeted to the mitochondria (Karbowski, 2004; Matsuda, 2008; Mitra, 2010; Patterson, 2002; Wu, 1987).

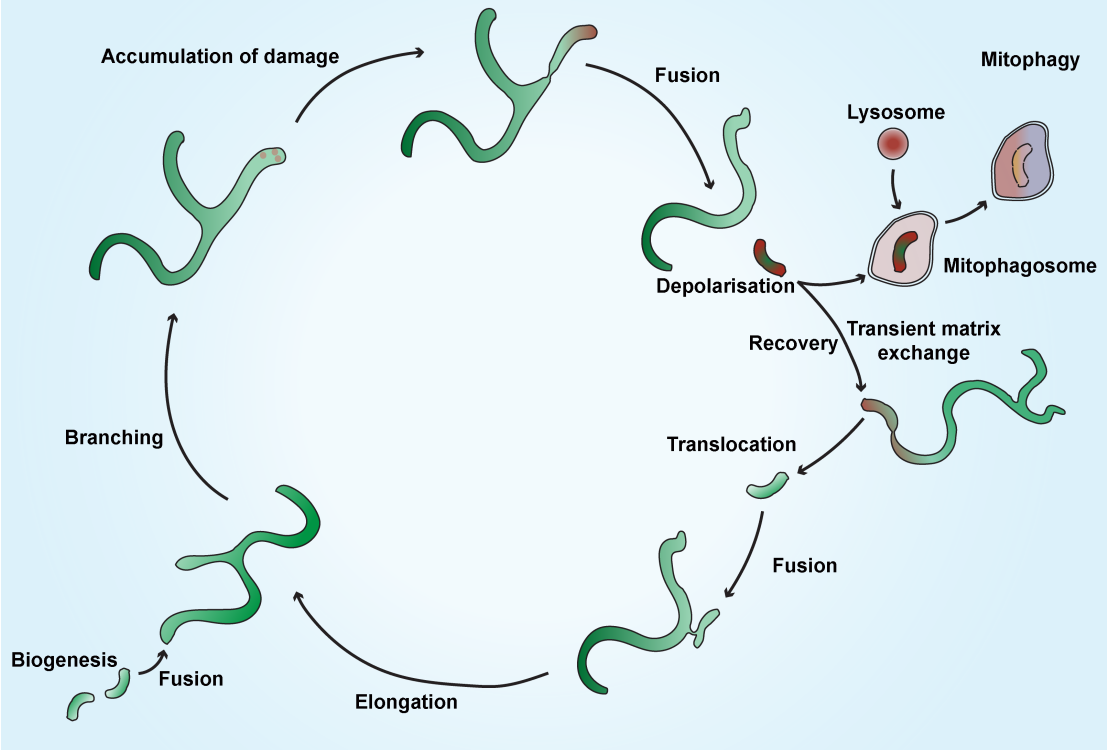

Fig.1.3.2. The mitochondrial fusion/fission cycle: The mitochondrial network within a cell constantly undergoes fission and fusion giving it an appearance of being under constant flux. The mitochondrial fragments do exhibit true movement as well, being ferried across the cell on dynein-kinesin filaments to fuse with other fragments to either transport metabolites or recover from damages. Quite often damaged mitochondrial fragments are targeted for destruction by mitophagy while some are recycled into the matrix on recovery. The mitochondrial network is regularly replenished by fresh mitochondrial units produced by biogenesis depending on the metabolic state of the cell.

The dynamics of mitochondria are the product of the constant fission, fusion, biogenesis and degradation of mitochondrial fragments and are governed by a specific set of cytoplasmic and mitochondria bound regulatory proteins (Ji et al., 2015; Korobova et al., 2013). Such behaviors of the mitochondria are well conserved in almost all cell types ranging from yeast to mammals and are indispensible for maintenance of optimal cellular health (Bereiter-Hahn and Voth, 1994; Hollenbeck, 1996; Sprague and Thorner, 1994). While the movements of the mitochondrial fragments appear random, according to the earliest observations by Lewis and Lewis and the detailed studies on the mitochondrial network performed recently, fine-tuned nature of mitochondrial behaviour affect and are affected by cellular bioenergetics, metabolism, survival, stress and disease conditions (Hickey et al., 2014; Huang et al., 2016; Lee et al., 2014; Sharp et al., 2015). Apart from contributing towards the maintenance of the cellular homeostasis and participating in the regulation of the above-mentioned processes, the dynamic nature of the mitochondrial network is also an important mechanism by which the network auto-regulates its own quality, thereby

serving as a means to eradicate and/or recycle damaged mitochondrial fragments (Chen et al., 2009; Held et al., 2015; Rambold et al., 2011; Shirihai et al., 2015).

The typical architecture of the mitochondrial network is largely cell-type specific is governed by the fusion/fission ratio prevalent in the cell. The ratio of the number of fusion events to the number of fission events is variable in terms of the conditions faced by the cells *in vivo* or *in vitro*. A pertinent example to illustrate this point would be to consider a case of metabolic deprivation faced by cells, which causes the fusion/fission ratio to tip in favour of fusion resulting in an elongation of the mitochondrial fragments and their eventual escape from starvation induced autophagy (Gomes et al., 2011). While this might appear to be a straight-forward mechanism to deal with loss of ATP resulting in from starvation, an intricate collaboration of several molecular pathways regulate the mediators of the fission-fusion process and are responsible for maintenance of the balance between the fission-fusion events. Alternatively, being able to supply ATP and affect local calcium concentration, the subcellular transport and localization of mitochondrial fragments are effective regulators of mitochondrial behavior (Guo et al., 2005; Verstreken et al., 2005). The mitochondrial fragments have been shown to relocate across the cytoplasm via interaction with dynein and kinesin tracks (Wu et al., 2011). Interestingly, while dynein acts as the molecular motor for mitochondrial transports, it is also responsible for the recruitment of mitochondrial fission mediator, dynamin-related protein-1 (Drp1) (Varadi et al., 2004).

1.3.3 Mitochondrial Fusion

The prime mediators for the mitochondrial fusion process are the mitofusin proteins, Mfn1 and Mfn2 and Optic Atrophy 1 (OPA1) (Alexander et al., 2000; Chen et al. 2003; Delettre et al., 2000; Santel and Fuller 2001) All three are GTPase proteins and belong to the dynamin superfamily of proteins. The double membraned nature of the mitochondria requires two separate fusion events that occur in tandem. The outer membrane fusion is mediated by the mitofusins, while the separate isoforms of the Opa proteins contribute towards the fusion of the inner membrane (Song et al., 2009; Mishra et al., 2014) The two processes were previously believed to be tightly coordinated but experimental evidence show that altering membrane potential can lead to an uncoupling indicating that they are governed by independent mechanisms (Olichon et al., 2003; Song et al., 2009; Twig et al., 2006). Apart from the mitofusins and OPA1, Phosphatidic acid generated from cardiolipin by the mitochondrial

phospholipase D promotes mitochondrial fusion in an Mfn dependent pathway (Choi et al., 2006; Vögtle et al., 2015)

The process of mitochondrial fusion share properties of virus-mediated and SNARE-mediated membrane fusion in biological systems and require the presence of both the mitofusins on the outer membranes of the adjacent mitochondria (Choi et al., 2006; Griffin et al., 2006) It is predicted that Mfn1 and Mfn2 form both homotypic and heterotypic dimers via their hydrophobic HR2 regions allowing close apposition of the mitochondrial membranes (Franco et al., 2016). Importantly, both mitofusins are necessary since knockdown of either result in an inhibition of mitochondrial fusion and pathological conditions (Chen et al., 2003; Chen et al., 2007; Song et al., 2015).

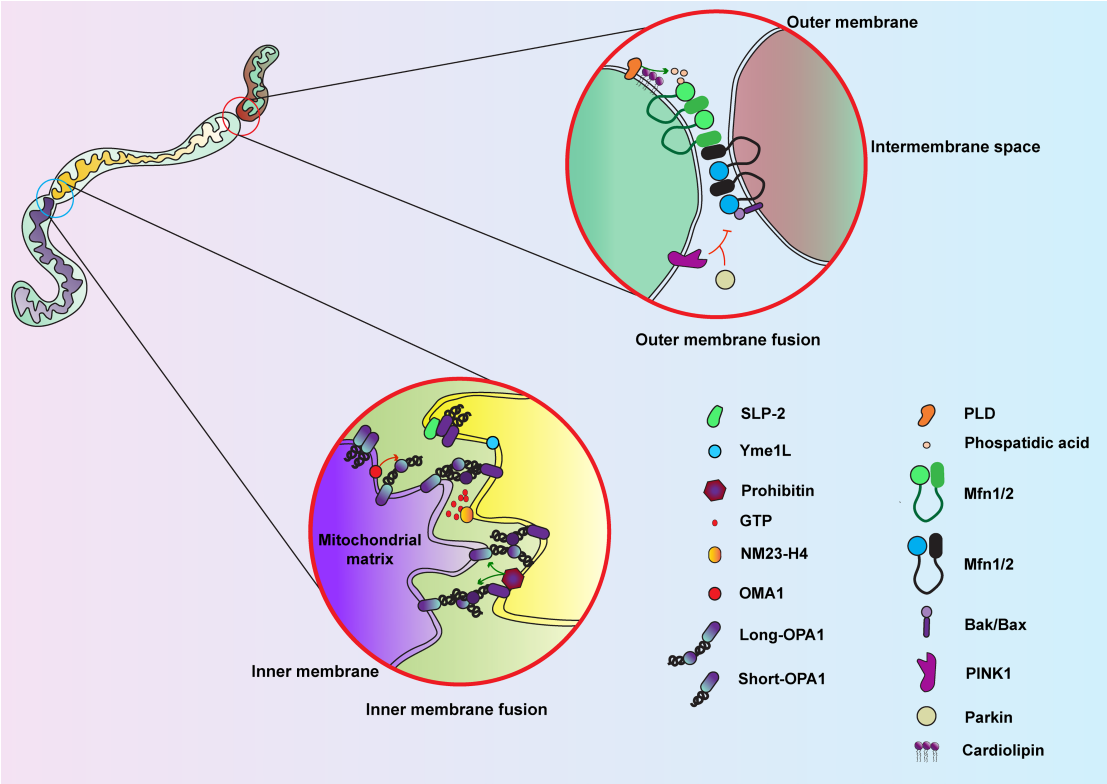

Fig.1.3.3. Mitochondrial fusion: Mitochondrial fusion is a two-step process. Inner membrane (IMM) fusion closely follows the mitofusin (Mfn1/2) driven outer membrane (OMM) fusion unless the IMM fusion promoting protein Opa is inhibited. The OMM fusion process is catalyzed by the juxtaposition of Mfn1/2 dimers on opposing mitochondrial fragments and is enhanced by several accessory events like association of Bak/Bax and PLD mediated production of phospatidic acid from cardiolipin. The long and short forms of OPA1 (L-OPA and S-OPA) are both found on the IMM. While the L-OPA is credited for the progression of IMM fusion, presence of both the forms are beneficial for fusion. The IMM proteins SLP-2 and Prohibitin stabilize the long form of OPA while NM23-H4 is responsible for the GTP required for driving the L-OPA mediated IMM fusion.

Structural studies show that such interaction of Mfn1 via its transmembrane region still leaves a significant gap between the two appositional mitochondria. It is believed that this gap might be closed by a GTP dependent conformational change in the Mfn1 structure (Franco et al., 2016; Koshiba et al., 2004). Control of mitochondrial

fusion is established by proteolysis and ubiquitination, both of which are, in turn, governed by cellular stress and metabolic conditions. During mitophagy, PTEN-induced putative kinase 1 (Pink1)- and Parkin-mediated ubiquitination leads to a proteasomal degradation of the mitofusins (Chen and Dorn, 2013; Gegg et al., 2010). In yeast, ubiquitination of the mitofusin homolog Fzo1 at specific residues might stabilize the protein or lead to its degradation (Cohen et al., 2011). In skeletal muscle cells, Mfn2 expression is transcriptionally regulated by Estrogen-related receptor-alpha transcription factor along with the nuclear coactivators PGC-1beta and PGC-1alpha under conditions of increased energy expenditure (Leisa et al., 2008; Soriano et al., 2006 Zorzano, 2009). Specific types of oxidative stress, which surprisingly can instigate fusion in isolated organelles, can also regulate Mitofusins. Oxidized glutathione induced dimerization of mitofusins lead to organelle tethering, a primary step in mitochondrial fusion (Desideri et al., 2012; Ryan and Stojanovski, 2012; Shutt et al., 2012). Finally, several recent studies have demonstrated intricate cell signalling pathways that regulate mitochondrial fusion. One prime example of such an event would be the phosphorylation of Mfn1 by the extra- cellular signal–regulated kinase tying the MAPK pathway to mitochondrial fusion (Pyakurel et al., 2015).

A successful fusion event leads to the exchange and intermingling of the mitochondrial matrix and cannot proceed without fusion of the inner membrane (Cipolat et al., 2004; Ishihara et al., 2004). The OPA1 protein, responsible for mitochondrial inner membrane fusion is indispensible for this event since knockdown of OPA1 in drosophila axons not only impairs inner membrane fusion, but also affects mitochondrial motility and distribution by reducing the number of over-all fusion events within the cell (Cipolat et al., 2004; Chen et al., 2005; Griparic et al., 2004; Wong et al., 2000) The Opa1 gene, implicated heavily in dominant optic atrophy, is transcribed to produce eight splice variant mRNAs for the long isoforms of OPA1 (Alexander et al., 2000; Delettre et al., 2001) These isoforms undergo further proteolytic cleavages at specific cleavage sites (conventionally termed as S1 or S2 sites) by mitochondrial proteases to generate the short isoforms of OPA1 (S-OPA) (Ehses et al., 2009; Song et al., 2007) It has now been shown that the long isoforms of OPA1 (L-OPA) along with the short ones are together responsible for mitochondrial fusion activity while the longer isoforms have little or no activity when expressed in absence of the smaller isoforms (Ehses et al., 2009). Proteolytic cleavage by the mitochondrial metalloprotease OMA1 is believed to limit OPA1's ability to participate in a fusion event since loss of membrane potential leads to spontaneous loss of the longer isoforms thus inhibiting mitochondrial fusion (Ehses et al., 2009; Quiros et al., 2012). Another regulator of OPA1 is the ATP dependent i-

AAA protease Yme1L. Located in the inner membrane of the mitochondria, it is believed to be responsible for the S1 cleavage of OPA1. Loss of Yme1L leads to increase in rates of transient fusion events termed as “Kiss and run” type fusion events and a fragmented mitochondrial network demonstrating that both S- and L-OPA are necessary for true fusion events (Anand et al., 2014; Liu et al., 2009; Ruan et al., 2013). In context of cellular physiology, such proteolytic cleavage of OPA1 by Yme1L is attributed to the OXOHOS-dependent induction of inner membrane fusion (Anand et al., 2014; Ruan et al., 2013). Interestingly, several cellular conditions seem to exert a form of control on the inner membrane fusion via control of the proteolytic cleavage events of OPA1 (Baricault et al. 2007; Merkwirth et al. 2008; Ehses et al. 2009). Low levels of ATP due to drug treatment or otherwise, loss of membrane potential and possibly accumulation of misfolded proteins lead to an immediate OMA1 induced cleavage at the S1 site of OPA1 thus establishing a control step prior to Pink1 Parkin pathway mediated inhibition of mitofusins (Frank et al., 2012; Twig et al., 2008; Uo et al., 2009).

Another mitochondrial inner membrane protein called Prohibitin, implicated in development and aging, has now been shown to regulate OPA activity by stabilizing L-OPA (Merkwirth et al., 2008; Merkwirth and Langer, 2009). Similar to Prohibitin, another inner membrane protein, Stomatin-Like Protein 2 (SLP-2), is also responsible for the stabilization of L-OPA and induces stress induced mitochondrial hyperfusion (Christie et al., 2011; Tondera et al., 2009) Additionally, OPA1 mediated mitochondrial fusion is dependent on the local GTP concentration. It has been shown that the mitochondrial diphospahtase kinase NM23-H4 catalyzes the production of GTP from GDP in presence of ATP and facilitates GTP loading onto OPA1 (Bernard et al., 2010; Griparic et al., 2004)

Mitochondrial fusion is intricately regulated and affected by the cellular metabolic status. Multiple studies have shown that the mitochondrial fragments undergo elongation under conditions of increased OXPHOS activity face by cells grown in galactose media, which instigates the cells to resort exclusively to the OXPHOS for ATP production (Auger et al., 2011; Coenan et al., 2004). Conversely, stimulation of OXPHOS activity in absence of metabolic stress also stimulates fusion and elongation of mitochondria, indicating that elongated mitochondria generated by mitochondrial fusion are more efficient at energy production (Gomes et al., 2011; Rambold et al., 2011; Tondera et al., 2009). Finally, several studies have shown that artificial augmentation of mitochondrial fusion by either overexpression of Mitofusins or OPA1 inhibit apoptosis, while their knockdown can lead to hyperfission and

induction of cell death pathways (Alaimo et al., 2014; Griparic et al., 2007; Papanicolaou et al., 2011).

Together these mechanisms provide an important link between the cellular conditions and regulation of mitochondrial architecture with regards to fusion events. While metabolic and stress responses are indispensible forces that govern fusion processes, alternation in rates of fusion affect cellular processes independent of OXPHOS activity.

1.3.4 Mitochondrial Fission

Being complimentary to mitochondrial fusion, Mitochondrial fission is just as critically important to cellular physiology and mitochondrial quality control. The key modulator of mitochondrial division and fission is the Dynamin-related protein Drp1 (Smirnova et al., 2001). Similar to its yeast homolog Dnm1, Drp1 is also a member of the large self-assembling GTPase family of Dynamin-related proteins (DRPs). As is characteristic of DRPs, Drp1 possesses a conserved GTPase domain and are unique in their structural and regulatory properties (Bleazard et al., 1999; Smirnova et al., 1999). Drp1 are singular in their capacity for GTP-induced self-assembly and assembly moderated GTP hydrolysis. Unlike regulatory GTPases, the affinity of Drp1 for GTP in its assembled state is considerably lower and exhibits faster rates of GTP hydrolysis (Gawlowski et al., 2012; Ugarte-Uribe et al., 2014). Other key components of mammalian mitochondrial fission mechanism are Fis1 and Mff along with the newly discovered MiD49 and MiD51, all of which are responsible for recruitment of Drp1 to the mitochondrial surface and facilitate fission (MacDonald et al., 2014; Palmer et al., 2013). Diacylglycerol, generated by the hydrolysis of phosphatidic acid by the protease Lipin-1, has been show to accumulate at fission site and facilitate fission, possibly by promoting actin polymerization and ER-mediated constriction of mitochondrial fission sites (Nishi et al., 2010; Willers and Cuezva, 2011).

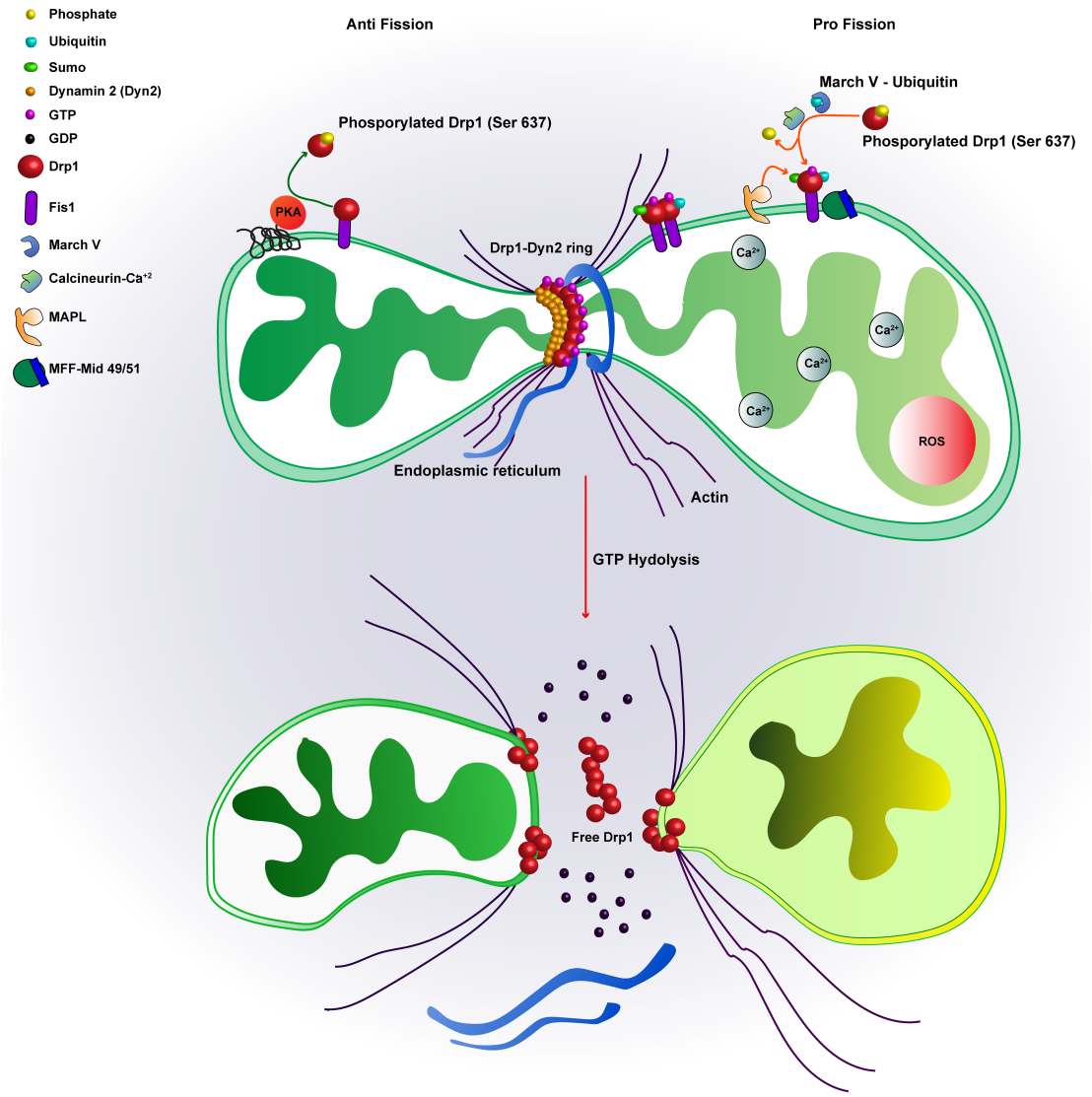

Fig.1.3.4. Mitochondrial Fission: Schematic of the mitochondrial fission assembly. Here the fission is promoted by the appearance of ROS and increase calcium influx, tagging the mitochondrial fragment on the right for either mitophagy or recycling. Such stress triggers the cytosolic regulatory proteins that modify Drp1 causing an increase in Drp1 translocation to the mitochondria and eventually forming the fission rings. Drp1, due to purely mechanistic reasons, can only form ring around a mitochondrial fragment that has been pre-constricted by the combined action of the endoplasmic reticulum and actin filaments. The Drp1 rings can, however, constrict the mitochondrial filament only till 100-120 nm. The final cleavage is carried out in a GTP dependent manner by the Dyn2 ring.

Unlike the fusion machinery which necessitates the presence of two distinct mechanisms and separate GTPase proteins (Mitofusins and OPA1) for the fusion of outer and inner membrane, the mitochondrial fission machinery can be driven solely by Drp1 in association with the membrane bound adaptors like Mff and Fis1 (Smirnova et al., 2001; Zhou et al., 2015). Drp1 is a nuclear-encoded protein and is predominantly cytosolic (Uo et al., 2009). Coordinated post-translational modifications limit its translocation to the mitochondrial surface or alternatively,

promote such translocation. Mammalian cells have been shown to express several splice variants of the Drp1 mRNA resulting in the presence of several isoforms of Drp1 (Luan et al., 2015). These variable isoform differ in their capacity to form higher order structures and capacity to bind the mitochondrial membrane bound adaptors such as Mff. Recent studies have also shown that alternative isoforms may have variations in the shape of their higher order structures to accommodate for the difference in the shape and thickness of mitochondrial fragments in different cell types (Otera et al., 2010; Sorensen et al., 2016). Structural studies of Drp1 have revealed a great deal about the structure of Drp1 and its relevance to the function of the protein. Drp1 has been shown to form multimeric spirals or helical ring like aggregates on the mitochondrial surface via its stalk like folds of middle and GTPase Effecter domain (Strack and Cribbs, 2012). While the cytosolic tetramers of Drp1 exhibits a low basal rate of GTP hydrolysis, this rate is enhance a 100 fold upon spiral formation and subsequent interaction between the GTPase domains of adjacent subunits around a mitochondrial fragment. Triggering of this enzymatic activity causes a GTP-dependent conformational change resulting in a constriction of the ring and eventual severing of both the inner and outer membrane of the mitochondria (Ingerman et al., 2005; Mears et al., 2011; Strack and Cribbs, 2012; van der Bliek and Payne, 2010).. The association of Drp1 with the mitochondria requires the presence of adaptor proteins on the outer membrane of the mitochondrial membrane facing the cytosol. Fis1, in concert with Mdv1 and Caf4, is essential for mitochondrial fission in yeast since they recruit the yeast homolog of Drp1, Dnm1 to the mitochondrial surface (Griffin et al., 2005; Koirala et al., 2010; Mozdy et al., 2000). While some studies show that the loss of Fis1 in mammals leads to slight defects in fission, the actual function of Fis1 is not clearly understood since deletion of Fis1 does not affect Drp1 distribution on the mitochondria (Loson et al., 2013; Otera et al., 2010). On the contrary, the tail-anchored mitochondrial fission factor (Mff) protein is essential for the recruitment of Drp1 to the mitochondrial membrane and its loss leads to elongation of mitochondrial fragments (Gandre-Babbe and van der Bliek, 2008). Mff appears on the mitochondrial surface as pre-arranged puncta independent of Drp1 and recruits Drp1 via its N-terminal cytosolic domain. Mitochondria in Mff knockdown cells exhibit similar morphology and interconnectivity observed in Drp1 knockdown cells (Otera et al., 2010)(Sorensen et al., 2016). While the mechanisms by which the mitochondrial elongation factor 1 (MiD51) and its variant MiD49 recruit Drp1 are not as clear cut as Mff's but it is well understood that they are essential for mitochondrial fission. ADP-bound MiD51 promotes the assembly of Drp1 spirals and eventual GTP hydrolysis (Loson et al.,

2014). However, over expression of either MiD51 or MiD49, while enhancing recruitment of Drp1, prevents the GTPase activity of Drp1, inhibits fission and induces fusion in a mitofusin independent manner (Palmer et al., 2011; Zhao et al., 2011). Knockdown of either one of these factors produce irregular morphology and distribution of the mitochondrial network. Interestingly, both MiD51 and MiD49 are capable recruiting Drp1 and initiating fission in absence of Mff and Fis1 (Palmer et al., 2011; Siengdee et al., 2015).

As mentioned previously the control of fission via Drp1 depends on a host of posttranslational modifications including, but not limited to, nitrosylation phosphorylation, sumoylation and ubiquitination (Cho et al., 2009; Figueroa-Romero et al., 2009; Karbowski et al., 2007). It is now understood that the adaptor proteins discussed above are subject to several modifications as well but such modifications are not as well characterized as in the case of Drp1 (Cherok et al., 2016; Zhang and Lin, 2016). One of the most well studied regulatory modifications of Drp1 is its phosphorylation, which can occur at multiple sites and are mediated by a variety of kinases under influence of specific pathways. Additionally, such phosphorylation can either activate or inhibit the capacity of Drp1 to induce fission depending on the site the phosphorylation occurs (Jahani-Asl and Slack, 2007). In response to a plethora of events such as forskolin mediated pharmacological activation, forced exercise or β -adrenergic stimulation Drp1 is phosphorylated at Ser 637 by protein kinase A (PKA) leading to an inhibition in its GTPase activity (Chang and Blackstone, 2007; Cribbs and Strack, 2007). Such negative regulation of Drp1 is also observed during nitrogen starvation and mTOR inhibition, which activates PKA by raising the cAMP levels. This effect is also observed during starvation-induced autophagy resulting in Drp1 inhibition and elongated mitochondria capable of increasing ATP production (Gomes et al., 2011; Rambold et al., 2011). The phosphorylation of Drp1 at Ser 637 by protein kinase A (PKA) is essential in terms of apoptotic resistance and is one of the primary indicators that blocking mitochondrial fission can inhibit apoptosis. Staurosporine induced cell death prevents PKA mediated phosphorylation of Drp1 at Ser 637 and Drp1 mutants with constitutively phosphorylated Ser 637 resist apoptosis induced by hydrogen peroxide and staurosporine (Cribbs and Strack, 2007). Interestingly, the cytosolic phosphatase calcineurin, activated by pro-apoptotic stimuli mediated rise in calcium, dephosphorylates Drp1 at Ser 637 to promote its activity and translocation to the mitochondria (Cereghetti et al., 2008). While phosphorylation of Drp1 at Ser 637 is mostly inhibitory with regards to its fission inducing activity, another phosphorylation at Ser 616 is responsible for the triggering of the fission event. This serine residue can be phosphorylated by protein kinase C

(PKC) activated by local concentrations of calcium or diacylgylcerol upon exposure to oxidative stress (Qi et al., 2011). Alternatively, Drp1 can also be phosphorylated at Ser 616 by the Ca2+/calmodulin-dependent protein kinase I alpha (CAMK-I) which in turn is activated by release of calcium from voltage dependent anion channels (VDACs) in the mitochondria. Phosphorylation at Ser 616 also enhances Drp1 binding to Fis1 and consequently promotes Drp1 binding to the mitochondria (Qi et al., 2011). Ser 616 phosphorylation has been investigated by several groups and has now been shown to be a phosphorylation residue for Rock kinase and CDK1/Cyclin B during hyperglycemia and cell division induced mitochondrial fission respectively (Taguchi et al., 2007; Wang et al., 2012b). It is speculated that fission events generally follow fusion close to the area of the event, since conditions that effect fission promoting phosphorylation arise from fusion events, such as phosphatidic acid mediated activation of Lipin1 that produces Diacylglycerol on the mitochondria (Choi et al., 2006; Nishi et al., 2010; van der Bliek et al., 2013). This is, however, not always the case. In events of massive membrane depolarization and fragmentation that occur due to presence of carbonyl cyanide m-chlorophenyl hydrazine (CCCP) or other pro-apoptotic signals, the near-total activation and mobilization occur without any corresponding fusion events (Frank et al., 2001). In such cases the rapid release of calcium from the mitochondria and the endoplasmic reticulum followed by activation of calcineurin results in the dephosphorylation of Drp1 at Ser 637 and fission of the mitochondrial network (Cereghetti et al., 2008; Cribbs and Strack, 2007; Scorrano et al., 2003). It must be noted that while most of the studies focused on the effect of the phosphor-modification of Drp1 and deduced the subsequent effects of the same, the broader picture must take into account the diverse effects manifested by the conditions that trigger these modifications. The effect of the modifications is presumably dependent on the conditions prevalent in the cell due to, for example, rise in the intracellular calcium or activation of the unfolded protein response from oxidative stress (Chang and Blackstone, 2010; Otera et al., 2013).

While phosphorylation of Drp1 is one of the major mechanisms by which diverse signalling pathways regulate mitochondrial fission, other previously mentioned modifications to Drp1 as well as its transcriptional regulation are utilized to exert control over mitochondrial fission. While oxidative and apoptotic stress induced by hydrogen peroxide and staurosporine lead to dephosphorylation of Drp1 at Ser 637, they also activate the tumour suppressor protein p53 and promote its nuclear translocation (Cribbs and Strack, 2007; Nicolier et al., 2009; Uberti et al., 1999). It has recently been shown that p53 can act as a transcription factor for Drp1 and increase the cytosolic levels of Drp1 (Li et al., 2010). Ubiquitination of Drp1 by the

mitochondrial ubiquitin E3 ligase MITOL/MARCH5 enhances the fission inducing activity of Drp1 and loss of MARCH5 leads to elongated and interconnected mitochondria. Interestingly, loss of MARCH5 also results in increased stabilization of Mfn2, which is hypothesized to be a target as well, demonstrating that ubiquitination affect mitochondrial architecture by targeting both fission and fusion regulators (Karbowski et al., 2007; Park et al., 2010). Similar to ubiquitination, studies have shown that SUMOylation can regulate fission as well. The mitochondria anchored protein ligase MAPL is an E3 ligase that SUMOylates Drp1 amongst other mitochondrial proteins. While overexpression of MAPL promotes mitochondrial fragmentation it is not deemed to be an essential necessity for fission induction (Braschi et al., 2009; Neuspiel et al., 2008). Recently, it has come to light the degradation of the deSUMOylating enzyme SENP3 during low oxygen/glucose conditions lead to stabilization of SUMOylated Drp1 protomers, preventing their translocation to the mitochondria and preventing mitochondrial fission, cytochrome *c* release and cell death (Guo et al., 2013a). Another deSUMOylating enzyme, SENP5, functions to deSUMOylate Drp1 as well but its effect appears to be radically conflicting. During G2/M phase of the cell cycle SENP5 deSUMOylates Drp1 on the mitochondrial membrane, promoting fission while overexpression of SENP5 prevents SUMO1-induced mitochondrial fragmentation by downregulating Drp1 (Zunino et al., 2009; Zunino et al., 2007). The effect of SUMOylated on Drp1 is a subject of debate since mono-SUMOylated Drp1 appears to be more stable and has an increased retention on the mitochondrial outer membrane. Finally, during staurosporine-induced apoptosis, which necessitates mitochondrial fragmentation, SUMOylation appears to be increased (Wasiak et al., 2007). In light of the conflicting evidences regarding the effect of SUMOylation on Drp1, it is speculated that the effect of Drp1 SUMOylation may be, context (other post-translational modification, location) and time (Cell cycle, Drp1 activity cycle) dependent.

1.3.5 Mitochondria in Infection

Given the plethora of interactions that regulate and are reregulated by the mitochondrial network, it is not hard to extrapolate the severity of the dysfunction that can arise as a result of impaired mitochondrial function and dynamics. Studies on the impact of mitochondria on the cellular processes has made it evident that any disruption in the mitochondrial biogenesis, replication and the pathways that control the same leads to fatal consequences with respect to cellular bioenergetics,

metabolism and immune status. Over the years several diverse and complex pathological conditions have been identified that result from mutations in the mitochondrial DNA, deletion or mutations in the nuclear genes encoding mitochondrial components, defects in the electron transport chain and finally, faulty regulation of mitochondrial dynamics (Angelini et al., 2009; Delettre et al., 2000; Dimauro and Davidzon, 2005; Jahani-Asl et al., 2015; Parker et al., 1994; Zuchner et al., 2004). Of recent, the role of mitochondria and mitochondrial dynamics in bacterial and viral infection has come in to focus (Castanier et al., 2010; Koterski et al., 2005). Mitochondrial ROS production (mtROS), signalling and metabolic control is indispensible for several essential immune responses, which include activation of the innate immune systems and the control of macrophage polarization and function (Haschemi et al., 2012; Mills and O'Neill, 2016; Seth et al., 2005; Tan et al., 2016). Mitochondrial dynamics and mtROS are essential for T-cell activation, production of cytokines and signalling via the T-cell receptors (Buck et al., 2016; Gill and Levine, 2013; Sena et al., 2013). Mitochondrial signalling and interactions have also been shown to be paramount for early response to viral infection and constitute an important part of the cellular antiviral response pathway (Castanier et al., 2010; Koshiba et al., 2011). Owing to the intimate connection that exists between the mitochondria and the cell death pathways, it has come to light that bacterial infection may in fact exploit this relationship for its own benefit (Galmiche et al., 2000; Muller et al., 2000; Nougayrede and Donnenberg, 2004). Considering the endosymbiotic nature of mitochondria, it is not hard to imagine that bacterial proteins might utilize mechanism similar to those used by mitochondrial proteins for targeting (Gray, 1982; Margulis, 1970). Studies shave shown that *Neisseria, H. pylori* and *E. coli* directly target certain effector proteins to the inner and outer membrane and the matrix of the host cell's mitochondria using the mitochondrial translocase complex (Jiang et al., 2011; Palframan et al., 2012; Papatheodorou et al., 2006). Finally, with the increased focus on the host-pathogen interaction, evidences regarding bacterial modulation of mitochondrial dynamics and architecture have surfaced. Transient calcium influx mediated mitochondrial fragmentation is observed upon *L. monocytogenes* infection. It is speculated that such fragmentation might be due to calcium-mediated activation of Drp1 and might serve to hinder metabolic processes required for the establishment of the infection (Stavru et al., 2011). Shigella infection induces apoptotic or necrotic cell death arising from the effect of the infection on the mitochondrial outer or inner membrane and has shown to induce mitochondrial fragmentation. Inhibition of Drp1 activity prevented such fragmentation and Drp1-assisted mitochondrial fragmentation is thought to assist in non-apoptotic cell death

induced by Shigella infection (Lum and Morona, 2014). Interestingly, a recent study shows that mitochondria assists the cytoskeletal protein septin in forming cages around Shigella to enhance their targeting by autophagosome (Sirianni et al., 2016). Previously, it has been shown that septins also assist in mitochondrial fission during cytokinesis while Drp1 interacts with septins to promote mitochondrial fragmentation (Glotzer, 2005). The study goes on to show that Shigella, in order to escape septin-mediated autophagosomal targeting, induces Drp1-mediated mitochondrial fragmentation since septins can only associate with the branched mitochondrial network (Sirianni et al., 2016). Finally, the vacuolating cytotoxin A (VacA) produced by the human gastric pathogen Helicobacter pylori has also shown to promote mitochondrial fragmentation via Drp1. In this case, VacA promotes Drp1 translocation to the mitochondria and, by a mechanism not fully understood, activates the GTPase function of Drp1 leading to mitochondrial fission and eventually, to apoptosis (Jain et al., 2011).

1.4 Aim of the Work

Previous studies have shown that *C. trachomatis* can effectively prevent initiation of apoptosis and, simultaneously, induce ROS production in cells to enhance infection. During ROS mediated stress the mitochondrial reticulum disintegrates into multiple punctiform particles indicating mitochondrial fragmentation. Formation of fission rings by the Dynamin-related protein, Drp1 on the surface of the mitochondrial constriction sites is essential for fragmentation. It has been shown that mitochondrial fission precedes apoptosis and inhibition of fission by Drp1 depletion or prevention of Drp1 translocation delays apoptosis by hindering caspases activation and cytochrome c release. The tumor suppressor protein p53 positively regulates Drp1, and is up regulated during stress-induced apoptosis. Of recent, many microRNA have been demonstrated to participate actively in regulation of apoptosis and mitochondrial dynamics.

Using a miRNA deep sequencing approach this work aims to show that *Chlamydia* infection differentially regulates several host miRNAs that are involved in apoptotic signalling. This work will focus on one such miRNA, miR-30c which targets the p53 mRNA and will attempt to illustrate that *Chlamydia* induced upregulation of miR-30c reduces Drp1 abundance by downregulating p53 expression. By studying the effects of artificial modulation of miR-30c, p53 and Drp1 on chlamydial growth we will attempt to corroborate these findings. Furthermore, super-resolution microscopy and Drp1 particle analysis will be utilized to ascertain the effect on *Chlamydia* induced depletion of Drp1 on the mitochondrial architecture and dynamics. Lastly, the effect of *Chlamydia* mediated changes on the mitochondria will be correlated to the mitochondrial fission induced changes in ATP concentrations and the effect of targeted ATP depletion on *Chlamydia* growth will be investigated.

In essence, this study will explore the ability of *Chlamydia* to modulate the host mitochondrial architecture and dynamics via altering the host miRNA expression profile to facilitate its own development.

Chapter 2. Results

2.1 Influence of *Chlamydia* infection on the host miRNA expression profile

The modulation of the host miRNA profile by bacterial pathogens, while largely a novel field, is the subject of much interest. Several detailed studies have been conducted on the differential regulation of host miRNAs by *Helicobacter pylori, Mycobacterium tuberculosis* and *Salmonella* (Chang et al., 2015; Maudet et al., 2014; Ren et al., 2015). However, the regulation of host miRNAs by intracellular pathogens is not well defined. Studies have been conducted with regards to *Listeria*, *Leishmania* and *Coxiella* but very few studies have focused on chlamydial infections in human cells (Igietseme et al., 2015; Izar et al., 2012; Millar et al., 2015; Yeruva et al., 2014). Considering the significant impact that chlamydial infections have on the host signalling pathways it is fair to assume that the involvement of miRNA in the modulation of these pathways within an infected cell is a fair possibility. Hence, we focused on deciphering a miRNA expression profile in HUVECs post *Chlamydia* infection.

2.1.1 *Chlamydia* infected HUVECs exhibit an altered miRNA expression profile

To determine the effect of Chlamydia infection on the host miRNA expression profile, a high throughput approach was employed to sequence the miRNOME of Chlamydia infected HUVECs (human umbilical endothelial cells). Upon analysis of deep sequencing data and comparison to non-infected control samples it was observed that the infected cells exhibit differential regulation of several miRNAs (Figure 2.1.1A and 2.1.1B). These changes are apparent after 12 and 24 hours of infection and, in case of specific miRNAs, were validated by Northern blot and qRT-PCR (Figure 2.1.2A and 2.1.2B).

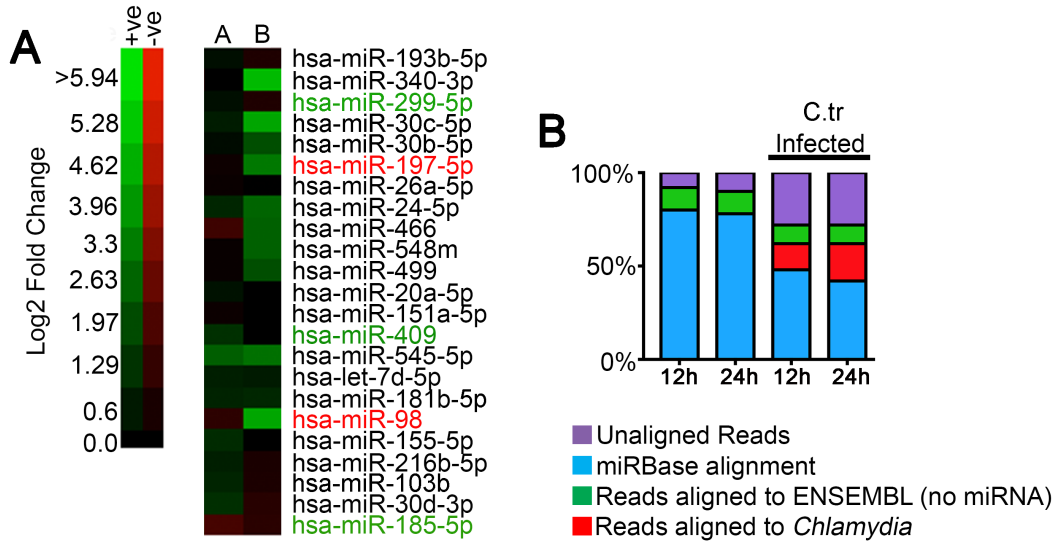

A: 12h C.tr infected normalised to 12h non-infected HUVECs
B: 24h C.tr infected normalised to 24h non-infected HUVECs

Figure 2.1.1: *Chlamydia* infected cells exhibit an altered miRNA expression profile.
(2.1.1A) A representative heat map was generated from the miRNA deep sequencing of control and Chlamydia infected HUVECs at different time points. The miRNA previously validated as pro-apoptotic are labelled in green while the ones, which exhibit anti-apoptotic tendencies, are labelled in red. (2.1.1B) The bar graph depicts the read distribution of the miRNA deep sequencing data. The mature miRNAs were mapped to the miRNA repository miRBase while the human and chlamydial genes were mapped against complete human and chlamydial genomes (Adapted from Chowdhury et al. 2017; JCB).

2.1.2 *Chlamydia* infection alters the expression of miRNAs involved in apoptotic signalling.

Deep sequencing results and analysis of specific miRNAs using DIANA-miRPath v2.0 web-server revealed that the miRNAs whose expressions were altered upon Chlamydia infection are also implicated to have roles in viral carcinogenesis, cell cycle, PI3K-AKT, p53 and cancer signalling pathways (Figure 2.1.2C). Specifically, several miRNAs were identified in the deep sequencing screen, which have been experimentally shown to be involved in cell death regulation and carcinogenesis (Fiori et al., 2014; Formosa et al., 2014; Li et al., 2012a; Wang et al., 2014; Wang et al., 2011b). The changes in the expression of these pro- or anti-apoptotic miRNAs were validated by qRT-PCR (Figure 2.1.1A and 2.1.2A).

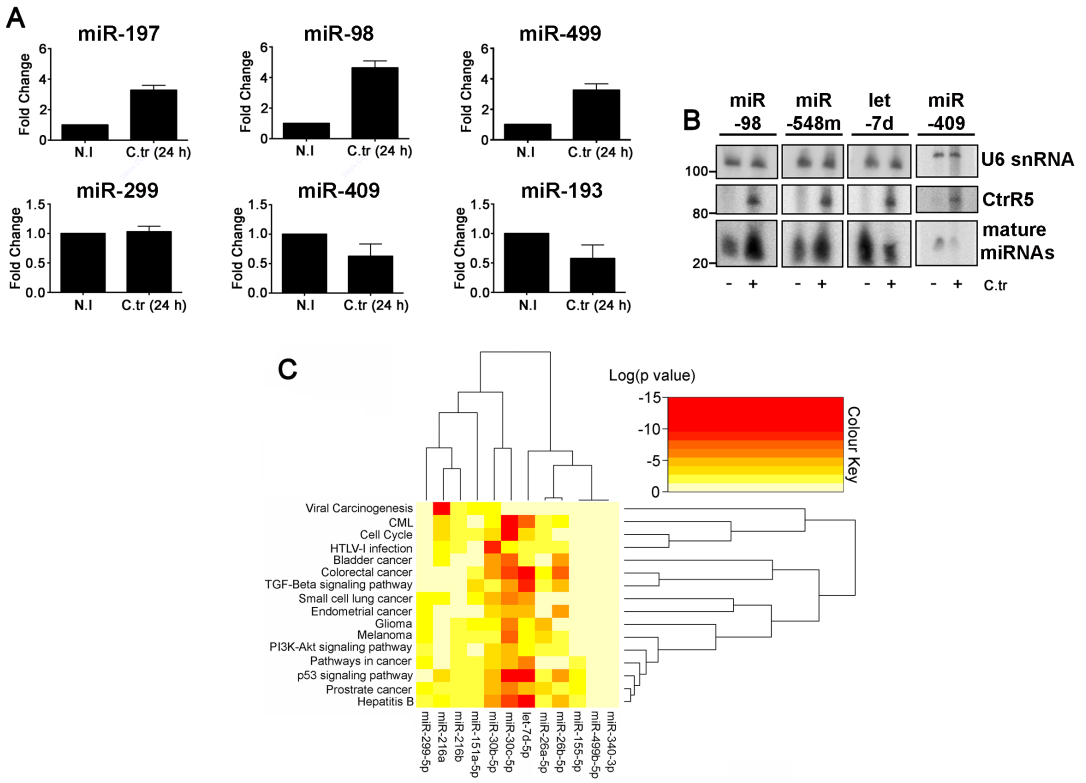

Figure 2.1.2: Validation and analysis of the *Chlamydia* induced changes in the miRNA profile. Several miRNAs were chosen in accordance to their relevance to cell death (miR-299, miR-409 and miR-193) or survival (miR-197, miR-98 and miR-499) pathways as depicted in previous studies. The change in expression of these miRNAs after 24 hours of *Chlamydia* infection in HUVECs, as depicted in the RNA sequencing results, was validated using qRT-PCR (2.1.2A) and northern blot (2.1.2B). All qRT-PCR results were normalized to non-infected HUVECs grown in culture for 24 hours. U6 snRNA was used as endogenous control for qRT-PCR. The northern blots were probed with oligo probes against specific miRNAs and U6 snRNA was used as endogenous control. The chlamydial small RNA CtrR5 was used as marker for chlamydial infection. (2.1.2C) A binary heat map was generated using the DIANA-miRPath v2.0 web-server representing the involvement of the depicted miRNA in the pathways listed on the left hand side column. The dendrogram clusters miRNAs on the basis of the pathways they affect. All pathways affected significantly are represented in deeper colours. All data represent mean ± S.D. Asterisks denote significance by unpaired *t* test: *, P < 0.05; **, P < 0.01; ***, P < 0.001 (Adapted from Chowdhury et al. 2017; JCB).

2.1.3 *Chlamydia* infection alters the expression of miR-30c in three different primary cell types.

Amongst the various differentially regulated miRNAs identified in the deep sequencing screen, one that held particular relevance to chlamydial pathogenesis was hsa-miR-30c-5p (hereafter referred to as miR-30c; Figure 2.1.3A). It had been previously shown that the miR-30 family (-a through -e) specifically targets the p53 mRNA and reduces its expression (Li et al., 2010). This observation is concordant with the previous observations of *Chlamydia*-induced downregulation of p53 (Gonzalez et al., 2014; Siegl et al., 2014). We validated the upregulation of miR-30c upon *Chlamydia* infection in HUVECs and primary epithelial cells of human fallopian

tube fimbriae (hFIMBs) by qRT-PCR and Northern blot (Figure 2.1.3B, 2.1.3C and 2.1.3D). To gauge the effect of miR-30c upon chlamydial growth and regulation we artificially modulated the expression of miR-30c using miRNA mimics, inhibitors and an anhydrous tetracycline (AHT) induced miR-30c sponge (Figure 2.1.4A and 2.1.4B). While the artificial over expression enhances chlamydia growth, inhibitor and sponge-mediated depletion of miR-30c hindered chlamydial infection and production of infectious progenies (Figure 2.1.4C and 2.1.4D).

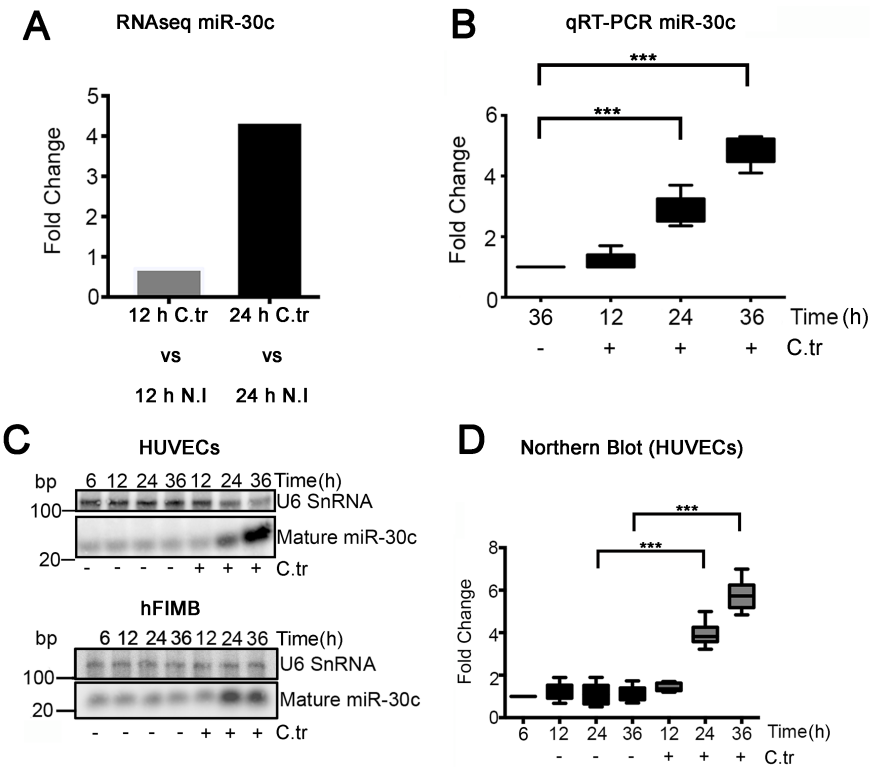

Figure 2.1.3: Regulation of miR-30c upon *Chlamydia* infection
(2.1.3A) The bar graph represents the changes in miR-30c expression upon Chlamydia infection after 12 and 24 hours of infection (normalized to uninfected HUVECs grown in culture for 12 and 24 hours) as obtained from the miRNA deep sequencing data. (2.1.3B)The box-plot represents the chlamydia-induced change in miR-30c expression levels was validated by qRT-PCR in HUVECs Cells were infected for 12, 24 and 36 hours and fold changes were normalised to miR-30c expression of non-infected cells at 36 hours. Fold change with qRT-PCR for HUVECs (± SD) at 24 hours = 2.96 ± 0.47 and 36 hours = 4.87 ± 0.46 (*n=6*). (2.1.3C) The chlamydia-induced change in miR-30c expression levels was validated by northern blots of total RNA from HUVECS and hFIMB cells. (2.1.3D) The box-plot represents a densitometric quantification of the change in miR-30c expression levels in HUVECs. Fold change with Northern blot for HUVECs (± SD) at 24 hours = 3.9 ± 0.58 and at 36 hours = 5.76 ± 0.72 (*n=5*). Fold changes were normalised to miR-30c expression in non-infected cells at 12, 12 and 36 hours respectively (*n=6* experiments). All data represent mean ± S.D. Asterisks denote significance by unpaired *t* test: *, P < 0.05; **, P < 0.01; ***, P < 0.001 (Adapted from Chowdhury et al. 2017; JCB).

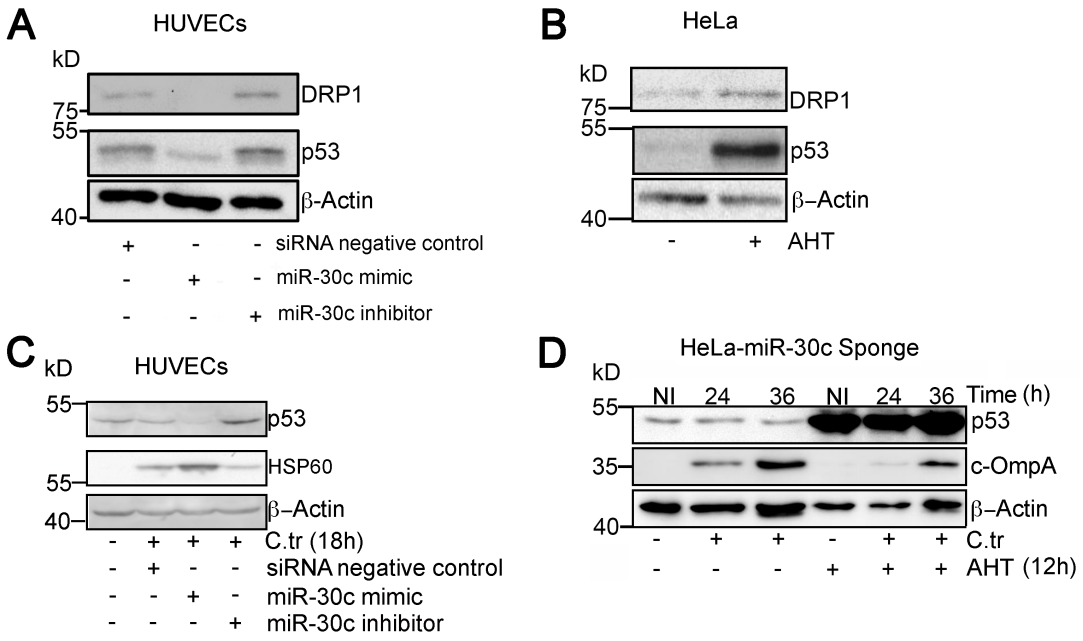

Figure 2.1.4: miR-30c alters p53 and Drp1 expression and affects *Chlamydia* infection.
(2.1.4A) Immunoblot of HUVECs transfected with miR-30c mimic and inhibitor. The blots were probed with antibodies against p53, Drp1 and Beta Actin. AllStar negative siRNA transfected HUVECs were used as a control sample. (2.1.4B) Immunoblot of HeLa cells expressing the miR-30c sponge. The expression of the sponge and its ability to specifically target miR-30c was determined by checking for an increase in the levels of p53, and Drp1 following AHT treatment. (2.1.4C) The immunoblot represents the effect of mimic and inhibitor mediated modulation of miR-30c on chlamydial growth. HUVECs were transfected with either AllStar negative siRNA, miR-30c mimic or inhibitor for 24 hours followed by Chlamydia infection for 18 hours. (2.1.4C) The immunoblot represents the effect of AHT mediated induction of miR-30c sponge on chlamydial growth. HeLa cells, lentivirally transduced with miR-30c sponge pLVTHM constructs were induced for 24 hours with AHT and infected with Chlamydia for indicated time spans. The blots were probed for p53 expression, chlamydial HSP60 (cHSP60) or chlamydia outer membrane protein A (cOMPA) and Beta Actin (Adapted from Chowdhury et al. 2017; JCB).

2.1.4 Artificial modulation of miR-30c affects p53 expression and mitochondrial morphology

It has been previously shown that alteration in the levels of miR-30 family of miRNAs in cardiomyocytes leads to changes in p53 expression. The p53 mRNA is targeted by all the members of miR-30 family by the virtue of a miR-30 specific binding site on its 3' UTR (Li et al., 2010). We show that this effect is conserved not only in HUVECs but also in HeLa cells since targeted downregulation of miR-30c using miRNA sponges (in HeLa) and inhibitors (in HUVECs) leads to a significant upregulation of p53 (Figure 2.1.4A and 2.1.4B). Additionally, confocal laser scanning microscopy (CLSM) of HUVECs and HeLa cells shows that miR-30c depletion induces a massive fragmentation of the mitochondrial reticulate network while overexpression of miR-30c in HUVECs promotes the formation of a fused mitochondrial architecture (Figure

2.1.5A, 2.1.5B, 2.1.5C 2.1.6A and 2.1.6B). Interestingly, the both these forms of the mitochondrial network, fragmented and fused, can be replicated by overexpression and siRNA mediated downregulation of the mitochondrial fission regulator Drp1, which, incidentally, is also upregulated upon inhibition of miR-30c (Figure 2.1.4A, 2.1.4B, 2.1.6A and 2.1.6B).

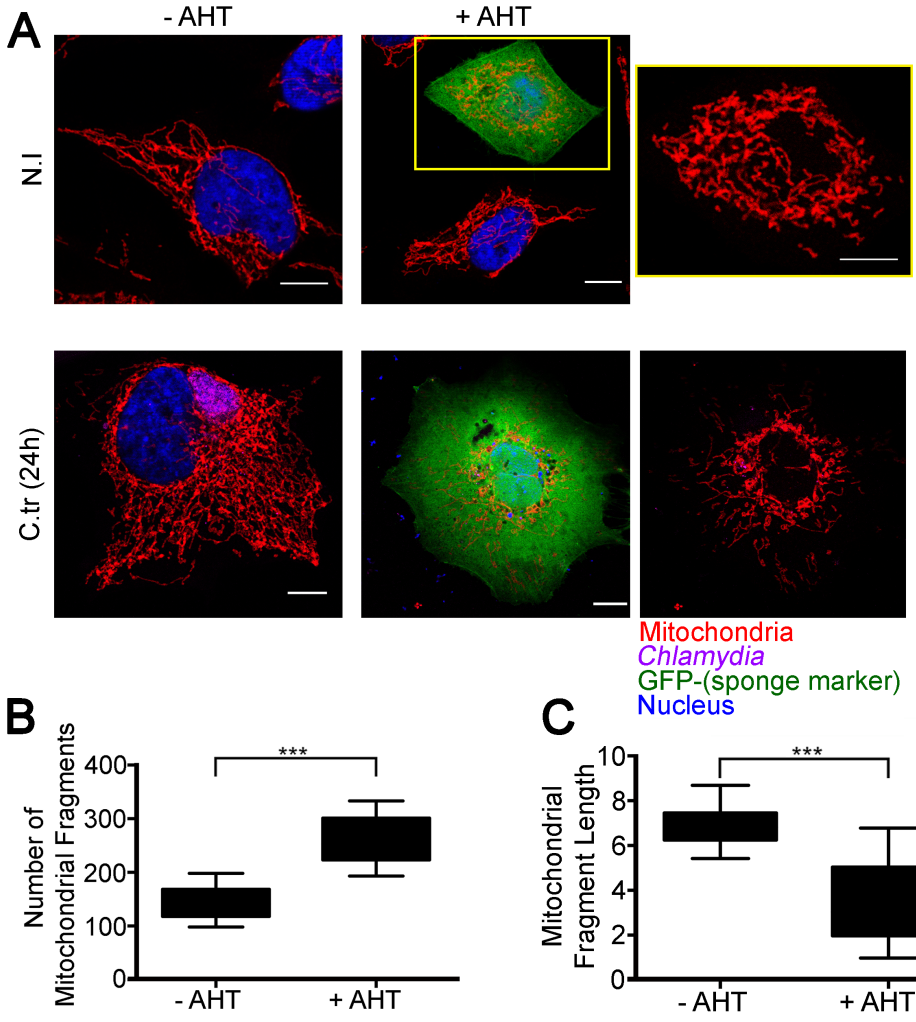

Figure 2.1.5: miR-30c modulation affects mitochondrial morphology
(2.1.5A) Confocal micrographs of AHT induced and non-induced HeLa cells prior to and post infection with Chlamydia for 24 hours. The expression of the sponge is indicated by the GFP signal (green). The mitochondrial network is labelled with MitoTracker deep red FM (Red) and chlamydial presence is labelled with cHSP60 (Cy3, magenta). The yellow box illustrates a zoomed picture of the fragmented mitochondrial network in an AHT induced, sponge expressing HeLa cell. Bars indicate 10µm. (2.1.5B and 2.1.5C) The box-plots represent quantification of individual mitochondrial fragment abundance and the length distribution of the fragments. in non-induced and AHT-induced miR-30c sponge cells. (*n=6*; ~20 cells were analyzed from random selection of ~10 ROI in each sample). All data represent mean ± S.D. Asterisks denote significance by unpaired *t* test: *, P < 0.05; **, P < 0.01; ***, P < 0.001 (Adapted from Chowdhury et al. 2017; JCB).

It has been previously shown that Drp1 is transcriptionally regulated by p53 since induction of oxidative stress induces p53 binding to Drp1 promoter sites thus enhancing Drp1 transcription and promoting mitochondrial fragmentation (Li et al., 2010; Merlo et al., 2014; Ottolini et al., 2013). Our experiments here demonstrate that artificial modulation of miR-30c not only regulates p53 expression in HUVECs and HeLa cells but also modifies the mitochondrial architecture.

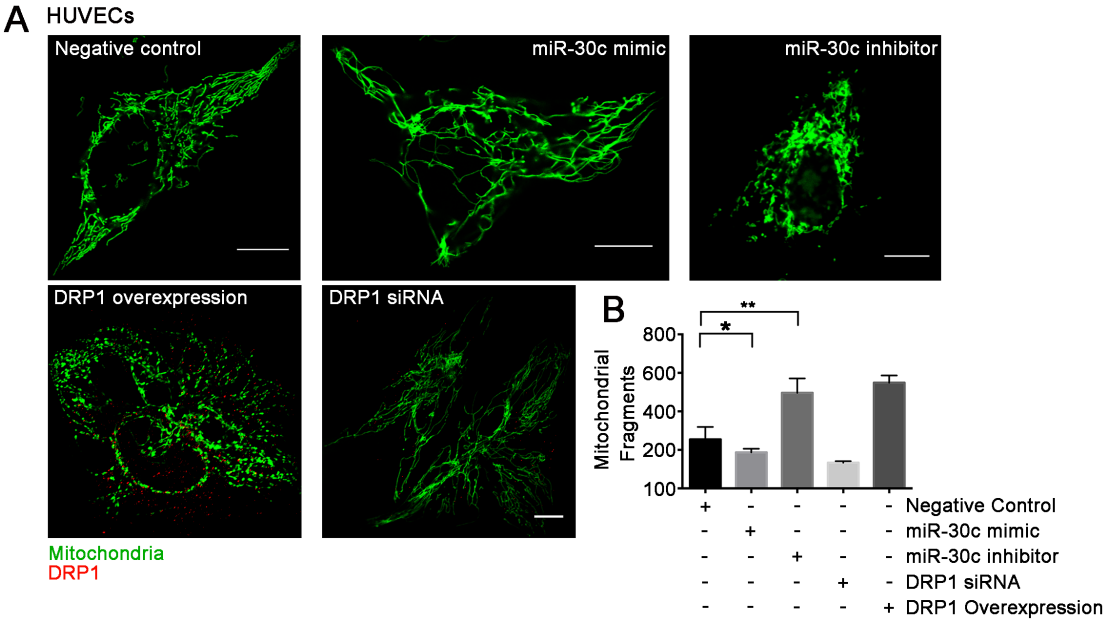

Figure 2.1.6 miR-30c modulation resembles Drp1 induced changes in the mitochondrial morphology
(2.1.6A) Confocal micrographs HUVECs stabling expressing mitochondrially targeted GFP (green), transfected with AllStar negative siRNA, miR-30c mimic and inhibitor, pcDNA-Drp1 overexpression vector and Drp1 siRNA. HUVECs transfected with pcDNA-Drp1 overexpression vector and Drp1 siRNA were stained with an antibody against Drp1 (Atto 647; red). (2.1.6B) The box-plot represents quantification of mitochondrial fragment abundance in all the above samples. (*n=5;* ~20 cells were analyzed per experiment). All data represent mean ± S.D. Asterisks denote significance by unpaired *t* test: *, P < 0.05; **, P < 0.01; ***, P < 0.001 (Adapted from Chowdhury et al. 2017; JCB).

2.1.5 *Chlamydia* infection induces p53 depletion in a miR-30c dependent manner

Our lab has previously demonstrated that chlamydial infection is facilitated by the downregulation of p53 and is affected by the p53-mediated downregulation of the pentose phosphate pathway. Siegl et al. also demonstrated that chlamydial infection effects a proteasomal degradation of p53 (Siegl et al., 2014). We now show that chlamydial infection also inhibits p53 abundance by inhibiting the expression of p53 in a miR-30c dependent manner. To this effect we performed reporter assays using a GFP reporter construct fused with wild-type and mutant p53 3' UTRs (Figure 2.1.7A). The mutant p53 3' UTR has a defective miR-30c binding site as described in Figure

7C. The immunoblots demonstrate that while the HUVECs transfected with the reporter constructs carrying the GFP fused to the wild type p53 3' UTR respond to *Chlamydia* infection by reducing GFP expression, this effect is absent in the reporter constructs carrying the GFP fused to the mutant p53 3' UTR (Figure 2.1.7B, 2.1.7C and 2.1.7D). This data clearly illustrates that amongst other mechanisms, Chlamydia also downregulates p53 expression by upregulation of miR-30c.

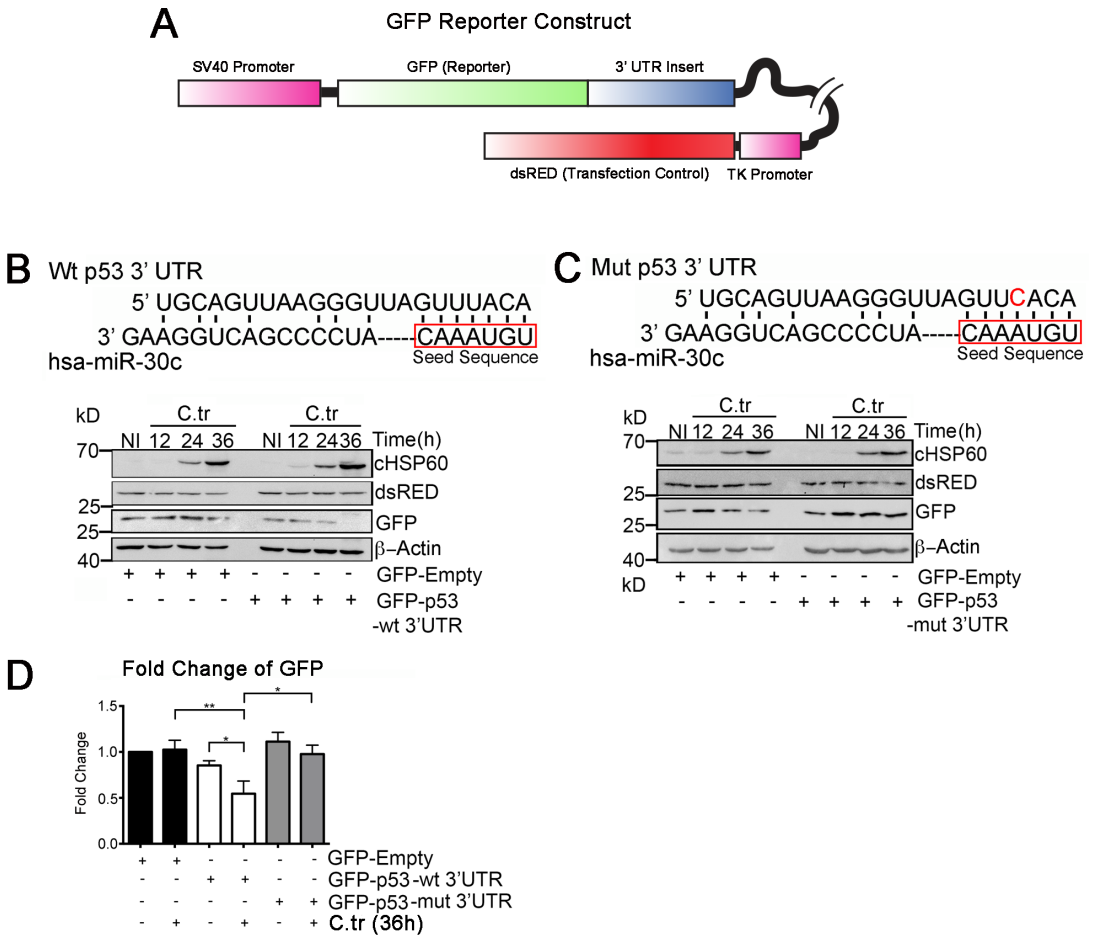

Figure 2.1.7 p53 depletion is effected by miR-30c elevation upon *Chlamydia* infection
(2.1.7A) Schematic diagram of the p53 3' UTR-GFP reporter construct. The vector was prepared using a psiCHECK-2 backbone by replacing the humanized *Renilla* luciferase with GFP and the humanized Firefly luciferase with dsRED. The GFP is spliced with p53 3' UTR and under control of the CMV promoter while the dsRED (under control of HSV-TK promoter) acts as the transfection control. (2.1.7B) The schematic represents the miR-30c seed sequence (red box) and its associated binding site on the p53 3'UTR. The immunoblot illustrates the effect of chlamydia infection on the GFP levels in HUVECs transfected with the p53 3' (wild type) UTR-GFP vector. (2.1.7C) The schematic represents the miR-30c seed sequence (red box) and its associated binding site on the mutated p53 3'UTR (mutation indicated with red 'C'). The immunoblot illustrates the effect of chlamydia infection on the GFP levels in HUVECs transfected with the p53 3' (mutated) UTR-GFP vector. The blots were probed with antibodies against GFP, cHSP60, dsRED and Beta Actin. (2.1.7C) The graph represents quantification of GFP expression in Chlamydia (36 hours) infected HUVECs transfected with the p53 3' (wild type) UTR-GFP vector or p53 3' (mutated) UTR-GFP vector. The expression of the chimeric GFP was normalized to the expression of the dsRED transfection control ($n=3$). All data represent mean ± S.D. Asterisks denote significance by Student's *t* test: *, $P < 0.05$; **, $P < 0.01$; ***, $P < 0.001$ (Adapted from Chowdhury et al. 2017; JCB).

2.2 *Chlamydia* requires a reduction of Drp1 expression and function to facilitate infection.

The importance of mitochondrial fusion and fission with respect to the metabolic health and the general cellular homeostasis has been demonstrated by a number of elegant studies over the last few years (Gomes et al., 2011; Yamamori et al., 2015). The subtle balance between fusion and fission events effects the over all architecture of the cellular mitochondrial network and is governed by a host of cytoplasmic and mitochondrial proteins (van der Bliek et al., 2013; Westermann, 2008). Drp1 is the major mitochondrial fission regulator, which upon activation translocates from the cytoplasm to the mitochondrial surface to aid in the fission process (Smirnova et al., 2001). In the recent years, bacterial interaction with the host mitochondrial dynamics has gained focus. Several pathogens have been shown to induce mitochondrial fission via modulation of Drp1 (Jain et al., 2011; Lum and Morona, 2014; Stavru et al., 2013). Given the dependence of *Chlamydia* on the host metabolism and the effect of miR-30c induced depletion of Drp1 in HUVECs, we investigated the effect of Chlamydia infection on Drp1 expression and mitochondrial localization.

2.2.1 *Chlamydia* infection leads to a loss of Drp1 expression

To deduce the effect of *Chlamydia* infection on Drp1 expression we infected several different cell lines and checked for expression of Drp1 mRNA after different durations of infection. All three primary cell lines, HUVECs, hFIMBs and Human foreskin fibroblast cells (HFF) showed a consistent downregulation of the Drp1 mRNA upon 24 and 36 hours of *Chlamydia* infection (Figure 2.2.1A). This was also reflected in the protein levels of Drp1 as illustrated by the immunoblots (Figure 2.2.1B and 2.2.1C). This result corroborates our previous findings of miR-30c upregulation and the resultant p53 depletion. In addition to the *Chlamydia*-mediated downregulation of Drp1 we were also able to demonstrate that, while artificially enforced overexpression of Drp1 significantly hinders chlamydial infection progression, siRNA mediated downregulation of Drp1 promotes *Chlamydia* growth in both HUVECs and HeLa (Figure 2.2.1B, 2.2.2A and 2.2.2B). This effect is also reflected in the inability of *Chlamydia* particles to produce infectious progenies when grown in an Drp1 overexpression environment compared to control or Drp1-depleted cells (Figure 2.2.2C). Taking into account the fission inducing function of Drp1 we overexpressed wild type Drp1 in HUVECs and checked for mitochondrial fragmentation. Drp1

overexpression, apart from hindering Chlamydia infection, also caused severe mitochondrial fragmentation in HUVECs (Figure 2.2.3A, 2.2.3B and 2.2.3C). Furthermore, we wanted to see if it was possible for Drp1 to affect *Chlamydia* growth and development in absence of p53. To this effect we overexpressed Drp1 In the p53 null lung cancer cell line H1299. It was observed that over expression of wild-type DRP in these cells prior to *Chlamydia* infection completely abrogated chlamydial infection and resulted in extensive fragmentation of the mitochondrial architecture (Figure 2.2.4A, 2.2.4B, 2.2.5A and 2.2.5B).

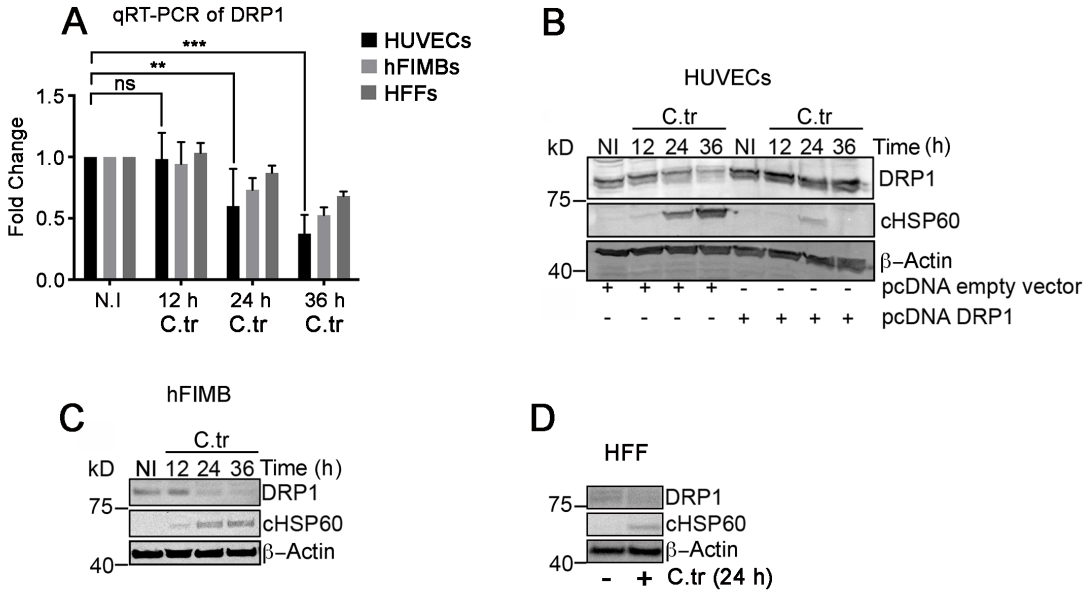

Figure 2.2.1 *Chlamydia* infection promotes a loss of Drp1 expression
(2.2.1A) The graph represents the quantification of qRTP-PCR for Drp1 mRNA levels in non-infected control and *Chlamydia* infected HUVECs, hFIMBs and HFF cells for 12, 24 and 36 hours. The fold change of Drp1 in HUVECs at 24 hours = 0.6 ± 0.30 and 36 hours = 0.325 ± 0.10 (*n=6*). (2.2.1B) The immunoblot represents the effect of *Chlamydia* growth on Drp1 protein levels in HUVECs and effect of Drp1 over expression on *Chlamydia* growth. (2.2.1C-2.2.1D) Immunoblot of hFIMB and HFF cells infected with *Chlamydia* for indicated timespans. The blots were probed with antibodies against Drp1, cHSP60 and Beta Actin. All blots were repeated a minimum of three times. Data in 2.1A represents mean ± S.D. Asterisks denote significance by Student's *t* test: *, P < 0.05; **, P < 0.01; ***, P < 0.001 (Adapted from Chowdhury et al. 2017; JCB).

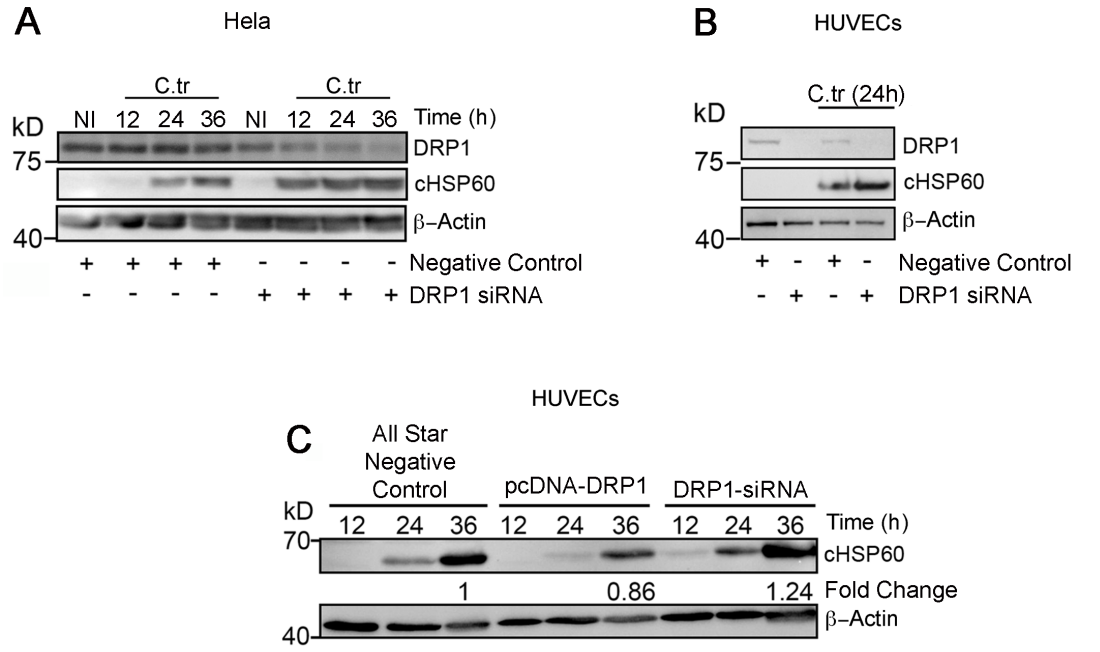

Figure 2.2.2 Artificial knockdown of Drp1 benefits *Chlamydia* growth
(2.2.2A) Immunoblot of HeLa transfected with siRNA Negative control or a siRNA pool against Drp1 followed by infection with C.tr for 12, 24 and 36 hours. (2.2.2B) Immunoblot of HUVECs transfected with siRNA Negative control or a siRNA against Drp1 followed by infection with C.tr for 24 hours. Blots were probed with antibodies against Drp1, cHSP60 and Beta Actin. (2.2.2C) Immunoblots depicting the infectivity assay performed with chlamydial lysates from 36 hours of infection in HUVECs transfected with siRNA negative control, pcDNA Drp1 overexpression vector or Drp1 siRNA pool. Blots were probed with antibodies against cHSP60 and Beta Actin. All blots were repeated a minimum of three times (Adapted from Chowdhury et al. 2017; JCB).

Curiously, this effect is not observed when the catalytically inactive form of Drp1 (Drp1-K38A) is expressed in H1299. The K38A mutation inhibits Drp1 function by preventing GTP binding and blocks mitochondrial fission (Smirnova et al., 2001; Song et al., 2011). Expression of this Drp1 mutant did not induce mitochondrial fragmentation in H1299 cells neither did it prevent the progression of chlamydial infection (Figure 2.2.4C, 2.2.4D, 2.2.5A and 2.2.5B). It can thus be interpreted that the mitochondrial fission inducing activity of Drp1 is inhibitory to chlamydial growth and loss of Drp1 is beneficial for a productive chlamydial infection cycle. Lastly, the inability of *Chlamydia* to flourish in the p53 null H1299 cell post wild type Drp1 over expression also demonstrates that functional Drp1 stabilization can inhibit *Chlamydia* development in absence of p53 and its regulatory effects on Drp1.

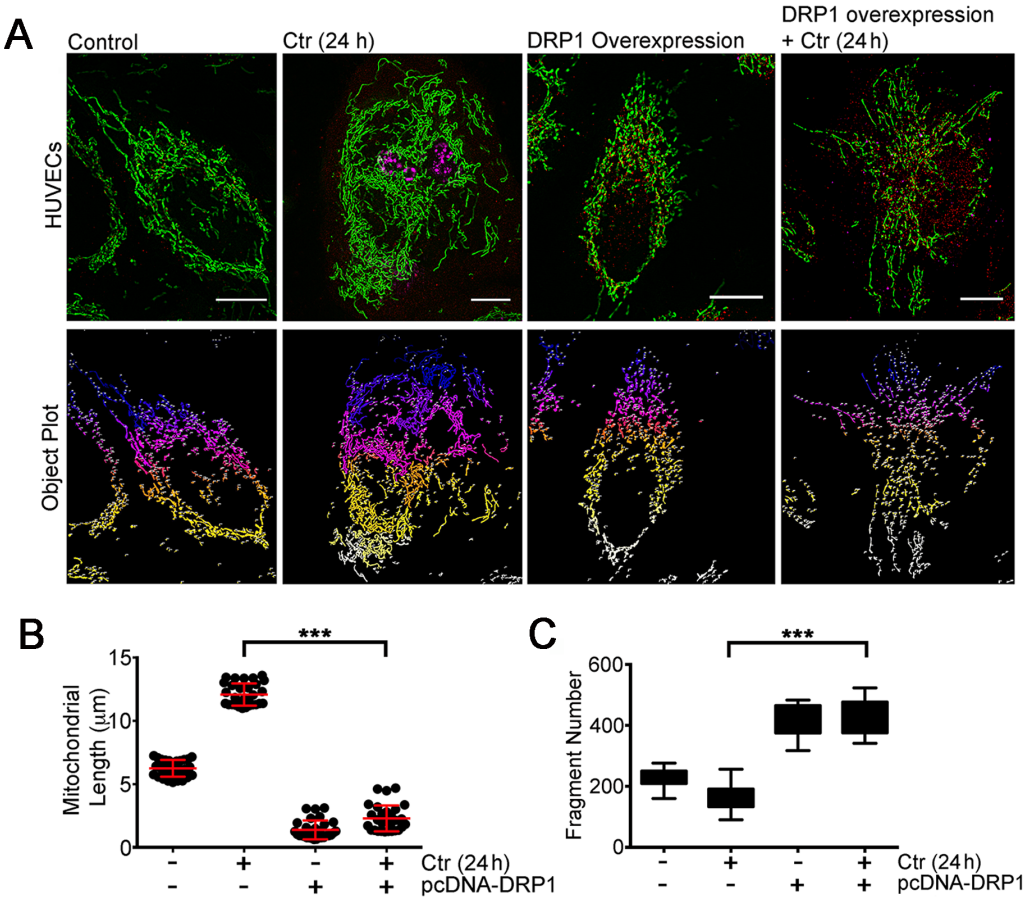

Figure 2.2.3 Enforced overexpression of Drp1 induces mitochondrial fragmentation in HUVECs. (2.2.3A) Structured illumination micrographs of control and non-infected mito-HUVECs (Green) transfected with Drp1 overexpression vector or vector control. The colorized panels illustrate the segmentations used for calculation of mitochondrial fragments. The samples were immunostained against Drp1 (Red) and cHSP60 (Magenta). Bars represent 10 µm. (2.2.3B) Graph represents the approximate length distribution of mitochondrial fragments in HUVECs infected with C.tr and transfected with Drp1 overexpression vector. The dots represent the mean mitochondrial fragment length of ~3 cells in an ROI chosen at random within samples. 30 such dots were plotted on the graph. Mean mitochondrial fragment length (µm; ± SD) in control = 6.25 ± 0.66, C.tr (24 h) = 12.08 ± 0.87, Drp1 overexpression = 1.39 ± 0.74, Drp1 overexpression + C.tr (24 h) = 2.3 ± 1.02. (2.2.3C) Graph represents the distribution of mitochondrial fragment count across HUVECs infected with C.tr and transfected with Drp1 over expression vector. Mean mitochondrial fragment count (± SD) in control = 240 ± 30.08, C.tr (24 h) = 133 ± 44.31, Drp1 overexpression = 388 ± 51.69 and Drp1 overexpression + C.tr (24h) = 399 ± 58.58 (*n=3* for panels 2.2.3B and 2.2.3C; ~30 cells were analyzed from random selection of ~10 ROI in each sample). All data represent mean ± S.D. Asterisks denote significance by one-way ANOVA followed by Tukey's multiple comparisons test for panel C and panel D: *, $P < 0.05$; **, $P < 0.01$; ***, $P < 0.001$; ns, non significant (Adapted from Chowdhury et al. 2017; JCB).

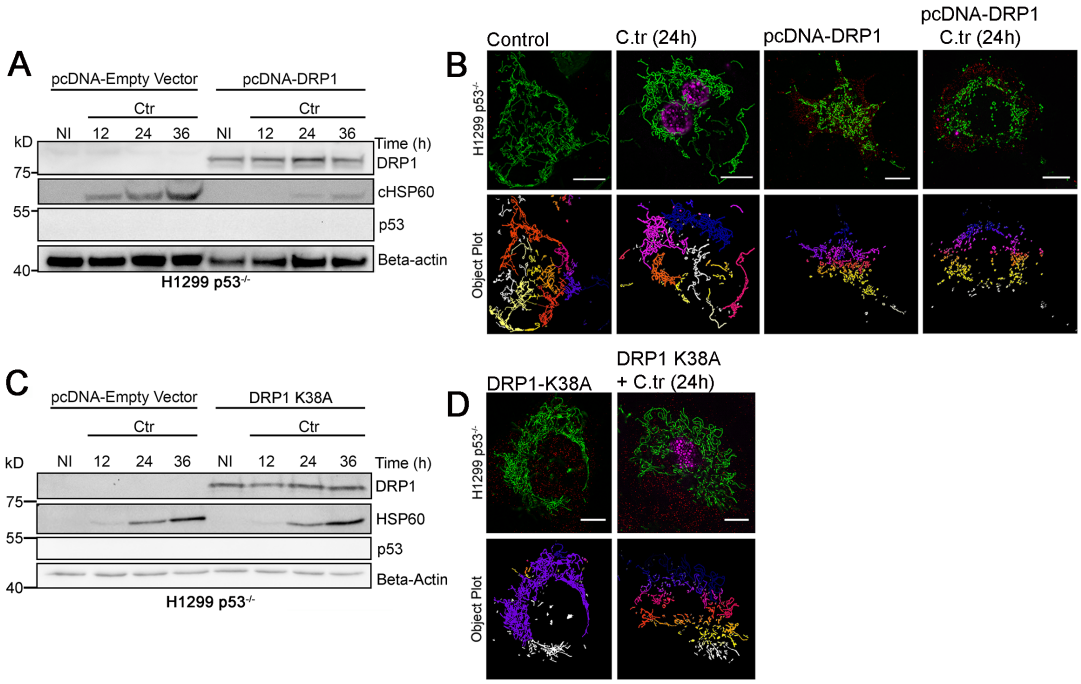

Figure 2.2.4 Enforced overexpression of functional Drp1 in H1299 p53$^{-/-}$ induces mitochondrial damage and hinders chlamydial growth.
(2.2.4A) Immunoblot represents the impact of Drp1 overexpression on *Chlamydia* growth in H1299 p53 null cells. The cells were transfected with vector control or pcDNA –Drp1 over expression vector followed by *Chlamydia* infection for indicated time spans. Blots were probed with antibodies against Drp1, cHSP60 and Beta Actin. (2.2.4B) Structured illumination micrographs of H1299 p53$^{-/-}$ cells expressing GFP targeted to mitochondria transfected with with vector control or pcDNA–Drp1 over expression vector followed by *Chlamydia* infection for 24 hours. The colorized panels illustrate the segmentations used for calculation of mitochondrial fragments. (2.2.4C-2.2.4D) Immunoblots and Structured illumination micrographs of H1299 p53 null cells transfected with vector control or the dominant negative mutant of Drp1 (Drp1$_{K38A}$) followed by *Chlamydia* infection for 24 hours. The samples for microscopy were immunostained against Drp1 (Red) and cHSP60 (Magenta). Bars represent 10 µm. All blots were repeated a minimum of three times (Adapted from Chowdhury et al. 2017; JCB).

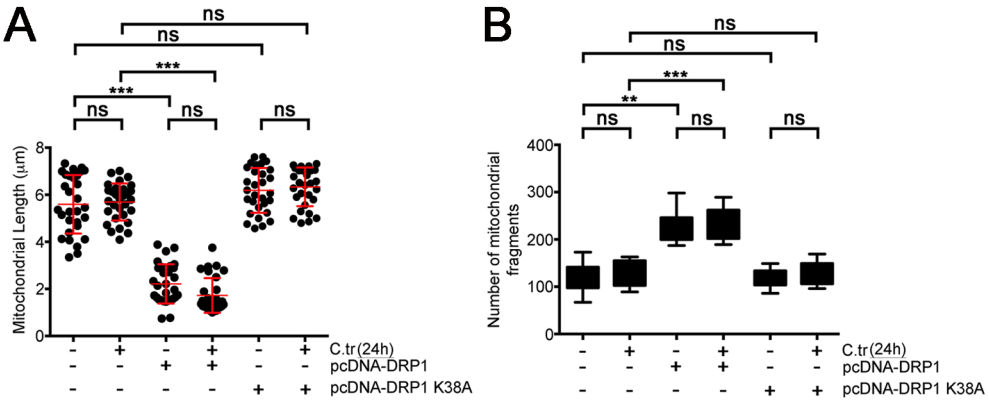

Figure 2.2.5 Functional Drp1 overexpression induces mitochondrial fission in absence of p53.
(2.2.4A) Analysis of mitochondrial fragment length distribution in H1299 p53$^{-/-}$ cells infected with C.tr and transfected with wild type Drp1 overexpression vector or dominant negative mutant of Drp1 (Drp1$_{K38A}$). The dots represent the mean mitochondrial fragment length of ~3 cells in an ROI chosen at random within samples. 30 such dots were plotted on the graph. Mean mitochondrial fragment length (µm; ± SD) in control = 5.59 ± 1.24, C.tr = 5.69 ± 0.78, Drp1 Overexpression = 2.21 ± 0.83, Drp1 overexpression + C.tr (24h) = 1.72 ± 0.73, Drp1 K38 overexpression = 6.18 ± 0.95 and Drp1 K38 overexpression +C.tr(24h) = 6.33 ± 0.82. (2.2.4B) Graph represents quantification of mitochondrial fragment count in

H1299 p53$^{-/-}$ cells infected with C.tr and transfected with wild type Drp1 overexpression vector or dominant negative mutant of Drp1 (Drp1$_{K38A}$). Mean mitochondrial fragment count (± SD) in control = 121.31 ± 27.56, C.tr = 130.56 ± 25.56, Drp1 Overexpression = 225.87 ± 29.63, Drp1 overexpression + C.tr (24h) = 233.43 ± 32.45, Drp1 K38 overexpression = 119.12 ± 32.45, Drp1 K38 Overexpression + C.tr infection (24h) = 128 ± 22.96 (*n*=3; ~30 cells were analyzed from random selection of ~10 ROI in each sample). All data represent mean ± S.D. Asterisks denote significance by one-way ANOVA followed by Tukey's multiple comparisons test for panel C and panel D: *, P < 0.05; **, P < 0.01; ***, P < 0.001; ns, non significant (Adapted from Chowdhury et al. 2017; JCB).

2.2.2 *Chlamydia* infected cells exhibit decreased Drp1 aggregate formation and mitochondrial colocalization.

Mammalian mitochondrial fission requires a ring-like assembly of Drp1 on mitochondrial constrictions sites ear-marked by the endoplasmic reticulum and the actin cytoskeleton (Ji et al., 2015; Korobova et al., 2013). The Drp1 ring has been shown to vary between 100 nm (constricted) to 360 nm (dilated) depending on whether they are the post cleavage form of the rings or have just assembled to initiate fission (Ingerman et al., 2005; Ji et al., 2015; Mears et al., 2011; Rosenbloom et al., 2014).

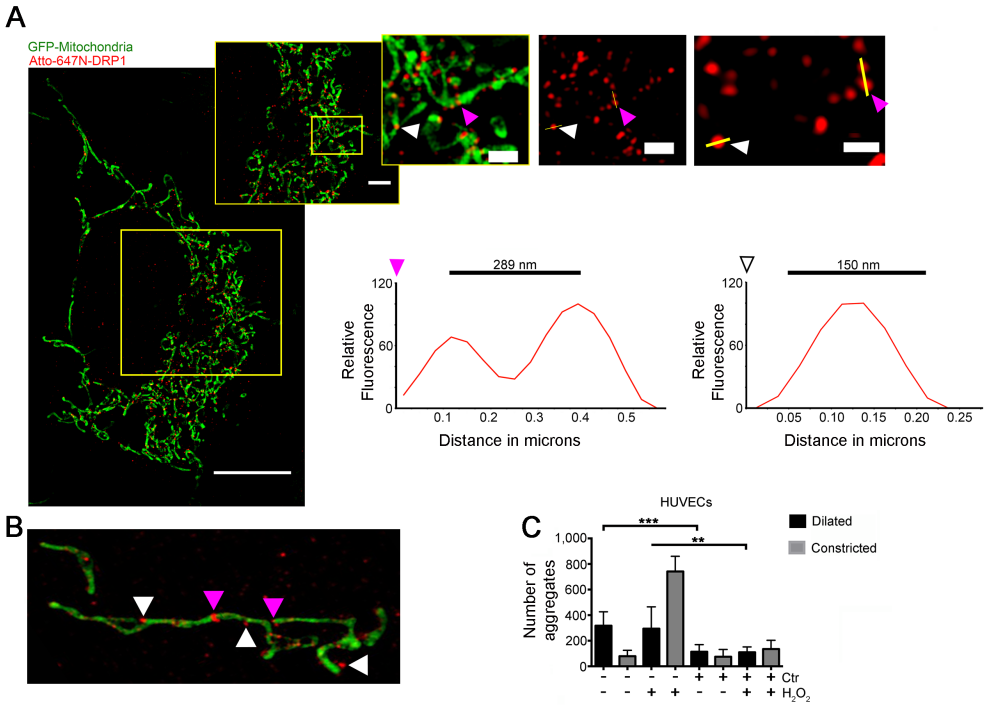

Figure 2.2.6 Identification and characterization of Drp1 aggregates in HUVECs
(2.2.6 A) Structured illumination micrograph of mito-HUVECs treated with H_2O_2 and immunostained against Drp1 (Red). The yellow enlargement boxes illustrate the two states of Drp1 ring-like aggregates in association with the mitochondrial fragments. The white arrow points towards a constricted ring in the process of cleaving the mitochondrial fragment. The pink arrow points at a dilated assembly just beginning its contraction. Bars represent 0.5 µm. The yellow cross section drawn across the aggregates provide intensity profiles illustrated in the line graphs. Diameter of a "dilated" ring is measured to be ~289nm ± 70nm (n=616) and the "constricted" ring is measured to be ~150nm ± 46nm (n=442) along the yellow bar drawn through the aggregates. (2.2.6 B) A representative structured illumination micrograph of a mitochondrial fragment decorated by several Drp1 assemblies along its length. (2.2.6C) The bar graph illustrates the distribution of constricted and dilated Drp1 aggregates in Chlamydia-

infected (24 hours) and uninfected HUVECs with or without 1 μM H_2O_2 (1 hour) treatment. ~6 (0.8 x 0.8 μm) sections were analyzed from each cell. 15 cells were chosen from a random selection of ~5 ROI in each sample *(n=10)*. Significance was calculated by Student's t test for panel L: *, P < 0.05; **, P < 0.01; ***, P < 0.001; ns, non significant (Adapted from Chowdhury et al. 2017; JCB).

Post assembly, Drp1 along with the Dynamin-2 GTPase protein cleaves the mitochondria in a GTP dependent manner (Lee et al., 2016). We performed structured illumination microscopy (SIM) of *Chlamydia* infected HUVECs stably expressing a mitochondrially targeted GFP to determine if *Chlamydia* infection affected the above mentioned assembly (Figure 2.2.6A and 2.2.6B). We observed that infected cells exhibit decreased number of Drp1 aggregates (both dilated and constricted) in *Chlamydia* infected cells (Figure 2.2.6C). Quantification of total number of Drp1 aggregates also showed that *Chlamydia* infected cells had significantly less number of aggregates (Figure 2.2.7A and 2.2.7B). At the same time, quantification of the degree of colocalization between the mitochondrial signal and Drp1 using plot profiling and COLOC2 analysis exhibited that *Chlamydia* infected cells had significantly less number of Drp1 aggregates associated with the mitochondria (Figure 2.2.8A, 2.2.8B and 2.2.8C). Interestingly, exposing *Chlamydia* infected cells to pro-fragmentation stress, such as hydrogen peroxide or cobalt chloride, does not increase the number of Drp1 aggregate count (dilated or constricted) or their colocalization with the mitochondria (Figure 2.2.6C, 2.2.7B and 2.2.8C). Artificial overexpression of Drp1 increases its colocalization with the mitochondrial and inhibits chlamydial growth as seen in (Figure 2.2.3A). This observation stands in line with the observation that treatment of *Chlamydia* infected HUVECs with hydrogen peroxide also does not deplete miR-30c or increase p53 expression as seen in control cells (Figure 2.2.9A and 2.2.9B). From these results it appears that the *Chlamydia* mediated downregulation of Drp1 serves to reduce the association of functional Drp1 rings with the mitochondria and thus interferes with the mitochondrial fission machinery.

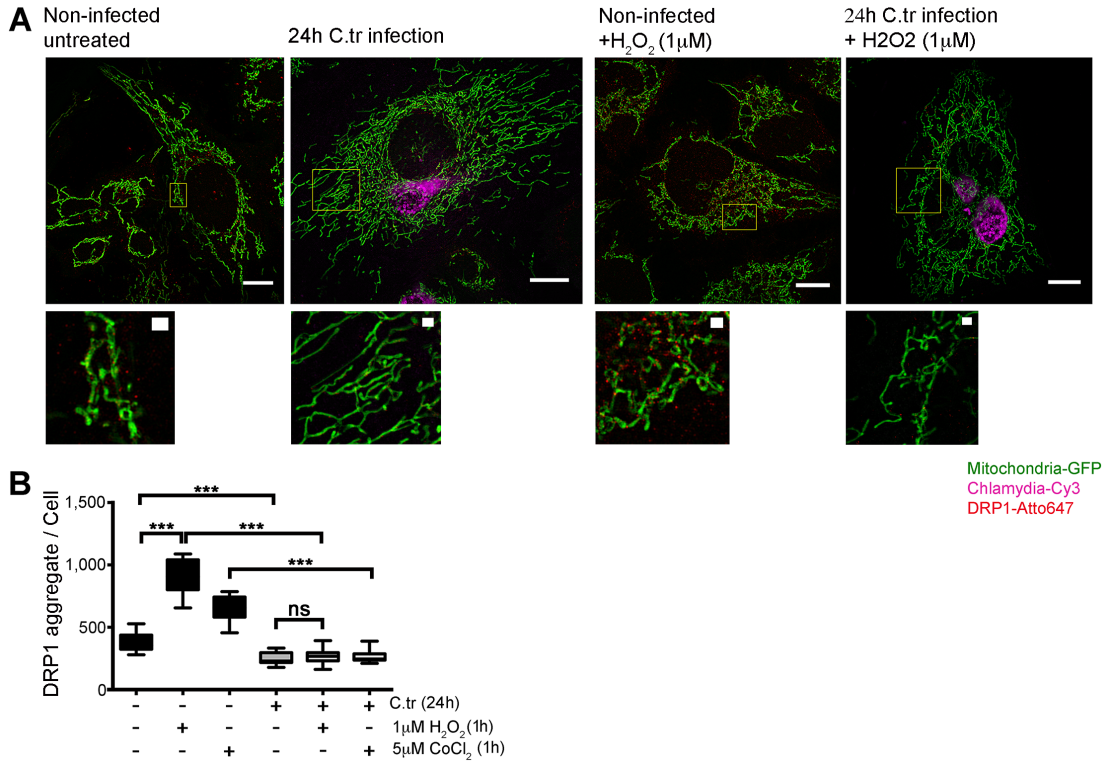

Figure 2.2.7 Chlamydial infection reduces Drp1 aggregates abundance in HUVECs
(2.2.7A) Structured illumination micrographs of control and *Chlamydia*-infected mito-HUVECs (Green) with and without 1 μM H_2O_2 (1 hour) treatment. The samples were immunostained against Drp1 (Red) and cHSP60 (Magenta). Bars represent 10 μm. The yellow enlargements illustrated the clustering of Drp1 aggregates (sized between 100 nm to 280 nm) on the mitochondrial fragments. (2.2.7B) Graph represents the number of Drp1 aggregate per cell (± SD) for non-infected and infected cells were 377.2 ± 65.86 and 251.8 ± 46.44 (~60 cells analyzed from random selection of 20 ROI in each sample. 2 or 3 random 10 μm x 10 μm ROIs were chosen in each selected cell. Significance was determined by Mann Whitney test; *n=10*; Adapted from Chowdhury et al. 2017; JCB).

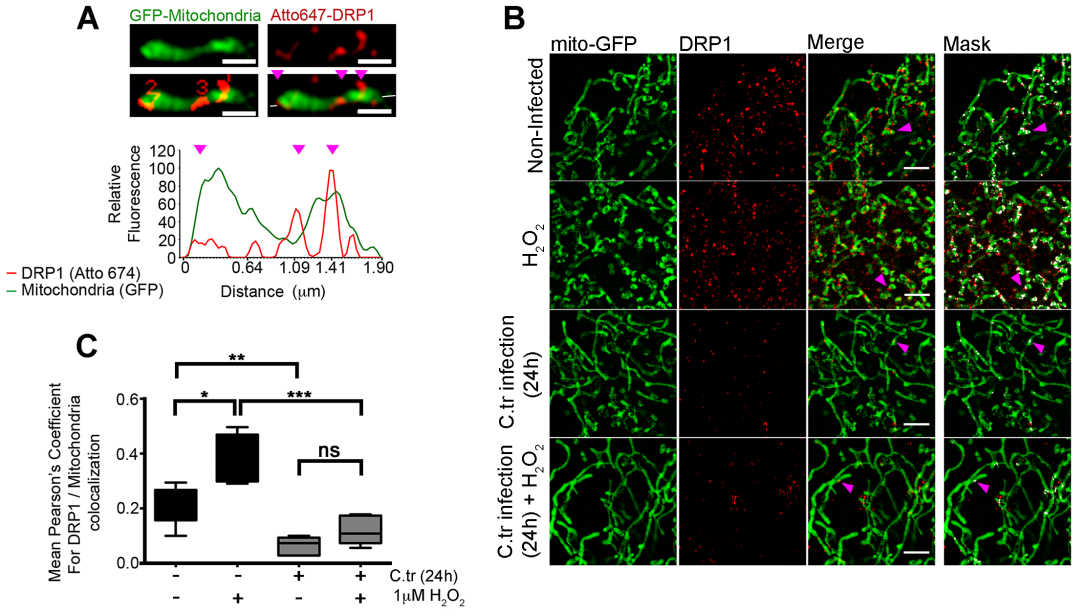

Figure 2.2.8 Chlamydial infections reduce the colocalization of Drp1 aggregates on mitochondrial fragments.

(2.2.8A) Representative structured illumination micrograph of a single mitochondrial fragment associated with three Drp1 aggregates. The graph depicts the fluorescence intensity profile plot of the green mitochondrial fragment with the red Drp1 aggregates on constriction sites (magenta arrowheads). The number of Drp1 aggregates was quantified and intensities in both channels were measured along the depicted axis (white line in last panel through the fragment). Bars represent 1µm. (2.2.8B) Structured illumination micrographs and colocalization analysis masks of control and *Chlamydia*-infected mito-HUVECs (Green) with and without 1 µM H_2O_2 (1 hour) treatment. The samples were immunostained against Drp1 (Red) and cHSP60 (Magenta). Bars represent 10 µm. (2.2.8C) The graph illustrates the degree of colocalization between the mitochondrial and Drp1 signal. The graph was plotted using values representing the Pearson's colocalization coefficient determined using the COLOC2 plugin from FIJI. (~20 cells were analyzed per sample. 2 or 3 random 10 µm x 10 µm ROIs were chosen in each selected cell. *n=10*). Bars represent 2µm. All data represent mean ± S.D. Asterisks denote significance by Student's *t* test. *, P < 0.05; **, P < 0.01; ***, P < 0.001; ns, non significant (Adapted from Chowdhury et al. 2017; JCB).

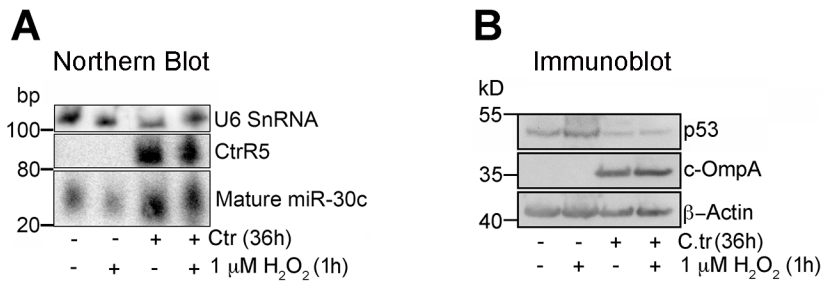

Figure 2.2.9 Oxidative stress mediated depletion and stabilization of p53 is inhibited upon *Chlamydia* infection
(2.2.9A) Northern blot of control and *Chlamydia* infected (36 hours) HUVECs treated with 1 µM H_2O_2 for 1 hour. The blot was probed with radiolabelled oilgos against miR-30c, U6 snRNA and the chlamydial small RNA CtrR5. (2.2.9B) The immunoblot illustrates the effect of chlamydial infection on H_2O_2 mediated stabilization of p53 in HUVECs. The cells were infected with Chlamydia for 36 hours and treated with 1 µM H_2O_2 for 1 hour prior to lysis. All blots were repeated a minimum of three times (Adapted from Chowdhury et al. 2017; JCB).

2.2.3 Diminution of p53 is essential for *Chlamydia* induced Drp1 depletion.

Depletion of p53 has been shown to be an absolutely necessity for the normal growth and development of C. *trachomatis* within human cells. *Chlamydia* requires the additional metabolic support obtained from the pentose phosphate pathway derepressed upon p53 depletion (Siegl et al., 2014). To further understand the role of p53 in the regulation of *Chlamydia* infection in terms of mitochondrial morphology and Drp1 expression we checked if artificial expression of p53 in H1299 had any effects on the Drp1 levels and the mitochondrial architecture of cell. We observed that replenishment of H1299 with p53 led to an upsurge in the Drp1 expression and aggregate abundance, its subsequent colocalization with the mitochondria and inhibition of chlamydial infection (Figure 2.2.10A, 2.2.10B, 2.2.10C, 2.2.10D and 2.2.10E). The overexpression vector of p53 produces the p53 mRNA without the 3' UTR thus its expression is subject, exclusively, to the regulation of the constitutive CMV promoter that drives the transcription. We investigated if it was possible for *Chlamydia*, in the absence of any miRNA-based regulation, to modulate the levels of

p53 and Drp1. To this effect we expressed p53 using the CMV promoter driven overexpression vector in H1299 cells post *Chlamydia* infection. We observed that post-infection transfection of p53 into *Chlamydia* infected H1299 cells also has a deleterious effect on chlamydial growth and is capable of promoting Drp1 expression (Figure 2.2.10B, 2.2.10C, 2.2.10D and 2.2.10E). Based on these results, we speculate that miR-30c mediated downregulation of p53 is essential for reduction of Drp1 expression and its subsequent accumulation on the mitochondria to promote fission.

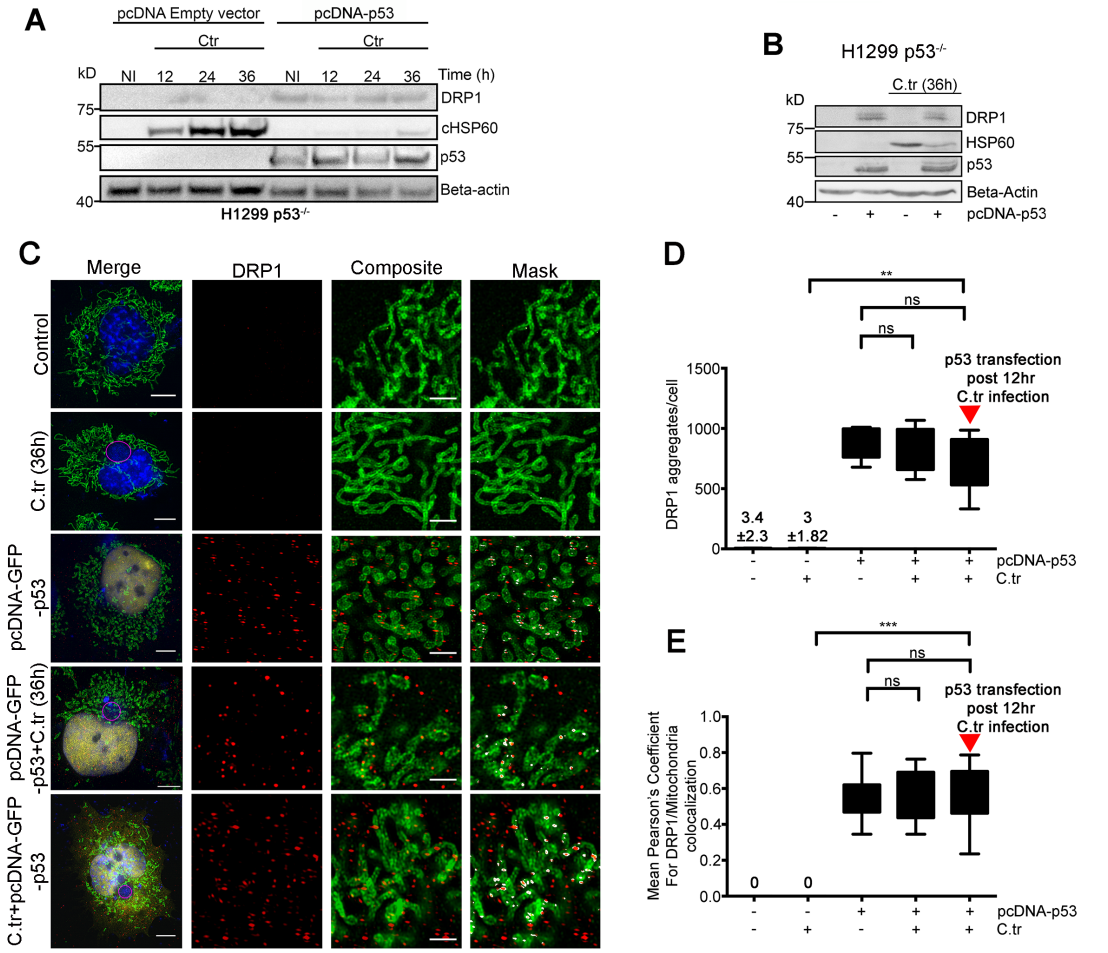

Figure 2.2.10 Artificial overexpression of p53 abrogates chlamydial growth and stabilizes Drp1 expression

(2.2.10A) Immunoblot represents the impact of Drp1 overexpression on chlamydial growth in H1299 p53 null cells. H1299 cells were transfected with vector control or pcDNA-p53 overexpression vector followed by *Chlamydia* infection for indicated timespans. (2.2.10A) Immunoblot illustrates the effect of p53 over expression on Drp1 expression and chlamydial growth before and after establishment of *Chlamydia* infection in H1299 p53 null cells. The blots were probed with antibodies against p53, cHSP60, Drp1 and Beta Actin. (2.10C) Structured illumination micrographs and COLOC2 analysis masks of H1299 p53 null cells transfected with pcDNA-p53-GFP overexpression vector. The samples were immunostained with antibodies against Drp1 (Red) and Tom20 (green). p53-GFP is indicated in yellow. The nucleus and chlamydial DNA (Purple ellipse) was stained using DAPI. Bars represent 2 µm. (2.2.10D) The abundance of Drp1 aggregates (sized between 100 nm to 280 nm) in control, pcDNA-p53-GFP transfected and/or chlamydia infected H1299 cells, is illustrated with the box plot. The red arrow marks the sample that was transfected with the pcDNA-p53-GFP overexpression vector post infection. Number of Drp1 aggregate per cell (± SD) for non-infected cells = 3.4 ± 2.24, C.tr (36 h) = 3 ±

1.73, p53 OE = 882.3 ± 124.82, p53 OE + Ctr (26h) = 790 ± 171.53 and C.tr (36h) ± p53 OE = 714.6 ± 215.07. (~30 cells analyzed from random selection of 20 ROI in each sample. Significance was determined by Mann Whitney test; *n*=*3*). (2.2.10E) The box plot illustrates the degree of colocalization between Drp1 (red) mitochondrial signals (green) upon p53-GFP over expression in H1299. The red arrow marks the sample that was transfected with the pcDNA-p53-GFP overexpression vector post infection. Peason's colocalization coefficient was used estimate the degrees of colocalization (~30 cells were analyzed per sample. 2 or 3 random 10µm x 10µm ROIs were chosen in each selected cell. *n*=*3*). All data represent mean ± S.D. Asterisks denote significance by unpaired *t* test *, P < 0.05; **, P < 0.01; ***, P < 0.001 (Adapted from Chowdhury et al. 2017; JCB).

2.3 Effect of chlamydial infection on the mitochondrial matrix.

Mammalian cells have been shown to respond to bacterial and fungal infection by producing reactive oxygen species (ROS) generated by, amongst other pathways, the NADPH oxidases (Fang, 2011; Paiva and Bozza, 2014; Pizzolla et al., 2012; Segal, 2008). The mitochondrial NADPH oxidase (Nox)/dual oxidase (Duox) family of proteins along with other cytosolic regulatory enzymes reduce O_2 to O_2^- utilizing electrons garnered from intracellular NADPH (Sirokmany et al., 2016). The superoxide O_2^- synthesized during the infection of *H. pylori, Salmonella* and *Shigella* assist in host defense by promoting the activation of pro-inflammatory cascades (Carneiro et al., 2009; Charles et al., 2008; Smoot et al., 2000). *Chlamydia* infection also promotes the production of ROS via a Nod-like receptor X1 (NLRX1) dependent pathway (Abdul-Sater et al., 2010; Boncompain et al., 2010). However, unlike other pathogens, ROS has a positive effect on chlamydial growth. ROS cleavage of caspase-1 is essential for the progression of chlamydial infection and inhibition of Nox dependent ROS production severely limits *Chlamydia* growth (Abdul-Sater et al., 2010). Increase in oxidative stress due by extrinsic or intrinsic factors promote mitochondrial dysfunction and induce mitochondrial fragmentation in a Drp1 dependent manner (Su et al., 2014; Wu et al., 2011). Apart from the obvious changes in the mitochondrial architecture, such ROS mediated stress also disturbs the mitochondrial matrix (Guo et al., 2013). To this effect we investigated the effect of *Chlamydia* infection on the mitochondrial matrix.

2.3.1 *Chlamydia* infection reversibly induces stress on the mitochondrial matrix

The mitochondrial matrix and, as a consequence, the mitochondrial network responds to subtle biochemical modulations within the cell. We speculated that the ROS promoting effect of *Chlamydia* might also have an effect on the mitochondrial matrix, even though the obvious signs of oxidative stress mediated mitochondrial damage was curiously absent. To this effect we used a modified dsRED variant called Timer that responds to oxidative stress by exhibiting a shift in fluorescence spectrum from green to red and targeted it for expression within the mitochondrial matrix (Figure 2.3.1A and 2.3.1B) (Ferree et al., 2013; Laker et al., 2014). Upon mitochondrial expression of the Timer protein (MitoTimer) within the HUVECs we observed that the protein responded to extrinsic sources of oxidative stress such as H_2O_2 (Figure 2.3.2A, 2.3.2B, 2.3.2C, 2.3.2D and 2.3.2E; Video 2.3.1 and 2.3.2). To

understand the effect of *Chlamydia* induced ROS production on the host mitochondrial matrix we infected MitoTimer expressing HUVEC and HFF cells with *Chlamydia* for different timespans and quantified the fraction of cell population expressing the red variant of the Timer protein using flow cytometry. We observed that the cells infected with *Chlamydia* for 8 hours exhibited a significant shift in the population towards the cells expressing the red variant of MitoTimer. Surprisingly, this effect is reduced in cells infected with *Chlamydia* for 16 hours most of which express the green MitoTimer. A second surge of infected cells expressing the red variant is seen 24 hours post infection during which ~44% (±3.8%; ± SD) cells are observed to express red MitoTimer. The expression of the oxidized timer is seen to plateau after 24 hours by which time even the non infected cells begin to show signs of red mitochondrial signal, possibly due to accumulation of metabolites. These changes are observed in both *Chlamydia*-infected HUVECs and HFF cells. Treatment of the uninfected HUVECs and HFFs with 1 μM H_2O_2 for 30 minutes leads to a major shift towards expression of the red MitoTimer while similar treatment prior to *Chlamydia* infection did not elicit a major shift towards the red MitoTimer (Figure 2.3.3A, 2.3.3B and 2.3.3C). Induction of ROS via oxidative stress promotes p53 expression and its nuclear translocation leads to an increase in Drp1 abundance (Li et al., 2010; Uberti et al., 1999). Cells treated with H_2O_2 have been shown to exhibit higher levels of p53 and/or p53 activity, Drp1 mediated mitochondrial fission and eventually, undergo apoptotic cell death (Qi et al., 2013; Roth et al., 2014; Uberti et al., 1999; Xie et al., 2001). While *Chlamydia* infected cells have been shown to be resistant to extrinsic pro-apoptotic stress the above experiments demonstrate that *Chlamydia*-induced oxidative stress reversibly stresses the mitochondrial matrix (Rajalingam et al., 2008; Sharma et al., 2011). Our previous results also demonstrate that the H_2O_2 induced downregulation of miR-30c, upregulation of p53 and Drp1 colocalization with the mitochondria are absent in *Chlamydia*-infected cells (Figure 2.2.9A and 2.2.9B). Lastly, in accordance to previous studies, the time points of infection during which the mitochondrial stress is exhibited roughly coincides with the time points when ROS is induced in infected cells (Boncompain et al., 2010).

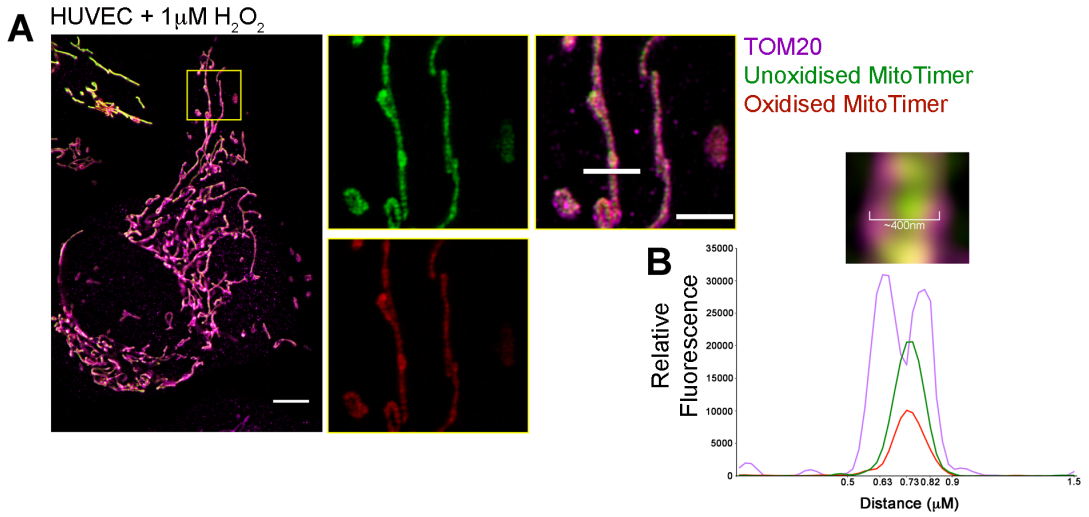

Figure 2.3.1. MitoTimer localizes to the mitochondria upon expression in HUVECs
(2.3.1A) Representative structured illumination micrograph of HUVECs expressing MitoTimer post treatment with 1 μM H_2O_2 for 15 minutes. The sample was immunostained with the mitochondrial outer membrane protein Tom20 to differentiate the OMM from the mitochondrial matrix. Bar represents 5μm. The inset (5μm x 5μm) show oxidized (red) and non-oxidized (green) fractions of the MitoTimer proteins and the Tom20 signal (purple). The final (rightmost) inset depicts the merged image with a 1.5 μm horizontal bar traversing the mitochondria. (2.3.1B) The graph was plotted with arbitrary intensity values obtained by plotting the intensity profile of oxidized (red) and non-oxidized (green) forms of the MitoTimer proteins and the Tom20 signal (purple) along the 1.5 μm horizontal bar traversing the mitochondria. (Adapted from Chowdhury et al. 2017; JCB).

2.3.2 Artificial p53 and Drp1 depletion can reduce ROS induced mitochondrial stress

Studies have shown that p53 is one of the critical effectors via which H_2O_2 mediated oxidative stress can activate specific pathways that lead to cell death, cell cycle arrest and senescence (Qi et al., 2013; Roth et al., 2014; Uberti et al., 1999; Xie et al., 2001). Additionally, H_2O_2 driven p53 activation has also been shown to promote Drp1 induced mitochondrial fission and miR-30c mediated p53 block prevents this effect (Li et al., 2010; Uberti et al., 1999). Since our previous observations illustrate that *Chlamydia* infection can downregulate both of these proteins, we attempted to gauge the effect of ROS induction on the mitochondrial matrix of HUVECs exhibiting targeted downregulation of p53 and Drp1. We transfected HUVECs expressing MitoTimer separately with p53 and Drp1 siRNAs and subjected them to treatments with H_2O_2 (1 μM; 30 minutes).

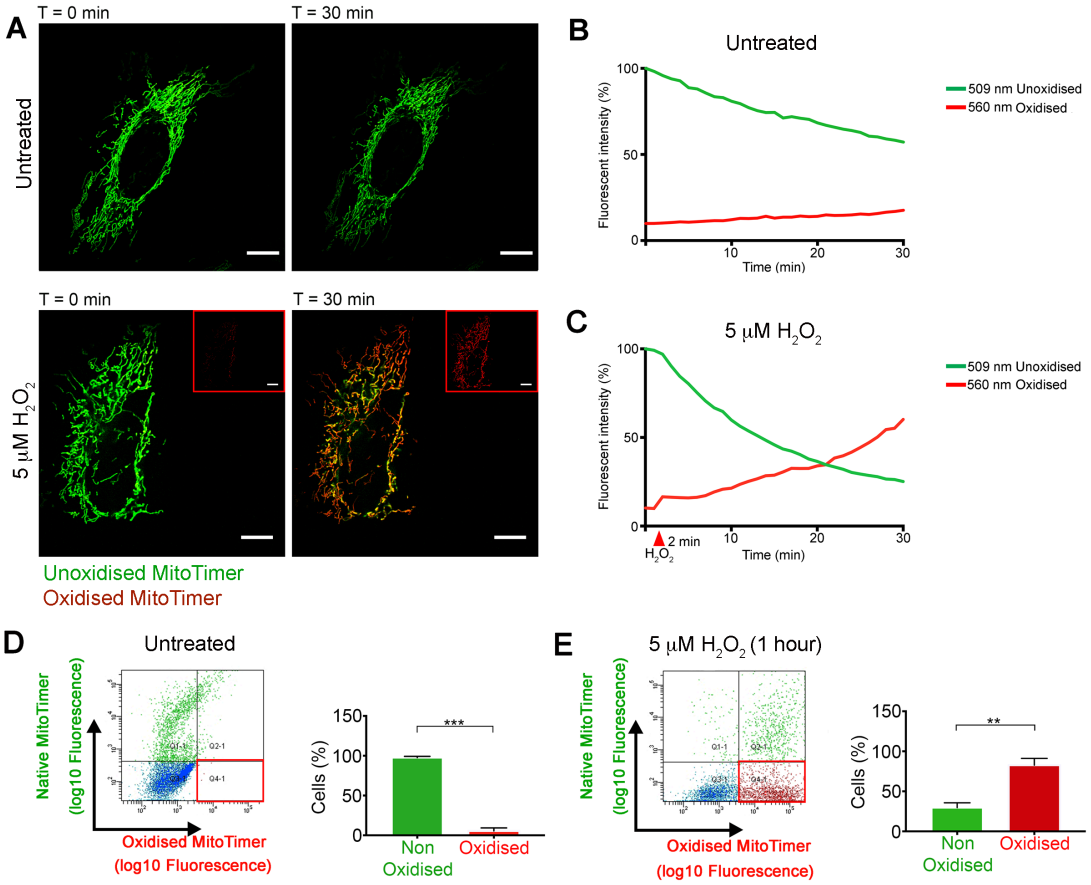

Figure 2.3.2 MitoTimer temporally alter its fluorescent properties on exposure to oxidative stress.

(2.3.2A) Freeze frames from confocal videomicrography of control and H_2O_2 (5 μM; 30 minutes) treated HUVECs expressing MitoTimer. The oxidized form of MitoTimer is depicted in red (596 nm) and the native form in green (500 nm). 5μM H_2O_2 was added into imaging media of indicated samples after 2 minutes of untreated imaging. Insets show the red channel images of the H_2O_2 treated cells at t=0 min and t=30 min. Images were captured every 60 seconds for 30 minutes. **See also** Video 2.3.1 and Video 2.3.2. (2.3.2B and 2.3.2C) The line graphs show the shift in fluorescence spectrum of the MitoTimer protein with time in presence and absence of H_2O_2 mediated oxidative stress. The arbitrary fluorescent intensity values were normalized to the starting fluorescent intensity value of the Timer protein in the green channel and depicted as percentage of that value. (2.3.2D and 2.3.2E) Scatter plots from flow cytometry depicting the shift in fluorescence spectrum of the MitoTimer protein in presence and absence of H_2O_2 mediated oxidative stress. The corresponding graphs indicate the percentage of total cells expressing the oxidized and non-oxidized form of the MitoTimer (Adapted from Chowdhury et al. 2017; JCB).

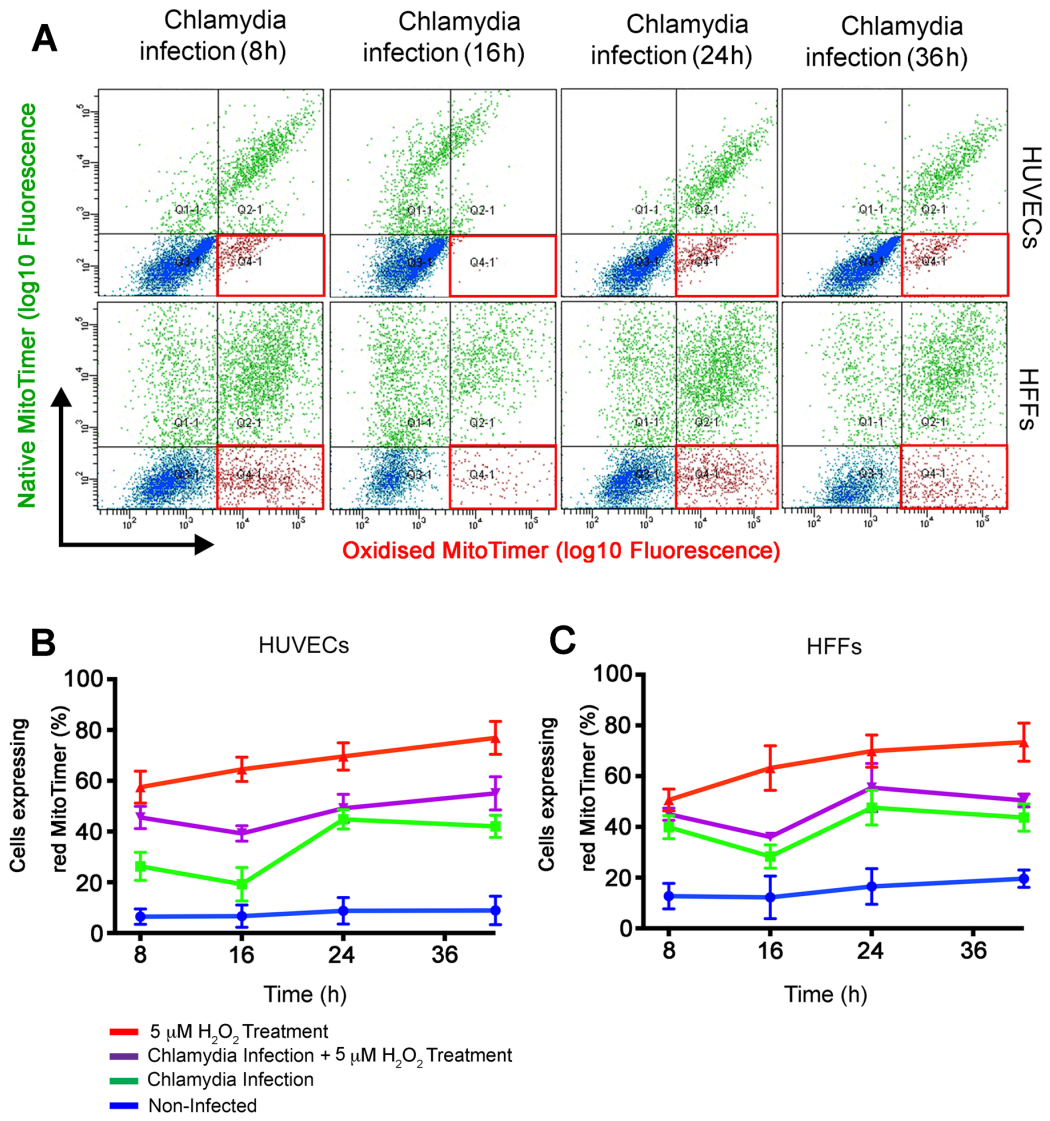

Figure 2.3.3 *Chlamydia* infection reversibly stresses the mitochondrial matrix.
(2.3.3A) Scatter plots from flow cytometry of MitoTimer expressing HUVECs and HFF cells post *Chlamydia* infection for indicated timespans. The red box indicates the fraction of cell population expressing the red MitoTimer. All samples were transfected 12 hours prior to infection. (2.3.3B-2.3.3C) The line graphs show the percentage of cell population expressing the red form of MitoTimer in control and Chlamydia infected HUVECs and HFFs. Indicated samples were also treated with with 5 μM H_2O_2 for 30 minutes, washed and allowed to grow for 8, 16, 24 and 36 hours. Another group of samples were pre-treated with 5 μM H_2O_2 for 30 minutes, washed and then infected with C.tr for 8, 16, 24 and 36 hours (n=3). All data represent mean ± S.D. Asterisks denote significance by Student's *t* test. *, P < 0.05; **, P < 0.01; ***, P < 0.001; ns, non significant. (**See also** Video 3.1 and 3.2; (Adapted from Chowdhury et al. 2017; JCB)).

The cells transfected with p53 siRNA exhibited significant resistance to the H_2O_2 mediated shift towards expression of the red variant of MitoTimer seen in control cells. A similar, but milder, ameliorative effect was also observed in cells transfected with Drp1 siRNA (Figure 2.3.4A and 2.3.4B). These results indicate that downregulation of p53 and Drp1 individually partially alleviate the stress inducing effects of H_2O_2 mediated oxidative stress on the mitochondrial matrix. We speculate

that reversibility of mitochondrial stress in *Chlamydia* infected cells could be, in part, attributed to the downregulation of p53 and Drp1.

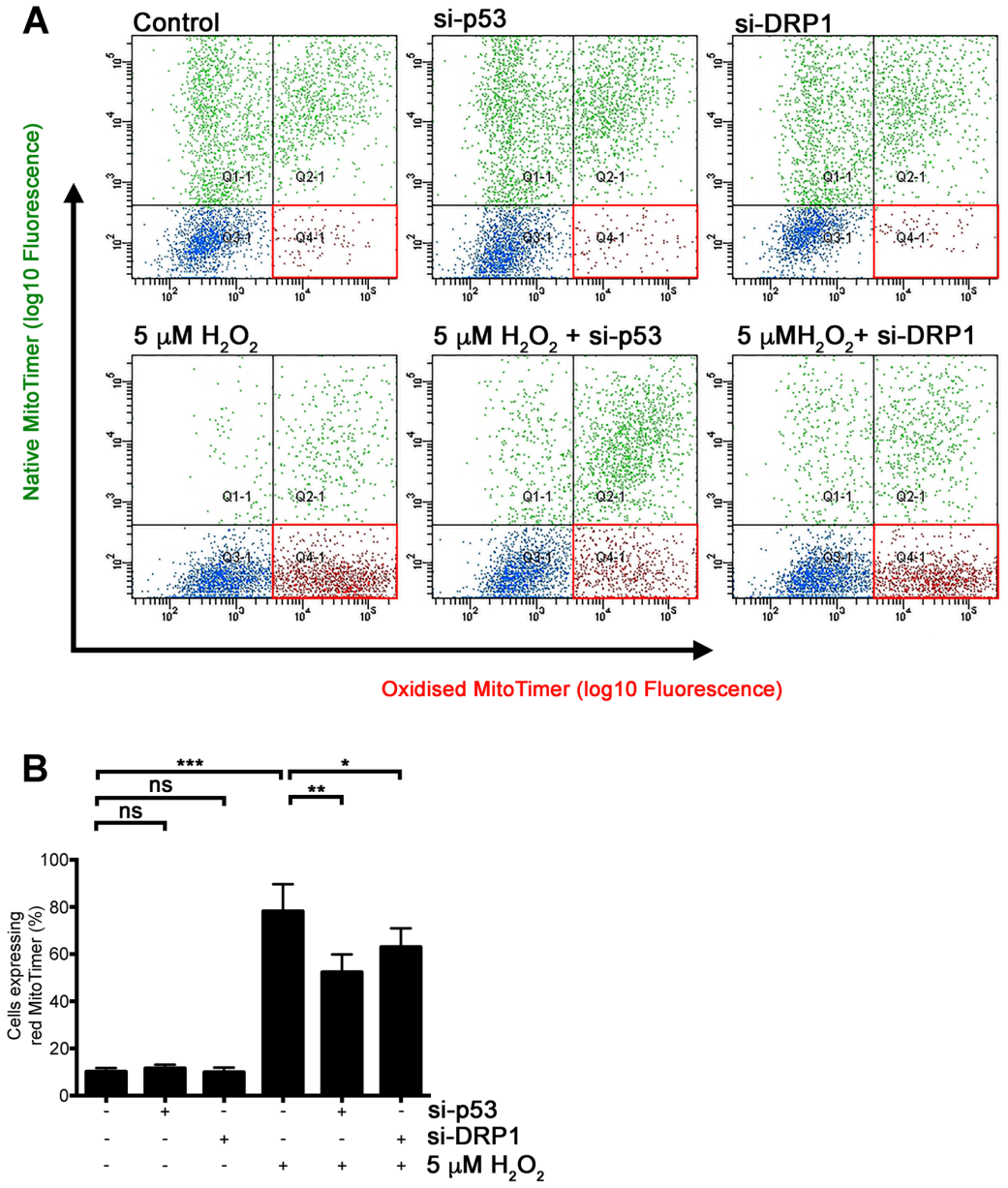

Figure 2.3.4 Artificial depletion of p53 and Drp1 alleviates ROS generated stress on the mitochondrial matrix

(2.3.4A-2.3.4B) Scatter plots and the corresponding graph illustrate the percentage of HUVECs expressing the oxidized form of MitoTimer post transfection with siRNA negative control, siRNAs against p53 and Drp1 and/or treated with 5 μM H_2O_2 for 15 minutes (*n=3;* Adapted from Chowdhury et al. 2017; JCB*)*.

2.4 *Chlamydia* infection affects the host mitochondrial architecture

Knockout and over expression studies have demonstrated that the mitochondrial network architecture and dynamics are heavily influenced by the abundance and functionality of the mitochondrial fission regulator Drp1 (Qi et al., 2013; Touvier et al., 2015). Drp1 is ubiquitously expressed in most of the mammalian cell types and is essential for mitochondrial division and stress-induced mitochondrial fragmentation, which also serves as a form of mitochondrial quality control (Shirakabe et al., 2016; Smirnova et al., 2001). It has been observed that under conditions of metabolite starvation, negative regulation of Drp1 and promotion of mitochondrial fusion generates elongated mitochondria (Gomes et al., 2011). These branched networks of mitochondria are more efficient at ATP production and are spared from targeted autophagy (Gomes et al., 2011; Rambold et al., 2011). *Chlamydiae* are dependent on the host metabolism for their growth and development and infection places an enormous stress on the cellular resources of ATP. We have seen that *Chlamydia* promotes Drp1 depletion via downregulation of p53 in a miR-30c dependent manner. This depletion of Drp1 reduces its mitochondrial colocalization and such colocalization has been shown to be essential for induction of mitochondrial fission. Thus we found it was important to explore the effect of *Chlamydia* infection on the overall mitochondrial architecture and dynamics of an infected cell.

2.4.1 *Chlamydia* infected HUVECs exhibit elongated mitochondria and are resistant to oxidative stress induced mitochondrial fragmentation

Concordant with the effect on the HUVEC mitochondrial network seen upon miR-30c and Drp1 inhibition, *Chlamydia* infected HUVECs exhibited a branched and elongated morphology that becomes increasingly evident with the progression of infection (Figure 2.4.1). *Chlamydia* infection effect a significant decrease in isolated mitochondrial fragments, an increase in the mitochondrial fragment length and over all mitochondrial area (Figure 2.4.2A, 2.4.2B and 2.4.2C). This effect was unsurprising in the light of observed depletion of Drp1 but the extent of the effect of infection on the mitochondrial network was unprecedented. The mean length of a mitochondrial fragment was found to increase from 7.607 (± 2.39; ±SD) to 10.98 (± 2.05; ±SD) upon Chlamydia infection (Figure 2.4.2C).

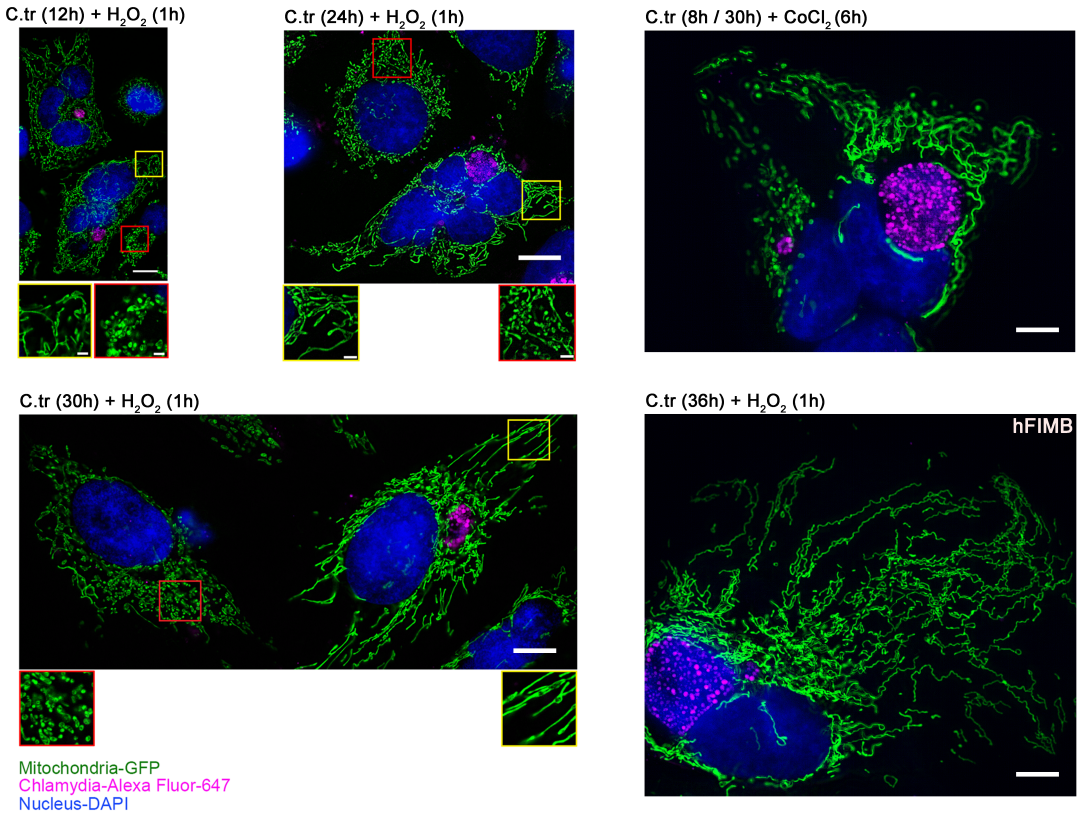

Figure 2.4.1 Chlamydia infection alters mitochondrial architecture
(2.4.1) Representative Structured illumination micrographs of Chlamydia infected mito-HUVECs and hFIMB (green). The cells were infected with Chlamydia for 12, 24 and 36 hours followed by 1 µM H_2O_2 for 1 hour or $CoCl_2$ for 6 hours. The samples were immunostained against cHSP60 (magenta) and the nucleus was stained with DAPI. Bar represents 10 µm. Red-bordered insets focus on uninfected cells while the yellow-bordered insets focus on infected cells. Bar represents 1.5 µm (Adapted from Chowdhury et al. 2017; JCB).

This effect bore close resemblance to the Drp1 knock down phenotype in HUVECs, which also exhibited elongated mitochondrial fragments and decreased occurrence of individual fragments (Figure 2.4.2A, 2.4.2B and 2.4.2C). As discussed above, mitochondrial fragmentation and induction of the fission machinery is a key event in apoptotic cascades and preventing mitochondrial fission inhibits apoptotic-signalling cascades. Given the strong apoptotic inhibition in *Chlamydia* infected cells we strove to see if H_2O_2 mediated oxidative stress could induce mitochondrial fragmentation within infected cells. Treatment of uninfected HUVECs with 1µM H_2O_2 for 1 hour resulted in massive mitochondrial fragmentation and, in some cells, even death. This effect was not observed in *Chlamydia* infected HUVECs whose mitochondrial network remained branched and unfragmented even after the above-mentioned treatment (Figure 2.4.2A, 2.4.2B and 2.4.2C). We attribute this curious effect of *Chlamydia* infection to the miR-30c mediated inhibition of the mitochondrial fission machinery. Furthermore, we speculate that this miR-30c mediated modification of the

mitochondrial architecture also allows *Chlamydia* infected cells to survive the oxidative stress produced a result of the infection.

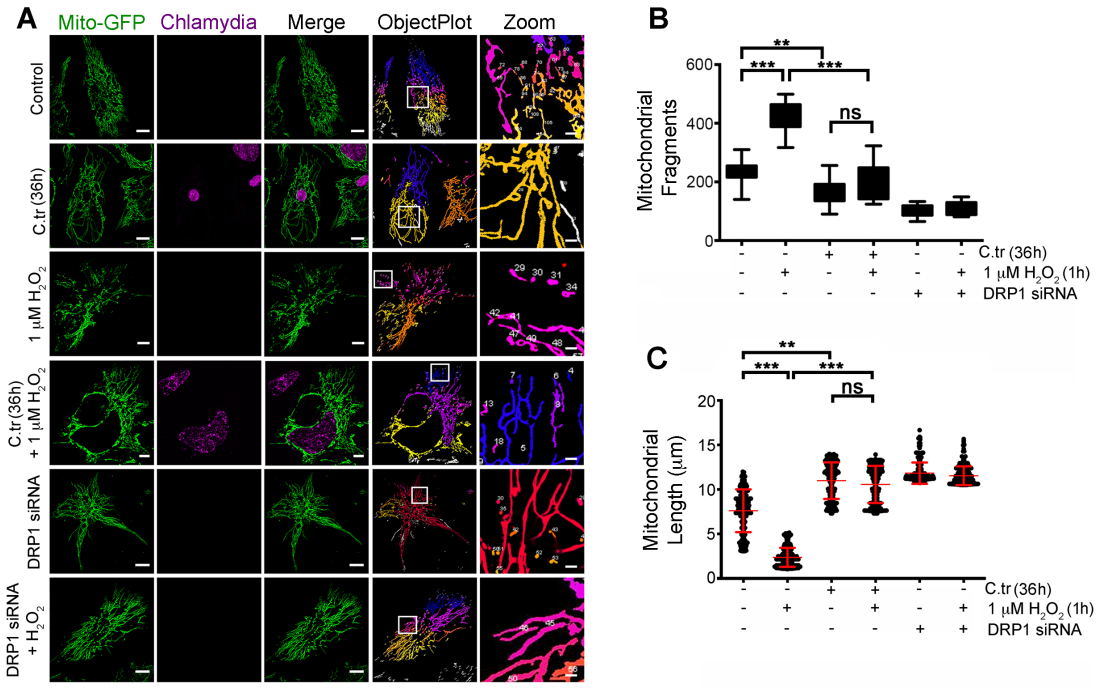

Figure 2.4.2 Chlamydia infection promotes mitochondrial elongation and inhibits oxidative stress mediated fragmentation
(2.4.2A) Confocal micrographs illustrating data processing, rolling ball thresholding and segmentation used for separating individual mitochondrial fragments. Mito-HUVECs were infected with *Chlamydia* (cHSP60; magenta) for 36 hours or transfected with Drp1 siRNA. Indicated samples were also treated with 1 μM H_2O_2. (2.4.2B) Graph depicts the abundance of individual mitochondrial fragments in samples. H_2O_2 is regarded as a positive control for fragmentation while siRNA mediated Drp1 knockdown is regarded as a negative control. Number of fragments in control (± SD) = 235.4 ± 36.34, H_2O_2 = 414.6 ± 50.39. C.tr = 169.1 ± 41.12 and C.tr + H_2O_2 = 198 ± 61.52 (*n=20* for panels c and d; ~30 cells were analyzed from random selection of ~10 ROI in each sample). (2.4.2C) Graph illustrates the distribution of mitochondrial fragment length across samples. The dots represent the mean mitochondrial fragment length of ~3 cells in an ROI chosen at random within samples. 200 such dots were plotted on the graph. Mean mitochondrial fragments length in control (± SD) = 7.607 ± 2.39, H_2O_2 = 2.36 ± 1.06, C.tr = 10.98 ± 2.05 and C.tr + H_2O_2 = 9.90 ± 1.84 (*n=20*; ~30 cells were analyzed from random selection of ~10 ROI in each sample). Asterisks denote significance by one-way ANOVA followed by Tukey's multiple comparisons test: *, P < 0.05; **, P < 0.01; ***, P < 0.001; ns, non significant (Adapted from Chowdhury et al. 2017; JCB).

2.4.2 Chlamydia infection alters the mitochondrial dynamics of infected cells

The dynamics of the mitochondrial particles and thus the network is subject to the ratio of the fusion/fission events orchestrated by the fusion and fission machinery (Jendrach et al., 2005; Karbowski et al., 2004; Wang et al., 2012; Wu et al., 2011). It is understandable that induction of mitochondrial fission by external oxidative stress would prompt an increase in rates of fission events thus induce mitochondrial fragmentation and an increase in the number of isolated mitochondrial particles (Wu et al., 2011). These particles exhibit random movements to attempt fusion in order to

be recycled or are targeted for destruction within mitophagosomes (Frank et al., 2012).

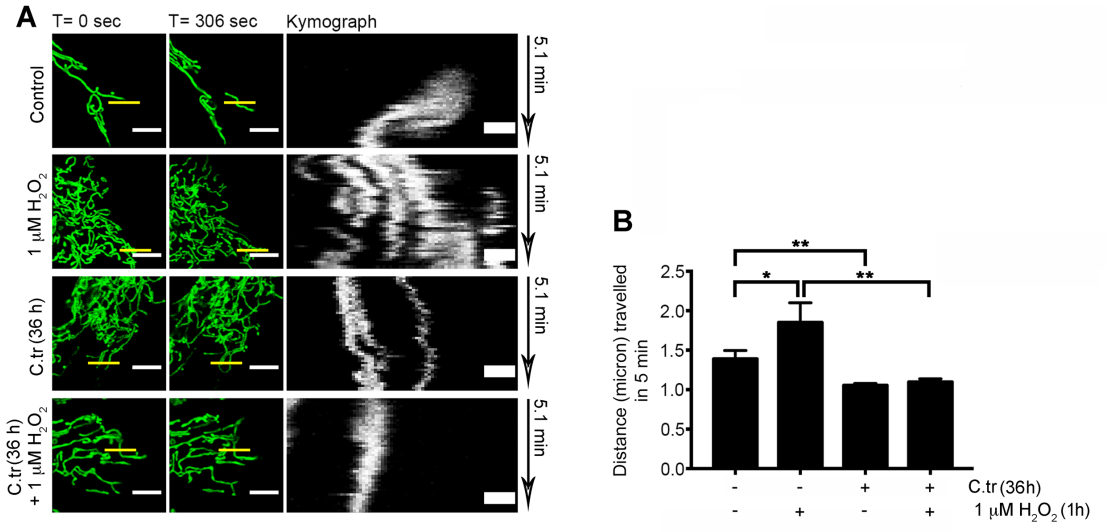

Figure 2.4.3 Stress induced mitochondrial motility is altered upon *Chlamydia* infection
(2.4.3A) Freeze frames (20 μm x 20μm) from confocal videomicrography of control and *Chlamydia* infected mito-HUVECs. Images are displayed at t = 0 and t = 306 seconds. White bars represent 5 μm. Yellow bars (0.5 μm in thickness) represent arbitrary lines drawn to determine lateral displacement of mitochondrial fragments with time as represented by the Kymograph panels (un-quantified). Indicated samples were also treated with 1 μM H_2O_2 treatment for 1 hour or with 1 μM H_2O_2 for 1 hour after 36 hours of *Chlamydia* infection. (2.4.3B) Graph illustrates the difference in the end mobility of mitochondrial fragments between corresponding samples. The distance moved by the mitochondrial fragments in 5 minutes was determined by analyzing Videos 2.4.1, 2.4.2, 2.4.3 and 2.4.4 with the mitoCRWLR macro (*n=5;* 3 ROIs were analyzed from individual cells with 6 cells being chosen at random from every sample). All data represent mean ± S.D. All data represent mean ± S.D. Asterisks denote significance by Student's *t* test. *, P < 0.05; **, P < 0.01; ***, P < 0.001; ns, non significant. **See also** Videos 2.4.1, 2.4.2, 2.4.3 and 2.4.4 (Adapted from Chowdhury et al. 2017; JCB).

Either way, ungoverned increase in fission and number of isolated mitochondrial particles lead to an increase in the apparent increase in the random movements of isolated mitochondrial particles. This effect is very clearly observed in the HUVECs treated with 1μM H_2O_2 for 1 hour (Figure 2.4.3A; Video 2.4.2). Using the novel MACRO script MitoCRWLR we measured and compared the distance moved by free ends of mitochondrial fragments in infected and non-infected cells. There is a significant decease in the mobility of mitochondrial fragments in both H_2O_2 treated and untreated *Chlamydia* infected cells (Figure 2.4.3A and 2.4.3B; Video 2.4.1, 2.4.2, 2.4.3 and 2.4.4). We attribute this decrease in motility to the loss in the number of individual fragments in chlamydia-infected cells, which contributes to the increase in the apparent motility of the mitochondrial network in control cells.

2.4.3 Ratio of fusion events to fission events is affected by *Chlamydia* infection

As described above, a delicate balance between the fusion and fission events governs the mitochondrial architecture and its maintenance. Changes to either the mitochondrial fusion or fission machinery affect this balance, giving rise to abnormal mitochondrial architecture and associated cellular implications (Karbowski et al., 2004). While mitochondrial fission has been found to be accessory to apoptotic induction and stress-mediated damage, it is also essential in regards to mitochondrial quality control, division and distribution (Qi et al., 2013; Shirakabe et al., 2016; Smirnova et al., 2001; Twig et al., 2008). Loss of mitochondrial fission can also lead to the collapse of the mitochondrial network and promote cell death albeit in a non-classical pathway (Uo et al., 2009; Westrate et al., 2014). However in context of chlamydial infection and associated effects such as increase in metabolic stress and ROS generation, inhibition of mitochondrial fission might provide protection to the mitochondrial network from stress-induced fragmentation. Thus, we quantified the so called mitochondrial fusion/fission ratio in non-infected and infected by manually tracking individual fission and fusion events occurring on mitochondrial segments of control and *Chlamydia* infected cells for a span of 3 hours (Figure 2.4.4 and 2.4.5; Video 2.4.6 and 2.4.7). It was observed that while the number of fusion events in both control and *Chlamydia*-infected cells remained more or less equal (slight decrease is seen in the *Chlamydia*-infected cells) fission events were quite rare in *Chlamydia*-infected cells. This is reflected in the ratio of fusion to fission events, which is slightly higher in *Chlamydia* infected cells when compared to control cells (Figure 2.4.6). This elevation of mitochondrial fusion/fission results in elongated mitochondrial fragments and the over all changes to the mitochondrial architecture in *Chlamydia* infected cells.

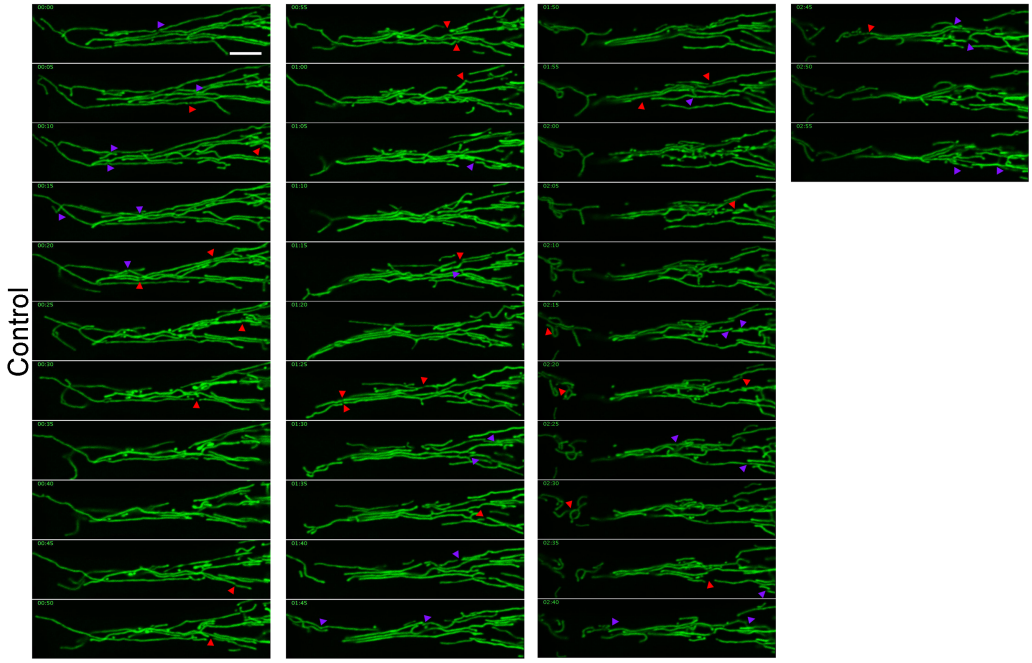

Figure 2.4.4 Control mito-HUVECs exhibit near equal rates of mitochondrial fusion and fission
Frame by frame montage from confocal videomicrograph of untreated, uninfected mito-HUVECs showing mitochondrial fusion (purple arrowheads) and fission events (red arrowheads). The samples were imaged for 3 hours with frames captured every 5 minutes (**See also** Video 2.4.6; Adapted from Chowdhury et al. 2017; JCB).

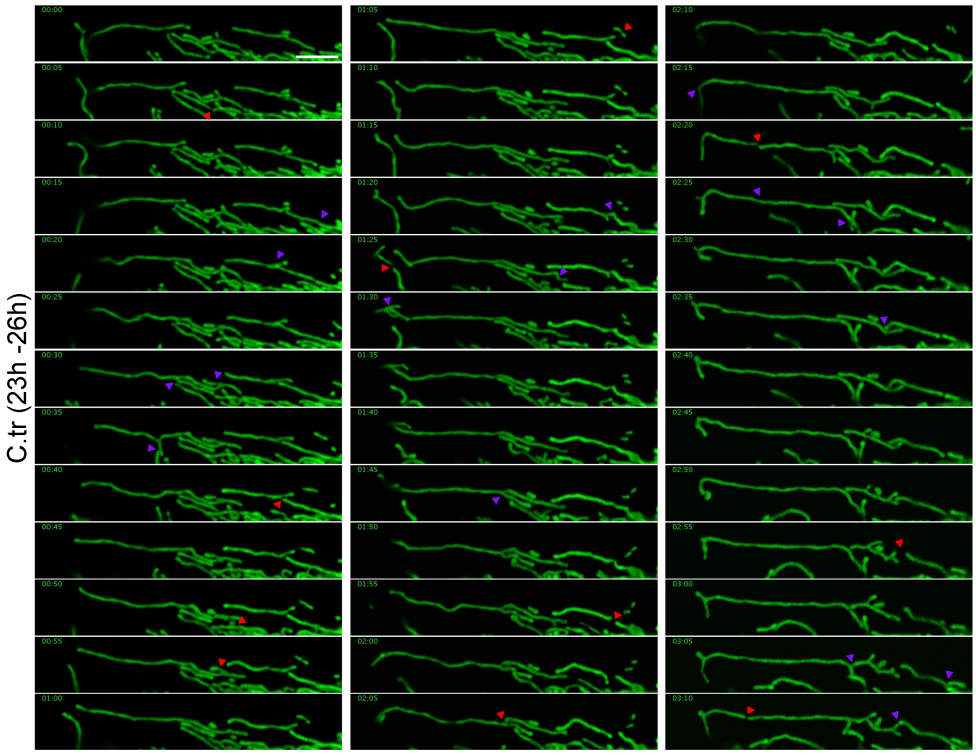

Figure 2.4.5 Chlamydia infected HUVECs exhibit lower rates of mitochondrial fission.
Frame by frame montage from confocal videomicrograph of *Chlamydia* infected (24 hours) mito-HUVECs showing mitochondrial fusion (purple arrowheads) and fission events (red arrowheads). The samples were imaged for 3 hours with frames captured every 5 minutes (**See also** Video 2.4.7; (Adapted from Chowdhury et al. 2017; JCB)).

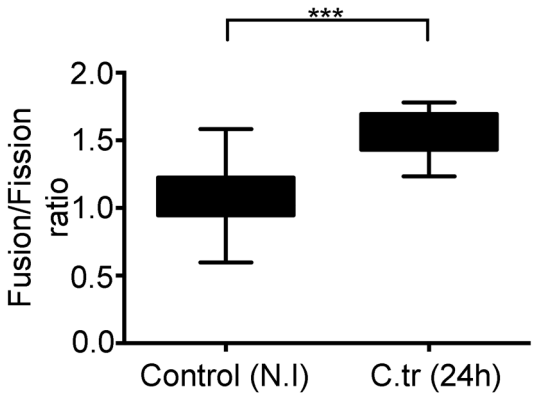

Figure 2.4.6 Fusion/Fission ratio is significantly elevated in Chlamydia infected HUVECs
Graph represents comparison between the fusion to fission ratios between non-infected and *Chlamydia* infected mito-HUVECs. Fusion/fission ratio in control (± SD) = 1.09±0.22 and and C.tr = 1.58±0.17 (*n=5;* 2 ROIs were analyzed from individual cells with 3 cells being chosen at random from every sample). Asterisks denote significance by Student's *t* test. *, P < 0.05; **, P < 0.01; ***, P < 0.001; ns, non significant (Adapted from Chowdhury et al. 2017; JCB).

2.5 Mitochondrial ATP production is essential for chlamydial growth and development

The effect of bacterial infection on host metabolism is of particular interest since it dictates, in a way, the fate of the cell and also tissue tropism of the bacterium. In certain cases, the interaction between the prokaryote and the eukaryotic host might be beneficial for both resulting in a symbiotic relationship, which is quite often the case with insects and protists (Chaston and Goodrich-Blair, 2010; Kupper et al., 2016). While this sort of symbiosis is not unusual between mammalian hosts and bacteria, the metabolic alterations effected by the presence of bacterial pathogens often disturb the cellular homeostasis. The former relationship is observed in the case of the gastric microbiota, which plays an important role in human health and disease (Bik et al., 2006). More commonly, pathogens such as *S. typhimurium*, *M. tuberculosis* and *L. monocytogenes,* effect major changes in the host metabolism. These changes often facilitate the progression of the invasion and the pathogenicity of the invading bacterium (Cawthraw et al., 2011; Eylert et al., 2008; Hartmann et al., 2008; Kim et al., 2010; Shin et al., 2011). It is well understood that the intracellular growth and development of Chlamydia is dependent on the metabolic capacities of the host cell. Chlamydia genome is equipped with metabolite transporters, which allow it to scavenge ATP amongst other metabolites such as amino acids, sphingolipids and nucleosides form the host cell (Karayiannis and Hobson, 1981; Robertson et al., 2009; Stephens et al., 1998; Tjaden et al., 1999). Indeed, Chlamydia infection has been shown to increase the rates of glycolysis in host cells (Moulder, 1970). At the same time, as discussed above the mitochondrial dynamics and architecture is closely tied to metabolic status of the host cell. In light of the inhibitory effect of Chlamydia infection on mitochondrial fission we felt it was prudent to investigate the role of mitochondrial source of ATP in infection progression.

2.5.1 miR-30c modulations affect cellular ATP levels

Several miRNAs have been shown to modulate cellular levels by directly targeting components of the respiratory chain (Nishi et al., 2010; Siengdee et al., 2015; Willers and Cuezva, 2011). Indeed both miR-30c depletion and miR-151-5p elevation have been implicated in loss of ATP levels in sperm cells (Zhou et al., 2015). While miR-151-5p elevation has a more direct role in ATP depletion since it targets the respiratory chain component Cytochrome b mRNA, we speculate that miR-30c might

indirectly affect ATP levels by promoting Drp1 dependent mitochondrial fragmentation. To investigate this line of reasoning, we measured the ATP levels of HUVECs transfected with miR-30c mimics and inhibitors. We also repeated these experiments after growing the cells in galactose containing media to prevent the mitochondria independent ATP production via glycolysis (Rossignol et al., 2004). While augmentation of miR-30c levels produced a mild but significant elevation of cellular levels, inhibition of miR-30c levels severely hindered ATP production and affected the cell viability of HUVECs grown in both normal and galactose supplemented media (Figure 2.5.1A and 2.5.1B). Additionally, sponge induced miR-30c depletion in HeLa cells also exhibited decreased ATP production when grown in galactose-supplemented media (Figure 2.5.2). We reasoned that this effect might arise due to the stabilization of p53 and Drp1 and eventual mitochondrial fragmentation seen upon miR-30c depletion. Thus we checked the effect of p53 and Drp1 overexpression on HeLa and H1299 $p53^{-/-}$ cells.

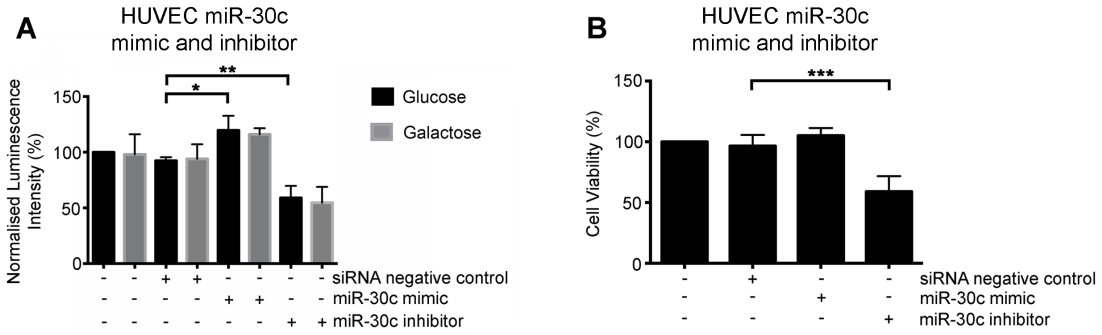

Figure 2.5.1 Artificial modulation of miR-30c affects mitochondrial ATP levels
(2.5.1A) Quantification of total ATP levels in HUVECs transfected with miR-30c mimic and inhibitor. Indicated samples were incubated in glucose free culture medium supplemented with galactose. The ATP luminescence was normalised to the ATP levels of untreated and un-transfected cells grown in glucose media. (2.5.1B) The cell viability of the corresponding samples were measured using MTT assay and represented as percentage of untreated and un-transfected cells. All data represent mean ± S.D. Asterisks denote significance by Student's *t* test *, P < 0.05; **, P < 0.01; ***, P < 0.001 (*n=3* for all panels; Adapted from Chowdhury et al. 2017; JCB).

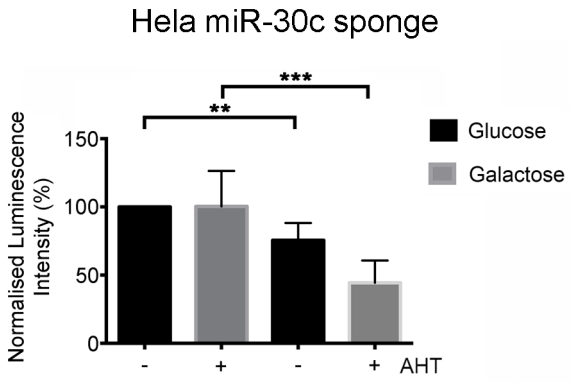

Figure 2.5.2 Induction of miR-30c sponge expression depletes mitochondrial ATP levels.
Quantification of total ATP levels in un-induced and AHT-induced HeLa-miR30c sponge cells. Indicated samples were incubated in glucose free culture medium supplemented with galactose. The ATP luminescence was normalised to the ATP levels of untreated and un-transfected cells grown in glucose media. Asterisks denote significance by Student's *t* test *, P < 0.05; **, P < 0.01; ***, P < 0.001 (*n=3;* Adapted from Chowdhury et al. 2017; JCB).

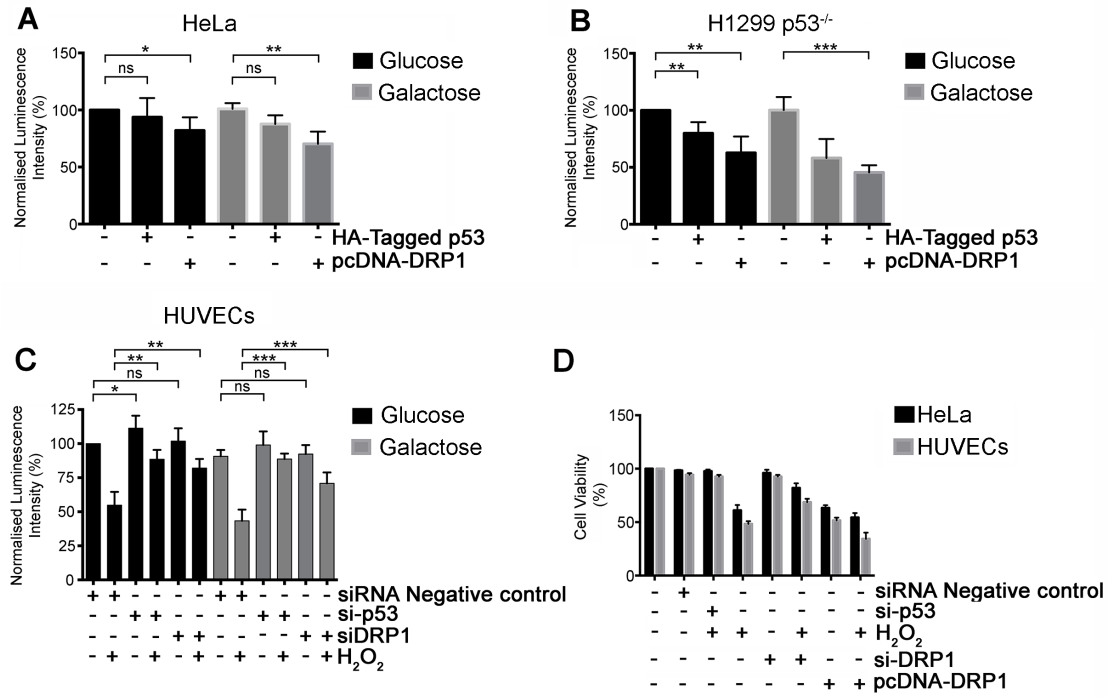

Figure 2.5.3 Artificial stabilization of p53 and Drp1 mildly affect mitochondrial ATP levels in HeLa and H1299 p53 null cells
(2.5.3A and 2.5.3B) The graphs depict the quantification of total ATP levels in HeLa and H1299 p53 null cells separately transfected with empty vector control, p53 and Drp1 overexpression vectors. Indicated samples were incubated in glucose free culture medium supplemented with galactose. (2.5.3C and 2.5.3D) Quantification of total ATP levels and viability of HUVECs and HeLa cells separately transfected with siRNAs against Drp1 and p53 and/or treated with and/or treated with 5 μM H_2O_2 for 15 minutes. Indicated samples were incubated in glucose free culture medium supplemented with galactose. The ATP luminescence was normalised to the ATP levels of untreated and un-transfected cells grown in glucose media. Asterisks denote significance by Student's *t* test *, P < 0.05; **, P < 0.01; ***, P < 0.001 (*n=3* for all panels; Adapted from Chowdhury et al. 2017; JCB).

Surprisingly, p53 and Drp1 overexpression did not have a significant effect on either of these cells the ATP levels when normalized to the cell viability (overexpression of

either protein has significantly affects the viability of HUVECs, HeLa and H1299 cells) of the cell lines (Figure 2.5.3A, 2.5.3B and 2.5.3D). Next we tested the effect of siRNA-mediated downregulation of p53 and Drp1 on the ATP levels of HUVECs. While such downregulation did not have any major effects on the ATP levels of control cells, it significantly abrogated the inhibitory effects of H_2O_2 (1 μM) treatment on HUVECs (Figure 2.5.3C). The results, when taken together, illustrate that while depletion of p53 and Drp1 might not enhance the cellular ATP production under normal conditions, miR-30c mediated downregulation of p53 and Drp1 prevents the oxidative stress induced loss of cellular ATP production. This line of reasoning leads us to speculate that the miR-30c dependent stabilization of the mitochondrial network seen during Chlamydia infection might contribute to the maintenance of normal ATP production in presence of oxidative stress generated as a result of the infection.

2.5.2 Mitochondrial ATP contributes to chlamydial growth and development.

To further understand the involvement of mitochondrial ATP in the intracellular growth and development of Chlamydia, we generated a stable HeLa cell line with inducible knockdown of the $F_1\beta$ subunit of the mitochondrial F_1F_O-ATPase. AHT treatment of these cells led to a massive depletion of the cellular ATP levels only when the cells were grown in galactose supplemented media, since HeLa, like other cancer cell lines, depends mainly on the glycolytic pathway for its ATP production (Figure 2.5.4A and 2.5.4B). Depletion of the $F_1\beta$ subunit also did not have any major effect on the cellular viability (Figure 2.5.4C).

High content image screening of the samples demonstrated that chlamydial growth and inclusion development were severely hampered in the ATH induced F1β subunit knockout HeLa cells grown in galactose (Figure 2.5.5A and 2.5.5B). A cell line with an inducible knockdown of metaxin 2 was used (Figure 2.5.4A, 2.5.4B and 2.5.4C). Metaxin 2 is a mitochondrial outer membrane protein and is known not to affect mitochondrial morphology and protein levels within the time frame of the experiment described above (Ott et al., 2012).

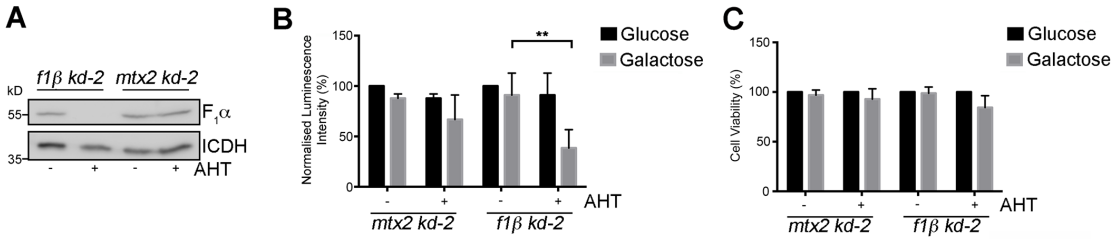

Figure 2.5.4 Knockdown of mitochondrial F_1F_O-ATPase subunit $F_1\beta$ depletes mitochondrial ATP levels
(2.5.4A) Immunoblot illustrates the depletion of $F_1\beta$ subunit and metaxin in isolated mitochondria from *f1βkd-2* and *mtx2kd-2* cells upon induction by AHT. The blots were probed with antibodies against $F_1\alpha$ subunit and Metaxin. Isocitrate Dehydrogenase (ICDH) was used as a loading control. (2.5.4B and 2.5.4C) The graphs represent the quantification of total endogenous ATP levels and viability of *f1βkd-2* and *mtx2kd-2* cells upon induction by AHT. Indicated samples were incubated either in glucose containing media or for 16 hours in glucose followed by 8 hours in galactose supplemented media. Asterisks denote significance by Student's *t* test *, P < 0.05; **, P < 0.01; ***, P < 0.001 (*n=3* for all panels; Adapted from Chowdhury et al. 2017; JCB).

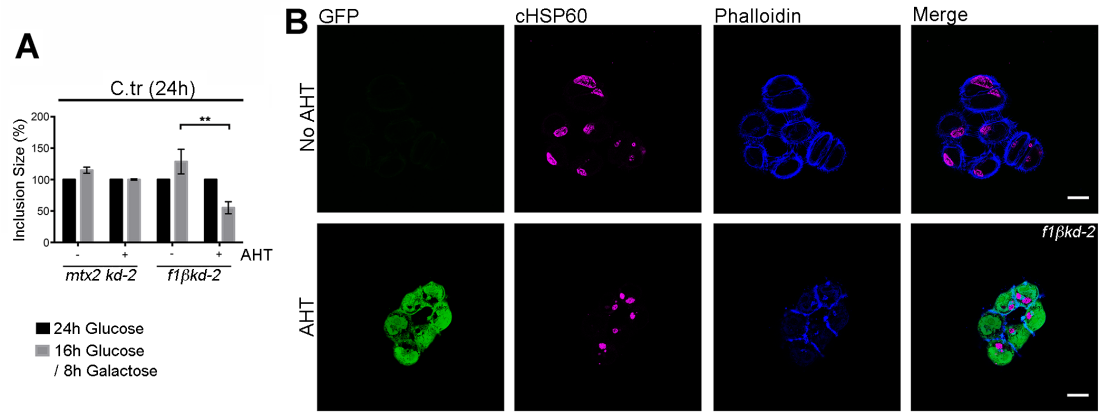

Figure 2.5.5 Knockdown of mitochondrial F_1F_O-ATPase subunit $F_1\beta$ hinders chlamydial growth
(2.5.5A) Quantification chlamydial inclusion sizes within non-induced and induced *mtx2kd-2* and *f1βkd-2* cells infected with *Chlamydia* for 24 hours. Indicated samples were grown in glucose containing media or for 16 hours in glucose followed by 8 hours in galactose supplemented media. (2.5.5B) Representative epifluorescence micrographs of non-induced and induced *f1βkd-2* cells infected with *Chlamydia* for 24 hours. Asterisks denote significance by Student's *t* test *, P < 0.05; **, P < 0.01; ***, P < 0.001 (*n=3* for all panels; Adapted from Chowdhury et al. 2017; JCB).

Chapter 3. Discussion

Since the discovery of miRNAs, a significant fraction of small RNA research has been focused on elucidating the regulation and the role of miRNAs in pathological conditions. The effort has been largely successful since currently there are several hundred miRNAs that are well known to be involved in conditions as diverse as leukemia and dementia (Luan et al., 2015; Sorensen et al., 2016). Discovery of differential regulation of miR-393 in *Arabidopsis thaliana* upon *Pseudomonas syringae* infection opened up an entirely new chapter of miRNA research: role of miRNA in infection. This development was, however, not entirely unprecedented keeping in mind the role of miRNA in the regulation of the T-cell and B-cell activation and differentiation and more importantly, their role in the modulation of the innate immunity (Luo et al., 2015; Rosa et al., 2007; Teteloshvili et al., 2015; Trifari et al., 2013; Zhang et al., 2009). The section on miRNAs in this work tries to throw some light on the broad range of function that miRNAs participate in. Several studies have made significant contributions towards the role of miRNAs in context of bacterial infection as discussed in section 1.2.8 (MicroRNAs in Infection). These studies have specifically pointed out that infection by pathogens such as H. pylori, Listeria and Salmonella amongst others tend to differentially regulate particular miRNAs that either assist in infection or promote the triggering of the innate immune system (Chang et al., 2015; Izar et al., 2012; Maudet et al., 2014; Schulte et al., 2011; Xiao et al., 2009).

Keeping in mind the broad range of effects that an intracellular pathogen such as *Chlamydia* can have on the host cell, it would not be surprising to find that cells infected with *Chlamydia* might exhibit a unique miRNA expression profile. Over the last decade it has become increasingly evident that chlamydial infection effects major alterations in the host signaling pathways. These alterations manifest right at the beginning of the infectious cycle (adhesion of the EBs to the host cells) increasingly altering the host cell metabolism, intracellular environment and cytoskeletal architecture to facilitate the growth and development of the pathogen within the cell (Ajonuma et al., 2010; Carabeo et al., 2002; Hackstadt et al., 1996; Jiwani et al., 2012; Mehlitz et al., 2010; Schramm et al., 1996). When one considers the extent to which miRNAs are involved in all of these processes in mammalian cells, there remains little doubt that the regulation of miRNAs, however minute, are affected by the infection process. One of the most striking aspect of a *Chlamydia* infected cell is its ability to withstand pro-apoptotic stress generated by a wide range of stimuli such

as tumor necrosis factor-α, etoposide, UV radiation and FAS antibody (Fan et al., 1998; Fischer et al., 2004; Rajalingam et al., 2008). This attribute of *Chlamydia* infected cells clearly demonstrates the alteration in the signaling pathways of the host and highlights the need to understand how the miRNOME of these cells respond to such changes or contribute to the establishment of the alterations. It is speculated that the need to protect the cells from apoptotic stimuli by Chlamydia is not just to ensure the completion of its life cycle since the epithelial or endothelial host cells infected by the pathogen live longer than the time necessary for the completion of the chlamydial developmental cycle. One possible reason for the *Chlamydia* induced apoptotic block is to protect the cell from the cytotoxic effects of the presence of *Chlamydia* itself (Fischer et al., 2004). Chlamydial growth necessitates alterations in signalling circuits that control metabolic pathways, cytoskeletal modulations and transcription of specific mRNA and production of oxidative stress at certain stages of development (Boncompain et al., 2010; Carabeo et al., 2002; Jiwani et al., 2012; Nicholson et al., 2003; Siegl et al., 2014). Such events can easily lead to activation of the pro-apoptotic pathways at any stage of the chlamydial developmental cycle and, to an extent, justifies the multiple strategies employed by *Chlamydia* to ensure host cell survival (Desouza et al., 2012; Rottner et al., 2011; Wensveen et al., 2011).

When considering the role of miRNAs in cellular health and homeostasis, it is impossible to focus on just one pathway since the miRNA network is intricately linked with all major cellular processes. While new implications of changes in the expression of a specific miRNAs are being discovered every day, certain families of miRNAs have been shown to be indispensible for the regulatory control of apoptosis, metabolism and cell cycle, to name a few. ApoptomiRs are a class of miRNAs that have been shown to regulate the apoptotic pathways via direct post-transcriptional regulation of diverse pro- and anti-apoptotic proteins. Deep sequencing studies have also identified several miRNAs that are differentially regulated during metabolic shifts in cells and during metabolic disorders. In many instances these sets of miRNAs overlap with each other and with Immuno-miRs, miRNAs regulating development of immune cells or immune pathways (Chen et al., 2016; Croci et al., 2016; Ferreira et al., 2014; Kroesen et al., 2015; Pinti et al., 2017; Ramirez et al., 2013; Rottiers and Naar, 2012; Vecchione and Croce, 2010).

Studies have shown that *Chlamydia* infection results in an altered transcriptional profile and engenders a significant metabolic shift while down regulating several and subverting pro-apoptotic proteins and pathways (Siegl et al., 2014; Xia et al., 2003). While miRNAs are important regulators of all these pathways, the mitochondrial

network is an essential focal point at which both, metabolic and apoptotic regulation converges. The architecture of the cellular mitochondrial network is both affects and is modulated by the metabolic status of the cell and is an integral part of apoptotic induction. miRNA mediated alteration in apoptotic response in leukemia affects mitochondrial dysfunction and promotes cytochrome c release while miR-143, a miRNA implicated in colon cancer, promotes apoptosis by interfering with mitochondrial function (Cimmino et al., 2005; Zheng et al., 2016). The mitochondrial network has been known to be dynamic and this mobility is crucial for mitochondrial function and for the metabolic homeostasis within the cell. Aberrant and excessive fragmentation of the mitochondrial network contributes to and is promoted during apoptotic induction. The miR-30 family has been shown to regulate the mitochondrial dynamics via a p53 dependent regulation of the mitochondrial fission regulator Drp1 (Li et al., 2010). Drp1 dependent mitochondrial fission is essential during apoptosis and is also inhibited by the downregulation of calcineurin by miR-499 (Wang et al., 2011a).

Chlamydia trachomatis is one of the most prevalent sexually transmitted pathogen and is a subject of keen interest in the field of obligate intracellular bacterial research. Till date, many elegant studies have helped in the understanding the intricacies of the host pathogen interactions during *Chlamydia* infection covering events from changes in signalling pathways during adhesion, infection induced metabolic shifts, alteration in exocytic and endocytic vesicular trafficking and modulation of cytoskeletal architecture to facilitate inclusion growth (Mehlitz et al., 2010; Robertson et al., 2009; Sharma et al., 2011; Stallmann and Hegemann, 2016; Xia et al., 2003; Ying et al., 2007). However, the effect of *Chlamydia* infection on the host cell microRNA circuitry has never been studied. In light of the effects and implication of miRNA regulation discussed above, examining the miRNA profile of *Chlamydia* infected cells might provide a deeper understanding of the cellular response to the presence of the chlamydial inclusion in the cytoplasm and the modifications engendered by the infection to facilitate chlamydial growth and survival within the cell. Such an approach would pinpoint miRNAs that are implicated in the regulation of cellular metabolism and/or apoptotic governance.

This work attempts, by means of miRNA deep sequencing, super resolution microscopy and biochemical assays, to link the effect of chlamydial infection on the mitochondrial morphology via alteration in the expression of a host miRNA. In the same context, this work tries to demonstrate the dependence of intracellular chlamydial growth on the host-encoded miR-30c and on the mitochondrial integrity of the host cell.

3.1 Infection induced changes in miRNA expression profile

The advent of RNA sequencing has allowed researchers to paint a detailed picture of the transcriptional landscape both in prokaryotes and eukaryotes. The development in the fields of RNA sequencing, with respect to the mechanistic finesse and the corresponding algorithmic approaches, has progressed in leaps and bound over the last decades. Not only the volume and the quality of data that can be gathered from a miniscule quantity of starting sample increased, the time taken for such in depth analysis has also been reduced to a matter of weeks. Such phenomenal advancements in the arena of sequencing technologies have made transcriptomic profiling of unique cellular conditions accessible to research groups working on diverse organisms and disease models. A typical workflow of a RNA sequencing or RNA-seq experiment begins with the isolation of the sample RNA from the tissues, cells, bacteria, viruses or host cells infected with pathogens of interest followed by appropriate quality control and preparation of a cDNA library (Accerbi et al., 2010; Castoldi et al., 2007; Eminaga et al., 2013; Hafner et al., 2012; Wang et al., 2008). This library is then amplified and used for deep sequencing. In this work we used RNA collected from uninfected and *Chlamydia* infected HUVECs at different time points to create the cDNA library and sequenced it on an Illumina HiSeq 2000 sequencer. A particular consideration that applies specifically to the sequencing of mature miRNAs is their lack of poly(A) tails and sequence difference between members of a single miRNA family (Cai et al., 2004; Cloonan et al., 2011). The poly(A) tails of mRNAs can be used for selective enrichment and as a universal primer binding site for cDNA preparation. Furthermore, miRNAs exhibit a considerable amount of sequence length and GC content variability, all of which contribute to a higher degree of complexity in the sequencing workflow when compared to mRNAs (Ebhardt et al., 2010; Kim et al., 2012). Taking all of these factors in consideration, next-generation sequencing for miRNA profiling has a higher hand over hybridization based or qRT-PCR-based methods not only because of its ability to distinguish between individual miRNAs differing by single nucleotides but also because it allows detection of novel miRNAs (Chiang et al., 2010; Newman et al., 2011).

In the present study, use of miRNA-seq allowed us to study a hitherto unknown expression profile of miRNAs upon *Chlamydia* infection. Of particular interest is the differential expression of several miRNAs previously implicated in the regulation of apoptotic pathways (Figure 2.1.1A, 2.1.2A and 2.1.2B). As discussed above, the intracellular life style of *Chlamydia* and its dependencies on the host metabolism

justifies the ability of *Chlamydia* to impose an apoptotic block on the host cell. While there are numerous evidences of protein-based strategies of *Chlamydia* induced apoptotic inhibition, we now show that there is an additional layer of regulation imposed by miRNAs that probably aids in enhancing the longevity of *Chlamydia* infected cells. Similar studies in other pathogens have revealed equally startling data where it has been demonstrated that *Listeria* infection promoted modulation of miRNAs involved in immune signalling while mycobacteria infection affects miRNAs involved in endo-lysosomal pathways and targets essential Rab proteins (Bettencourt et al., 2013; Izar et al., 2012; Vegh et al., 2015). Similarly *Salmonella* infected macrophages and epithelial cells also exhibit changes in the expression of miRNAs involved in cell cycle, immune regulation and modulation of cytoskeletal structures (Hoeke et al., 2013; Maudet et al., 2014; Schulte et al., 2011). Additionally, the Salmonella infection also promotes depletion of the host SUMOylation pathway proteins Ubc-9 and PIAS1 via the upregulation of miR-30e to ensure its intracellular survival (Verma et al., 2015). In this work, using the webtool DIANA-miRPath v2.0, we demonstrate that the miRNAs regulated upon *Chlamydia* infection, apart from participating in apoptotic regulation, are also involved in a variety of cancer signalling pathways (Figure 2.1.2C). This finding is significant particularly in the light of the speculations that *Chlamydia* infection could increase the risk of cervical and ovarian cancer (Madeleine et al., 2007; Ness et al., 2003). Bacterial infection mediated oncogenesis was first described in *Helicobacter pylori* infected patients (Forman et al., 1991; Suganuma et al., 2008). Expression of miR-21, one of the most well studied miRNAs, is elevated upon *H. pylori* infection (Zhang et al., 2008). Elevation of miR-21 is reported widely in several oncogenic conditions including gastric and ovarian cancer and is a robust inhibitor of apoptosis (Buscaglia and Li, 2011; Riccioni et al., 2015; Yan et al., 2008). It is well known that apoptosis evasion and inhibition of pro-apoptotic pathways are hallmarks of tumorigenic growth and cancer development. While it is fascinating to find miRNAs involved in oncogenesis being regulated upon *Chlamydia* infection, it is not altogether surprising given the potent anti-apoptotic tendencies of *Chlamydia* infected cells.

Chlamydia induced downregulation of the tumour suppressor protein p53 furthers fuels the speculation of the pathogen's ability to promote oncogenesis. Our group previously demonstrated that *Chlamydia* infection promoted the proteasomal degradation of p53 and promoted a significant metabolic shift in HUVECs to facilitate the infection process (Siegl et al., 2014). In this work we show that along with proteasomal degradation, *Chlamydia* also enforces a translational block on p53 by upregulating the expression of miR-30c. miR-30c is upregulated upon *Chlamydia*

infection in HUVECs and hFIMBs (Figure 3A to 3D) and by specifically targeting miR-30c using miRNA sponges and inhibitors, we show that the presence of miR-30c is indispensable for the establishment of *Chlamydia* infection in HeLa and primary HUVEC cells (Figure 4C and 4D). The upregulation of miR-30c appears to be particularly essential for chlamydial growth and development within primary cells like HUVECs, HFF and hFIMB cells. Primary or non-transformed cells, unlike cell of cancerous origin, such as HeLa, strongly depend on the mitochondrial source of ATP (Ward and Thompson, 2012). Since it had been demonstrated previously that the members of the miR-30 family are able to modulate Drp1 mediated mitochondrial fission, we speculated that *Chlamydia* mediated stabilization of miR-30c could have a role on the mitochondrial architecture of the host cell.

The miR-30c family comprises of five members, miR-30a through e, and has been implicated in multiple pathogenic conditions particularly in cardiovascular diseases and breast cancer. While in case of breast cancer miR-30c enhances the invasiveness of metastatic breast cancer cells, miR-30c depletion has been shown to promote apoptosis and enhances cell proliferation in myocardial cell models (Dobson et al., 2014; Liu et al., 2016a; Ward and Thompson, 2012). All miR-30 family members share a conserved binding site on the p53 3' UTR and can regulate the expression of p53 to an extent upon artificial modulation while depletion of miR-30c promotes ROS generation and downregulates mitochondrial oxygen consumption (Wang et al., 2017a). This effect is also observed in case of miR-30c modulation in HUVECs (Fig 4A and 4B). Furthermore, as has been shown before, we also found that miR-30c modulation can deplete the mitochondrial fission regulator Drp1 since p53 is an essential transcription factor responsible for the stress-induced transcription of the Drp1 mRNA (Li et al., 2010; Wang et al., 2017a).

Several groups working on mitochondrial dynamics have investigated the effect of Drp1 inhibition and overexpression on the mitochondrial morphology in great detail. It is well established that Drp1 mediated fission is essential not only for the healthy recycling of mitochondrial particles, mitochondrial biogenesis but also for the pre-apoptotic fragmentation of mitochondria (Frank et al., 2001; Roth et al., 2014; Smirnova et al., 2001). Presence of oxidative stress or any general pro-apoptotic stimuli promote Drp1 dependent mitochondrial fragmentation and such fragmentation essential for the proper execution of the apoptotic cascade. Inhibition of mitochondrial fission via blockage or depletion of Drp1 stalls the release of cytochrome c and apoptotic process (Qi et al., 2013; Su et al., 2014). Alternatively, Drp1 dependent mitochondrial fission is also prevented during conditions of nutrient starvation to promote mitochondrial elongation and enhance the OXPHOS reactions

(Gomes et al., 2011). In order to understand if *Chlamydia* mediated enhancement of miR-30c levels had any effect on the mitochondrial architecture we investigated the mitochondrial morphology in HUVECs upon artificial modulation of miR-30c. Inhibition of miR-30c in both HeLa cells and in HUVECs promoted massive fragmentation of the mitochondria along with loss of cell viability while artificial augmentation of miR-30c in HUVECs engendered a hyper-fused architecture of the mitochondrial resembling a Drp1 knockdown phenotype (Figure 5A-5D; 6A and 6B). This observation bolstered our speculation that *Chlamydia* infection affects the mitochondrial morphology and function and thus we focused our attention towards the investigation of the mitochondrial form and function upon *Chlamydia* infection.

3.2 Infection induced alteration in the mitochondrial architecture

While the intracellular rearrangement that follows the establishment of *Chlamydia* infection has generated great interest in the field of intracellular pathogen research, the role or the effect of the infection on the mitochondrial architecture has remained largely unexplored. Studies have focused on the nutrient acquisition by the chlamydial inclusion from the mitochondria and this dependency of *Chlamydia* was further exemplified by our experiments that demonstrate the depletion of Drp1 in HUVECs and hFIMBs upon *Chlamydia* infection. Drp1, as described in section 1.3.4, forms ring like aggregates on the mitochondrial surface and uses GTP hydrolysis to cleave mitochondrial fragments (Ingerman et al., 2005). Artificial stabilization of Drp1 has been shown to lead to mitochondrial hyperfission, loss of ATP levels and eventual cell death (Bras et al., 2007). This effect of Drp1 modulation was particularly interesting since mitochondrial ATP synthesis is indispensible in primary cells such as HUVECs. To understand the effect of Drp1 on *Chlamydia* infection we overexpressed wild type and mutant Drp1 molecules in HUVECs and observed that while *Chlamydia* infection depleted the endogenous Drp1, artificial overexpression of wild type Drp1 completely abrogated *Chlamydia* infection. Alternatively, siRNA mediated downregulation of Drp1 or expression of dominant negative mutant Drp1 promoted *Chlamydia* growth and development. These observations further confirmed the chlamydial dependency on the integrity of the mitochondrial network.

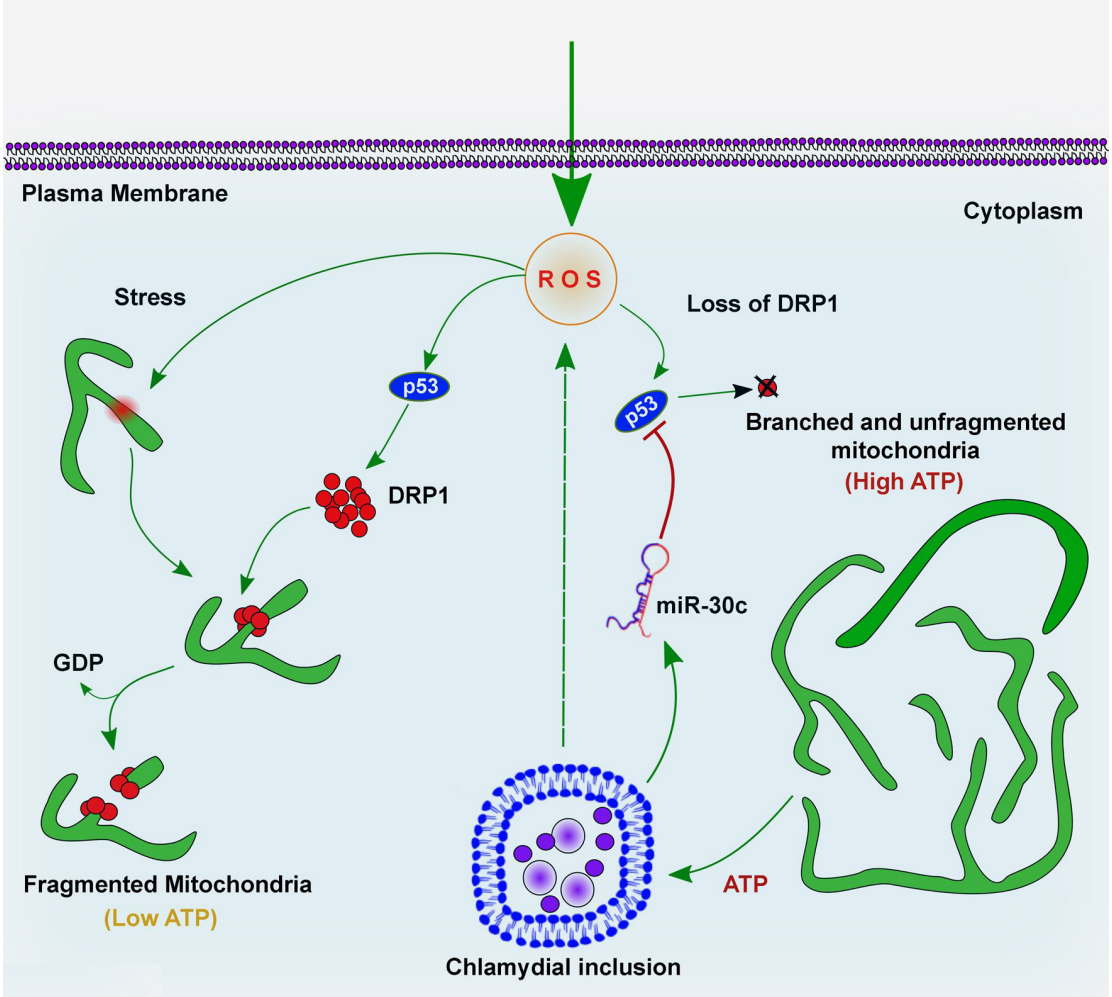

Fig 3.2.1. A schematic representation of the miR-30c mediated protective effect of *Chlamydia* infection on the mitochondrial network of the host cell

The study of mitochondria and its fusion/fission machinery has been greatly enhanced by the advances in confocal and super-resolution microscopy. Groups working on advanced super-resolution microscopy have often used the Drp1 induced mitochondrial fission events as way of challenging the limits of optical resolution of novel imaging protocols (Jakobs and Wurm, 2014; Ji et al., 2015; Rosenbloom et al., 2014). While STED, dSTORM and PALM all have their own area of specialized usage and have been applied to the study of mitochondria and its fission/fusion machinery, **S**tructured **I**llumination **M**icroscopy (SIM) has carved out its own niche owing to the ease of access and simplicity of sample preparation. SIM enhances optical resolution up to two fold by illuminating the samples with spatially structured excitation light. This technique results in the acquisition of data in form of Moiré fringes that is well beyond the resolution observed on a normal confocal microscope (Gustafsson, 2000; Gustafsson, 2005). The accessory software that accompanies a SIM platform usually extracts this data by reconstructing a series of images taken in

this fashion (Muller et al., 2016). The lateral resolution of the data acquired by SIM approaches ~100 nm while the axial resolution is around 300 nm. Samples prepared for SIM can be stained using common organic dyes and recently, it has even been possible to preform live cell imaging on SIM platforms (Gustafsson et al., 2008; Kner et al., 2009). The only downside to this technology is the need for complex calculations that are required for the reconstruction of the final image. However, most SIM platforms are accompanied by suitable processing software capable of carrying out these calculations. The application of super resolution microscopy in current day bioscience research can be illustrated by the fact that the Noble prize in 2014 was awarded to E. Betzig, S. Hell and W. Morener for the their contributions towards the development of super resolution fluorescence microscopy. The increased resolution achieved by the advancements have not just contributed towards a better picture of the intracellular landscape but also aided the understanding of organellar dynamics and architecture.

In this work we used SIM in order to track the availability of Drp1 aggregates in *Chlamydia*-infected cells and quantify their colocalization on the mitochondrial surface. We observed that *Chlamydia* infection induced depletion of Drp1 transcription reduced the abundance of Drp1 aggregates in HUVECs and significantly curtailed their localization on the mitochondrial surface. Drp1 has been described as the essential point of control to regulate the fission of mitochondria. This is emphasized by the fact that Drp1 under goes a plethora of post-translational modification that governs its cytoplasmic localization, protein stability, mitochondrial translocation and its ability to cause fission (Filichia et al., 2016; Gawlowski et al., 2012; Horn et al., 2011; Jahani-Asl and Slack, 2007; Prudent et al., 2015). Recently it has been shown that the formation of the ring-like Drp1 aggregates is aided by mitochondria associated endoplasmic reticulum that pre-constricts the mitochondrial fragments, and by another dynamin family protein Dyn2 that carries out the final cut of the mitochondria at the fission sites (Ji et al., 2015; Lee et al., 2016). However, as evidenced in prior studies, loss of the Drp1 protein is inhibitory to mitochondrial fission and this effect is also observed upon *Chlamydia* infection. The *Chlamydia* induced block on Drp1 transcription via loss of p53, mediated by miR-30, reduced the availability of Drp1 and resulted in a hyper-fused architecture of the mitochondrial network. Both p53 and Drp1 respond to ROS generated by extrinsic or intrinsic sources. Hydrogen peroxide is a well-known agent that induces cell death by the mitochondrial pathways and has been shown to deplete miR-30c, stabilize p53 and upregulate Drp1 expression (Uberti et al., 1999; Watanabe et al., 2014). Interestingly, *Chlamydia* infected cells not only are resistant to such ROS induced p53 stabilization

and loss of miR-30c, but also exhibit minimal mitochondrial fragmentation upon H_2O_2 treatment. We believe, amongst other reasons, such a resistance to ROS mediated mitochondrial fragmentation is enforced by the miR-30c dependent depletion of p53 and Drp1 thus providing a line of defense against the mitochondrial fragmentation induced apoptotic events.

The resistance of *Chlamydia*-infected cells to ROS mediated mitochondrial fragmentation is of significant interest since it is well known that chlamydial growth and development needs ROS production within the host cell. It has been shown that *Chlamydia* periodically induces ROS via the NLRX1 - NADPH oxidase pathway (Abdul-Sater et al., 2010; Boncompain et al., 2010). While ROS production in the host cell upon infection by other pathogens such as *Salmonella* and *Helicobacter* aid in the orchestration of the innate immune response cascades, in case of *Chlamydia* ROS is necessary for activation of caspase-1, an essential step for chlamydial growth (Abdul-Sater et al., 2009; Handa et al., 2010; Mehta et al., 1998). However, any amount of ROS produced within the host cell, however minute, is likely to affect the mitochondrial function and morphology to a certain extent (Li et al., 2009). While we observed that the mitochondrial architecture was well preserved upon *Chlamydia* infection, this did not reflect the internal environment of the mitochondrial matrix. To understand the effect of *Chlamydia* induced ROS on the mitochondrial matrix we utilized the novel stress responsive protein MitoTimer (Ferree et al., 2013; Laker et al., 2014). While several commercial kits are available for detecting cellular and mitochondrial superoxide production (DFCDA; MitoSOX) we were unable to use them in conjunction with *Chlamydia* infection since most of these stains also stained the chlamydial inclusion along with the mitochondria. The MitoTimer protein targeted to the mitochondria proved to be an excellent tool to detect stress within the mitochondrial matrix at specific time points of chlamydial growth. We observed that the mitochondrial matrix within infected cells was reversibly stressed at 8 and 24 hours post infection. Furthermore the mitochondrial matrix of these cells was protected against the effects of extrinsic ROS stress created by the addition of H_2O_2 to the culture media. While artificial downregulation of p53 and Drp1 also abrogated the effect of H_2O_2 on the mitochondrial matrix of non-infected cells we speculate that *Chlamydia* infected cells might also have additional mechanisms to safeguard mitochondria against such effects.

One of the primary reasons for *Chlamydia* to protect the mitochondrial integrity, both structurally and in terms of matrix environment, besides preventing apoptosis would be to ensure the supply of metabolites necessary for chlamydial development, especially ATP. Chlamydial growth can be hampered by the loss of the mitochondrial

TIM/TOM complexes, however the actual reason for such an effect was not known. During the course of this work, we became aware of the close dependence that exhibits on the host mitochondrial ATP production. This was particularly true in cases where, as a part of the experimental setup, the glycolytic pathway in HeLa cells was inhibited along with a knockdown of the $F_1\beta$ subunit of the mitochondrial F_1F_O-ATPase. This rendered the HeLa cells significantly incapable of producing ATP either by glycolysis or via the mitochondrial respiratory chain. Unsurprisingly, under such conditions, *Chlamydia* failed to propagate. The effect of miR-30c modulation on the mitochondria seemed likely to affect ATP production since elongated mitochondria have been shown to be more efficient in producing ATP and mitochondrial fission blockages have been observed under condition of nutrition starvation. Most interestingly, miR-30c depletion in HUVECs and HeLa cells exhibited strong ATP depletion under condition of glycolytic blockage. We speculated that this effect might be due to the stabilization of p53 and Drp1 upon miR-30c depletion, however, artificial stabilization of either protein did not significantly affect ATP production. Oxidative stress affects the ATP production of a cell by altering the mitochondrial fusion/fission ratio. A decrease in the fusion/fission ratio due to elevation of Drp1 leads to a fragmented mitochondrial architecture, which is less efficient in producing ATP (Sarin et al., 2013; Touvier et al., 2015). We rationalized that the effect of ROS generated during the growth of *Chlamydia* must need to be neutralized somehow in order to keep the production of ATP unharmed. Upon comparing the levels of ATP in cells transfected with Drp1 and p53 siRNAs and treated with H_2O_2 we found that depletion of either protein protected the cells against the disruptive effects of H_2O_2 generated ROS on the cellular ATP production. These results indicated that the upregulation of miR-30c upon infection perhaps serves to partially ameliorate the effects of infection induced oxidative stress.

The mitochondrial architecture of the cell is governed by a fine tuned mechanism that responds to stress, nutritional deprivation, survival, and apoptotic signals (Dahlmans et al., 2016; Suen et al., 2008; Wang et al., 2017b). In each of the above cases the fusion and fission machinery reacts by both promoting the branching and elongation of the mitochondrial fragments or by inducing fragmentation of the network. ROS mediated mitochondrial fragmentation is catalyzed by Drp1 dependent mitochondrial fission that creates smaller mitochondrial particles, which can then be targeted for mitophagy. Alternatively, under nutritional stress, indiscriminate autophagy also leads to organelle loss. Under such conditions Drp1 is phosphorylated to prevent mitochondrial fragmentation and fusion is promoted to elongate the mitochondrial fragments (Frank et al., 2012; Gomes et al., 2011; Lee et al., 2012). Using live cell

video-microscopy, we checked if the fusion/fission ratio of the mitochondrial network in HUVECs was affected by *Chlamydia* infection. While we found a minimal change in the rates of mitochondrial fusion upon *Chlamydia* infection, the rates of mitochondrial fission was significantly decreased thus increasing the over all fusion/fission ratio in the infected cell. This scenario is reminiscent of a cell facing nutritional stress owing to the high demands of metabolites engendered by the presence of *Chlamydia*. However, unlike cells facing nutritional stress we did not find any increase in the rates of fusion and the decease in the rates of fission was a result of Drp1 depletion and not by negative phosphorylation of Drp1.

Taken together, this work attempts to demonstrate the effect of chlamydial infection and growth on the host mitochondrial form and integrity via the regulation of a host miRNA. The results here suggest an indispensible dependency of *C. trachomatis* on the mitochondrial fission machinery and encourage further investigations into the regulation of *Chlamydia* induced alterations in the host cell architecture.

3.3 Future perspectives

Through the course of this work we have tried to establish the impact that *Chlamydia* infection has on the miRNA profile of HUVECs. We describe a *Chlamydia* induced up regulation of miR-30c, a miRNA known to affect the mitochondrial dynamics via a p53 mediated down regulation of the mitochondrial fission regulator Drp1. However, we have not established a pathway by which miR-30c is regulated upon infection. The focus on miR-30c has been quite recent and very few studies have been preformed on the signalling pathways that regulate miR-30c transcription. While miR-30c-1 is produced as a mirtron from the intronic region of the host gene NFYC (chromosome1), miR-30c-2 is present as an independent gene locus on chromosome 6. Bioinformatic analysis of he putative promoter region of both the loci revealed binding sites for the transcription factors C/EBPα (Katzerke et al., 2013), GATA-4, NF-κB-p50:p50 dimer and NFATc2. *C. trachomatis* can be linked to the C/EBP and NFκB signalling pathways both, which are essential for infection-induced IL-8 induction (Buchholz and Stephens, 2006). These preliminary results open up a path for determining the means by which *Chlamydia* can modulate the transcription of miR-30c.

The idea that *C. trachomatis* regulates the mitochondrial morphology upon infection is novel, however, *C. psittaci* has been shown to form close contact sites with the mitochondria (Matsumoto et al., 1991). While we have no concrete proof of such

contact between *C. trachomatis* and the mitochondrial network, given the extreme dependence that the pathogen shows on the mitochondrial network of primary cells this area needs to be revisited. Using the advanced electron microscopy techniques available today, i.e. high pressure freezing and Cryo-Electron tomography it would be possible to visualize if such interaction are indeed happening between *Chlamydia trachomatis* and the mitochondrial network.

Finally, the elongation of mitochondrial fragments observed upon *Chlamydia* infection is, as mentioned before, reminiscent of the mitochondrial branching and elongation observed upon severe nutritional stress. The elongation of mitochondria not only serves to enhance ATP production but also spares the mitochondrial fragments from mitophagy. No studies regarding the mitophagy or regulation of the mitophagy machinery, especially with relation to PINK1/PARKIN regulation exist in *Chlamydia* infected cells. Based on our observation of Drp1 down regulation it would be interesting to check if mitophagy in an infected cell is blocked simply due to the depletion of Drp1 or there are additional regulatory mechanisms at play for mitochondrial recycling. This study would also engender a further investigation into the role of mitochondrial biogenesis upon *Chlamydia* infection. In essence we hope that this study will open up several new frontiers of mitochondrial biology with respect to infection biology.

Chapter 4. Methods

4.1 Eukaryotic Cell Biology

4.1.1 Eukaryotic cell culture and maintenance

All cell lines used in this work are detailed in Table 5.1. The cell lines were grown at 37°C in a water-saturated atmosphere supplemented with 5% CO_2. HeLa229, H1299 $p53^{-/-}$ and hFIMB cells were cultured in RPMI-1640 supplemented with 10% FCS. HUVECs were cultured in Medium 200 supplemented with Low Serum Growth Supplement (LSGS). HFF cells were cultured in Fibroblast Basal Medium supplemented with 15% FCS.

HUVECs and hFIMBS, being primary cells were not maintained via continuous culture like HeLa229 or H1299 $p53^{-/-}$ cell lines. All experiments performed with HUVECs and hFIMBS utilized cells not more than 5 passages old. For passaging, cells were washed with warm (37°C) 1x PBS followed by incubation with Trypsin/EDTA (1.5 ml for HeLa229, H1299 $p53^{-/-}$; 1:1 mix of Trypsin/EDTA and PBS for HUVECs and hFIMBS) for 2-3 minutes. Post detachment the cell suspension is mixed with complete growth medium and gently agitated by pipetting to avoid cell clumping. The cells are seeded as per requirement. For experiments involving miRNA transfection and/ or mitochondrial studies, HUVECS and hFIMBs were freshly thawed and cultivated overnight in T75 (HUVECs) or T25 (hFIMBs) flasks. The following day, cells are split into three subsequent flasks and seeded as per requirement.

4.1.2 Cryopreservation and thawing of cell lines

All cell lines were cataloged and stocked in ultra low temperature (liquid nitrogen tank) to ensure viability and data preservation. For long-term cryopreservation, a T75 flask of the cell line was trypsinized as described above followed by a brief (5 min; 4°C) centrifugation at 800 g. The cell pellet is suspended in 1 ml cell freezing medium (80% FCS, 15% LSGS-supplemented medium-200 and 5% DMSO for HUVECs; 90% FCS and 10% DMSO for all other cell lines) and pipetted into cryotubes. The cyrotubes are subjected to gradual cooling (-1°C/min) within isopropanol filled freezing chamber within an -80°C freezer. After 24 hours the cells are transferred the to liquid nitrogen tank.

Cells were subjected to a gradual thawing process at room temperature followed by suspension of the cell-cell-freezing mixture in 6 ml of warm complete growth media. This mixture is then centrifuged at 800 g (5 min; 4°C) to remove traces of DMSO. The cell pellet is then suspended in warm growth media and plated as needed.

4.1.3 Transfection of cells

Transfection of plasmid DNA into HUVECs and HFFs were performed using Lipofectamine2000 (Invitrogen) or X-tremeGENE HP DNA Transfection Reagent (Roche) according to the manufacturer's protocol. Transfection of miRNA mimics, inhibitors and siRNAs into HUVECs and HFFs were performed using RNAiFect Transfection Reagent (QIAGEN) according to the manufacturer's protocol. Transfection of plasmid DNA into all other cell lines were performed using PEI according to the protocol described by Longo et al. (Longo et al., 2013). Transfection of miRNA mimics, inhibitors and siRNAs into HeLa229 and H1299 $p53^{-/-}$ were performed using HiPerFect Transfection Reagent (QIAGEN) or X-tremeGENE HP DNA Transfection Reagent (Roche) according to the manufacturer's protocol.
Transfection of siRNAs against Drp1, miR-30c inhibitor, Drp1 or p53 over expression plasmids induced severe cellular stress and loss of viability in HUVECs. To ensure cell viability, transfection with the above mentioned constructs were repeated several times with different DNA/siRNA-transfection ratios. For miRNA mimics, inhibitors and siRNAs the optimal ratio was found to be 1.5 nM of miRNA mimic with 4 µl of RNAiFect Transfection Reagent, 2.5 nM of miRNA inhibitor or siRNA with 4 µl of RNAiFect Transfection Reagent, 300 µg – 600 µg of Drp1 or p53 overexpression vector with 4 µl X-tremeGENE HP DNA Transfection Reagent. All the calculations were made with reference to one well of a 12 well plate (70% confluency; ~ 3 $x10^5$ cells). All the mixtures were made in 100 µl of Opti-MEM®. The transfection mixtures are added drop-wise to HUVECs pre-incubated in warm Opti-MEM® (400 µl) and mildly shaken in a clockwise the anti-clockwise direction. The cells are incubated with the transfection mixtures over night (~ 8-12 hours) and 200 µl of fresh complete growth medium is added to the cells. The cells are either harvested for western blot or processed for imaging after another 4 hours. For infection, the medium along with the transfection mixture is removed 4 hours after addition of 200 µl fresh complete growth medium. The cells are washed with warm 1x PBS and processed as required. Similar steps were taken to ensure the viability of hFIMBs and HFFs during transfection. All constructs used and/or created for this work are listed in Table 5.4 and 5.5

4.1.4 Chemical treatment of cells

As per the requirements of the experiments the cells were often treated with H_2O_2 (Sigma) or $CoCl_2$ (Roth). To this effect the chemicals were dissolved or diluted in ultrapure cell culture grade water to generate appropriate dilutions. H_2O_2 or $CoCl_2$ treatment of HUVECs was carried out in 500 µl in 12 well plates. For all other cell types except for HFF, treatments were carried in RPMI supplemented with 5% FCS.
To inhibit cytoplasmic glycolytic pathways for the experiments requiring ATP measurements, the cells were treated with galactose. Briefly, All cells were grown in appropriate cell culture media containing glucose and growth supplements for 16 hours. Post 16 hours, the cells were washed with warm 1x PBS and incubated in galactose (10 mM) supplemented media for 8 hours.

4.1.5 Generation of Lentivirus particles and custom cell lines

293T cells were transfected with the lentivirus vector pLVTHM containing appropriate inserts to generate lentiviral particles carrying pre-sequence GFP (pLVTHM vector created by Dr. Vera Kozak-Pavlovic), miR-30c sponge (pLVTHM vector created by Dr. Bhupesh Prusty) and shRNAs against the $F_1\beta$ subunit and metaxin 2 (*f1βKd-2* and *mtx2kd-2* cell lines created by Anastasija Reimer*)*. The production of infectious lentiviral particles necessitates the presence of accessory plasmids that encode envelope and packaging proteins. To this effect, 15 cm^3 plates of 293T cells were transfected simultaneously with the appropriate pLVTHM, VSVG (envelope plasmid) and psPAX2 (envelope plasmid) using the calcium phosphate method. For this process 20 µg of pLVTHM, 10 µg of VSVG and 15 µg of psPAX2 plasmids were mixed together followed by addition of 400 µl of $CaCl_2$ and 1.6 ml ultra pure H_2O. The addition of all the components was accompanied by gentle tapping. Following 2 minutes of incubation, 2 ml of HBS was added drop wise to the mixture while simultaneous bubbling mediated agitation is performed using a Pasteur pipette. The transfection reagent is then added to the cells drop wise and mixed by a gentle clockwise swirl of the plate. Cells are incubated with is mixture overnight (max ~ 8 hours) and then washed with 1x PBS.
The supernatant containing the lentiviral particles are collected 36 hours post transfection (following the appearance of GFP if the pLVTHM carries the GFP reporter) followed by two more collections every 24 hours. Fresh media is added to the cell plate very gently after every collection. The supernatant is centrifuged at 2000 rpm for 7 minutes followed by filtration step through a 0.45 µm filter to remove

cellular debris. The lentiviral particles are further concentrated by an additional centrifugation step at 30000 g (4°C; 90 minutes) and suspension in 1 ml of FCS-free RPMI per 10 ml of supernatant.

Target cells are seeded in 12 well plates the day before infection and incubated with different concentrations of the supernatant are added as mixtures with growth media supplemented with 5% FCS for 2-3 days. To increase the efficiency of viral transduction, polybrene, a cationic polymer, is added along with the concentrated supernatant. The cells expressing the pLVTHM encoded GFP marker are then sorted by flow cytometry and propagated to generate single cell clones.

HeLa cells that stably express a Tet-repressor (HeLa–KRAB) were transduced with the corresponding lentiviral particles to create drug inducible miR-30c sponge, *f1βKd-2* and *mtx2kd-2* cell lines. Post transduction these cell lines express the GFP marker and the corresponding sponge or the shRNAs only upon induction with anhydrous tetracycline. To select single cell clones, the transduced cells were briefly pulsed with AHT and sorted by flow cytometry to segregate the cells expressing both GFP (from pLVTHM) and ds-RED (from pLVTHM-tTR-KRAB-Red). The single cells were then propagated in fresh media without AHT.

To create HUVECs stably expressing GFP targeted to the mitochondria (mito-HUVECs), the cells were seeded in 6 well plates and incubated with 1:1 mixture of concentrated lentiviral supernatant and LSGS supplemented medium 200 along with polybrene for 5 days. At the end of 4 days a small colony of mito-HUVEC was observed which exhibited cell division while the others were mostly senescent. This colony was expanded over a time period of several months since their doubling time was found to be quite high at the beginning. Single cells were sorted for mito-GFP from this expanded colony and cryopreserved for future use. Additionally to ensure the identity of the cells we checked for the expression for the HUVEC marker VE-Cadherin.

4.1.6 Flow cytometry

Flow cytometry using a BD FACS Aria III was used to sort cells for single cell population selection and for detection of fluorescence shifts in MitoTimer. For single cell population section of mitochondrial GFP expressing HUVECs and H1299 cells, the fraction of the cell population excited by the FITC (509 nm) laser line was sorted into 6 well plates (HUVECs) or individual cells were sorted into 96 well microtitre plates (H1299) and allowed to propagate. For the selection of miR-30c sponge cells, one T25 flask was briefly pulsed AHT (12 hours) to induce GFP production and

single cells excited both by the FITC (509 nm; GFP expression) and PE (560 nm; KRAB dsRED expression) were sorted into 96 well microtitre plates and allowed to grow in AHT free RPMI.

For MitoTimer experiments, HUVECs or HFF cells were plated in 6 well plates and infected or treated as per the needs of the experiments. At endpoints (time scales of the experiments is illustrated in Figure 4.1.6), the cells are trypsinized, suspended in 500 µl of full growth medium and pipetted into FACS tubes. The fluorescence readings of the cells expressing MitoTimer were measured simultaneously in FITC (509 nm; un-oxidised Timer) and PE (560 nm; oxidized Timer) channels.

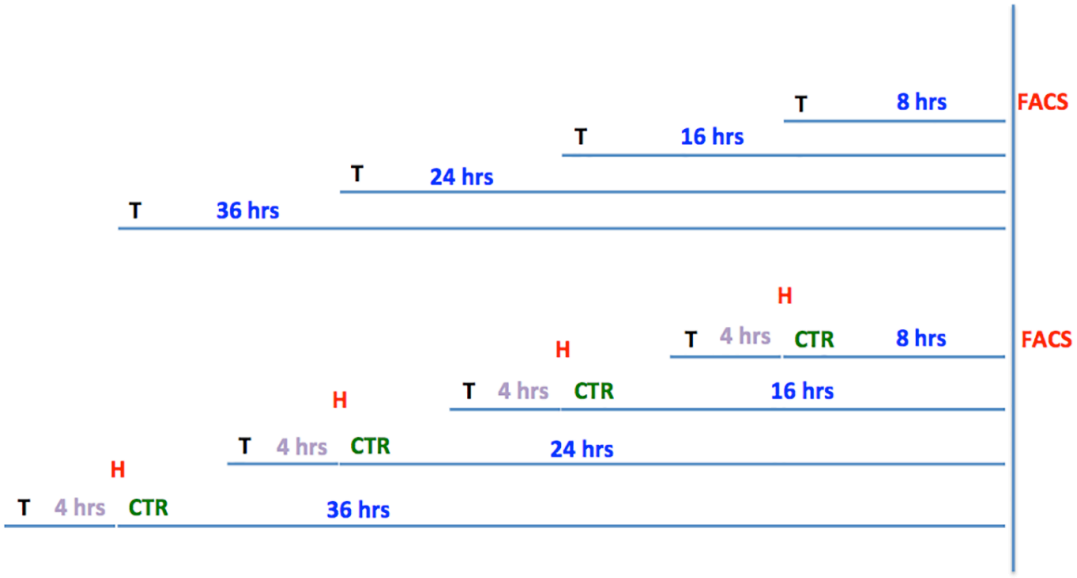

Fig. 4.1.6. Schematic representation of the time spans represented in the MitoTimer experiment. T represents the point of transfection of the MitoTimer construct. Four hours post transfection one set of the cells is pulsed with hydrogen peroxide. Both untreated and treated samples are then infected with *Chlamydia* (CTR). All samples are washed every four hours to avoid timer oxidation by secondary metabolites in the media. At the end of the time points the cells are detached using trypsin and the fluorescence is quantified using FACS.

4.2 Chlamydial Biology

4.2.1. Chlamydial propagation and stock preparation

All infections in this work were performed with C. trachomatis LGV serovar L2. Since *Chlamydia* are intracellular obligate pathogens, their cultivation and propagation can be accomplished exclusively within live cell cultures. Live EBs are isolated out of Chlamydia infected cells, aliquoted and stored at -80°C for future use. To propagate *Chlamydia,* one T75 cell culture flask is seeded with HeLa at 70-80% final confluency and infected with *Chlamydia* at MOI 1 and allowed to grow for 48 hours at 35°C (5% CO_2). The infected cells along with the chlamydial particles are scraped out using a rubber policeman and collected in 50 ml centrifuge tubes, which contain around 7 ml of glass beads. The tubes are then vortexed at high speed for around 3 minutes to break the cells. In parallel to the infection, 6 T150 cell culture flasks are seeded with HeLa at a final confluency of 70%. The cell lysate along with the chlamydial particles obtained form the T75 is inoculated into the T150 flasks and the infection is allowed to progress till 48 hours. The cell lysate along with the chlamydial particles are collected from these T150 flasks and vortexed vigorously together with glass beads. Cellular debris is removed by centrifuging these the lysates at 2000 rpm for 10 minutes in a pre-cooled (4°C) centrifuge. The supernatant is then transferred into autoclaved SS34-centrifuge tubes and centrifuged at 30,000 g in a pre-cooled (4°C) Sorvall centrifuge for 30 minutes. The supernatant is discarded and the chlamydial pellet is resuspended in 6 ml ice-cold SPG buffer. Another centrifugation step is performed at 30,000 g in a pre-cooled (4°C) Sorvall centrifuge for 30 minutes and the pellet is subsequently resuspended in fresh 6 ml ice-cold SPG buffer. The suspension is homogenized by passing it though a G20 needle (3x) and a G18 needle (1x). The homogenized suspension is then aliquoted in 25 µl fraction in autoclaved Eppendorf tubes and stored at -80°C.

To calculate the infectious units of *Chlamydia* (IFU)/ml, different dilutions of the chlamydial suspension (1:1000, 1:5000 and 1:10,000) were used to infect HeLa cells seeded on glass slides in 12 well plates for 24 hours. The samples were stained against cHSP60 and the cell periphery was marked with Phalloidin staining. The slides were imaged using the 40X objective of an epifluorescence microscope and 10 fields were captured per slide. Number of visible inclusion and cells were counted using the Object Count algorithm of FIJI. The IFU/ml was counted using the following formula:

IFU/ml = (IFU/well) x (Number of wells / 0.1 ml) x (dilution factor).

4.2.2. *C. trachomatis* infection of eukaryotic cells

Cells were seeded as per experimental set up in 12-well or 24 well plates, on glass slides for fixed cell microscopy or in 35mm glass bottom live cell imaging chambers (ibidi) and grown for 24 hours under the cell culture conditions described above. Prior to infection, the growth medium was aspirated, the cells are washed with warm 1x PBS and incubated with fresh medium supplemented with 5% FCS. The all cells except for HUVECs and hFIMBs were infected with *Chlamydia* at MOI 1. HUVECs and hFIMBs were infected at MOI 0.5. The 5% FCS medium is replaced with full growth medium after 2.5 hours and allowed to grow for the time spans necessitated by the experimental set up. Post infection with Chlamydia, all cells were grown at 35°C.

4.2.3. *C. trachomatis* infectivity assay

Chlamydial infectivity assay was performed using chlamydial lysates from different cell types expression various shRNAs or miRNA sponges and cells transfected with miRNA mimics, inhibitors, siRNAs or p53 and Drp1 overexpression vectors to quantify the efficiency of progeny formation. The Infectivity assays were performed according to the protocol described by Siegl et al. (Siegl et al., 2014). Briefly, Chlamydia infected and non – infected cells were lysed using autoclaved glass beads and one-hundredth of the lysates were used to infect a second set of cells plated the previous day. The cells were incubated for 12, 24 and 36 hours and subsequently lysed for immunoblot analysis.

4.3 Molecular biology

4.3.1. Total RNA extraction

Total RNA isolation, including the small RNA, from all cell types including *Chlamydia* infected cells was performed using miRNAeasy Kit (Qiagen) according to manufacturers protocol. The cells were seesed in 12 well or 6 well plates and treated, transfected and/or infected with *Chlamydia* for necessary time points as per the requirements of the experiment and lysed with the Phenol/guanidine-based QIAzol Lysis Reagent prior to RNA extraction. The quantity and quality of RNA was determined by NanoDrop spectrophotometry and denaturing agarose gel electrophoresis. Additional quality control of RNA prepared for sequencing was done on the 2100 Bioanalyzer instrument using a RNA analysis kit (Agilent). Isolated RNA was used for downstream applications like qRT-PCR, RNA sequencing and Northern blot or stored at -80°C for future use.

4.3.2. MicroRNA sequencing

Total RNA along with the small RNA fraction was isolated from non-infected control and Chlamydia infected HUVECs was used for RNA sequencing. The cells were infected with Chlamydia for 12 and 24 hours. The non-infected cells were grown in 6 well plates for 12 and 24 hours before processing. The total RNA was screened for quality and quantity as described above. Library preparation was performed by Vertis biotechnology AG and the RNA sequencing was performed on an Ilumina HiSeq 2000 sequencer at the Max Planck Genome Centre Cologne, Cologne, 519 Germany, as described in Maudet et al. (Maudet et al., 2014).

4.3.3. Northern Blot

Northern blots using total RNA from samples were performed to analyze changes in miRNA expression under different experimental conditions and to validate the results of the miRNA deep sequencing (in case of certain miRNAs). All blots were preformed according to the protocol published by the Narry Kim Lab (http://www.narrykim.org/en/protocols). Briefly, 15-25 µg of total RNA was mixed with an equal volume of 2x RNA gel loading dye and denatured by boiling at 95°C. The sample was then loaded on to a 12.5% urea-polyacrylamide gel (prepared with

DEPC treated ingredients) and separated by running the gel at 350 V for approximately 4.5 hours. The samples are run alongside a Decade RNA marker (Ambion) radiolabelled with [gamma-P32] Adenosine 5'-triphosphate using polynucleotide kinase (PNK) according to manufacturer's protocol.

Post separation the RNA is transferred onto a positively charged nylon membrane under wet blot transfer conditions at constant amperage of 406 mA (4°C; 2 hours). Post transfer the RNA is cross-linked to the nylon membrane on a UV transilluminator (3 min). The cross-linked membrane is pre-hybridized using ULTRAhyb hybridization buffer pre-warmed to 65°C for one hour followed by overnight hybridization with the radiolabelled probe of choice at 42°C.

DNA oligonucleotides (Table 5.7) were ordered according to specifications and 10 pmol was labelled with 1-3 µl of γ-32P-ATP and T4- PNK in the supplied buffer (PNK-A) for 1 hour at 37°C following which the PNK is inactivated by boiling at 95°C. The labelled probe is stored at -20°C. For hybridization, the probes can be diluted or directly added to the ULTRAhyb hybridization buffer. 10 µl of a 1:1 radiolabelled probe – DEPC water mixture was used for hybridization in all northern blots.

Post hybridization, the membrane is washed 3 times (5 minutes each) in pre-warmed Northern washing buffer and once (1 min) with DEPC water at 42°C.The membranes are dried with tissue paper, sealed in plastic films and exposed to phospho-storage films for 12 to 36 hours depending on the strength of the signal. The plates are scanned on the Typhoon scanner the data is analyzed using FIJI.

4.3.4. Generation of cDNA by reverse transcription

The total RNA isolated from samples were used to generate complementary DNA (cDNA) for quantitative analysis by qPCR. The cDNA from both the mRNA and miRNA fractions of the total RNA samples was generated using the miScript II RT Kit (Qiagen). 1 µg of the total RNA sample was used as starting material. The HiSpec buffer provided with the kit was used in all cases along with the Oligo-dT-universal tag primer to generate cDNA. This cDNA could be used for qPCR of miRNAs using a miRNA specific forward primer and also for qPCR of mRNAs using custom designed oligonucleotide primers.

4.3.5. Quantification of mRNAs and miRNAs by qPCR

Quantification of p53 and Drp1 expression was performed using custom designed oligonucleotide primers (Table 5.6) in conjunction with the PerfeCTa SYBR® Green FastMix according to manufacturer's protocol. The cDNA prepared as described as

above was diluted by adding 200 µl of RNase-free water to each 20 µl reverse-transcription reaction and 5 µl of this dilution was used in each 20 µl SYBR® Green reaction mixture along with gene specific primer sets and dNTPs. Reactions were allowed to run for 40 cycles with an initial hold step at 95°C, where each cycle was as follows: 95°C for 15 seconds and 60°C for 1 minute. qPCR of miRNAs was performed using miScript SYBR® Green PCR Kit or miRCURY LNA™ Universal RT microRNA PCR system according to manufacture's protocol. In case of miScript SYBR® Green PCR Kit miRNA-specific forward primers were used to prime the reaction along with a universal reverse primer (Table 5.8). In case of miRCURY LNA™ Universal RT microRNA PCR system, specific LNA primer sets were used (Table 5.8). All reactions were run on the StepOnePlus™ Real Time PCR system with ramp rates and cycling parameters set according to manufacture's protocol.

4.3.6. Plasmid isolation

E. coli carrying plasmid of interest was grown overnight in LB supplement with the antibiotic of choice and centrifuged to obtain pellet for plasmid prep. Plasmid isolation was performed either with NucleoBond®PC100 Midiprep Kit or with NucleoSpin® Plasmid minikit (Machery Nagel). For midipreps ~40 ml of overnight culture was used while 2.5 – 5 ml overnight culture was used for minipreps. The plasmid isolation was performed according to manufacturer's protocol and stored at -20°C till further use.

4.3.7. Polymerase Chain Reaction (PCR)

Non-quantitative amplifications of DNA fragments by PCR were preformed to amplify inserts of Drp1, p53, GFP and others for creating necessary vectors. MolTaq (Molzym), a standard Taq DNA polymerase, was used for colony PCRs and to check for the presence of inserts. High-fidelity polymerases such as ReproFast polymerase (Genaxxon) or iProof™ polymerase (BIO-RAD) were used for insert amplification from cDNA. Reaction mixtures were prepared as recommended by the manufacturers with suitable buffers and products were amplified under suitable cycling parameters dictated by the enzyme properties (elongation time for ReproFast: 1min/kb; iProof™: 30sec/kb) and the melting temperature of the oligonucleotide primers (Table 5.6). PCR products were separated according to size by agarose gel electrophoresis and visualized after Intas HD Green (Intas) staining under UV light.

4.3.8. DNA digestion and ligation

Digestion of plasmid vectors and DNA fragments and their subsequent ligation was performed to create overexpression and other reporter vectors used in this work. T4 DNA ligase and restriction enzymes (along with their corresponding buffers) were bought from Fermentas or NEB and used as directed by the manufacturer. Restriction enzyme and buffer compatibility was checked online using the Double Digest tool (Thermo). Digested products were separated according to size by agarose gel electrophoresis and purified using the GeneJET^{TM} Gel Extraction Kit (Thermo). Ligated products were checked for positive ligation by agarose gel electrophoresis. All novel vectors created for this work were sequenced to check for unwanted mutations or mismatches at SeqLab sequence laboratories, Göttingen (Microsynth).

4.3.9. psiGFP-dsRED 3' UTR reporter vector construction

To ascertain the effect of miRNAs upon infection we created a destabilized GFP vector using the psiCHECK-2 vector (Promega) backbone. The reporter vector also designed to express a dsRED (under the control of a separated TK promoter and unaffected by 3' UTR inserts) to serve as a transfection control. The psiCHECK-2 vector carries a Renilla luciferase cassette driven by a SV 40 promoter that serves as the 3' UTR reporter. Artificial 3' UTRs can be inserted into the MCS following the Renilla luciferase cassette. We amplified the EGFP gene from the pEGFP-N1 vector (Clontech) using a GFP forward primer (EGFP-F) and a reverse primer encoding the proline-glutamate-serine-threonine-rich (PEST) sequence from the mouse ornithine decarboxylase gene (EGFP-PEST-R). This PEST-GFP insert was used to replace the Renilla luciferase cassette. The synthetic firefly luciferase is the native transfection control gene in psiCHECK-2 vector. We replaced synthetic firefly luciferase with a dsRED insert. The complete vector map is represented in Figure 3.3.1.

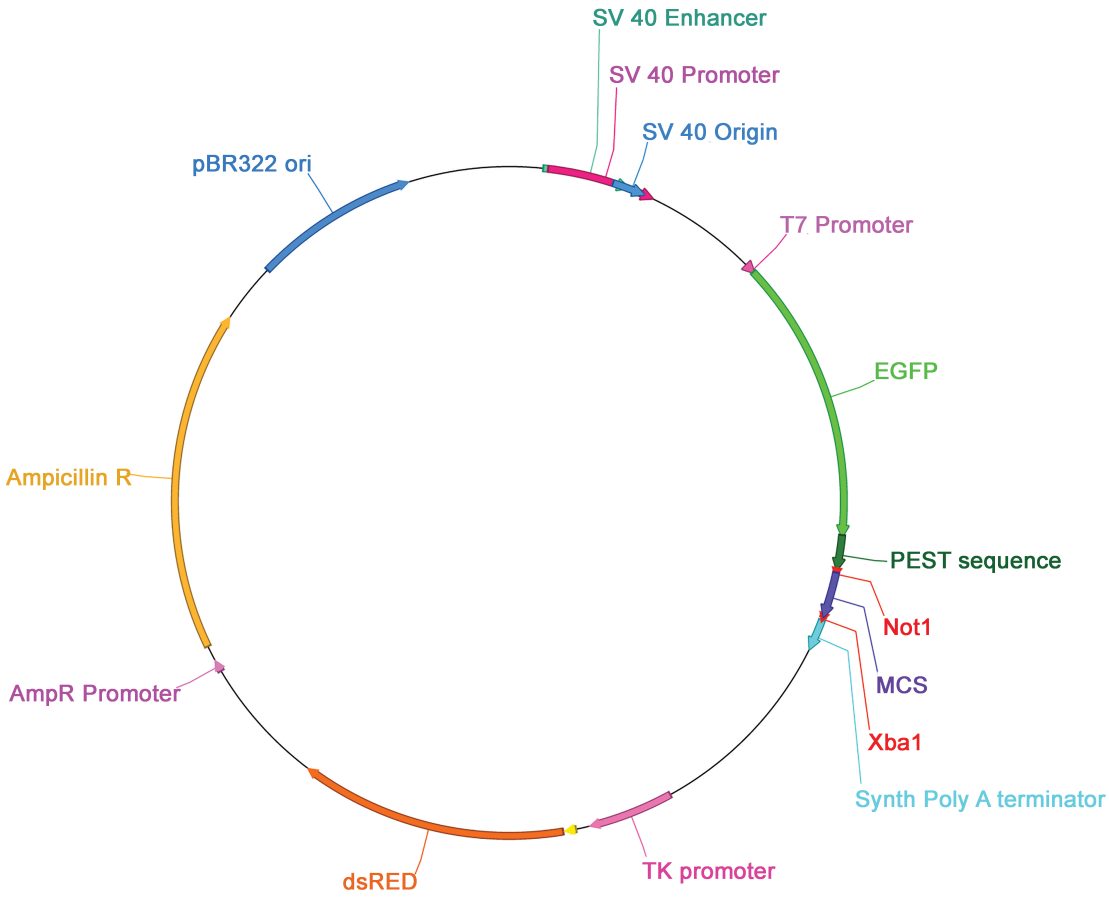

Fig. 4.3.9. Schematic representation of the psiGFP-dsRED 3' UTR reporter construct

4.3.10. Designing of wild type and mutant p53 3'UTR inserts

The psiGFP-dsRED 3' UTR reporter modified to carry the wild type and the mutant p53 3'UTRs. The psiGFP-dsRED 3' UTR vector carrying the wild type vector (psiGFP-p53UTR^{WT}-dsRED) was created by inserting the wild type p53 3' UTR from HUVEC cDNA (using the p53-3'UTR^{WT}-F and p53-3'UTR^{WT}-R primers) and inserting them in the MCS following the PEST-GFP by vector digestion and subsequent ligation. The psiGFP- p53-3'UTR^{MUT}-dsRED vector was prepared by altering the miR-30c binding site (GTTCACA) on the p53 3' UTR by site directed mutagenesis (SDM) (using the p53-3'UTR^{MUT}-F and p53-3'UTR^{MUT}-R SDM primers). SDM was performed by introduction of a point mutation in the above-mentioned sequence using the Quick-change site-directed mutagenesis protocol. Briefly, the oligonucleotides p53-3'UTR^{MUT}-F and p53-3'UTR^{MUT}-R, carrying a single nucleotide change compared to the p53UTR^{WT} 3'UTR were extended using the Phusion DNA polymerase (Thermo) to generate a mutated plasmid with staggered nicks. The Type IIM restriction endonuclease, DpnI, was used to digest the original template at 37°C

(1 hour) followed by an inactivation step (80°C; 20 min). DpnI acts specifically on methylated DNA, thus spares the newly synthesized DNA produced in the PCR reaction. All insertions and presence of mutation were confirmed by sequencing.

4.4 Biochemical methods

4.4.1. SDS-PAGE

Denaturing SDS-PAGE (sodium dodecyl sulphate polyacrylamide gel electrophoresis) was performed to check the regulation of host protein expression due to infection, transfection of over expression vectors or siRNA/shRNA/miRNA mimic or inhibitors. Samples grown and treated as per requirements of the experiments were lysed using 2x Laemmli buffer and denatured by boiling at 94°C for 10 minutes. The proteins were then separated according to mass by running these samples in 10-12% polyacrylamide gel across a constant voltage for ~ 1.5 – 2 hours. For proper estimation of the protein sizes, the samples were run alongside 5 – 6 µl of PageRuler Prestained Protein Ladder (Thermo).

4.4.2. Semi-dry western blot

Post separation by SDS-PAGE the proteins are transferred from the gel to a PVDF membrane by the process of semi-dry western blotting. The proteins transferred onto the membrane are thus made accessible to detection by antibody binding. To this effect, the methanol activated PVDF membranes are sandwiched with the polyacrylamide gel containing the size-separated proteins, layered on both the membrane and the gel side with 2x Whatman paper slices. The Whatman papers slices are cut according to the size of the gel and soaked in 1x western transfer buffer. Pior to placement of the gel in the transfer sandwich, it is soaked in 1x transfer buffer for 5 minutes. The sandwich is then transferred to the semi-dry transfer apparatus with the PVDF membrane oriented towards the anode and the gel towards the cathode. Once placed inside the transfer apparatus, care is taken to remove bubbles between the gel and the membrane. The apparatus is tightly sealed using clamps and transfer is performed at 1mA/cm^2 for 2 hours.

Post transfer, the membrane is briefly rinsed in TBS-T and blocked using 5% milk made in TBS-T for 1 hour. Following blocking, the membrane is briefly rinsed in TBS-T and incubated with a primary antibody (Table 5.10) of choice at 4°C for a time period dictated by the efficiency of the antibody (usually overnight). After incubation with the antibody, the membrane is washed 3 times (~10 minutes each) with TBS-T and then incubated with a corresponding HRP-conjugated secondary antibody (Table 5.11) for 1 hour (R.T.). Following the secondary antibody incubation the, membrane is subjected to a final wash (3x; ~10 minutes each), incubated with ECL-

mix for 2-3 minutes and visualized on the Intas imager system. The images of the bolts were acquired as raw tiffs and used as either representative figures or quantified for protein expression using FIJI. The same membrane was used for detection of expression of multiple protein targets. In some cases the membrane was stripped of the primary and secondary antibody bindings by incubating it in stripping buffer (37°C; 20 minutes).

4.4.3. Cell Viability Assay

To assess the viability of cells post transfection or treatment as dictated by the experimental conditions, MTT based colorimetric cell viability assay was performed. The cells were plated in 96 well flat-bottomed colourless microtitre plates and infected, treated or transfected as necessary. The cells were then incubated with 20 µl of 5 mg/ml MTT solution for 4 hours. Post incubation, the MTT solution and media was aspirated and 170 µl of DMSO was added to dissolve the resulting formazan and produce a coloured solution. The absorbance of this solution was determined using an Infinite 200 PRO multimode reader (Tecan).

4.4.4. Measurement of total ATP content

Total ATP measurements of infected or transfected cells were performed using the Luminescent ATP Detection Assay Kit (Abcam) according to manufacturer's protocol. Briefly, cells were plated in 96 well flat-bottomed white microtitre plates and infected, treated or transfected as necessary. The cells were also incubated in either normal growth medium or media supplemented with galactose as necessary. The measurements were carried out on an Infinite 200 PRO multimode reader (Tecan).

4.5 Imaging and microscopy

4.5.1 Immunostaining and fixed cell microscopy

Immunostaining of cells fixed on glass coverslips was performed for the visualization of the morphological variations of the mitochondrial architecture, Drp1 abundance and localization amongst other things. Prior to transfection, infection or chemical treatment, cells were plated on glass slides within 12 well plates and allowed to grow overnight (24-30 hours for HUVECs) to reach 60-70% confluency. Post transfections with siRNAs, miRNA mimics or inhibitors and necessary constructs, the cells were infected with *Chlamydia* as dictated by the needs of the experiment. At the end point of the experiment, the growth medium was removed and the cells were washed with 1x PBS and fixed with 4% paraformaldehyde for 20 minutes. After fixing, the paraformaldehyde was washed away with 1x PBS and the samples were permeabilized with 0.2% Triton-X100 (in PBS) for 15 minutes followed by blocking in 2% FCS for 45 minutes. The fixed, permeabilized and blocked cells were then incubated with primary antibodies (in blocking buffer; Table 5.10) of choice for 1 hour in a humid chamber (R.T.). The cell were then washed 3 times with 1x PBS and incubated with the corresponding secondary antibodies (in blocking buffer; Table 5.11) for 1 hour. After 3 washes with 1x PBS, a post staining fixation step was performed with 4% paraformaldehyde for 20 minutes. DAPI or Hoechst stains were used to demarcate the nucleus. Following a final washing step with 1x PBS, the glass cover slips were mounted on glass slides in 2.5% Mowiol-DABCO (Carl Roth, Germany). Confocal imaging of the samples were done on a Leica TCS SP5 confocal microscope using a 63x oil immersion UV objective with a numerical aperture of 1.4. Super resolution imaging for quantification of Drp1 aggregates, their sizes and localization on the mitochondria was performed using Structured Illumination Microscopy on a Zeiss ELYRA S.1 SR-SIM structured illumination platform using a Plan-APOCHROMAT 63x oil immersion objective with a numerical aperture of 1.4. The images were reconstructed using the SIM algorithm provided with the ZEN 2012 image-processing platform with a SIM module.

4.5.2. Live cell Confocal video-microscopy

The intricate details of fission, fusion and the over all dynamic motility of the HUVEC mitochondrial fragments under different condition was captured by performing live cell video-microscopy on a Leica TCS SP5 confocal microscope using a 63x oil

immersion UV objective. HUVECs were plated in μ-Dish 35 mm, high Glass Bottom (ibidi) and grown for 24-30 hours prior to transfection, infection or chemical treatment. Ten minutes before imaging the growth media was replaced with 2.5 ml of re-warmed RPMI-1640 containing 25mM HEPES buffer (without phenol-red; with Ca^{2+}/Mg^{2+}) and incubated at 37°C for 10 minutes. The dishes were then transferred to a Live-cell incubation chamber (Life Imaging Systems) attached to the Leica TCS SP5 confocal microscope, pre warmed to 37°C. In certain cases the chemical treatment with H_2O_2 was performed *in situ* at the chamber. Images acquisition was preformed using the LAS software package. All images, unless specified otherwise, were acquired at a resolution of 1024x1024 and recorded in 8-bit mode at pre-defined time intervals.

4.6 Computational Analysis

4.6.1 Computational analysis of RNA-Seq data

Computational analysis of miRNA sequencing data was performed using the READemption pipeline v0.3.3 (Forstner et al., 2014) in conjunction with Segemehl v0.1.7 (Otto et al., 2014). This process was utilized to map the transcripts obtained from the miRNA sequencing against human mature miRNA sequences from the miRBase data base as described by Maudet et al., 2014 (Maudet et al., 2014), and also to the human and chlamydial genomes (NCBI references NC_021049 and NC_021052). 14 nucleotide parameter cut-offs for minimum read length and 95% minimum similarity were used in the analysis. DESeq 1.12.1 (Anders and Huber, 2010) was used for analysis differential miRNA gene expression between infected and non-infected samples collected across same time spans. Pathway based interaction analysis and pathway based grouping of selected miRNAs was performed using the DIANA-miRPath v2.0 webtool (Vlachos et al., 2012).

4.6.2. Computational analysis of imaging data

All computational steps and analysis performed on the confocal and SIM imaging data were performed using the image processing platform FIJI (Moll et al., 2006) with additional plugins and custom designed MACRO scripts. Quantification of Chlamydia inclusions and Drp1 fission rings were performed using the Object Counter plugin following appropriate background subtraction and thresholding using the Rolling ball background subtraction model. The original micrographs used for Drp1 quantification was processed by applying a predetermined threshold calculated by measuring the average pixel intensity of the Drp1 channel in control samples. All subsequent images were normalized using this thresholding parameter. To determine minimum and maximum ring diameters of dilated and constricted Drp1 rings, several hundred random ring diameters were measured using the Profile function of ZEN 2012 image-processing platform and the Plot Profile plugin in FIJI. This data was used to calculate the maximum (360 nm; dilated) and minimum (100

nm; constricted) threshold of object detection by the Object Profile algorithm (Ingerman et al., 2005; Ji et al., 2015; Mears et al., 2011; Rosenbloom et al., 2014). This diametric range was maintained in the thresholding and classification process of Drp1 ring. All rings above 180 nm were classified as dilated while those below were tagged as constricted rings. Areas of mitochondrial constriction were determined by plotting the absolute intensity along the length of the mitochondrial fragment. Spots with low mitochondrial GFP signal and high Drp1 signals were tagged as potential fission sites.

The degree of colocalisation of Drp1 aggregates on the mitochondrial surface was determined using the COLOC2 plugin from FIJI (White et al., 2015; http://github.com/fiji/Colocalisation_Analysis). The quantification of colocalization was calculated and represented as Pearson's colocalisation coefficient.

The object plot plugin was further modified to calculate the length distribution of mitochondrial fragments. To achieve this, an equal threshold was applied to all images and the mitochondrial GFP signal was converted to binary. These binary images were then fed as data to the object plot plugin and the algorithm was used to segregate the mitochondrial fragments as individual particles or continuous fragments based on their degree of connectivity to adjacent particles or to the over all network. The areas covered by these fragments were then calculated as micron squared values. Using the Profile function from the ZEN 2012 image-processing platform the width of ~300 individual mitochondrial fragments from HUVECs and H1299 cells were measured and averaged. These values were then used to divide the area covered by the mitochondrial fragments in HUVECs (0.39 nm) and H1299 (0.46 nm) to provide the approximate length of individual mitochondrial particles. The mitochondrial fragments with extensive connections to the adjacent particles were categorized as unfragmented while those that exhibited no visible connections were tagged as individual fragments. Cells which contained more that 300 mitochondrial fragments unassociated with the mitochondrial network or other mitochondrial particles were categorized as hyper-fragmented and those with less than 160 such fragments were considered as hyper-fused.

The end-mobility of mitochondrial fragments was determined using the novel MACRO script (written as a part of this work) called MitoCRWLR. Live cell video micrographs processed using this script were opened in the FIJI platform and converted to binary. The script then measures the "differences" between two consecutive frames of the video and uses the "Analyze particles" function of FIJI to calculate the area of the mitochondrial GFP signal in each frame. Simultaneously, the total area of the visible mitochondrial fraction was recorded by the script and used to normalize the differences. These normalized differences between the mitochondrial end-mobility of treated, infected and control cells were determined in triplicate and plotted on graphs.

4.7 Statistical Analysis

Statistical analysis of all data points collected in experiments mentioned in this work was performed using GraphPad Prism 6.0. All experimental data represented have been replicated at least 3 or more times and the error bars depicted in the graphs represent the mean ± SD of such replicates. Normality of distribution was tested in cases of mitochondrial length distribution and fragment count using D'Agostino-Pearson normality test. Statistical significance of the data represented was calculated using Student's *t*-test or one-way ANOVA followed by Tukey's multiple comparisons test. All image analysis was performed on 6 or more replicates for each biological condition.

Chapter 5. Materials

5.I Cell Lines

Table 5.1: Cell Lines

Name	Description	Media	Source
HUVEC	Human Umbilical Cord Endothelial Cells	Medium 200	ATCC
Mito-HUVEC	HUVECs stably expressing mitochondrial presence tagged GFP	Medium 200	This work
FIMB	Human fimbrial epithelial cells from fallopian tube biopsy	RPMI 1640	This work
Mito-FIMB	FIMBs stably expressing mitochondrial presence tagged GFP	RPMI 1640	This work
H1299 p53$^{-/-}$	Epithelial cells from a metastatic site of the human lung	RPMI 1640	Prof. Dr. Martin Eliers
Mito- H1299 p53$^{-/-}$	H1299 p53$^{-/-}$ stably expressing mitochondrial presence tagged GFP	RPMI 1640	This work
293T	Human embryonic kidney epithelial cells	DMEM	ATCC
HeLa229	Human cervix adenocarcinoma cells	RPMI 1640	ATCC
HeLa229-miR-30c-sponge	HeLa cells inducibly expressing a sponge against miR-30c	RPMI 1640	Dr. B. Prusty
f_1βkd-2 HeLa	HeLa cells inducibly expressing a shRNA against F_1β subunit of the mitochondrial F_1F_O-ATPase	RPMI 1640	Dr. V. Kozak-Pavlovic
Metaxin 2-HeLa	HeLa cells inducibly expressing a shRNA against Metaxin 2	RPMI 1640	(Ott et al., 2012)
HFF	Human Foreskin Fibroblast cells	Fibroblast Basal Medium	ATCC

5.2 Bacterial strains

Table 5.2: *E.Coli* strains

Cell Line	Description
***E.coli* DH5α**	Cloning *Coli*
***E.coli* XL1blue**	Cloning
***E.coli* JM101**	Epithelial cells from a metastatic site of the human lung

The *E.coli* strains were grown on LB agar plates or in LB medium.

Table 5.3: *Chlamydia* strains

Species	Serovar	Description	Source
C.trachomatis	LGV L2 (434)	Wildtype *Chlamydia*	ATCC
C.trachomatis* *pGFP::SW2	LGV L2 (434)	*C.trachomatis* transformed with pGFP::SW2 plasmid. Selected with 100 units of PenG/ml	Dr. A. Mehlitz
***C.trachomatis* pmCherry::SW2**	LGV L2 (434)	*C.trachomatis* transformed with pmCherry::SW2 plasmid. Selected with 100 units of PenG/ml	Dr. A. Mehlitz
***C.trachomatis* pCFP::SW2**	LGV L2 (434)	*C.trachomatis* transformed with pmCFP::SW2 plasmid. Selected with 100 units of PenG/ml	This work

5.3 Plasmids and Constructs

Table 5.4: Plasmids

Plasmid	Comment	Source
pcDNA3	Expression vector for eukaryotic cells	Invitrogen
pcDNA3-FLAG	Expression vector for fusing a C-terminal FLAG tag to a protein	Dr. V. Kozak-Pavlovic
pEGFP-N1	Expression vector for expressing and visualizing a protein of interest fused to GFP	Clontech
pDsRED-N1	Expression vector for expressing and visualizing a protein of interest fused to DsRED	Clontech
pmCherry-N1	Expression vector for expressing and visualizing a protein of interest fused to mCherry	Clontech
mEos3.2-N1	Expression vector for expressing and visualizing a protein of interest fused to mEos3.1	Addgene (Plasmid #54525)
pcDNA3-presequence	Expression vector for expressing a protein of interest fused to the mitochondrial presequence and targeting it to the mitochondrial matrix	Dr. V. Kozak-Pavlovic
psiCHECK-2	Reporter system for expression of Renilla luciferase fused to artificial 3'UTR sequences	Promega
pMitoTIMER	Expression vector for expressing and visualizing a Timer protein fused to the mitochondrial presequence and targeting it to the mitochondrial matrix	Addgene (Plasmid #52659)
pLVTHM	Second-generation lentivector expressing shRNA from H1 promoter and GFP for direct cloning of shRNA	Addgene (Plasmid # 12250)
pcDNA3-p53	Expression vector for overexpression of wildtype p53	(Marin et al., 2000)
pcDNA3-Drp1K38A	Expression vector for a catalytically inactive Dominant negative form of Drp1	Addgene (Plasmid # 45161)
pcDNA3-Drp1K38A	Expression vector for a catalytically inactive Dominant negative form of Drp1	Addgene (Plasmid # 45161)

Table 5.5: Vector Constructs

Plasmid	Comment	Source
pcDNA3-Drp1	Full length Drp1 was amplified from cDNA of HUVECs and cloned into pcDNA3	This work
pEGFP-p53	Full length p53 was amplified pcDNA3-p53 and cloned pcDNA3 carrying a EGFP sequence. The p53 sequence was cloned with its amino terminus towards the GFP separated by two amino acids originating from an EcoRI restriction site	Dr. V. Kozak-Pavlovic
psiGFP-dsRED	The Renilla luciferase in psiCHECK-2 vector was replaced with a destabilized GFP while the synthetic firefly luciferase was replaced with dsRED to create an empty 3'UTR reporter construct	This work
psiGFP-p53UTR^{WT}-dsRED	The wild type 3'UTR of p53 from HUVECs was cloned downstream of the destabilized GFP to create a GFP reported construct under the control of the p53 3'UTR	This work
psiGFP-p53UTR^{mut}-dsRED	Reporter construct expressing a destabilized GFP under the control of a mutant p53 3' UTR. The binding site for miR-30c was altered using site directed mutagenesis.	This work
Mito-mEos3.2-N1	Full length mEos3.1 was amplified from mEos3.2-N1 and cloned into pcDNA3-presequence	This work
pcDNA3-presequence-GFP	Full length mEos3.1 was amplified from pEGFP-N1 and cloned into pcDNA3-presequence	Dr. V. Kozak-Pavlovic
pLVTHM-miR30c sponge	Lentiviral construct for inducible expression of the miR-30c sponge created by cloning the miR-30c oligo into the empty pLVTHM construct	Dr. B. Prusty
pLVTHM-f_1βkd-shRNA	Lentiviral construct for shRNA mediated knockdown of the F_1β subunit of the mitochondrial F_1F_O-ATPase created by cloning the f_1βkd-shRNA into the empty pLVTHM construct	Dr. V. Kozak-Pavlovic
pLVTHM-presequence GFP	Lentiviral construct for stable expression of GFP targeted to the mitochondrial matrix	Dr. V. Kozak-Pavlovic

5.4 Oligonucleotides

Table 5.6: Oligonucleotides used for cloning and q-RT-PCR

Name	Sequence (5'→ 3')	Comment
Drp1-F	TCAGGCGGCCGCAGCGCATGGCCTGCCGGGA	Cloning/NotI
Drp1-R	CTAGCTCGAGCTACTCTATACGGTTATGTTCCAAAG	Cloning/XhoI
EGFP-F	ATAGGCTAGCATGGTGAGCAAGGGCGAGGAG	Cloning into psiGFP-dsRED/NheI
EGFP-PEST-R	ACTGCTCGAGATTAATGACGGTCCATCCCGCTCTCCTGGGCACAAGACATGGGCAGCGTGCCATCATCCTGCTCCTCCACCTCCGGCGGGAAGCCATGCTTGTACAGCTCGTCCATG	Cloning into psiGFP-dsRED with a destabilizing PEST sequence/XhoI
dsRED-F	ATCGGGGCCCCATGGCCTCCTCCGAGAACG	Cloning into psiGFP-dsRED/ApaI
dsRED-R	CGATTCTAGACAGGAACAGGTGGTGGCG	Cloning into psiGFP-dsRED/XbaI
mEos3.2-F	ATGCGAATTCAGTGCGATTAAGCCAGACATG	Cloning into pcDNA-presequence/EcoRI
mEos3.3-R	ATCGCTCGAGTTATCGTCTGGCATTGTCAGG	Cloning into pcDNA-presequence/XhoI
miR-30c sponge	CGCGTCCCCCTGAGGATGTAGGATGTTTACATGACTGAGGATGTAGGATGTTTACAAGCGGCTGAGGATGTAGGATGTTTACACCCGGTGCATGACTAAGCTAGCCTGAGGATGTAGGATGTTTACACGACTGAGGATGTAGGATGTTTACAACGCGCTGAGGATGTAGGATGTTTACATTTTTGGAAAT	Cloning into pLVTHM/MluI and ClaI
p53-3'UTR^{WT}-F	TAGAATCTCGAGCCCTAGGGGTCTTGGCCATTC	Cloning/XhoI
p53-3'UTR^{WT}-R	TAGAATGCGGCCGCGCAGTCAGACAGCTTCTTTATTTGACT	Cloning/NotI
p53-3'UTR^{MUT}-F	TCTTGCAGTTAAGGGTTA**GTTCAC**AATCAGCCACATTCTAGGT	Site directed mutagenesis

p53-3'UTR^{MUT}-R	AGAACGTCAATTCCCAAT**CAAGTGT**TAGT CGGTGTAAGATCCA	Site directed mutagenesis
Drp1-F	GCGCTGATCCCGCGTCAT	qRT-PCR
Drp1-R	CCGCACCCACTGTGTTGA	qRT-PCR
p53-F	TCAACAAGATGTTTTGCCAACTG	qRT-PCR
p53-R	ATGTGCTGTGACTGACTGACTGCTT	qRT-PCR
GAPDH-F	CGTCTTCACCACCATGGAGAAGGC	qRT-PCR
GAPDH-R	AAGGCCATGCCAGTGAGCTTCCC	qRT-PCR

Table 5.7: Oligonucleotides used as probes for northern blot

Name	Sequence (5'→ 3')
hsa/rno-U6 snRNA	CACGAATTTGCGTGTCATCCTT
5s rRNA (human)	CATCCAAGTACTACCAGGCCC
hsa-miR-30a	TTCCAGTCGAGGATGTTTAC
hsa-miR-30b	AGCTGAGTGTAGGATGTTTACA
hsa-miR-30c	GCTGAGAGTGTAGGATGTTTACA
hsa-miR-30d	CTTCCAGTCGGGGATGTTTACA
hsa-miR-30e	AGCTTCCAGTCAAGGATGTTTACA
hsa-miR-409	ATGCAAAGTTGCTCGGGTA
hsa-miR-21	TCAACATCAGTCTGATAAGCTA
hsa-miR-193	TCATCTCGCCCGCAAAGACC
hsa-miR-98	ACAATACAACTTACTACCTCA
hsa-miR-548m	CAAAAACCACAAATACCTTT
C.trR5 (chlamydial)	CAGCACCCCTCTGAGTTCTCCC

All oligonucleotides used for cloning, q-RT-PCR and Northern blotting were purchased from Sigma-Aldrich Chemie GmbH and diluted in ultrapure water as per manufacturer's instructions. All qRT-PCR for microRNAs were performed with miScript primer assays from Qiagen using the miScript PCR system or with the microRNA LNA™ PCR primers using miRCURY LNA™ Universal RT microRNA PCR system as per manufacturer's protocol. The primer assays and LNA™ PCR primers used are listed in Table 2-7.

Table 5.8: miScript Primer assays or LNA PCR Primer used for validation of target miRNA regulation

Target	Name	Source
miR-30a	Hs_miR-30a-5p_1 miScript Primer Assay	Qiagen
miR-30b	Hs_miR-30b_1 miScript Primer Assay	Qiagen
miR-30c	Hs_miR-30c_2 miScript Primer Assay	Qiagen
miR-30d	Hs_miR-30d_2 miScript Primer Assay	Qiagen
miR-30e	Hs_miR-30e_1 miScript Primer Assay	Qiagen
U6 snRNA	Hs_RNU6-2_11 miScript Primer Assay	Qiagen
miR-193	hsa-miR-193a-5p LNA™ PCR primer set, UniRT	Exiqon
miR-98	hsa-miR-98-5p LNA™ PCR primer set, UniRT	Exiqon
miR-299	hsa-miR-299-5p LNA™ PCR primer set, UniRT	Exiqon
miR-197	hsa-miR-197-5p LNA™ PCR primer set, UniRT	Exiqon
miR-24	hsa-miR-24-1-5p LNA™ PCR primer set, UniRT	Exiqon
miR-499	hsa-miR-499a-5p LNA™ PCR primer set, UniRT	Exiqon
U6 snRNA	miRCURY LNA™ Universal RT microRNA PCR reference gene primer set	Exiqon

Table 5.9: SiRNA oligonucleotides directed against mRNA targets, miRNA mimics and inhibitors for and against miR-30.

Target	Sequence	Source
Negative Control	AllStars Negative Control siRNA	Qiagen/ SI03650318
Drp1	FlexiTube GeneSolution GS10059 for DNM1L (4 siRNAs); SI04320092 (FlexiTube siRNA) SI04274235 (FlexiTube siRNA); SI04202464 (FlexiTube siRNA); SI02661365 (FlexiTube siRNA)	Qiagen/ GS10059
p53	5' TACAGAACATGTCTAAGCATGCTGGGGACT 5' AGTCCCCAGCATGCTTAGACATGTTCTGTA	Dharmacon
miR-30c mimic	Syn-hsa-miR-30c-5p miScript miRNA Mimic	Qiagen/ MSY0000244
miR-30c inhibitor	Anti-hsa-miR-30c-5p miScript miRNA Inhibitor	Qiagen/ MIN0000244

5.5 Antibodies

Table 5.10: Primary antibodies

Antibody	Source	Dilution	Company
Beta-Actin	Mouse monoclonal	1:5000 WB	Sigma Aldrich (A5441)
c-OmpA	Rabbit monoclonal		Kindly gifted by Dr. Fischer
c-HSP60 (*C.tr*)	Mouse monoclonal	1:1000 WB 1:400 IF	Santa Cruz (sc-57840)
Caspase-3	Rabbit Polyclonal	1:1000 WB	Cell Signaling (9662)
Drp1	Mouse monoclonal	1:500 WB 1:200 IF	Santa Cruz (sc-271583)
Drp1	Rabbit polyclonal	1:400 WB 1:200 IF	Genetex (GTX31901)
dsRED (E-8)	Mouse monoclonal	1:1000 WB	Santa Cruz (sc-390909)
$F_1\alpha$	Mouse Monoclonal	1:1000 WB	BD Biosciences
GFP	Mouse monoclonal	1:2000 WB	Santa Cruz (sc-9996)
p53	Mouse monoclonal	1:1000 WB 1:500 IF	Santa Cruz (sc-390909)

Table 5.11: Secondary antibodies

Antibody	Source	Dilution	Company
Anti-mouse IgG Cy3™-linked Antibody	Goat	1:200 IF	Dianova
Anti-rabbit IgG Cy3™-linked Antibody	Goat	1:200 IF	Dianova
Anti-mouse IgG Cy5™-linked Antibody	Goat	1:200 IF	Dianova
Anti-rabbit IgG Cy5™-linked Antibody	Goat	1:200 IF	Dianova
Anti-rabbit-IgG - Atto 647N	Goat	1:500 IF	Sigma-Aldrich (50185-1ML-F)
ECL™ anti-mouse IgG HRP linked Antibody	Goat	1:2500 WB	Santa Cruz (sc-2005)
ECL™ anti-rabbit IgG HRP linked Antibody	Goat	1:2500 WB	Santa Cruz (sc-2005)

5.6 Commercial Kits

Table 5.12: Commercial kits

Kit	Description	Company
miRNeasy Mini Kit	Isolation of microRNA and total RNA from tissues and cells	Qiagen
miScript II RT Kit	Reverse transcription of total RNA containing miRNA	Qiagen
miScript SYBR® Green PCR Kit	miRNA detection by real-time PCR	Qiagen
miRCURY LNA™ Universal RT microRNA PCR system	LNA™-based system designed for detection of microRNA by quantitative real-time PCR	Exiqon
RevertAid First Strand cDNA Synthesis Kit	Synthesis of first strand cDNA from mRNA templates	Thermo-Fisher
PerfeCTa SYBR® Green FastMix	Master mix for quantitative real-time PCR	Quantabio
NucleoSpin® Plasmid	Plasmid DNA extraction	Macherey-Nagel
GeneJET™ Gel Extraction Kit	Gel extraction and DNA purification	Thermo Scientific
Luminescent ATP Detection Assay Kit	Total cellular ATP measurement	AbCam
Decade™ Markers System	Low range RNA marker (150-10 nucleotides) system for radiolabelling	Thermo-Fisher

Table 5.13: Commercial Staining kits used for Immunofluorescence staining.

Name	Description	Source
Alexa Fluor® 549 Phalloidin	DNA-directed DNA polymerase	Genaxxon Biosciences
Alexa Fluor® 660 Phalloidin	High-Fidelity DNA-directed DNA polymerase	Invitrogen
MitoTracker® Deep Red FM	Bovine pancreatic ribonuclease for RNA eradication	Carl-Roth

5.7 Media

Table 5.14 Medium for Cell Cultivation and processing

Medium	Supplier/Ingredients
Medium 200	Thermo Fisher
Low serum growth supplement	Thermo Fisher
Fibroblast Basal Medium	ATCC
RPMI-1640	GIBCO
Fetal Calf Serum (FCS)	PAA
Opti-MEM® Reduced serum Medium	GIBCO
Live cell imaging media	RPMI 1640NPR (GIBCO) + 25 mM HEPES (GIBCO)
Cell Freezing medium	FCS+ 10% (v/v) DMSO

Table 5.15 Medium bacterial growth and processing

Medium	Ingredients
SPG buffer	75 g Sucrose, 0.53 g KH_2PO_4, 1.22 g Na_2HPO_4, 0.72 g L-glutamic acid, pH adjusted to 7.4 and sterile filtered.
$CaCl_2$ buffer	50 mM $CaCl_2$, 10 mM TrisHCl pH adjusted to 7.4
Transformation B1	30 mM $C_2H_3K0_2$, 50 mM $MnCl_2$, 100 mM KCl, 10 mM $CaCl_2$, 15% (v/v) glycerin pH adjusted to 5.8
Transformation B1	10 mM MOPS, 75 mM $CaCl_2$, 10 mM KCl, 15% (v/v) glycerin pH adjusted to 7.0
LB Medium	10 g Tryptone, 5 g yeast extract, 10 g NaCl
LB Agar	10 g Tryptone, 5 g yeast extract, 10 g NaCl, 15 g agar
SOC	2% (w/v) bacto-tryptone, 0.5% (w/v) yeast extract, 10 mM NaCl, 2.5 mM KCl, 10 mM $MgCl_2$, 10 mM $MgSO_4$, 20 mM glucose

5.8 Reagents and Solutions

Table 5.16: Buffers, reagents and solutions used in this work

Name	Ingredients
4% PFA/Sucrose fixing solution	4%(w/v) PFA, 4%(w/v) sucrose in 1x PBS, pH adjusted to 7.4
Permeabilization solution	0.02% Triton-X-100 in 1x PBS
Blocking Solution (IF)	2% FCS in 1x PBS
Mowiol/DABCO mounting medium	2.4 g of Mowiol, 6 g of glycerol, 6 ml of H_2O, 12 ml of 0.2 M Tris-Cl (pH 8.5) and 2.5%(w/v) DABCO.
Phospate-buffered Saline (10x)	80g NaCl, 2 g KCl, 14.4g Na_2HPO_4, 2.4 g KH_2PO_4,
50x TAE	242 g Tris, 57.1 ml acetic acid, 37.2 g EDTA, 1 L H_2O(ad.)
SDS upper PAGE buffer	0.5 M Tris HCl pH 6.8, 0.04 % (w/v) SDS
SDS lower PAGE buffer	1.5 M Tris HCl pH 8.8, 0.04 % (w/v) SDS
10% APS (WB)	5 g APS, 50 mL H_2O
10% SDS lower PAGE gel solution	2.5 ml SDS lower buffer, 3.4 ml 30 % acrylamide, 4.1 ml H2O, 75 µl 10 % APS, 7.5 µl TEMED (10 ml)
12% SDS lower PAGE gel solution	2.5 ml SDS lower buffer, 4 ml 30 % acrylamide, 3.5 ml H2O, 75 µl 10 % APS, 7.5 µl TEMED (10 ml)
Upper gel solution for PAGE	2.5 ml SDS upper buffer, 1.25 ml 30 % acrylamide, 6.25 ml H2O, 100 µl 10 % APS, 20 µl TEMED (10 ml)
Laemmli Loading buffer (2X) for PAGE	100 mM Tris HCl pH 6.8, 4 % (w/v) SDS, 20 % (v/v) glycerol, 1.5 % (v/v) β-mercaptoethanol, bromophenol blue
10x SDS-PAGE running buffer	30.3 g Tris, 144.1 g glycine, 10 g SDS
1x Semi Dry Transfer buffer	192 mM glycine, 0.1 % (w/v) SDS, 25 mM Tris, 20 % (v/v) methanol
10x TBS-T	60.5 g Tris, 87.5 g NaCl, 5 ml Tween20, pH adjusted to 7.5 with HCl
Blocking solution (WB)	5 % (w/v) dry milk powder or BSA in TBS-T

WB Developing Solution 1	100 mM Tris HCl pH 8.6, 2.5 mM Luminol, 0.4 mM p-coumaric acid
WB Developing Solution 2	100 mM Tris HCl pH 8.6, 0.02 % H2O2
Stripping Solution (WB)	1.5g glycine, 0.1g SDS, 1ml Tween 20, 100ml di water, pH adjusted to 2.2 with HCl
5x TBE (Northern)	54 g Tris base, 27.5 boric acid, 20 ml 0.5 M EDTA (pH 8.0) dissolved in DEPC treated H_2O
20x SSC (Northern)	175.3 g NaCl (final 3M), 88.2 g sodium citrate (final 0.3M) 1 L DEPC treated H_2O (ad.) pH adjusted to 7.0 with HCl
20% APS (Northern)	5 g APS, 50 mL DEPC treated H_2O
RNA Gel Loading buffer	95% (v/v) Formamide, 18mM EDTA 9 (pH 8.8), 0.025% (w/v) SDS, 0.025% (w/v) bromophenol blue, 0.025% (w/v) xylene cyanol FF
12.5% Urea-polyacrylamide Gel (Northern)	12ml 5x TBE, 15.3 ml 40 % acrylamide, 366 µl APS, 60 µl TEMED, 60 mL DEPC treated H_2O (ad.)
Northern Washing Solution 1	2x SSC. 0.05% (w/v) SDS
Northern Washing Solution 2	0.1x SSC. 0.1% (w/v) SDS
10 mM H_2O_2	10.2 ul 30% H_2O_2, 10 ml ultrapure H_2O
10 mM $CoCl_2$	23.79 mg $CoCl_2$ (Hexahydrate), 10 ml ultrapure H_2O
10 mg/ml Anhydrous Tetracycline (AHT)	100 mg AHT, 10 ml Ethanol (99.9%)
MTT solution	5 mg/ml MTT in DPBS
MTT solvent	4 mM HCl, 0.1% Nonidet P-40 in Isopropanol

Table 5.17: Commercial Enzymes used in this work.

Name	Description	Source
MolTaq DNA polymerase	DNA-directed DNA polymerase	Molzyme
iProof™ High-Fidelity DNA polymerase	High-Fidelity DNA-directed DNA polymerase	Bio-Rad
Ribonuclease A (RNase A)	Bovine pancreatic ribonuclease for RNA eradication	Carl-Roth
Deoxyribonuclease I (DNase I)	Hyperactive DNase I DNA eradication	Ambion
Proteinase K	protein eradication	Carl-Roth
T4 DNA Ligase	DNA-DNA ligation	Thermo-Fisher
T4 Polynucleotide Kinase	Catalyzes the exchange of phosphate groups between 5'-P-oligo-polynucleotides in presence of ATP	Thermo-fisher

5.9 Technical Equipment

Table 5.18: Devices used in this work.

Devices	Manufacturer
TCS SP5 confocal microscope (63x oil immersion UV objective; N.A. 1.4)	Leica
Bioanalyzer 2100	Agilent Tech.
Chemiluminescence camera system	Intas
Cold centrifuge CT15RE	Himac
DMIL light microscope	Leica
ELYRA S.1 SR-SIM structured illumination platform	Zeiss
FACS Aria	BD Biosciences
Hera Cell 240i incubator	Thermo
Hera Safe sterile bench	Thermo
Nanodrop spectrophotometer	Thermo Scientific
PerfectBlue™ 'Semi-Dry'-Electro-blotter	Peqlab
Phospho-storage plates	FujiFilm
Plate reader infinite 200	TECAN
Spectrophotometer Ultrospec 3100 pro	Amersham
StepOnePlus™ Real-Time PCR	Thermo Scientific
Thermal cycler 2720	Thermo Scientific
Typhoon Scanner	GE Life Sciences/
UV transilluminator	Biostep
Vertical gel electrophoresis chamber for Northern Blot	Hoefer

5.10 Software

Table 5.19: Software used in this work.

Software	Purpose
FIJI	Image analysis; MACRO coding
Adobe® Illustrator	Illustration
Adobe® Photoshop CS4	Figure preparation
ApE	Plasmid Editor and Sequence analysis
DIANA TOOLS - TarBase v7.0	miRNA pathways analysis http://diana.imis.athena-innovation.gr
EndNote X2	Reference bibliography
GraphPad-Prism6	Statistical Analysis
Integrated Genome Browser, v4.6	Affymetrix
LabImage Chemostar (Intas)	Image acquisition on Intas imager
LAS AF confocal microscopy software	Image acquisition on Leica SP5 confocal system
Mac OSX-El Capitan	Operating System
MATLAB	Data processing
Microsoft Office for Mac	Utilities
Python 2.7.10	Coding
R	Statistical Analysis
RNAstructure	RNA secondary structure prediction http://rna.urmc.rochester.edu/RNAstructureWeb
Serial Cloner 2.5	Sequence analysis; primer design
ZEN 20 12 image- processing platform	SIM image acquisition and reconstruction
StepOneTM software v2.3 (Thermo Scientific)	qRT-PCR data acquisition and analysis

Supplementary

S.1. Videos

Video 2.3.1 and Video 2.3.2: HUVECs transfected with MitoTimer with and without treatment of 1μM H_2O_2.

Video 2.4.1, Video 2.4.2, Video 2.4.3 and Video 2.4.4: Video segments used as inputs to the mitoCRWLR MACRO to calculate the end-to-end movements of mitochondrial fragments.

Video 2.4.6 and Video 2.4.7: Representative videos of mitochondrial dynamics in control and *Chlamydia* infected HUVECs used to calculate mitochondrial fusion/fission dynamics.

The videos are included in the attached CD-ROM (back cover) along with the electronic version of the thesis

S.2. MACRO codes

S.2.1. MitoCRWLR

```
/*make selection and save binary*/

open();
waitForUser ("make a selection");
run("Crop");
setOption("BlackBackground", true);
run("Convert to Mask", "method=IsoData background=Default calculate black");
saveAs("Tiff", "/Users/Roy/Desktop/bin1.tif");


run("Set Measurements...", "area standard stack display add redirect=None
decimal=3");
origtitle=getTitle();
odir=getDirectory("image");
run("Set Scale...", "distance=0");


getDimensions(w, h, c, z, t);
 if (c>1){
          run("Split Channels");
          selectWindow("C2"+"-"+origtitle);
          close();
          }

orig=getImageID();
ot=getTitle();
run("Subtract Background...", "rolling=50 sliding disable stack");
run("Median...", "radius=1 stack");
setAutoThreshold("Default dark");
```

```
run("Convert to Mask", "stack");
setSlice(1);
run("Analyze Particles...", "size=1-Infinity clear summarize ");
getRawStatistics(n, mean, min, max, std, histogram);
selectWindow("Summary of "+ot);
lines = split(getInfo(), "\n");
headings = split(lines[0], "\t");
values = split(lines[1], "\t");
mitoar=values[2];
mitoct=values[1];
close("Summary of "+ot);

print(ot+" Mito Area (Px):"+ mitoar);

newImage("Result", "8-bit", w, h, t-1);
setBatchMode(true);
resstack=getImageID();

for(i=1; i<=t-1; i++) {
        //print(i);
        selectImage(orig);
        setSlice(i);
        run("Duplicate...", "title=[first] ");
        firid=getImageID();
        selectImage(orig);
        setSlice(i+1);
        run("Duplicate...", "title=[second] ");
        secid=getImageID();
        imageCalculator("Difference create", "first","second");
        //imageCalculator("Subtract create", "second", "first");
        resid=getImageID();
        //run ("Select None");
        run("Copy");
        selectImage(resstack);
        setSlice(i);
        run("Paste");
        selectImage(firid);
        close;
        selectImage(secid);
        close;
        selectImage(resid);
        close;
}
setBatchMode(false);
selectImage(resstack);

run("Invert", "stack");
setAutoThreshold("Default");
//setThreshold(0, 128);
run("Convert to Mask", "stack");
run("Analyze Particles...", "size=1-Infinity clear summarize stack");
selectWindow("Summary of Result");
lines = split(getInfo(), "\n");
headings = split(lines[0], "\t");
values = split(lines[1], "\t");
```

```
nsum=0;
nv=newArray(lines.length);
for (i=1; i<lines.length; i++){
	values = split(lines[i], "\t");
	//print(values[2]);
	norm=((values[2])/mitoar);
	nv[i]=norm;
	nsum=nsum+norm;
}
aravg=arrayAverage(nv);
arsd=arrayStdDev(nv);
print (ot+": normalizedSum:"+nsum+", elements:"+ i + ", AVG:"+ aravg + ", SD:"+
arsd);
saveAs("Results", odir+"\\"+ot+".xls");

selectImage(resstack);
close();
selectImage(orig);
close;

//Returns the mean of an array
function arrayAverage(array) {
	sum=0;
	for (a=0; a<lengthOf(array); a++) {
		sum+=array[a];
	}
	return sum/lengthOf(array);
}

//Returns the standard deviation of an array
function arrayStdDev(array) {
	sumsqd=0;
	mean=arrayAverage(array);
	for (a=0; a<lengthOf(array); a++) {
		sumsqd+=pow(array[a]-mean, 2);
	}
	return pow(sumsqd/lengthOf(array), 0.5);
}
```

Bibliography

Abdul-Sater, A.A., E. Koo, G. Hacker, and D.M. Ojcius. 2009. Inflammasome-dependent caspase-1 activation in cervical epithelial cells stimulates growth of the intracellular pathogen Chlamydia trachomatis. *The Journal of biological chemistry*. 284:26789-26796.

Abdul-Sater, A.A., N. Said-Sadier, V.M. Lam, B. Singh, M.A. Pettengill, F. Soares, I. Tattoli, S. Lipinski, S.E. Girardin, P. Rosenstiel, and D.M. Ojcius. 2010. Enhancement of reactive oxygen species production and chlamydial infection by the mitochondrial Nod-like family member NLRX1. *The Journal of biological chemistry*. 285:41637-41645.

Accerbi, M., S.A. Schmidt, E. De Paoli, S. Park, D.H. Jeong, and P.J. Green. 2010. Methods for isolation of total RNA to recover miRNAs and other small RNAs from diverse species. *Methods in molecular biology*. 592:31-50.

Agaisse, H., and I. Derre. 2015. STIM1 Is a Novel Component of ER-Chlamydia trachomatis Inclusion Membrane Contact Sites. *PloS one*. 10:e0125671.

Ajonuma, L.C., K.L. Fok, L.S. Ho, P.K. Chan, P.H. Chow, L.L. Tsang, C.H. Wong, J. Chen, S. Li, D.K. Rowlands, Y.W. Chung, and H.C. Chan. 2010. CFTR is required for cellular entry and internalization of Chlamydia trachomatis. *Cell biology international*. 34:593-600.

Akira, S., and K. Takeda. 2004. Toll-like receptor signalling. *Nature reviews. Immunology*. 4:499-511.

Al-Younes, H.M., T. Rudel, V. Brinkmann, A.J. Szczepek, and T.F. Meyer. 2001. Low iron availability modulates the course of Chlamydia pneumoniae infection. *Cellular microbiology*. 3:427-437.

Al-Zeer, M.A., H.M. Al-Younes, M. Kerr, M. Abu-Lubad, E. Gonzalez, V. Brinkmann, and T.F. Meyer. 2014. Chlamydia trachomatis remodels stable microtubules to coordinate Golgi stack recruitment to the chlamydial inclusion surface. *Molecular microbiology*. 94:1285-1297.

Altmann, R. 1890. Elementarorganismen und ihre Beziehungen zu den Zellen. Veit, Leipzig.

Amann, R., N. Springer, W. Schonhuber, W. Ludwig, E.N. Schmid, K.D. Muller, and R. Michel. 1997. Obligate intracellular bacterial parasites of acanthamoebae related to Chlamydia spp. *Applied and environmental microbiology*. 63:115-121.

Ambros, V., B. Bartel, D.P. Bartel, C.B. Burge, J.C. Carrington, X. Chen, G. Dreyfuss, S.R. Eddy, S. Griffiths-Jones, M. Marshall, M. Matzke, G. Ruvkun, and T. Tuschl. 2003. A uniform system for microRNA annotation. *Rna*. 9:277-279.

Aubert, H. 1852. *Zeitschrift für wissenschaftliche Zoologie*. 4:388-399.

Auyeung, V.C., I. Ulitsky, S.E. McGeary, and D.P. Bartel. 2013. Beyond secondary structure: primary-sequence determinants license pri-miRNA hairpins for processing. *Cell*. 152:844-858.

Azuma-Mukai, A., H. Oguri, T. Mituyama, Z.R. Qian, K. Asai, H. Siomi, and M.C. Siomi. 2008. Characterization of endogenous human Argonautes and their miRNA partners in RNA silencing. *Proceedings of the National Academy of Sciences of the United States of America*. 105:7964-7969.

Banerjee, A., F. Schambach, C.S. DeJong, S.M. Hammond, and S.L. Reiner. 2010. Micro-RNA-155 inhibits IFN-gamma signaling in CD4+ T cells. *European journal of immunology*. 40:225-231.

Barsig, J., and S.H. Kaufmann. 1997. The mechanism of cell death in Listeria

monocytogenes-infected murine macrophages is distinct from apoptosis. *Infection and immunity*. 65:4075-4081.

Bartel, D.P., and C.Z. Chen. 2004. Micromanagers of gene expression: the potentially widespread influence of metazoan microRNAs. *Nature reviews. Genetics*. 5:396-400.

Bastidas, R.J., C.A. Elwell, J.N. Engel, and R.H. Valdivia. 2013. Chlamydial intracellular survival strategies. *Cold Spring Harbor perspectives in medicine*. 3:a010256.

Bedson, S.P. 1955. Psittacosis. *Proceedings of the Royal Society of Medicine*. 48:633-636.

Bedson, S.P., and J.V. Gostling. 1954. A study of the mode of multiplication of psittacosis virus. *British journal of experimental pathology*. 35:299-308.

Behm-Ansmant, I., J. Rehwinkel, T. Doerks, A. Stark, P. Bork, and E. Izaurralde. 2006. mRNA degradation by miRNAs and GW182 requires both CCR4:NOT deadenylase and DCP1:DCP2 decapping complexes. *Genes & development*. 20:1885-1898.

Belair, C., J. Baud, S. Chabas, C.M. Sharma, J. Vogel, C. Staedel, and F. Darfeuille. 2011. Helicobacter pylori interferes with an embryonic stem cell micro RNA cluster to block cell cycle progression. *Silence*. 2:7.

Belland, R.J., S.P. Ouellette, J. Gieffers, and G.I. Byrne. 2004. Chlamydia pneumoniae and atherosclerosis. *Cellular microbiology*. 6:117-127.

Bernstein, E., A.A. Caudy, S.M. Hammond, and G.J. Hannon. 2001. Role for a bidentate ribonuclease in the initiation step of RNA interference. *Nature*. 409:363-366.

Bettencourt, P., S. Marion, D. Pires, L.F. Santos, C. Lastrucci, N. Carmo, J. Blake, V. Benes, G. Griffiths, O. Neyrolles, G. Lugo-Villarino, and E. Anes. 2013. Actin-binding protein regulation by microRNAs as a novel microbial strategy to modulate phagocytosis by host cells: the case of N-Wasp and miR-142-3p. *Frontiers in cellular and infection microbiology*. 3:19.

Bik, E.M., P.B. Eckburg, S.R. Gill, K.E. Nelson, E.A. Purdom, F. Francois, G. Perez-Perez, M.J. Blaser, and D.A. Relman. 2006. Molecular analysis of the bacterial microbiota in the human stomach. *Proceedings of the National Academy of Sciences of the United States of America*. 103:732-737.

Bohme, L., M. Albrecht, O. Riede, and T. Rudel. 2010. Chlamydia trachomatis-infected host cells resist dsRNA-induced apoptosis. *Cellular microbiology*. 12:1340-1351.

Bonci, D., V. Coppola, M. Musumeci, A. Addario, R. Giuffrida, L. Memeo, L. D'Urso, A. Pagliuca, M. Biffoni, C. Labbaye, M. Bartucci, G. Muto, C. Peschle, and R. De Maria. 2008. The miR-15a-miR-16-1 cluster controls prostate cancer by targeting multiple oncogenic activities. *Nature medicine*. 14:1271-1277.

Boncompain, G., B. Schneider, C. Delevoye, O. Kellermann, A. Dautry-Varsat, and A. Subtil. 2010. Production of reactive oxygen species is turned on and rapidly shut down in epithelial cells infected with Chlamydia trachomatis. *Infection and immunity*. 78:80-87.

Boncompain, G., C. Muller, V. Meas-Yedid, P. Schmitt-Kopplin, P.B. Lazarow, and A. Subtil. 2014. The intracellular bacteria Chlamydia hijack peroxisomes and utilize their enzymatic capacity to produce bacteria-specific phospholipids. *PloS one*. 9:e86196.

Borchert, G.M., W. Lanier, and B.L. Davidson. 2006. RNA polymerase III transcribes human microRNAs. *Nature structural & molecular biology*. 13:1097-1101.

Boss, I.W., P.E. Nadeau, J.R. Abbott, Y. Yang, A. Mergia, and R. Renne. 2011. A Kaposi's sarcoma-associated herpesvirus-encoded ortholog of microRNA

miR-155 induces human splenic B-cell expansion in NOD/LtSz-scid IL2Rgammanull mice. *Journal of virology*. 85:9877-9886.

Brand, R.A. 2010. Biographical sketch: Otto Heinrich Warburg, PhD, MD. *Clinical orthopaedics and related research*. 468:2831-2832.

Bras, M., V.J. Yuste, G. Roue, S. Barbier, P. Sancho, C. Virely, M. Rubio, S. Baudet, J.E. Esquerda, H. Merle-Beral, M. Sarfati, and S.A. Susin. 2007. Drp1 mediates caspase-independent type III cell death in normal and leukemic cells. *Molecular and cellular biology*. 27:7073-7088.

Braun, J.E., E. Huntzinger, and E. Izaurralde. 2013. The role of GW182 proteins in miRNA-mediated gene silencing. *Advances in experimental medicine and biology*. 768:147-163.

Braun, J.E., E. Huntzinger, M. Fauser, and E. Izaurralde. 2011. GW182 proteins directly recruit cytoplasmic deadenylase complexes to miRNA targets. *Molecular cell*. 44:120-133.

Buchholz, K.R., and R.S. Stephens. 2006. Activation of the host cell proinflammatory interleukin-8 response by Chlamydia trachomatis. *Cellular microbiology*. 8:1768-1779.

Budak, H., R. Bulut, M. Kantar, and B. Alptekin. 2016. MicroRNA nomenclature and the need for a revised naming prescription. *Briefings in functional genomics*. 15:65-71.

Buscaglia, L.E., and Y. Li. 2011. Apoptosis and the target genes of microRNA-21. *Chinese journal of cancer*. 30:371-380.

Cai, X., C.H. Hagedorn, and B.R. Cullen. 2004. Human microRNAs are processed from capped, polyadenylated transcripts that can also function as mRNAs. *Rna*. 10:1957-1966.

Calin, G.A., C.D. Dumitru, M. Shimizu, R. Bichi, S. Zupo, E. Noch, H. Aldler, S. Rattan, M. Keating, K. Rai, L. Rassenti, T. Kipps, M. Negrini, F. Bullrich, and C.M. Croce. 2002. Frequent deletions and down-regulation of micro- RNA genes miR15 and miR16 at 13q14 in chronic lymphocytic leukemia. *Proceedings of the National Academy of Sciences of the United States of America*. 99:15524-15529.

Campo-Paysaa, F., M. Semon, R.A. Cameron, K.J. Peterson, and M. Schubert. 2011. microRNA complements in deuterostomes: origin and evolution of microRNAs. *Evolution & development*. 13:15-27.

Carabeo, R.A., D.J. Mead, and T. Hackstadt. 2003. Golgi-dependent transport of cholesterol to the Chlamydia trachomatis inclusion. *Proceedings of the National Academy of Sciences of the United States of America*. 100:6771-6776.

Carabeo, R.A., S.S. Grieshaber, E. Fischer, and T. Hackstadt. 2002. Chlamydia trachomatis induces remodeling of the actin cytoskeleton during attachment and entry into HeLa cells. *Infection and immunity*. 70:3793-3803.

Carlin, J.M., and J.B. Weller. 1995. Potentiation of interferon-mediated inhibition of Chlamydia infection by interleukin-1 in human macrophage cultures. *Infection and immunity*. 63:1870-1875.

Carneiro, L.A., L.H. Travassos, F. Soares, I. Tattoli, J.G. Magalhaes, M.T. Bozza, M.C. Plotkowski, P.J. Sansonetti, J.D. Molkentin, D.J. Philpott, and S.E. Girardin. 2009. Shigella induces mitochondrial dysfunction and cell death in nonmyleoid cells. *Cell host & microbe*. 5:123-136.

Castoldi, M., V. Benes, M.W. Hentze, and M.U. Muckenthaler. 2007. miChip: a microarray platform for expression profiling of microRNAs based on locked nucleic acid (LNA) oligonucleotide capture probes. *Methods*. 43:146-152.

Cawthraw, S., J.L. Pennings, H.M. Hodemaekers, R. de Jonge, A.H. Havelaar, B.

Hoebee, L. Johnson, A. Best, E. Kennedy, R.M. La Ragione, D.G. Newell, and R. Janssen. 2011. Gene expression profiles induced by Salmonella infection in resistant and susceptible mice. *Microbes and infection*. 13:383-393.

Chang, C.J., C.H. Chao, W. Xia, J.Y. Yang, Y. Xiong, C.W. Li, W.H. Yu, S.K. Rehman, J.L. Hsu, H.H. Lee, M. Liu, C.T. Chen, D. Yu, and M.C. Hung. 2011. p53 regulates epithelial-mesenchymal transition and stem cell properties through modulating miRNAs. *Nature cell biology*. 13:317-323.

Chang, H., N. Kim, J.H. Park, R.H. Nam, Y.J. Choi, H.S. Lee, H. Yoon, C.M. Shin, Y.S. Park, J.M. Kim, and D.H. Lee. 2015. Different microRNA expression levels in gastric cancer depending on Helicobacter pylori infection. *Gut and liver*. 9:188-196.

Charles, J.F., M.B. Humphrey, X. Zhao, E. Quarles, M.C. Nakamura, A. Aderem, W.E. Seaman, and K.D. Smith. 2008. The innate immune response to Salmonella enterica serovar Typhimurium by macrophages is dependent on TREM2-DAP12. *Infection and immunity*. 76:2439-2447.

Chaston, J., and H. Goodrich-Blair. 2010. Common trends in mutualism revealed by model associations between invertebrates and bacteria. *FEMS microbiology reviews*. 34:41-58.

Chaturvedi, A.K., C.A. Gaydos, P. Agreda, J.P. Holden, N. Chatterjee, J.J. Goedert, N.E. Caporaso, and E.A. Engels. 2010. Chlamydia pneumoniae infection and risk for lung cancer. *Cancer epidemiology, biomarkers & prevention : a publication of the American Association for Cancer Research, cosponsored by the American Society of Preventive Oncology*. 19:1498-1505.

Chau, S., E.Y. Tso, W.S. Leung, and K.S. Fung. 2015. Three cases of atypical pneumonia caused by Chlamydophila psittaci. *Hong Kong medical journal = Xianggang yi xue za zhi*. 21:272-275.

Chekulaeva, M., H. Mathys, J.T. Zipprich, J. Attig, M. Colic, R. Parker, and W. Filipowicz. 2011. miRNA repression involves GW182-mediated recruitment of CCR4-NOT through conserved W-containing motifs. *Nature structural & molecular biology*. 18:1218-1226.

Chekulaeva, M., R. Parker, and W. Filipowicz. 2010. The GW/WG repeats of Drosophila GW182 function as effector motifs for miRNA-mediated repression. *Nucleic acids research*. 38:6673-6683.

Chen, W.M., W.H. Sheu, P.C. Tseng, T.S. Lee, W.J. Lee, P.J. Chang, and A.N. Chiang. 2016. Modulation of microRNA Expression in Subjects with Metabolic Syndrome and Decrease of Cholesterol Efflux from Macrophages via microRNA-33-Mediated Attenuation of ATP-Binding Cassette Transporter A1 Expression by Statins. *PloS one*. 11:e0154672.

Chiang, H.R., L.W. Schoenfeld, J.G. Ruby, V.C. Auyeung, N. Spies, D. Baek, W.K. Johnston, C. Russ, S. Luo, J.E. Babiarz, R. Blelloch, G.P. Schroth, C. Nusbaum, and D.P. Bartel. 2010. Mammalian microRNAs: experimental evaluation of novel and previously annotated genes. *Genes & development*. 24:992-1009.

Chien, C.H., Y.M. Sun, W.C. Chang, P.Y. Chiang-Hsieh, T.Y. Lee, W.C. Tsai, J.T. Horng, A.P. Tsou, and H.D. Huang. 2011. Identifying transcriptional start sites of human microRNAs based on high-throughput sequencing data. *Nucleic acids research*. 39:9345-9356.

Chowdhury, S.R., A. Reimer, M. Sharan, V. Kozjak-Pavlovic, A. Eulalio, B.K. Prusty, M. Fraunholz, K. Karunakaran, and T. Rudel. 2017. Chlamydia preserves the mitochondrial network necessary for replication via microRNA-dependent inhibition of fission. The Journal of cell biology. 216:1071-1089

Chu, C.Y., and T.M. Rana. 2006. Translation repression in human cells by

microRNA-induced gene silencing requires RCK/p54. *PLoS biology*. 4:e210.

Cimmino, A., G.A. Calin, M. Fabbri, M.V. Iorio, M. Ferracin, M. Shimizu, S.E. Wojcik, R.I. Aqeilan, S. Zupo, M. Dono, L. Rassenti, H. Alder, S. Volinia, C.G. Liu, T.J. Kipps, M. Negrini, and C.M. Croce. 2005. miR-15 and miR-16 induce apoptosis by targeting BCL2. *Proceedings of the National Academy of Sciences of the United States of America*. 102:13944-13949.

Cloonan, N., S. Wani, Q. Xu, J. Gu, K. Lea, S. Heater, C. Barbacioru, A.L. Steptoe, H.C. Martin, E. Nourbakhsh, K. Krishnan, B. Gardiner, X. Wang, K. Nones, J.A. Steen, N.A. Matigian, D.L. Wood, K.S. Kassahn, N. Waddell, J. Shepherd, C. Lee, J. Ichikawa, K. McKernan, K. Bramlett, S. Kuersten, and S.M. Grimmond. 2011. MicroRNAs and their isomiRs function cooperatively to target common biological pathways. *Genome biology*. 12:R126.

Coller, J., and R. Parker. 2005. General translational repression by activators of mRNA decapping. *Cell*. 122:875-886.

Collier, L.H. 1990. In: Topley and Wilson's Principles of Bacteriology, Virology and Immunity. 8th Edition. *Published Edward Arnold, London,*:17.

Croci, S., A. Zerbini, L. Boiardi, F. Muratore, A. Bisagni, D. Nicoli, E. Farnetti, G. Pazzola, L. Cimino, A. Moramarco, A. Cavazza, B. Casali, M. Parmeggiani, and C. Salvarani. 2016. MicroRNA markers of inflammation and remodelling in temporal arteries from patients with giant cell arteritis. *Annals of the rheumatic diseases*. 75:1527-1533.

Dahlmans, D., A. Houzelle, P. Schrauwen, and J. Hoeks. 2016. Mitochondrial dynamics, quality control and miRNA regulation in skeletal muscle: implications for obesity and related metabolic disease. *Clinical science*. 130:843-852.

Dai, W., and Z. Li. 2014. Conserved type III secretion system exerts important roles in Chlamydia trachomatis. *International journal of clinical and experimental pathology*. 7:5404-5414.

Dai, Y., P. Jia, Y. Fang, H. Liu, X. Jiao, J.C. He, and X. Ding. 2016. miR-146a is essential for lipopolysaccharide (LPS)-induced cross-tolerance against kidney ischemia/reperfusion injury in mice. *Scientific reports*. 6:27091.

Dang, L.T., N.D. Lawson, and J.E. Fish. 2013. MicroRNA control of vascular endothelial growth factor signaling output during vascular development. *Arteriosclerosis, thrombosis, and vascular biology*. 33:193-200.

De Lay, N., D.J. Schu, and S. Gottesman. 2013. Bacterial small RNA-based negative regulation: Hfq and its accomplices. *The Journal of biological chemistry*. 288:7996-8003.

Delevoye, C., M. Nilges, P. Dehoux, F. Paumet, S. Perrinet, A. Dautry-Varsat, and A. Subtil. 2008. SNARE protein mimicry by an intracellular bacterium. *PLoS pathogens*. 4:e1000022.

Denli, A.M., B.B. Tops, R.H. Plasterk, R.F. Ketting, and G.J. Hannon. 2004. Processing of primary microRNAs by the Microprocessor complex. *Nature*. 432:231-235.

Derre, I. 2015. Chlamydiae interaction with the endoplasmic reticulum: contact, function and consequences. *Cellular microbiology*. 17:959-966.

Derry, M.C., A. Yanagiya, Y. Martineau, and N. Sonenberg. 2006. Regulation of poly(A)-binding protein through PABP-interacting proteins. *Cold Spring Harbor symposia on quantitative biology*. 71:537-543.

Desouza, M., P.W. Gunning, and J.R. Stehn. 2012. The actin cytoskeleton as a sensor and mediator of apoptosis. *Bioarchitecture*. 2:75-87.

Di Carlo, V., E. Grossi, P. Laneve, M. Morlando, S. Dini Modigliani, M. Ballarino, I. Bozzoni, and E. Caffarelli. 2013. TDP-43 regulates the microprocessor

complex activity during in vitro neuronal differentiation. *Molecular neurobiology*. 48:952-963.

Didiano, D., and O. Hobert. 2008. Molecular architecture of a miRNA-regulated 3' UTR. *Rna*. 14:1297-1317.

Diebel, K.W., A.L. Smith, and L.F. van Dyk. 2010. Mature and functional viral miRNAs transcribed from novel RNA polymerase III promoters. *Rna*. 16:170-185.

Dixon, M. 1929. OXIDATION MECHANISMS IN ANIMAL TISSUES. *Biological Reviews*. 4:352-397.

Dobson, J.R., H. Taipaleenmaki, Y.J. Hu, D. Hong, A.J. van Wijnen, J.L. Stein, G.S. Stein, J.B. Lian, and J. Pratap. 2014. hsa-mir-30c promotes the invasive phenotype of metastatic breast cancer cells by targeting NOV/CCN3. *Cancer cell international*. 14:73.

Doxaki, C., S.C. Kampranis, A.G. Eliopoulos, C. Spilianakis, and C. Tsatsanis. 2015. Coordinated Regulation of miR-155 and miR-146a Genes during Induction of Endotoxin Tolerance in Macrophages. *Journal of immunology*. 195:5750-5761.

Du, K., Q. Zheng, M. Zhou, L. Zhu, B. Ai, and L. Zhou. 2011. Chlamydial antiapoptotic activity involves activation of the Raf/MEK/ERK survival pathway. *Current microbiology*. 63:341-346.

Dueck, A., C. Ziegler, A. Eichner, E. Berezikov, and G. Meister. 2012. microRNAs associated with the different human Argonaute proteins. *Nucleic acids research*. 40:9850-9862.

Durieux, C. 1945. [Not Available]. *Comptes rendus des seances de la Societe de biologie et de ses filiales*. 139:759-761.

Ebhardt, H.A., A. Fedynak, and R.P. Fahlman. 2010. Naturally occurring variations in sequence length creates microRNA isoforms that differ in argonaute effector complex specificity. *Silence*. 1:12.

El-Shami, M., D. Pontier, S. Lahmy, L. Braun, C. Picart, D. Vega, M.A. Hakimi, S.E. Jacobsen, R. Cooke, and T. Lagrange. 2007. Reiterated WG/GW motifs form functionally and evolutionarily conserved ARGONAUTE-binding platforms in RNAi-related components. *Genes & development*. 21:2539-2544.

Elkayam, E., C.D. Kuhn, A. Tocilj, A.D. Haase, E.M. Greene, G.J. Hannon, and L. Joshua-Tor. 2012. The structure of human argonaute-2 in complex with miR-20a. *Cell*. 150:100-110.

Elkind, M.S., M.L. Tondella, D.R. Feikin, B.S. Fields, S. Homma, and M.R. Di Tullio. 2006. Seropositivity to Chlamydia pneumoniae is associated with risk of first ischemic stroke. *Stroke*. 37:790-795.

Emde, A., and E. Hornstein. 2014. miRNAs at the interface of cellular stress and disease. *The EMBO journal*. 33:1428-1437.

Eminaga, S., D.C. Christodoulou, F. Vigneault, G.M. Church, and J.G. Seidman. 2013. Quantification of microRNA expression with next-generation sequencing. *Current protocols in molecular biology*. Chapter 4:Unit 4 17.

Engstrom, P., M. Bergstrom, A.C. Alfaro, K. Syam Krishnan, W. Bahnan, F. Almqvist, and S. Bergstrom. 2015. Expansion of the Chlamydia trachomatis inclusion does not require bacterial replication. *International journal of medical microbiology : IJMM*. 305:378-382.

Esen, M., B. Schreiner, V. Jendrossek, F. Lang, K. Fassbender, H. Grassme, and E. Gulbins. 2001. Mechanisms of Staphylococcus aureus induced apoptosis of human endothelial cells. *Apoptosis : an international journal on programmed cell death*. 6:431-439.

Eulalio, A., E. Huntzinger, and E. Izaurralde. 2008. GW182 interaction with Argonaute is essential for miRNA-mediated translational repression and mRNA decay.

Nature structural & molecular biology. 15:346-353.

Eulalio, A., F. Tritschler, and E. Izaurralde. 2009b. The GW182 protein family in animal cells: new insights into domains required for miRNA-mediated gene silencing. *Rna*. 15:1433-1442.

Eulalio, A., F. Tritschler, R. Buttner, O. Weichenrieder, E. Izaurralde, and V. Truffault. 2009a. The RRM domain in GW182 proteins contributes to miRNA-mediated gene silencing. *Nucleic acids research*. 37:2974-2983.

Everett, K.D., R.M. Bush, and A.A. Andersen. 1999. Emended description of the order Chlamydiales, proposal of Parachlamydiaceae fam. nov. and Simkaniaceae fam. nov., each containing one monotypic genus, revised taxonomy of the family Chlamydiaceae, including a new genus and five new species, and standards for the identification of organisms. *International journal of systematic bacteriology*. 49 Pt 2:415-440.

Eylert, E., J. Schar, S. Mertins, R. Stoll, A. Bacher, W. Goebel, and W. Eisenreich. 2008. Carbon metabolism of Listeria monocytogenes growing inside macrophages. *Molecular microbiology*. 69:1008-1017.

Eystathioy, T., A. Jakymiw, E.K. Chan, B. Seraphin, N. Cougot, and M.J. Fritzler. 2003. The GW182 protein colocalizes with mRNA degradation associated proteins hDcp1 and hLSm4 in cytoplasmic GW bodies. *Rna*. 9:1171-1173.

Eystathioy, T., E.K. Chan, S.A. Tenenbaum, J.D. Keene, K. Griffith, and M.J. Fritzler. 2002. A phosphorylated cytoplasmic autoantigen, GW182, associates with a unique population of human mRNAs within novel cytoplasmic speckles. *Molecular biology of the cell*. 13:1338-1351.

Fabian, M.R., and N. Sonenberg. 2012. The mechanics of miRNA-mediated gene silencing: a look under the hood of miRISC. *Nature structural & molecular biology*. 19:586-593.

Fabian, M.R., G. Mathonnet, T. Sundermeier, H. Mathys, J.T. Zipprich, Y.V. Svitkin, F. Rivas, M. Jinek, J. Wohlschlegel, J.A. Doudna, C.Y. Chen, A.B. Shyu, J.R. Yates, 3rd, G.J. Hannon, W. Filipowicz, T.F. Duchaine, and N. Sonenberg. 2009. Mammalian miRNA RISC recruits CAF1 and PABP to affect PABP-dependent deadenylation. *Molecular cell*. 35:868-880.

Fabian, M.R., M.K. Cieplak, F. Frank, M. Morita, J. Green, T. Srikumar, B. Nagar, T. Yamamoto, B. Raught, T.F. Duchaine, and N. Sonenberg. 2011. miRNA-mediated deadenylation is orchestrated by GW182 through two conserved motifs that interact with CCR4-NOT. *Nature structural & molecular biology*. 18:1211-1217.

Fainardi, E., M. Castellazzi, S. Seraceni, E. Granieri, and C. Contini. 2008. Under the microscope: focus on Chlamydia pneumoniae infection and multiple sclerosis. *Current neurovascular research*. 5:60-70.

Fan, T., H. Lu, H. Hu, L. Shi, G.A. McClarty, D.M. Nance, A.H. Greenberg, and G. Zhong. 1998. Inhibition of apoptosis in chlamydia-infected cells: blockade of mitochondrial cytochrome c release and caspase activation. *The Journal of experimental medicine*. 187:487-496.

Fang, F.C. 2011. Antimicrobial actions of reactive oxygen species. *mBio*. 2.

Fassi Fehri, L., M. Koch, E. Belogolova, H. Khalil, C. Bolz, B. Kalali, H.J. Mollenkopf, M. Beigier-Bompadre, A. Karlas, T. Schneider, Y. Churin, M. Gerhard, and T.F. Meyer. 2010. Helicobacter pylori induces miR-155 in T cells in a cAMP-Foxp3-dependent manner. *PloS one*. 5:e9500.

Ferree, A.W., K. Trudeau, E. Zik, I.Y. Benador, G. Twig, R.A. Gottlieb, and O.S. Shirihai. 2013. MitoTimer probe reveals the impact of autophagy, fusion, and motility on subcellular distribution of young and old mitochondrial protein and on relative mitochondrial protein age. *Autophagy*. 9:1887-1896.

Ferreira, A.F., L.G. Moura, I. Tojal, L. Ambrosio, B. Pinto-Simoes, N. Hamerschlak, G.A. Calin, C. Ivan, D.T. Covas, S. Kashima, and F.A. Castro. 2014. ApoptomiRs expression modulated by BCR-ABL is linked to CML progression and imatinib resistance. *Blood cells, molecules & diseases*. 53:47-55.

Fields, K.A. 2012. Chlamydiales. *In* Intracellular Pathogens 1. Vol. 1. M. Tan and M. Bavoil, editors. ASM press, Washinton, D. C.

Filichia, E., B. Hoffer, X. Qi, and Y. Luo. 2016. Inhibition of Drp1 mitochondrial translocation provides neural protection in dopaminergic system in a Parkinson's disease model induced by MPTP. *Scientific reports*. 6:32656.

Fiori, M.E., C. Barbini, T.L. Haas, N. Marroncelli, M. Patrizii, M. Biffoni, and R. De Maria. 2014. Antitumor effect of miR-197 targeting in p53 wild-type lung cancer. *Cell death and differentiation*. 21:774-782.

Fischer, S.F., J. Vier, S. Kirschnek, A. Klos, S. Hess, S. Ying, and G. Hacker. 2004. Chlamydia inhibit host cell apoptosis by degradation of proapoptotic BH3-only proteins. *The Journal of experimental medicine*. 200:905-916.

Fordham, J.B., A.R. Naqvi, and S. Nares. 2015. Regulation of miR-24, miR-30b, and miR-142-3p during macrophage and dendritic cell differentiation potentiates innate immunity. *Journal of leukocyte biology*. 98:195-207.

Forman, D., D.G. Newell, F. Fullerton, J.W. Yarnell, A.R. Stacey, N. Wald, and F. Sitas. 1991. Association between infection with Helicobacter pylori and risk of gastric cancer: evidence from a prospective investigation. *Bmj*. 302:1302-1305.

Formosa, A., E.K. Markert, A.M. Lena, D. Italiano, E. Finazzi-Agro, A.J. Levine, S. Bernardini, A.V. Garabadgiu, G. Melino, and E. Candi. 2014. MicroRNAs, miR-154, miR-299-5p, miR-376a, miR-376c, miR-377, miR-381, miR-487b, miR-485-3p, miR-495 and miR-654-3p, mapped to the 14q32.31 locus, regulate proliferation, apoptosis, migration and invasion in metastatic prostate cancer cells. *Oncogene*. 33:5173-5182.

Frank, F., N. Sonenberg, and B. Nagar. 2010. Structural basis for 5'-nucleotide base-specific recognition of guide RNA by human AGO2. *Nature*. 465:818-822.

Frank, M., S. Duvezin-Caubet, S. Koob, A. Occhipinti, R. Jagasia, A. Petcherski, M.O. Ruonala, M. Priault, B. Salin, and A.S. Reichert. 2012. Mitophagy is triggered by mild oxidative stress in a mitochondrial fission dependent manner. *Biochimica et biophysica acta*. 1823:2297-2310.

Frank, S., B. Gaume, E.S. Bergmann-Leitner, W.W. Leitner, E.G. Robert, F. Catez, C.L. Smith, and R.J. Youle. 2001. The role of dynamin-related protein 1, a mediator of mitochondrial fission, in apoptosis. *Developmental cell*. 1:515-525.

Frohlich, K.S., K. Haneke, K. Papenfort, and J. Vogel. 2016. The target spectrum of SdsR small RNA in Salmonella. *Nucleic acids research*. 44:10406-10422.

Fujii, T., K. Shimada, A. Asano, Y. Tatsumi, N. Yamaguchi, M. Yamazaki, and N. Konishi. 2016. MicroRNA-331-3p Suppresses Cervical Cancer Cell Proliferation and E6/E7 Expression by Targeting NRP2. *International journal of molecular sciences*. 17.

Fukunaga, R., B.W. Han, J.H. Hung, J. Xu, Z. Weng, and P.D. Zamore. 2012. Dicer partner proteins tune the length of mature miRNAs in flies and mammals. *Cell*. 151:533-546.

Gawlowski, T., J. Suarez, B. Scott, M. Torres-Gonzalez, H. Wang, R. Schwappacher, X. Han, J.R. Yates, 3rd, M. Hoshijima, and W. Dillmann. 2012. Modulation of dynamin-related protein 1 (Drp1) function by increased O-linked-beta-N-acetylglucosamine modification (O-GlcNAc) in cardiac myocytes. *The Journal of biological chemistry*. 287:30024-30034.

Geraci, N.S., J.C. Tan, and M.A. McDowell. 2015. Characterization of microRNA expression profiles in Leishmania-infected human phagocytes. *Parasite immunology*. 37:43-51.

Ghildiyal, M., and P.D. Zamore. 2009. Small silencing RNAs: an expanding universe. *Nature reviews. Genetics*. 10:94-108.

Gomes, L.C., G. Di Benedetto, and L. Scorrano. 2011. During autophagy mitochondria elongate, are spared from degradation and sustain cell viability. *Nature cell biology*. 13:589-598.

Gonzalez, E., M. Rother, M.C. Kerr, M.A. Al-Zeer, M. Abu-Lubad, M. Kessler, V. Brinkmann, A. Loewer, and T.F. Meyer. 2014. Chlamydia infection depends on a functional MDM2-p53 axis. *Nature communications*. 5:5201.

Grayston, J.T., L.A. Campbell, C.C. Kuo, C.H. Mordhorst, P. Saikku, D.H. Thom, and S.P. Wang. 1990. A new respiratory tract pathogen: Chlamydia pneumoniae strain TWAR. *The Journal of infectious diseases*. 161:618-625.

Greub, G. 2010. International Committee on Systematics of Prokaryotes Subcommittee on the taxonomy of the Chlamydiae. Minutes of the inaugural closed meeting, 21 March 2009, Little Rock, AR, USA. *International Journal of Systematic and Evolutionary Microbiology*. 60:2691-2693.

Grey, F., H. Meyers, E.A. White, D.H. Spector, and J. Nelson. 2007. A human cytomegalovirus-encoded microRNA regulates expression of multiple viral genes involved in replication. *PLoS pathogens*. 3:e163.

Grieshaber, N.A., J.B. Sager, C.A. Dooley, S.F. Hayes, and T. Hackstadt. 2006b. Regulation of the Chlamydia trachomatis histone H1-like protein Hc2 is IspE dependent and IhtA independent. *Journal of bacteriology*. 188:5289-5292.

Grieshaber, N.A., S.S. Grieshaber, E.R. Fischer, and T. Hackstadt. 2006a. A small RNA inhibits translation of the histone-like protein Hc1 in Chlamydia trachomatis. *Molecular microbiology*. 59:541-550.

Griffiths-Jones, S., J.H. Hui, A. Marco, and M. Ronshaugen. 2011. MicroRNA evolution by arm switching. *EMBO reports*. 12:172-177.

Griffiths-Jones, S., R.J. Grocock, S. van Dongen, A. Bateman, and A.J. Enright. 2006. miRBase: microRNA sequences, targets and gene nomenclature. *Nucleic acids research*. 34:D140-144.

Gu, X., Z. Su, and Y. Huang. 2009. Simultaneous expansions of microRNAs and protein-coding genes by gene/genome duplications in early vertebrates. *Journal of experimental zoology. Part B, Molecular and developmental evolution*. 312B:164-170.

Guo, C., L. Sun, X. Chen, and D. Zhang. 2013. Oxidative stress, mitochondrial damage and neurodegenerative diseases. *Neural regeneration research*. 8:2003-2014.

Guo, L., and Z. Lu. 2010. The fate of miRNA* strand through evolutionary analysis: implication for degradation as merely carrier strand or potential regulatory molecule? *PloS one*. 5:e11387.

Guo, L., J. Yu, H. Yu, Y. Zhao, S. Chen, C. Xu, and F. Chen. 2015. Evolutionary and expression analysis of miR-#-5p and miR-#-3p at the miRNAs/isomiRs levels. *BioMed research international*. 2015:168358.

Gustafsson, M.G. 2000. Surpassing the lateral resolution limit by a factor of two using structured illumination microscopy. *Journal of microscopy*. 198:82-87.

Gustafsson, M.G. 2005. Nonlinear structured-illumination microscopy: wide-field fluorescence imaging with theoretically unlimited resolution. *Proceedings of the National Academy of Sciences of the United States of America*. 102:13081-13086.

Gustafsson, M.G., L. Shao, P.M. Carlton, C.J. Wang, I.N. Golubovskaya, W.Z.

Cande, D.A. Agard, and J.W. Sedat. 2008. Three-dimensional resolution doubling in wide-field fluorescence microscopy by structured illumination. *Biophysical journal*. 94:4957-4970.

Ha, M., and V.N. Kim. 2014. Regulation of microRNA biogenesis. *Nature reviews. Molecular cell biology*. 15:509-524.

Haase, A.D., L. Jaskiewicz, H. Zhang, S. Laine, R. Sack, A. Gatignol, and W. Filipowicz. 2005. TRBP, a regulator of cellular PKR and HIV-1 virus expression, interacts with Dicer and functions in RNA silencing. *EMBO reports*. 6:961-967.

Hackstadt, T. 2012. Chlamydiales. *In* Intracellular Pathogens 1. M. Tan and M. Bavoil, editors. ASM press, Washinton, D. C.

Hackstadt, T., D.D. Rockey, R.A. Heinzen, and M.A. Scidmore. 1996. Chlamydia trachomatis interrupts an exocytic pathway to acquire endogenously synthesized sphingomyelin in transit from the Golgi apparatus to the plasma membrane. *The EMBO journal*. 15:964-977.

Hafner, M., N. Renwick, T.A. Farazi, A. Mihailovic, J.T. Pena, and T. Tuschl. 2012. Barcoded cDNA library preparation for small RNA profiling by next-generation sequencing. *Methods*. 58:164-170.

Hahn, D.L., R.W. Dodge, and R. Golubjatnikov. 1991. Association of Chlamydia pneumoniae (strain TWAR) infection with wheezing, asthmatic bronchitis, and adult-onset asthma. *Jama*. 266:225-230.

Halberstadter, L., and S. von Prowazek. 1907a. Uber Zellelnschlusse parasitrer Natur belm Trachom. *Arb. GesundhAmte.* 26:7.

Halberstadter, L., and S. von Prowazek. 1907b. Zur atiologie des trachoms. *Deutsche Medizinische Wochenschrift*. 33:1285–1287.

Han, J., Y. Lee, K.H. Yeom, J.W. Nam, I. Heo, J.K. Rhee, S.Y. Sohn, Y. Cho, B.T. Zhang, and V.N. Kim. 2006. Molecular basis for the recognition of primary microRNAs by the Drosha-DGCR8 complex. *Cell*. 125:887-901.

Handa, O., Y. Naito, and T. Yoshikawa. 2010. Helicobacter pylori: a ROS-inducing bacterial species in the stomach. *Inflammation research : official journal of the European Histamine Research Society ... [et al.]*. 59:997-1003.

Harrop, G.A., G.W. Rake, and M.F. Shaffer. 1940. A Group of Laboratory Infections Ascribed to Lymphogranuloma Venereum. *Transactions of the American Clinical and Climatological Association*. 56:154-159.

Hartmann, H., H.K. Eltzschig, H. Wurz, K. Hantke, A. Rakin, A.S. Yazdi, G. Matteoli, E. Bohn, I.B. Autenrieth, J. Karhausen, D. Neumann, S.P. Colgan, and V.A. Kempf. 2008. Hypoxia-independent activation of HIF-1 by enterobacteriaceae and their siderophores. *Gastroenterology*. 134:756-767.

Hatch, T.P., E. Al-Hossainy, and J.A. Silverman. 1982. Adenine nucleotide and lysine transport in Chlamydia psittaci. *Journal of bacteriology*. 150:662-670.

Hegemann, J.H., and K. Moelleken. 2012. Chlamydiales. *In* Intracellular Pathogens 1. Vol. 1. M. Tan and M. Bavoil, editors. ASM press, Washinton, D. C.

Heimberg, A.M., R. Cowper-Sal-lari, M. Semon, P.C. Donoghue, and K.J. Peterson. 2010. microRNAs reveal the interrelationships of hagfish, lampreys, and gnathostomes and the nature of the ancestral vertebrate. *Proceedings of the National Academy of Sciences of the United States of America*. 107:19379-19383.

Herbert, K.M., G. Pimienta, S.J. DeGregorio, A. Alexandrov, and J.A. Steitz. 2013. Phosphorylation of DGCR8 increases its intracellular stability and induces a progrowth miRNA profile. *Cell reports*. 5:1070-1081.

Hibio, N., K. Hino, E. Shimizu, Y. Nagata, and K. Ui-Tei. 2012. Stability of miRNA 5'terminal and seed regions is correlated with experimentally observed

miRNA-mediated silencing efficacy. *Scientific reports*. 2:996.

Hock, J., and G. Meister. 2008. The Argonaute protein family. *Genome biology*. 9:210.

Hoeke, L., J. Sharbati, K. Pawar, A. Keller, R. Einspanier, and S. Sharbati. 2013. Intestinal Salmonella typhimurium infection leads to miR-29a induced caveolin 2 regulation. *PloS one*. 8:e67300.

Horn, S.R., M.J. Thomenius, E.S. Johnson, C.D. Freel, J.Q. Wu, J.L. Coloff, C.S. Yang, W. Tang, J. An, O.R. Ilkayeva, J.C. Rathmell, C.B. Newgard, and S. Kornbluth. 2011. Regulation of mitochondrial morphology by APC/CCdh1-mediated control of Drp1 stability. *Molecular biology of the cell*. 22:1207-1216.

Hsu, S.D., H.Y. Huang, C.H. Chou, Y.M. Sun, M.T. Hsu, and A.P. Tsou. 2015. Integrated analyses to reconstruct microRNA-mediated regulatory networks in mouse liver using high-throughput profiling. *BMC genomics*. 16 Suppl 2:S12.

Hu, H.Y., Z. Yan, Y. Xu, H. Hu, C. Menzel, Y.H. Zhou, W. Chen, and P. Khaitovich. 2009. Sequence features associated with microRNA strand selection in humans and flies. *BMC genomics*. 10:413.

Huntzinger, E., D. Kuzuoglu-Ozturk, J.E. Braun, A. Eulalio, L. Wohlbold, and E. Izaurralde. 2013. The interactions of GW182 proteins with PABP and deadenylases are required for both translational repression and degradation of miRNA targets. *Nucleic acids research*. 41:978-994.

Huntzinger, E., J.E. Braun, S. Heimstadt, L. Zekri, and E. Izaurralde. 2010. Two PABPC1-binding sites in GW182 proteins promote miRNA-mediated gene silencing. *The EMBO journal*. 29:4146-4160.

Hutchison, R., R.A. Rowlands, and S.L. Simpson. 1930. A Study of Psittacosis. *British medical journal*. 1:633-646.

Huttenhofer, A., J. Cavaille, and J.P. Bachellerie. 2004. Experimental RNomics: a global approach to identifying small nuclear RNAs and their targets in different model organisms. *Methods in molecular biology*. 265:409-428.

Hutvagner, G., and M.J. Simard. 2008. Argonaute proteins: key players in RNA silencing. *Nature reviews. Molecular cell biology*. 9:22-32.

Hybiske, K., and R.S. Stephens. 2007. Mechanisms of host cell exit by the intracellular bacterium Chlamydia. *Proceedings of the National Academy of Sciences of the United States of America*. 104:11430-11435.

Igietseme, J.U., Y. Omosun, O. Stuchlik, M.S. Reed, J. Partin, Q. He, K. Joseph, D. Ellerson, B. Bollweg, Z. George, F.O. Eko, C. Bandea, H. Liu, G. Yang, W.J. Shieh, J. Pohl, K. Karem, and C.M. Black. 2015. Role of Epithelial-Mesenchyme Transition in Chlamydia Pathogenesis. *PloS one*. 10:e0145198.

Iliffe-Lee, E.R., and G. McClarty. 1999. Glucose metabolism in Chlamydia trachomatis: the 'energy parasite' hypothesis revisited. *Molecular microbiology*. 33:177-187.

Immunity. R.S. Stephens, editor. ASM Press, Washington, D.C. 139-169.

Inada, T., and S. Makino. 2014. Novel roles of the multi-functional CCR4-NOT complex in post-transcriptional regulation. *Frontiers in genetics*. 5:135.

Ingerman, E., E.M. Perkins, M. Marino, J.A. Mears, J.M. McCaffery, J.E. Hinshaw, and J. Nunnari. 2005. Dnm1 forms spirals that are structurally tailored to fit mitochondria. *The Journal of cell biology*. 170:1021-1027.

Iwasaki, Y.W., K. Kiga, H. Kayo, Y. Fukuda-Yuzawa, J. Weise, T. Inada, M. Tomita, Y. Ishihama, and T. Fukao. 2013. Global microRNA elevation by inducible Exportin 5 regulates cell cycle entry. *Rna*. 19:490-497.

Izar, B., G.K. Mannala, M.A. Mraheil, T. Chakraborty, and T. Hain. 2012. microRNA response to Listeria monocytogenes infection in epithelial cells. *International*

journal of molecular sciences. 13:1173-1185.

Jahani-Asl, A., and R.S. Slack. 2007. The phosphorylation state of Drp1 determines cell fate. *EMBO reports*. 8:912-913.

Jain, P., Z.Q. Luo, and S.R. Blanke. 2011. Helicobacter pylori vacuolating cytotoxin A (VacA) engages the mitochondrial fission machinery to induce host cell death. *Proceedings of the National Academy of Sciences of the United States of America*. 108:16032-16037.

Jakobs, S., and C.A. Wurm. 2014. Super-resolution microscopy of mitochondria. *Current opinion in chemical biology*. 20:9-15.

Jendrach, M., S. Pohl, M. Voth, A. Kowald, P. Hammerstein, and J. Bereiter-Hahn. 2005. Morpho-dynamic changes of mitochondria during ageing of human endothelial cells. *Mechanisms of ageing and development*. 126:813-821.

Jewett, T.J., E.R. Fischer, D.J. Mead, and T. Hackstadt. 2006. Chlamydial TARP is a bacterial nucleator of actin. *Proceedings of the National Academy of Sciences of the United States of America*. 103:15599-15604.

Ji, W.K., A.L. Hatch, R.A. Merrill, S. Strack, and H.N. Higgs. 2015. Actin filaments target the oligomeric maturation of the dynamin GTPase Drp1 to mitochondrial fission sites. *eLife*. 4:e11553.

Jiwani, S., R.J. Ohr, E.R. Fischer, T. Hackstadt, S. Alvarado, A. Romero, and T.J. Jewett. 2012. Chlamydia trachomatis Tarp cooperates with the Arp2/3 complex to increase the rate of actin polymerization. *Biochemical and biophysical research communications*. 420:816-821.

Jiwani, S., S. Alvarado, R.J. Ohr, A. Romero, B. Nguyen, and T.J. Jewett. 2013. Chlamydia trachomatis Tarp harbors distinct G and F actin binding domains that bundle actin filaments. *Journal of bacteriology*. 195:708-716.

Johannes, S., and L.A. Page. 1971. Taxonomy of the Chlamydiae: Reasons for Classifying Organisms of the Genus Chlamydia, Family Chlamydiaceae, in a Separate Order, Chlamydiales ord. nov. . *International journal of systematic bacteriology* 21:332-334.

Jonas, S., and E. Izaurralde. 2015. Towards a molecular understanding of microRNA-mediated gene silencing. *Nature reviews. Genetics*. 16:421-433.

Joshi, R., B. Khandelwal, D. Joshi, and O.P. Gupta. 2013. Chlamydophila pneumoniae infection and cardiovascular disease. *North American journal of medical sciences*. 5:169-181.

Jung, H.J., and Y. Suh. 2014. Regulation of IGF -1 signaling by microRNAs. *Frontiers in genetics*. 5:472.

Jutras, I., L. Abrami, and A. Dautry-Varsat. 2003. Entry of the lymphogranuloma venereum strain of Chlamydia trachomatis into host cells involves cholesterol-rich membrane domains. *Infection and immunity*. 71:260-266.

Kabeiseman, E.J., K. Cichos, T. Hackstadt, A. Lucas, and E.R. Moore. 2013. Vesicle-associated membrane protein 4 and syntaxin 6 interactions at the chlamydial inclusion. *Infection and immunity*. 81:3326-3337.

Kadener, S., J. Rodriguez, K.C. Abruzzi, Y.L. Khodor, K. Sugino, M.T. Marr, 2nd, S. Nelson, and M. Rosbash. 2009. Genome-wide identification of targets of the drosha-pasha/DGCR8 complex. *Rna*. 15:537-545.

Kahane, S., D. Greenberg, M.G. Friedman, H. Haikin, and R. Dagan. 1998. High prevalence of "Simkania Z," a novel Chlamydia-like bacterium, in infants with acute bronchiolitis. *The Journal of infectious diseases*. 177:1425-1429.

Kalckar, H.M. 1991. 50 years of biological research--from oxidative phosphorylation to energy requiring transport regulation. *Annual review of biochemistry*. 60:1-37.

Karayiannis, P., and D. Hobson. 1981. Amino acid requirements of a Chlamydia trachomatis genital strain in McCoy cell cultures. *Journal of clinical microbiology*. 13:427-432.

Karbowski, M., D. Arnoult, H. Chen, D.C. Chan, C.L. Smith, and R.J. Youle. 2004. Quantitation of mitochondrial dynamics by photolabeling of individual organelles shows that mitochondrial fusion is blocked during the Bax activation phase of apoptosis. *The Journal of cell biology*. 164:493-499.

Kataoka, N., M. Fujita, and M. Ohno. 2009. Functional association of the Microprocessor complex with the spliceosome. *Molecular and cellular biology*. 29:3243-3254.

Katzerke, C., V. Madan, D. Gerloff, D. Brauer-Hartmann, J.U. Hartmann, A.A. Wurm, C. Muller-Tidow, S. Schnittger, D.G. Tenen, D. Niederwieser, and G. Behre. 2013. Transcription factor C/EBPalpha-induced microRNA-30c inactivates Notch1 during granulopoiesis and is downregulated in acute myeloid leukemia. *Blood*. 122:2433-2442.

Kawamata, T., and Y. Tomari. 2010. Making RISC. *Trends in biochemical sciences*. 35:368-376.

Khvorova, A., A. Reynolds, and S.D. Jayasena. 2003. Functional siRNAs and miRNAs exhibit strand bias. *Cell*. 115:209-216.

Kim, K., Y.S. Lee, and R.W. Carthew. 2007. Conversion of pre-RISC to holo-RISC by Ago2 during assembly of RNAi complexes. *Rna*. 13:22-29.

Kim, M.J., H.C. Wainwright, M. Locketz, L.G. Bekker, G.B. Walther, C. Dittrich, A. Visser, W. Wang, F.F. Hsu, U. Wiehart, L. Tsenova, G. Kaplan, and D.G. Russell. 2010. Caseation of human tuberculosis granulomas correlates with elevated host lipid metabolism. *EMBO molecular medicine*. 2:258-274.

Kim, S.J., M. Khan, J. Quan, A. Till, S. Subramani, and A. Siddiqui. 2013. Hepatitis B virus disrupts mitochondrial dynamics: induces fission and mitophagy to attenuate apoptosis. *PLoS pathogens*. 9:e1003722.

Kim, V.N., J. Han, and M.C. Siomi. 2009. Biogenesis of small RNAs in animals. *Nature reviews. Molecular cell biology*. 10:126-139.

Kim, Y.K., and V.N. Kim. 2007. Processing of intronic microRNAs. *The EMBO journal*. 26:775-783.

Kim, Y.K., J. Yeo, B. Kim, M. Ha, and V.N. Kim. 2012. Short structured RNAs with low GC content are selectively lost during extraction from a small number of cells. *Molecular cell*. 46:893-895.

Klase, Z., P. Kale, R. Winograd, M.V. Gupta, M. Heydarian, R. Berro, T. McCaffrey, and F. Kashanchi. 2007. HIV-1 TAR element is processed by Dicer to yield a viral micro-RNA involved in chromatin remodeling of the viral LTR. *BMC molecular biology*. 8:63.

Kner, P., B.B. Chhun, E.R. Griffis, L. Winoto, and M.G. Gustafsson. 2009. Super-resolution video microscopy of live cells by structured illumination. *Nature methods*. 6:339-342.

Kokes, M., and R.H. Valdivia. 2012. Chlamydiales. *In* Intracellular Pathogens 1. Vol. 1. M. Tan and M. Bavoil, editors. ASM press, Washinton, D. C.

Kolliker, A. 1856. *Zeitschrift für wissenschaftliche Zoologie*. 8:311-325.

Korhonen, J.T., M. Puolakkainen, A. Haveri, A. Tammiruusu, M. Sarvas, and R. Lahesmaa. 2012. Chlamydia pneumoniae entry into epithelial cells by clathrin-independent endocytosis. *Microbial pathogenesis*. 52:157-164.

Korobova, F., V. Ramabhadran, and H.N. Higgs. 2013. An actin-dependent step in mitochondrial fission mediated by the ER-associated formin INF2. *Science*. 339:464-467.

Kozomara, A., and S. Griffiths-Jones. 2011. miRBase: integrating microRNA annotation and deep-sequencing data. *Nucleic acids research*. 39:D152-157.

Krebs, H.A., and W.A. Johnson. 1937. Metabolism of ketonic acids in animal tissues. *The Biochemical journal*. 31:645-660.

Kroesen, B.J., N. Teteloshvili, K. Smigielska-Czepiel, E. Brouwer, A.M. Boots, A. van den Berg, and J. Kluiver. 2015. Immuno-miRs: critical regulators of T-cell development, function and ageing. *Immunology*. 144:1-10.

Krol, J., I. Loedige, and W. Filipowicz. 2010. The widespread regulation of microRNA biogenesis, function and decay. *Nature reviews. Genetics*. 11:597-610.

Kumar, Y., and R.H. Valdivia. 2008. Actin and intermediate filaments stabilize the Chlamydia trachomatis vacuole by forming dynamic structural scaffolds. *Cell host & microbe*. 4:159-169.

Kupper, M., C. Stigloher, H. Feldhaar, and R. Gross. 2016. Distribution of the obligate endosymbiont Blochmannia floridanus and expression analysis of putative immune genes in ovaries of the carpenter ant Camponotus floridanus. *Arthropod structure & development*. 45:475-487.

Kuzuoglu-Ozturk, D., E. Huntzinger, S. Schmidt, and E. Izaurralde. 2012. The Caenorhabditis elegans GW182 protein AIN-1 interacts with PAB-1 and subunits of the PAN2-PAN3 and CCR4-NOT deadenylase complexes. *Nucleic acids research*. 40:5651-5665.

Lai, E.C. 2004. Predicting and validating microRNA targets. *Genome biology*. 5:115.

Lai, X., A. Bhattacharya, U. Schmitz, M. Kunz, J. Vera, and O. Wolkenhauer. 2013. A systems' biology approach to study microRNA-mediated gene regulatory networks. *BioMed research international*. 2013:703849.

Lai, X., O. Wolkenhauer, and J. Vera. 2016. Understanding microRNA-mediated gene regulatory networks through mathematical modelling. *Nucleic acids research*. 44:6019-6035.

Laker, R.C., P. Xu, K.A. Ryall, A. Sujkowski, B.M. Kenwood, K.H. Chain, M. Zhang, M.A. Royal, K.L. Hoehn, M. Driscoll, P.N. Adler, R.J. Wessells, J.J. Saucerman, and Z. Yan. 2014. A novel MitoTimer reporter gene for mitochondrial content, structure, stress, and damage in vivo. *The Journal of biological chemistry*. 289:12005-12015.

Landthaler, M., D. Gaidatzis, A. Rothballer, P.Y. Chen, S.J. Soll, L. Dinic, T. Ojo, M. Hafner, M. Zavolan, and T. Tuschl. 2008. Molecular characterization of human Argonaute-containing ribonucleoprotein complexes and their bound target mRNAs. *Rna*. 14:2580-2596.

Lee, H.Y., K. Zhou, A.M. Smith, C.L. Noland, and J.A. Doudna. 2013. Differential roles of human Dicer-binding proteins TRBP and PACT in small RNA processing. *Nucleic acids research*. 41:6568-6576.

Lee, J., S. Giordano, and J. Zhang. 2012. Autophagy, mitochondria and oxidative stress: cross-talk and redox signalling. *The Biochemical journal*. 441:523-540.

Lee, J.E., L.M. Westrate, H. Wu, C. Page, and G.K. Voeltz. 2016. Multiple dynamin family members collaborate to drive mitochondrial division. *Nature*. 540:139-143.

Lee, R.C., R.L. Feinbaum, and V. Ambros. 1993. The C. elegans heterochronic gene lin-4 encodes small RNAs with antisense complementarity to lin-14. *Cell*. 75:843-854.

Lee, Y., C. Ahn, J. Han, H. Choi, J. Kim, J. Yim, J. Lee, P. Provost, O. Radmark, S. Kim, and V.N. Kim. 2003. The nuclear RNase III Drosha initiates microRNA processing. *Nature*. 425:415-419.

Lee, Y., I. Hur, S.Y. Park, Y.K. Kim, M.R. Suh, and V.N. Kim. 2006. The role of PACT in the RNA silencing pathway. *The EMBO journal*. 25:522-532.

Lee, Y., K. Jeon, J.T. Lee, S. Kim, and V.N. Kim. 2002. MicroRNA maturation: stepwise processing and subcellular localization. *The EMBO journal*. 21:4663-4670.

Lee, Y., M. Kim, J. Han, K.H. Yeom, S. Lee, S.H. Baek, and V.N. Kim. 2004. MicroRNA genes are transcribed by RNA polymerase II. *The EMBO journal*. 23:4051-4060.

Lewis, M.R., and W.H. Lewis. 1914. Mitochondria in Tissue Culture. *Science*. 39:330-333.

Li, C., H. Nie, M. Wang, L. Su, J. Li, B. Yu, M. Wei, J. Ju, Y. Yu, M. Yan, Q. Gu, Z. Zhu, and B. Liu. 2012a. MicroRNA-409-3p regulates cell proliferation and apoptosis by targeting PHF10 in gastric cancer. *Cancer letters*. 320:189-197.

Li, J., S. Donath, Y. Li, D. Qin, B.S. Prabhakar, and P. Li. 2010. miR-30 regulates mitochondrial fission through targeting p53 and the dynamin-related protein-1 pathway. *PLoS genetics*. 6:e1000795.

Li, M., J. Wang, Y. Fang, S. Gong, M. Li, M. Wu, X. Lai, G. Zeng, Y. Wang, K. Yang, and X. Huang. 2016. microRNA-146a promotes mycobacterial survival in macrophages through suppressing nitric oxide production. *Scientific reports*. 6:23351.

Li, N., T. Brun, M. Cnop, D.A. Cunha, D.L. Eizirik, and P. Maechler. 2009. Transient oxidative stress damages mitochondrial machinery inducing persistent beta-cell dysfunction. *The Journal of biological chemistry*. 284:23602-23612.

Li, S.C., Y.L. Liao, M.R. Ho, K.W. Tsai, C.H. Lai, and W.C. Lin. 2012b. miRNA arm selection and isomiR distribution in gastric cancer. *BMC genomics*. 13 Suppl 1:S13.

Li, Y., and K.V. Kowdley. 2012. MicroRNAs in common human diseases. *Genomics, proteomics & bioinformatics*. 10:246-253.

Li, Y., C. Qiu, J. Tu, B. Geng, J. Yang, T. Jiang, and Q. Cui. 2014. HMDD v2.0: a database for experimentally supported human microRNA and disease associations. *Nucleic acids research*. 42:D1070-1074.

Lian, S.L., S. Li, G.X. Abadal, B.A. Pauley, M.J. Fritzler, and E.K. Chan. 2009. The C-terminal half of human Ago2 binds to multiple GW-rich regions of GW182 and requires GW182 to mediate silencing. *Rna*. 15:804-813.

Liew, F.Y., D. Xu, E.K. Brint, and L.A. O'Neill. 2005. Negative regulation of toll-like receptor-mediated immune responses. *Nature reviews. Immunology*. 5:446-458.

Liston, A., A.S. Papadopoulou, D. Danso-Abeam, and J. Dooley. 2012. MicroRNA-29 in the adaptive immune system: setting the threshold. *Cellular and molecular life sciences : CMLS*. 69:3533-3541.

Liu, J., M.A. Valencia-Sanchez, G.J. Hannon, and R. Parker. 2005. MicroRNA-dependent localization of targeted mRNAs to mammalian P-bodies. *Nature cell biology*. 7:719-723.

Liu, X., M. Li, Y. Peng, X. Hu, J. Xu, S. Zhu, Z. Yu, and S. Han. 2016a. miR-30c regulates proliferation, apoptosis and differentiation via the Shh signaling pathway in P19 cells. *Experimental & molecular medicine*. 48:e248.

Liu, Y., W. Nie, Y. Jin, A. Zhuo, Y. Zang, and Q. Xiu. 2016b. B and T Lymphocyte Attenuator is a Target of miR-155 during Naive CD4+ T Cell Activation. *Iranian journal of immunology : IJI*. 13:89-99.

Longbottom, D., and M. Livingstone. 2006. Vaccination against chlamydial infections of man and animals. *Veterinary journal*. 171:263-275.

Lu, F., A. Weidmer, C.G. Liu, S. Volinia, C.M. Croce, and P.M. Lieberman. 2008. Epstein-Barr virus-induced miR-155 attenuates NF-kappaB signaling and stabilizes latent virus persistence. *Journal of virology*. 82:10436-10443.

Lu, H., Z. Qi, L. Lin, L. Ma, L. Li, H. Zhang, L. Feng, and Y. Su. 2016. The E6-TAp63beta-Dicer feedback loop involves in miR-375 downregulation and epithelial-to-mesenchymal transition in HR-HPV+ cervical cancer cells. *Tumour biology : the journal of the International Society for Oncodevelopmental Biology and Medicine*.

Luan, C., Z. Yang, and B. Chen. 2015. The functional role of microRNA in acute lymphoblastic leukemia: relevance for diagnosis, differential diagnosis, prognosis, and therapy. *OncoTargets and therapy*. 8:2903-2914.

Lum, M., and R. Morona. 2014. Dynamin-related protein Drp1 and mitochondria are important for Shigella flexneri infection. *International journal of medical microbiology : IJMM*. 304:530-541.

Luo, S., Y. Liu, G. Liang, M. Zhao, H. Wu, Y. Liang, X. Qiu, Y. Tan, Y. Dai, S. Yung, T.M. Chan, and Q. Lu. 2015. The role of microRNA-1246 in the regulation of B cell activation and the pathogenesis of systemic lupus erythematosus. *Clinical epigenetics*. 7:24.

Ma, J.B., K. Ye, and D.J. Patel. 2004. Structural basis for overhang-specific small interfering RNA recognition by the PAZ domain. *Nature*. 429:318-322.

MacCardle, R. 1964. Introduction. *In* Cytology and Cell Physiology. G. Bourne, editor. Academic Press.

Macrae, I.J., K. Zhou, F. Li, A. Repic, A.N. Brooks, W.Z. Cande, P.D. Adams, and J.A. Doudna. 2006. Structural basis for double-stranded RNA processing by Dicer. *Science*. 311:195-198.

Madeleine, M.M., T. Anttila, S.M. Schwartz, P. Saikku, M. Leinonen, J.J. Carter, M. Wurscher, L.G. Johnson, D.A. Galloway, and J.R. Daling. 2007. Risk of cervical cancer associated with Chlamydia trachomatis antibodies by histology, HPV type and HPV cofactors. *International journal of cancer*. 120:650-655.

Mah, S.M., C. Buske, R.K. Humphries, and F. Kuchenbauer. 2010. miRNA*: a passenger stranded in RNA-induced silencing complex? *Critical reviews in eukaryotic gene expression*. 20:141-148.

Majeed, M., J.D. Ernst, K.E. Magnusson, E. Kihlstrom, and O. Stendahl. 1994. Selective translocation of annexins during intracellular redistribution of Chlamydia trachomatis in HeLa and McCoy cells. *Infection and immunity*. 62:126-134.

Majoros, W.H., and U. Ohler. 2007. Spatial preferences of microRNA targets in 3' untranslated regions. *BMC genomics*. 8:152.

Maniataki, E., and Z. Mourelatos. 2005. A human, ATP-independent, RISC assembly machine fueled by pre-miRNA. *Genes & development*. 19:2979-2990.

Martinez, I., A.S. Gardiner, K.F. Board, F.A. Monzon, R.P. Edwards, and S.A. Khan. 2008. Human papillomavirus type 16 reduces the expression of microRNA-218 in cervical carcinoma cells. *Oncogene*. 27:2575-2582.

Matsumoto, A., and G.P. Manire. 1970. Electron microscopic observations on the effects of penicillin on the morphology of Chlamydia psittaci. *Journal of bacteriology*. 101:278-285.

Matsumoto, A., H. Bessho, K. Uehira, and T. Suda. 1991. Morphological studies of the association of mitochondria with chlamydial inclusions and the fusion of chlamydial inclusions. *Journal of electron microscopy*. 40:356-363.

Maudet, C., M. Mano, U. Sunkavalli, M. Sharan, M. Giacca, K.U. Forstner, and A. Eulalio. 2014. Functional high-throughput screening identifies the miR-15 microRNA family as cellular restriction factors for Salmonella infection. *Nature communications*. 5:4718.

Mauxion, F., C.Y. Chen, B. Seraphin, and A.B. Shyu. 2009. BTG/TOB factors impact

deadenylases. *Trends in biochemical sciences*. 34:640-647.

Mears, J.A., L.L. Lackner, S. Fang, E. Ingerman, J. Nunnari, and J.E. Hinshaw. 2011. Conformational changes in Dnm1 support a contractile mechanism for mitochondrial fission. *Nature structural & molecular biology*. 18:20-26.

Mehlitz, A., S. Banhart, A.P. Maurer, A. Kaushansky, A.G. Gordus, J. Zielecki, G. Macbeath, and T.F. Meyer. 2010. Tarp regulates early Chlamydia-induced host cell survival through interactions with the human adaptor protein SHC1. *The Journal of cell biology*. 190:143-157.

Mehta, A., S. Singh, and N.K. Ganguly. 1998. Role of reactive oxygen species in Salmonella typhimurium-induced enterocyte damage. *Scandinavian journal of gastroenterology*. 33:406-414.

Meijer, C.J., J.J. Calame, E.J. de Windt, E.K. Risse, O.P. Bleker, P. Kenemans, W.G. Quint, and M.J. Meddens. 1989. Prevalence of Chlamydia trachomatis infection in a population of asymptomatic women in a screening program for cervical cancer. *European journal of clinical microbiology & infectious diseases : official publication of the European Society of Clinical Microbiology*. 8:127-130.

Meisgen, F., N. Xu, T. Wei, P.C. Janson, S. Obad, O. Broom, N. Nagy, S. Kauppinen, L. Kemeny, M. Stahle, A. Pivarcsi, and E. Sonkoly. 2012. MiR-21 is up-regulated in psoriasis and suppresses T cell apoptosis. *Experimental dermatology*. 21:312-314.

Meng, F., R. Henson, H. Wehbe-Janek, H. Smith, Y. Ueno, and T. Patel. 2007. The MicroRNA let-7a modulates interleukin-6-dependent STAT-3 survival signaling in malignant human cholangiocytes. *The Journal of biological chemistry*. 282:8256-8264.

Mereschkowski, K. 1905. Theorie der zwei Plasmaarten als Grundlage der Symbiogenesis, einer neuen Lehre von der Ent‐stehung der Organismen. *Biologisches Centralblatt*. 30:353-367.

Merlo, P., B. Frost, S. Peng, Y.J. Yang, P.J. Park, and M. Feany. 2014. p53 prevents neurodegeneration by regulating synaptic genes. *Proceedings of the National Academy of Sciences of the United States of America*. 111:18055-18060.

Meshesha, M.K., I. Veksler-Lublinsky, O. Isakov, I. Reichenstein, N. Shomron, K. Kedem, M. Ziv-Ukelson, Z. Bentwich, and Y.S. Avni. 2012. The microRNA Transcriptome of Human Cytomegalovirus (HCMV). *The open virology journal*. 6:38-48.

Michaelis, L. 1900. Die vitale Farbung, eine Darstellungsmethode der Zellgranula. *Archiv für mikroskopische Anatomie*. 55:558-557.

Mihailescu, R. 2015. Gene expression regulation: lessons from noncoding RNAs. *Rna*. 21:695-696.

Millar, J.A., R. Valdes, F.R. Kacharia, S.M. Landfear, E.D. Cambronne, and R. Raghavan. 2015. Coxiella burnetii and Leishmania mexicana residing within similar parasitophorous vacuoles elicit disparate host responses. *Frontiers in microbiology*. 6:794.

Miyagawa, Y.M., T.; Yaoi, H.; Ishii, N.; Okanishi, J. 1935. Studies on the Virus of Lymphogranuloma Inguinale Nicolas, Favre & Durand. Fourth Report: Cultivation of the Virus on the Chorio-Allantoic Membrane of the Chicken Embryo. *Japanese Journal of Experimental Medicine* 13:733-738.

Moazed, D. 2009. Small RNAs in transcriptional gene silencing and genome defence. *Nature*. 457:413-420.

Monack, D.M., B. Raupach, A.E. Hromockyj, and S. Falkow. 1996. Salmonella typhimurium invasion induces apoptosis in infected macrophages. *Proceedings of the National Academy of Sciences of the United States of*

America. 93:9833-9838.

Monteys, A.M., R.M. Spengler, J. Wan, L. Tecedor, K.A. Lennox, Y. Xing, and B.L. Davidson. 2010. Structure and activity of putative intronic miRNA promoters. *Rna*. 16:495-505.

Monticelli, S., K.M. Ansel, C. Xiao, N.D. Socci, A.M. Krichevsky, T.H. Thai, N. Rajewsky, D.S. Marks, C. Sander, K. Rajewsky, A. Rao, and K.S. Kosik. 2005. MicroRNA profiling of the murine hematopoietic system. *Genome biology*. 6:R71.

Moore, E.R., and S.P. Ouellette. 2014. Reconceptualizing the chlamydial inclusion as a pathogen-specified parasitic organelle: an expanded role for Inc proteins. *Frontiers in cellular and infection microbiology*. 4:157.

Moulder, J.W. 1966. The relation of the psittacosis group (Chlamydiae) to bacteria and viruses. *Annual review of microbiology*. 20:107-130.

Moulder, J.W. 1970. Glucose Metabolism of L Cells Before and After Infection with Chlamydia psittaci. *Journal of bacteriology*. 104:1189-1196.

Moulder, J.W. 1991. Interaction of chlamydiae and host cells in vitro. *Microbiological reviews*. 55:143-190.

Muller, M., V. Monkemoller, S. Hennig, W. Hubner, and T. Huser. 2016. Open-source image reconstruction of super-resolution structured illumination microscopy data in ImageJ. *Nature communications*. 7:10980.

Myers, G.S., S.A. Mathews, M. Eppinger, C. Mitchell, K.K. O'Brien, O.R. White, F. Benahmed, R.C. Brunham, T.D. Read, J. Ravel, P.M. Bavoil, and P. Timms. 2009. Evidence that human Chlamydia pneumoniae was zoonotically acquired. *Journal of bacteriology*. 191:7225-7233.

Nam, Y., C. Chen, R.I. Gregory, J.J. Chou, and P. Sliz. 2011. Molecular basis for interaction of let-7 microRNAs with Lin28. *Cell*. 147:1080-1091.

Nans, A., H.R. Saibil, and R.D. Hayward. 2014. Pathogen-host reorganization during Chlamydia invasion revealed by cryo-electron tomography. *Cellular microbiology*. 16:1457-1472.

Nass, M.M., and S. Nass. 1963. Intramitochondrial Fibers with DNA Characteristics. I. Fixation and Electron Staining Reactions. *The Journal of cell biology*. 19:593-611.

Navarro, L., P. Dunoyer, F. Jay, B. Arnold, N. Dharmasiri, M. Estelle, O. Voinnet, and J.D. Jones. 2006. A plant miRNA contributes to antibacterial resistance by repressing auxin signaling. *Science*. 312:436-439.

Nelson, D.E. 2012. Chlamydiales. *In* Intracellular Pathogens 1. Tan M and B. PM, editors. ASM Press, Washinton, D. C.

Ness, R.B., M.T. Goodman, C. Shen, and R.C. Brunham. 2003. Serologic evidence of past infection with Chlamydia trachomatis, in relation to ovarian cancer. *The Journal of infectious diseases*. 187:1147-1152.

Newman, M.A., V. Mani, and S.M. Hammond. 2011. Deep sequencing of microRNA precursors reveals extensive 3' end modification. *Rna*. 17:1795-1803.

Nicholson, A.W. 2014. Ribonuclease III mechanisms of double-stranded RNA cleavage. *Wiley interdisciplinary reviews. RNA*. 5:31-48.

Nicholson, T.L., L. Olinger, K. Chong, G. Schoolnik, and R.S. Stephens. 2003. Global stage-specific gene regulation during the developmental cycle of Chlamydia trachomatis. *Journal of bacteriology*. 185:3179-3189.

Nishi, H., K. Ono, Y. Iwanaga, T. Horie, K. Nagao, G. Takemura, M. Kinoshita, Y. Kuwabara, R.T. Mori, K. Hasegawa, T. Kita, and T. Kimura. 2010. MicroRNA-15b modulates cellular ATP levels and degenerates mitochondria via Arl2 in neonatal rat cardiac myocytes. *The Journal of biological chemistry*. 285:4920-

4930.

Noland, C.L., and J.A. Doudna. 2013. Multiple sensors ensure guide strand selection in human RNAi pathways. *Rna*. 19:639-648.

Nonaka, T., T. Kuwabara, H. Mimuro, A. Kuwae, and S. Imajoh-Ohmi. 2003. Shigella-induced necrosis and apoptosis of U937 cells and J774 macrophages. *Microbiology*. 149:2513-2527.

Nottrott, S., M.J. Simard, and J.D. Richter. 2006. Human let-7a miRNA blocks protein production on actively translating polyribosomes. *Nature structural & molecular biology*. 13:1108-1114.

O'Connell, R.M., K.D. Taganov, M.P. Boldin, G. Cheng, and D. Baltimore. 2007. MicroRNA-155 is induced during the macrophage inflammatory response. *Proceedings of the National Academy of Sciences of the United States of America*. 104:1604-1609.

O'Donnell, K.A., E.A. Wentzel, K.I. Zeller, C.V. Dang, and J.T. Mendell. 2005. c-Myc-regulated microRNAs modulate E2F1 expression. *Nature*. 435:839-843.

Ochoa, S. 1938. Enzymic phosphorylations in invertebrate muscle. *The Biochemical journal*. 32:237-242.

Ochoa, S. 1939. Enzymic synthesis of cocarboxylase in animal tissues. *The Biochemical journal*. 33:1262-1270.

Okamura, K., A. Ishizuka, H. Siomi, and M.C. Siomi. 2004. Distinct roles for Argonaute proteins in small RNA-directed RNA cleavage pathways. *Genes & development*. 18:1655-1666.

Okamura, K., N. Liu, and E.C. Lai. 2009. Distinct mechanisms for microRNA strand selection by Drosophila Argonautes. *Molecular cell*. 36:431-444.

Olsen, P.H., and V. Ambros. 1999. The lin-4 regulatory RNA controls developmental timing in Caenorhabditis elegans by blocking LIN-14 protein synthesis after the initiation of translation. *Developmental biology*. 216:671-680.

Omsland, A., J. Sager, V. Nair, D.E. Sturdevant, and T. Hackstadt. 2012. Developmental stage-specific metabolic and transcriptional activity of Chlamydia trachomatis in an axenic medium. *Proceedings of the National Academy of Sciences of the United States of America*. 109:19781-19785.

Ott, C., K. Ross, S. Straub, B. Thiede, M. Gotz, C. Goosmann, M. Krischke, M.J. Mueller, G. Krohne, T. Rudel, and V. Kozjak-Pavlovic. 2012. Sam50 functions in mitochondrial intermembrane space bridging and biogenesis of respiratory complexes. *Molecular and cellular biology*. 32:1173-1188.

Ottolini, D., T. Cali, A. Negro, and M. Brini. 2013. The Parkinson disease-related protein DJ-1 counteracts mitochondrial impairment induced by the tumour suppressor protein p53 by enhancing endoplasmic reticulum-mitochondria tethering. *Human molecular genetics*. 22:2152-2168.

Ozsolak, F., L.L. Poling, Z. Wang, H. Liu, X.S. Liu, R.G. Roeder, X. Zhang, J.S. Song, and D.E. Fisher. 2008. Chromatin structure analyses identify miRNA promoters. *Genes & development*. 22:3172-3183.

Page, L.A. 1968. Proposal for the recognition of two species in the genus Chlamydia. *International Journal of Systematic and Evolutionary Microbiology*. 18:51-66.

Paiva, C.N., and M.T. Bozza. 2014. Are reactive oxygen species always detrimental to pathogens? *Antioxidants & redox signaling*. 20:1000-1037.

Park, J.E., I. Heo, Y. Tian, D.K. Simanshu, H. Chang, D. Jee, D.J. Patel, and V.N. Kim. 2011. Dicer recognizes the 5' end of RNA for efficient and accurate processing. *Nature*. 475:201-205.

Paroo, Z., X. Ye, S. Chen, and Q. Liu. 2009. Phosphorylation of the human microRNA-generating complex mediates MAPK/Erk signaling. *Cell*. 139:112-

122.

Pasquinelli, A.E., B.J. Reinhart, F. Slack, M.Q. Martindale, M.I. Kuroda, B. Maller, D.C. Hayward, E.E. Ball, B. Degnan, P. Muller, J. Spring, A. Srinivasan, M. Fishman, J. Finnerty, J. Corbo, M. Levine, P. Leahy, E. Davidson, and G. Ruvkun. 2000. Conservation of the sequence and temporal expression of let-7 heterochronic regulatory RNA. *Nature*. 408:86-89.

Paumet, F., J. Wesolowski, A. Garcia-Diaz, C. Delevoye, N. Aulner, H.A. Shuman, A. Subtil, and J.E. Rothman. 2009. Intracellular bacteria encode inhibitory SNARE-like proteins. *PloS one*. 4:e7375.

Petersen, C.P., M.E. Bordeleau, J. Pelletier, and P.A. Sharp. 2006. Short RNAs repress translation after initiation in mammalian cells. *Molecular cell*. 21:533-542.

Pillai, R.S., S.N. Bhattacharyya, C.G. Artus, T. Zoller, N. Cougot, E. Basyuk, E. Bertrand, and W. Filipowicz. 2005. Inhibition of translational initiation by Let-7 MicroRNA in human cells. *Science*. 309:1573-1576.

Pinti, M.V., Q.A. Hathaway, and J.M. Hollander. 2017. Role of microRNA in metabolic shift during heart failure. *American journal of physiology. Heart and circulatory physiology*. 312:H33-H45.

Pizzolla, A., M. Hultqvist, B. Nilson, M.J. Grimm, T. Eneljung, I.M. Jonsson, M. Verdrengh, T. Kelkka, I. Gjertsson, B.H. Segal, and R. Holmdahl. 2012. Reactive oxygen species produced by the NADPH oxidase 2 complex in monocytes protect mice from bacterial infections. *Journal of immunology*. 188:5003-5011.

Prudent, J., R. Zunino, A. Sugiura, S. Mattie, G.C. Shore, and H.M. McBride. 2015. MAPL SUMOylation of Drp1 Stabilizes an ER/Mitochondrial Platform Required for Cell Death. *Molecular cell*. 59:941-955.

Qi, X., N. Qvit, Y.C. Su, and D. Mochly-Rosen. 2013. A novel Drp1 inhibitor diminishes aberrant mitochondrial fission and neurotoxicity. *Journal of cell science*. 126:789-802.

Rajalingam, K., M. Sharma, C. Lohmann, M. Oswald, O. Thieck, C.J. Froelich, and T. Rudel. 2008. Mcl-1 is a key regulator of apoptosis resistance in Chlamydia trachomatis-infected cells. *PloS one*. 3:e3102.

Rambold, A.S., B. Kostelecky, N. Elia, and J. Lippincott-Schwartz. 2011. Tubular network formation protects mitochondria from autophagosomal degradation during nutrient starvation. *Proceedings of the National Academy of Sciences of the United States of America*. 108:10190-10195.

Ramirez, C.M., L. Goedeke, N. Rotllan, J.H. Yoon, D. Cirera-Salinas, J.A. Mattison, Y. Suarez, R. de Cabo, M. Gorospe, and C. Fernandez-Hernando. 2013. MicroRNA 33 regulates glucose metabolism. *Molecular and cellular biology*. 33:2891-2902.

Ramkaran, P., S. Khan, A. Phulukdaree, D. Moodley, and A.A. Chuturgoon. 2014. miR-146a polymorphism influences levels of miR-146a, IRAK-1, and TRAF-6 in young patients with coronary artery disease. *Cell biochemistry and biophysics*. 68:259-266.

Reinhart, B.J., F.J. Slack, M. Basson, A.E. Pasquinelli, J.C. Bettinger, A.E. Rougvie, H.R. Horvitz, and G. Ruvkun. 2000. The 21-nucleotide let-7 RNA regulates developmental timing in Caenorhabditis elegans. *Nature*. 403:901-906.

Ren, N., G. Gao, Y. Sun, L. Zhang, H. Wang, W. Hua, K. Wan, and X. Li. 2015. MicroRNA signatures from multidrugresistant Mycobacterium tuberculosis. *Molecular medicine reports*. 12:6561-6567.

Retzius, G. 1890. Muskelfibrille und Sarcoplasma. *Biol Untersuch Stockholm (N.F.)*. 1:51-88.

Ribeiro, J., and H. Sousa. 2014. MicroRNAs as biomarkers of cervical cancer development: a literature review on miR-125b and miR-34a. *Molecular biology reports*. 41:1525-1531.

Ribeiro, J., J. Marinho-Dias, P. Monteiro, J. Loureiro, I. Baldaque, R. Medeiros, and H. Sousa. 2015. miR-34a and miR-125b Expression in HPV Infection and Cervical Cancer Development. *BioMed research international*. 2015:304584.

Riccioni, R., V. Lulli, G. Castelli, M. Biffoni, R. Tiberio, E. Pelosi, F. Lo-Coco, and U. Testa. 2015. miR-21 is overexpressed in NPM1-mutant acute myeloid leukemias. *Leukemia research*. 39:221-228.

Roberts, A.P., A.P. Lewis, and C.L. Jopling. 2011. The role of microRNAs in viral infection. *Progress in molecular biology and translational science*. 102:101-139.

Robertson, D.K., L. Gu, R.K. Rowe, and W.L. Beatty. 2009. Inclusion biogenesis and reactivation of persistent Chlamydia trachomatis requires host cell sphingolipid biosynthesis. *PLoS pathogens*. 5:e1000664.

Rodriguez, A., E. Vigorito, S. Clare, M.V. Warren, P. Couttet, D.R. Soond, S. van Dongen, R.J. Grocock, P.P. Das, E.A. Miska, D. Vetrie, K. Okkenhaug, A.J. Enright, G. Dougan, M. Turner, and A. Bradley. 2007. Requirement of bic/microRNA-155 for normal immune function. *Science*. 316:608-611.

Rodriguez, A., S. Griffiths-Jones, J.L. Ashurst, and A. Bradley. 2004. Identification of mammalian microRNA host genes and transcription units. *Genome research*. 14:1902-1910.

Rosa, A., M. Ballarino, A. Sorrentino, O. Sthandier, F.G. De Angelis, M. Marchioni, B. Masella, A. Guarini, A. Fatica, C. Peschle, and I. Bozzoni. 2007. The interplay between the master transcription factor PU.1 and miR-424 regulates human monocyte/macrophage differentiation. *Proceedings of the National Academy of Sciences of the United States of America*. 104:19849-19854.

Rosenbloom, A.B., S.H. Lee, M. To, A. Lee, J.Y. Shin, and C. Bustamante. 2014. Optimized two-color super resolution imaging of Drp1 during mitochondrial fission with a slow-switching Dronpa variant. *Proceedings of the National Academy of Sciences of the United States of America*. 111:13093-13098.

Rossignol, R., R. Gilkerson, R. Aggeler, K. Yamagata, S.J. Remington, and R.A. Capaldi. 2004. Energy substrate modulates mitochondrial structure and oxidative capacity in cancer cells. *Cancer research*. 64:985-993.

Roth, D., P.H. Krammer, and K. Gulow. 2014. Dynamin related protein 1-dependent mitochondrial fission regulates oxidative signalling in T cells. *FEBS letters*. 588:1749-1754.

Rottiers, V., and A.M. Naar. 2012. MicroRNAs in metabolism and metabolic disorders. *Nature reviews. Molecular cell biology*. 13:239-250.

Rottner, M., S. Tual-Chalot, H.A. Mostefai, R. Andriantsitohaina, J.M. Freyssinet, and M.C. Martinez. 2011. Increased oxidative stress induces apoptosis in human cystic fibrosis cells. *PloS one*. 6:e24880.

Ruby, J.G., A. Stark, W.K. Johnston, M. Kellis, D.P. Bartel, and E.C. Lai. 2007. Evolution, biogenesis, expression, and target predictions of a substantially expanded set of Drosophila microRNAs. *Genome research*. 17:1850-1864.

Rzomp, K.A., L.D. Scholtes, B.J. Briggs, G.R. Whittaker, and M.A. Scidmore. 2003. Rab GTPases are recruited to chlamydial inclusions in both a species-dependent and species-independent manner. *Infection and immunity*. 71:5855-5870.

Sachse, K., and E. Grossmann. 2002. [Chlamydial diseases of domestic animals--zoonotic potential of the agents and diagnostic issues]. *DTW. Deutsche tierarztliche Wochenschrift*. 109:142-148.

Sagan, L. 1967. On the origin of mitosing cells. *Journal of theoretical biology*. 14:255-274.

Saka, H.A., J.W. Thompson, Y.S. Chen, Y. Kumar, L.G. Dubois, M.A. Moseley, and R.H. Valdivia. 2011. Quantitative proteomics reveals metabolic and pathogenic properties of Chlamydia trachomatis developmental forms. *Molecular microbiology*. 82:1185-1203.

Sakha, S., T. Muramatsu, K. Ueda, and J. Inazawa. 2016. Exosomal microRNA miR-1246 induces cell motility and invasion through the regulation of DENND2D in oral squamous cell carcinoma. *Scientific reports*. 6:38750.

Santos-Rosa, H., R. Schneider, A.J. Bannister, J. Sherriff, B.E. Bernstein, N.C. Emre, S.L. Schreiber, J. Mellor, and T. Kouzarides. 2002. Active genes are tri-methylated at K4 of histone H3. *Nature*. 419:407-411.

Sapp, J. 2007. Mitochondria and Their Host: Morphology to Molecular Phylogeny. *In* Origin of Mitochondria and Hydrogenosomes. W. Martin and M. Muller, editors. Springer-Verlag, Berlin Heidelberg.

Sarin, M., Y. Wang, F. Zhang, K. Rothermund, Y. Zhang, J. Lu, S. Sims-Lucas, D. Beer-Stolz, B.E. Van Houten, J. Vockley, E.S. Goetzman, J.A. Graves, and E.V. Prochownik. 2013. Alterations in c-Myc phenotypes resulting from dynamin-related protein 1 (Drp1)-mediated mitochondrial fission. *Cell death & disease*. 4:e670.

Sarkar, A., S. Moller, A. Bhattacharyya, M. Behnen, J. Rupp, G. van Zandbergen, W. Solbach, and T. Laskay. 2015. Mechanisms of apoptosis inhibition in Chlamydia pneumoniae-infected neutrophils. *International journal of medical microbiology : IJMM*. 305:493-500.

Schachter, J. 1999. Infection and disease epidemiology. *In* Chlamydia: Intracellular Biology, Pathogenesis, and

Schachter, J., G. Causse, and M.L. Tarizzo. 1976. Chlamydiae as agents of sexually transmitted diseases. *Bulletin of the World Health Organization*. 54:245-254.

Schatz, G., E. Haslbrunner, and H. Tuppy. 1964. Deoxyribonucleic Acid Associated with Yeast Mitochondria. *Biochemical and biophysical research communications*. 15:127-132.

Schirle, N.T., and I.J. MacRae. 2012. The crystal structure of human Argonaute2. *Science*. 336:1037-1040.

Schneider, R., A.J. Bannister, F.A. Myers, A.W. Thorne, C. Crane-Robinson, and T. Kouzarides. 2004. Histone H3 lysine 4 methylation patterns in higher eukaryotic genes. *Nature cell biology*. 6:73-77.

Schramm, N., C.R. Bagnell, and P.B. Wyrick. 1996. Vesicles containing Chlamydia trachomatis serovar L2 remain above pH 6 within HEC-1B cells. *Infection and immunity*. 64:1208-1214.

Schulte, J.H., S. Horn, T. Otto, B. Samans, L.C. Heukamp, U.C. Eilers, M. Krause, K. Astrahantseff, L. Klein-Hitpass, R. Buettner, A. Schramm, H. Christiansen, M. Eilers, A. Eggert, and B. Berwanger. 2008. MYCN regulates oncogenic MicroRNAs in neuroblastoma. *International journal of cancer*. 122:699-704.

Schulte, L.N., A. Eulalio, H.J. Mollenkopf, R. Reinhardt, and J. Vogel. 2011. Analysis of the host microRNA response to Salmonella uncovers the control of major cytokines by the let-7 family. *The EMBO journal*. 30:1977-1989.

Segal, A.W. 2008. The function of the NADPH oxidase of phagocytes and its relationship to other NOXs in plants, invertebrates, and mammals. *The international journal of biochemistry & cell biology*. 40:604-618.

Seggerson, K., L. Tang, and E.G. Moss. 2002. Two genetic circuits repress the Caenorhabditis elegans heterochronic gene lin-28 after translation initiation. *Developmental biology*. 243:215-225.

Sempere, L.F., C.N. Cole, M.A. McPeek, and K.J. Peterson. 2006. The phylogenetic distribution of metazoan microRNAs: insights into evolutionary complexity and constraint. *Journal of experimental zoology. Part B, Molecular and developmental evolution*. 306:575-588.

Sharma, M., N. Machuy, L. Bohme, K. Karunakaran, A.P. Maurer, T.F. Meyer, and T. Rudel. 2011. HIF-1alpha is involved in mediating apoptosis resistance to Chlamydia trachomatis-infected cells. *Cellular microbiology*. 13:1573-1585.

Shin, J.H., J.Y. Yang, B.Y. Jeon, Y.J. Yoon, S.N. Cho, Y.H. Kang, D.H. Ryu, and G.S. Hwang. 2011. (1)H NMR-based metabolomic profiling in mice infected with Mycobacterium tuberculosis. *Journal of proteome research*. 10:2238-2247.

Shirakabe, A., P. Zhai, Y. Ikeda, T. Saito, Y. Maejima, C.P. Hsu, M. Nomura, K. Egashira, B. Levine, and J. Sadoshima. 2016. Drp1-Dependent Mitochondrial Autophagy Plays a Protective Role Against Pressure Overload-Induced Mitochondrial Dysfunction and Heart Failure. *Circulation*. 133:1249-1263.

Shmaryahu, A., M. Carrasco, and P.D. Valenzuela. 2014. Prediction of bacterial microRNAs and possible targets in human cell transcriptome. *Journal of microbiology*. 52:482-489.

Siddiqui, N., M.J. Osborne, D.R. Gallie, and K. Gehring. 2007. Solution structure of the PABC domain from wheat poly (A)-binding protein: an insight into RNA metabolic and translational control in plants. *Biochemistry*. 46:4221-4231.

Siegl, C., B.K. Prusty, K. Karunakaran, J. Wischhusen, and T. Rudel. 2014. Tumor suppressor p53 alters host cell metabolism to limit Chlamydia trachomatis infection. *Cell reports*. 9:918-929.

Siengdee, P., N. Trakooljul, E. Murani, M. Schwerin, K. Wimmers, and S. Ponsuksili. 2015. MicroRNAs Regulate Cellular ATP Levels by Targeting Mitochondrial Energy Metabolism Genes during C2C12 Myoblast Differentiation. *PloS one*. 10:e0127850.

Simonelig, M. 2011. Developmental functions of piRNAs and transposable elements: a Drosophila point-of-view. *RNA biology*. 8:754-759.

Sirokmany, G., A. Donko, and M. Geiszt. 2016. Nox/Duox Family of NADPH Oxidases: Lessons from Knockout Mouse Models. *Trends in pharmacological sciences*. 37:318-327.

Skalsky, R.L., and B.R. Cullen. 2010. Viruses, microRNAs, and host interactions. *Annual review of microbiology*. 64:123-141.

Skalsky, R.L., M.A. Samols, K.B. Plaisance, I.W. Boss, A. Riva, M.C. Lopez, H.V. Baker, and R. Renne. 2007. Kaposi's sarcoma-associated herpesvirus encodes an ortholog of miR-155. *Journal of virology*. 81:12836-12845.

Slack, F.J., M. Basson, Z. Liu, V. Ambros, H.R. Horvitz, and G. Ruvkun. 2000. The lin-41 RBCC gene acts in the C. elegans heterochronic pathway between the let-7 regulatory RNA and the LIN-29 transcription factor. *Molecular cell*. 5:659-669.

Smirnova, E., L. Griparic, D.L. Shurland, and A.M. van der Bliek. 2001. Dynamin-related protein Drp1 is required for mitochondrial division in mammalian cells. *Molecular biology of the cell*. 12:2245-2256.

Smoot, D.T., T.B. Elliott, H.W. Verspaget, D. Jones, C.R. Allen, K.G. Vernon, T. Bremner, L.C. Kidd, K.S. Kim, J.D. Groupman, and H. Ashktorab. 2000. Influence of Helicobacter pylori on reactive oxygen-induced gastric epithelial cell injury. *Carcinogenesis*. 21:2091-2095.

Snavely, E.A., M. Kokes, J.D. Dunn, H.A. Saka, B.D. Nguyen, R.J. Bastidas, D.G. McCafferty, and R.H. Valdivia. 2014. Reassessing the role of the secreted protease CPAF in Chlamydia trachomatis infection through genetic approaches. *Pathogens and disease*. 71:336-351.

Song, G., Y. Zhang, and L. Wang. 2009. MicroRNA-206 targets notch3, activates apoptosis, and inhibits tumor cell migration and focus formation. *The Journal of biological chemistry*. 284:31921-31927.

Song, J.J., S.K. Smith, G.J. Hannon, and L. Joshua-Tor. 2004. Crystal structure of Argonaute and its implications for RISC slicer activity. *Science*. 305:1434-1437.

Song, W., J. Chen, A. Petrilli, G. Liot, E. Klinglmayr, Y. Zhou, P. Poquiz, J. Tjong, M.A. Pouladi, M.R. Hayden, E. Masliah, M. Ellisman, I. Rouiller, R. Schwarzenbacher, B. Bossy, G. Perkins, and E. Bossy-Wetzel. 2011. Mutant huntingtin binds the mitochondrial fission GTPase dynamin-related protein-1 and increases its enzymatic activity. *Nature medicine*. 17:377-382.

Sorensen, S.S., A.B. Nygaard, and T. Christensen. 2016. miRNA expression profiles in cerebrospinal fluid and blood of patients with Alzheimer's disease and other types of dementia - an exploratory study. *Translational neurodegeneration*. 5:6.

Stallmann, S., and J.H. Hegemann. 2016. The Chlamydia trachomatis Ctad1 invasin exploits the human integrin beta1 receptor for host cell entry. *Cellular microbiology*. 18:761-775.

Stavru, F., A.E. Palmer, C. Wang, R.J. Youle, and P. Cossart. 2013. Atypical mitochondrial fission upon bacterial infection. *Proceedings of the National Academy of Sciences of the United States of America*. 110:16003-16008.

Steiner, F.A., and R.H. Plasterk. 2006. Knocking out the Argonautes. *Cell*. 127:667-668.

Stephens, R.S., G. Myers, M. Eppinger, and P.M. Bavoil. 2009. Divergence without difference: phylogenetics and taxonomy of Chlamydia resolved. *FEMS immunology and medical microbiology*. 55:115-119.

Stephens, R.S., S. Kalman, C. Lammel, J. Fan, R. Marathe, L. Aravind, W. Mitchell, L. Olinger, R.L. Tatusov, Q. Zhao, E.V. Koonin, and R.W. Davis. 1998. Genome sequence of an obligate intracellular pathogen of humans: Chlamydia trachomatis. *Science*. 282:754-759.

Stoner, B.P., and S.E. Cohen. 2015. Lymphogranuloma Venereum 2015: Clinical Presentation, Diagnosis, and Treatment. *Clinical infectious diseases : an official publication of the Infectious Diseases Society of America*. 61 Suppl 8:S865-873.

Stuart, E.S., W.C. Webley, and L.C. Norkin. 2003. Lipid rafts, caveolae, caveolin-1, and entry by Chlamydiae into host cells. *Experimental cell research*. 287:67-78.

Su, H., S. Meng, Y. Lu, M.I. Trombly, J. Chen, C. Lin, A. Turk, and X. Wang. 2011. Mammalian hyperplastic discs homolog EDD regulates miRNA-mediated gene silencing. *Molecular cell*. 43:97-109.

Su, Y.C., H.W. Chiu, J.C. Hung, and J.R. Hong. 2014. Beta-nodavirus B2 protein induces hydrogen peroxide production, leading to Drp1-recruited mitochondrial fragmentation and cell death via mitochondrial targeting. *Apoptosis : an international journal on programmed cell death*. 19:1457-1470.

Suen, D.F., K.L. Norris, and R.J. Youle. 2008. Mitochondrial dynamics and apoptosis. *Genes & development*. 22:1577-1590.

Suganuma, M., K. Yamaguchi, Y. Ono, H. Matsumoto, T. Hayashi, T. Ogawa, K. Imai, T. Kuzuhara, A. Nishizono, and H. Fujiki. 2008. TNF-alpha-inducing protein, a carcinogenic factor secreted from H. pylori, enters gastric cancer cells. *International journal of cancer*. 123:117-122.

Sun, F., H. Fu, Q. Liu, Y. Tie, J. Zhu, R. Xing, Z. Sun, and X. Zheng. 2008. Downregulation of CCND1 and CDK6 by miR-34a induces cell cycle arrest.

FEBS letters. 582:1564-1568.

Suzuki, H.I., K. Yamagata, K. Sugimoto, T. Iwamoto, S. Kato, and K. Miyazono. 2009. Modulation of microRNA processing by p53. *Nature*. 460:529-533.

Swarts, D.C., K. Makarova, Y. Wang, K. Nakanishi, R.F. Ketting, E.V. Koonin, D.J. Patel, and J. van der Oost. 2014. The evolutionary journey of Argonaute proteins. *Nature structural & molecular biology*. 21:743-753.

Szaszak, M., P. Steven, K. Shima, R. Orzekowsky-Schroder, G. Huttmann, I.R. Konig, W. Solbach, and J. Rupp. 2011. Fluorescence lifetime imaging unravels C. trachomatis metabolism and its crosstalk with the host cell. *PLoS pathogens*. 7:e1002108.

Taganov, K.D., M.P. Boldin, K.J. Chang, and D. Baltimore. 2006. NF-kappaB-dependent induction of microRNA miR-146, an inhibitor targeted to signaling proteins of innate immune responses. *Proceedings of the National Academy of Sciences of the United States of America*. 103:12481-12486.

Takimoto, K., M. Wakiyama, and S. Yokoyama. 2009. Mammalian GW182 contains multiple Argonaute-binding sites and functions in microRNA-mediated translational repression. *Rna*. 15:1078-1089.

Tang, F.F., H.L. Chang, Y.T. Huang, and K.C. Wang. 1957. Studies on the etiology of trachoma with special reference to isolation of the virus in chick embryo. *Chinese medical journal*. 75:429-447.

Tang, G., B.J. Reinhart, D.P. Bartel, and P.D. Zamore. 2003. A biochemical framework for RNA silencing in plants. *Genes & development*. 17:49-63.

Tang, S., A. Patel, and P.R. Krause. 2009. Novel less-abundant viral microRNAs encoded by herpes simplex virus 2 latency-associated transcript and their roles in regulating ICP34.5 and ICP0 mRNAs. *Journal of virology*. 83:1433-1442.

Tang, X., Y. Zhang, L. Tucker, and B. Ramratnam. 2010. Phosphorylation of the RNase III enzyme Drosha at Serine300 or Serine302 is required for its nuclear localization. *Nucleic acids research*. 38:6610-6619.

Taylor, D.H., E.T. Chu, R. Spektor, and P.D. Soloway. 2015. Long non-coding RNA regulation of reproduction and development. *Molecular reproduction and development*. 82:932-956.

Teteloshvili, N., K. Smigielska-Czepiel, B.J. Kroesen, E. Brouwer, J. Kluiver, A.M. Boots, and A. van den Berg. 2015. T-cell Activation Induces Dynamic Changes in miRNA Expression Patterns in CD4 and CD8 T-cell Subsets. *MicroRNA*. 4:117-122.

Thai, T.H., D.P. Calado, S. Casola, K.M. Ansel, C. Xiao, Y. Xue, A. Murphy, D. Frendewey, D. Valenzuela, J.L. Kutok, M. Schmidt-Supprian, N. Rajewsky, G. Yancopoulos, A. Rao, and K. Rajewsky. 2007. Regulation of the germinal center response by microRNA-155. *Science*. 316:604-608.

Thomson, N.R., C. Yeats, K. Bell, M.T. Holden, S.D. Bentley, M. Livingstone, A.M. Cerdeno-Tarraga, B. Harris, J. Doggett, D. Ormond, K. Mungall, K. Clarke, T. Feltwell, Z. Hance, M. Sanders, M.A. Quail, C. Price, B.G. Barrell, J. Parkhill, and D. Longbottom. 2005. The Chlamydophila abortus genome sequence reveals an array of variable proteins that contribute to interspecies variation. *Genome research*. 15:629-640.

Thygeson, P. 1958. The present status of laboratory research in trachoma. *Bulletin of the World Health Organization*. 19:129-152.

Tili, E., J.J. Michaille, A. Cimino, S. Costinean, C.D. Dumitru, B. Adair, M. Fabbri, H. Alder, C.G. Liu, G.A. Calin, and C.M. Croce. 2007. Modulation of miR-155 and miR-125b levels following lipopolysaccharide/TNF-alpha stimulation and their possible roles in regulating the response to endotoxin shock. *Journal of*

immunology. 179:5082-5089.

Tipples, G., and G. McClarty. 1993. The obligate intracellular bacterium Chlamydia trachomatis is auxotrophic for three of the four ribonucleoside triphosphates. *Molecular microbiology*. 8:1105-1114.

Tjaden, J., H.H. Winkler, C. Schwoppe, M. Van Der Laan, T. Mohlmann, and H.E. Neuhaus. 1999. Two nucleotide transport proteins in Chlamydia trachomatis, one for net nucleoside triphosphate uptake and the other for transport of energy. *Journal of bacteriology*. 181:1196-1202.

Tokumaru, S., M. Suzuki, H. Yamada, M. Nagino, and T. Takahashi. 2008. let-7 regulates Dicer expression and constitutes a negative feedback loop. *Carcinogenesis*. 29:2073-2077.

Tomari, Y., T. Du, and P.D. Zamore. 2007. Sorting of Drosophila small silencing RNAs. *Cell*. 130:299-308.

Touvier, T., C. De Palma, E. Rigamonti, A. Scagliola, E. Incerti, L. Mazelin, J.L. Thomas, M. D'Antonio, L. Politi, L. Schaeffer, E. Clementi, and S. Brunelli. 2015. Muscle-specific Drp1 overexpression impairs skeletal muscle growth via translational attenuation. *Cell death & disease*. 6:e1663.

Trifari, S., M.E. Pipkin, H.S. Bandukwala, T. Aijo, J. Bassein, R. Chen, G.J. Martinez, and A. Rao. 2013. MicroRNA-directed program of cytotoxic CD8+ T-cell differentiation. *Proceedings of the National Academy of Sciences of the United States of America*. 110:18608-18613.

Tsai, C.Y., Y.Y. Liu, K.H. Liu, J.T. Hsu, T.C. Chen, C.T. Chiu, and T.S. Yeh. 2017. Comprehensive profiling of virus microRNAs of Epstein-Barr virus-associated gastric carcinoma: highlighting the interactions of ebv-Bart9 and host tumor cells. *Journal of gastroenterology and hepatology*. 32:82-91.

Turchinovich, A., L. Weiz, A. Langheinz, and B. Burwinkel. 2011. Characterization of extracellular circulating microRNA. *Nucleic acids research*. 39:7223-7233.

Twig, G., B. Hyde, and O.S. Shirihai. 2008. Mitochondrial fusion, fission and autophagy as a quality control axis: the bioenergetic view. *Biochimica et biophysica acta*. 1777:1092-1097.

Uberti, D., E. Yavin, S. Gil, K.R. Ayasola, N. Goldfinger, and V. Rotter. 1999. Hydrogen peroxide induces nuclear translocation of p53 and apoptosis in cells of oligodendroglia origin. *Brain research. Molecular brain research*. 65:167-175.

Uo, T., J. Dworzak, C. Kinoshita, D.M. Inman, Y. Kinoshita, P.J. Horner, and R.S. Morrison. 2009. Drp1 levels constitutively regulate mitochondrial dynamics and cell survival in cortical neurons. *Experimental neurology*. 218:274-285.

Valencia-Sanchez, M.A., J. Liu, G.J. Hannon, and R. Parker. 2006. Control of translation and mRNA degradation by miRNAs and siRNAs. *Genes & development*. 20:515-524.

van der Bliek, A.M., Q. Shen, and S. Kawajiri. 2013. Mechanisms of mitochondrial fission and fusion. *Cold Spring Harbor perspectives in biology*. 5.

Vanover, J., J. Sun, S. Deka, J. Kintner, M.M. Duffourc, and R.V. Schoborg. 2008. Herpes simplex virus co-infection-induced Chlamydia trachomatis persistence is not mediated by any known persistence inducer or anti-chlamydial pathway. *Microbiology*. 154:971-978.

Vecchione, A., and C.M. Croce. 2010. Apoptomirs: small molecules have gained the license to kill. *Endocrine-related cancer*. 17:F37-50.

Vegh, P., D.A. Magee, N.C. Nalpas, K. Bryan, M.S. McCabe, J.A. Browne, K.M. Conlon, S.V. Gordon, D.G. Bradley, D.E. MacHugh, and D.J. Lynn. 2015. MicroRNA profiling of the bovine alveolar macrophage response to Mycobacterium bovis infection suggests pathogen survival is enhanced by

microRNA regulation of endocytosis and lysosome trafficking. *Tuberculosis*. 95:60-67.

Vella, M.C., E.Y. Choi, S.Y. Lin, K. Reinert, and F.J. Slack. 2004. The C. elegans microRNA let-7 binds to imperfect let-7 complementary sites from the lin-41 3'UTR. *Genes & development*. 18:132-137.

Verbeke, P., L. Welter-Stahl, S. Ying, J. Hansen, G. Hacker, T. Darville, and D.M. Ojcius. 2006. Recruitment of BAD by the Chlamydia trachomatis vacuole correlates with host-cell survival. *PLoS pathogens*. 2:e45.

Verma, S., G. Mohapatra, S.M. Ahmad, S. Rana, S. Jain, J.K. Khalsa, and C.V. Srikanth. 2015. Salmonella Engages Host MicroRNAs To Modulate SUMOylation: a New Arsenal for Intracellular Survival. *Molecular and cellular biology*. 35:2932-2946.

Vermeulen, A., L. Behlen, A. Reynolds, A. Wolfson, W.S. Marshall, J. Karpilow, and A. Khvorova. 2005. The contributions of dsRNA structure to Dicer specificity and efficiency. *Rna*. 11:674-682.

Vo, N., M.E. Klein, O. Varlamova, D.M. Keller, T. Yamamoto, R.H. Goodman, and S. Impey. 2005. A cAMP-response element binding protein-induced microRNA regulates neuronal morphogenesis. *Proceedings of the National Academy of Sciences of the United States of America*. 102:16426-16431.

Voth, D.E., D. Howe, and R.A. Heinzen. 2007. Coxiella burnetii inhibits apoptosis in human THP-1 cells and monkey primary alveolar macrophages. *Infection and immunity*. 75:4263-4271.

Wada, T., J. Kikuchi, and Y. Furukawa. 2012. Histone deacetylase 1 enhances microRNA processing via deacetylation of DGCR8. *EMBO reports*. 13:142-149.

Wan, G., X. Zhang, R.R. Langley, Y. Liu, X. Hu, C. Han, G. Peng, L.M. Ellis, S.N. Jones, and X. Lu. 2013. DNA-damage-induced nuclear export of precursor microRNAs is regulated by the ATM-AKT pathway. *Cell reports*. 3:2100-2112.

Wang, H.W., C. Noland, B. Siridechadilok, D.W. Taylor, E. Ma, K. Felderer, J.A. Doudna, and E. Nogales. 2009. Structural insights into RNA processing by the human RISC-loading complex. *Nature structural & molecular biology*. 16:1148-1153.

Wang, J., Y. Jiao, L. Cui, and L. Jiang. 2017a. miR-30 functions as an oncomiR in gastric cancer cells through regulation of P53-mediated mitochondrial apoptotic pathway. *Bioscience, biotechnology, and biochemistry*. 81:119-126.

Wang, J., Z. Jia, C. Zhang, M. Sun, W. Wang, P. Chen, K. Ma, Y. Zhang, X. Li, and C. Zhou. 2014. miR-499 protects cardiomyocytes from H 2O 2-induced apoptosis via its effects on Pdcd4 and Pacs2. *RNA biology*. 11:339-350.

Wang, J.X., J.Q. Jiao, Q. Li, B. Long, K. Wang, J.P. Liu, Y.R. Li, and P.F. Li. 2011a. miR-499 regulates mitochondrial dynamics by targeting calcineurin and dynamin-related protein-1. *Nature medicine*. 17:71-78.

Wang, L., G. Yang, L. Qi, X. Li, L. Jia, J. Xie, S. Qiu, P. Li, R. Hao, Z. Wu, X. Du, W. Li, and H. Song. 2016. A Novel Small RNA Regulates Tolerance and Virulence in Shigella flexneri by Responding to Acidic Environmental Changes. *Frontiers in cellular and infection microbiology*. 6:24.

Wang, S., W. Xiao, S. Shan, C. Jiang, M. Chen, Y. Zhang, S. Lu, J. Chen, C. Zhang, Q. Chen, and M. Long. 2012. Multi-patterned dynamics of mitochondrial fission and fusion in a living cell. *PloS one*. 7:e19879.

Wang, S., Y. Mao, S. Xi, X. Wang, and L. Sun. 2017b. Nutrient Starvation Sensitizes Human Ovarian Cancer SKOV3 Cells to BH3 Mimetic via Modulation of Mitochondrial Dynamics. *Anatomical record*. 300:326-339.

Wang, S., Y. Tang, H. Cui, X. Zhao, X. Luo, W. Pan, X. Huang, and N. Shen. 2011b.

Let-7/miR-98 regulate Fas and Fas-mediated apoptosis. *Genes and immunity*. 12:149-154.

Wang, S.P., and J.T. Grayston. 1970. Immunologic relationship between genital TRIC, lymphogranuloma venereum, and related organisms in a new microtiter indirect immunofluorescence test. *American journal of ophthalmology*. 70:367-374.

Wang, W.X., B.R. Wilfred, D.A. Baldwin, R.B. Isett, N. Ren, A. Stromberg, and P.T. Nelson. 2008. Focus on RNA isolation: obtaining RNA for microRNA (miRNA) expression profiling analyses of neural tissue. *Biochimica et biophysica acta*. 1779:749-757.

Wang, X., X. Xu, Z. Ma, Y. Huo, Z. Xiao, Y. Li, and Y. Wang. 2011c. Dynamic mechanisms for pre-miRNA binding and export by Exportin-5. *Rna*. 17:1511-1528.

Warburg, O. 1928. The Chemical Constitution of Respiration Ferment. *Science*. 68:437-443.

Ward, P.S., and C.B. Thompson. 2012. Metabolic reprogramming: a cancer hallmark even warburg did not anticipate. *Cancer cell*. 21:297-308.

Watanabe, T., M. Saotome, M. Nobuhara, A. Sakamoto, T. Urushida, H. Katoh, H. Satoh, M. Funaki, and H. Hayashi. 2014. Roles of mitochondrial fragmentation and reactive oxygen species in mitochondrial dysfunction and myocardial insulin resistance. *Experimental cell research*. 323:314-325.

Wensveen, F.M., N.L. Alves, I.A. Derks, K.A. Reedquist, and E. Eldering. 2011. Apoptosis induced by overall metabolic stress converges on the Bcl-2 family proteins Noxa and Mcl-1. *Apoptosis : an international journal on programmed cell death*. 16:708-721.

Westermann, B. 2008. Molecular machinery of mitochondrial fusion and fission. *The Journal of biological chemistry*. 283:13501-13505.

Westrate, L.M., A.D. Sayfie, D.M. Burgenske, and J.P. MacKeigan. 2014. Persistent mitochondrial hyperfusion promotes G2/M accumulation and caspase-dependent cell death. *PloS one*. 9:e91911.

Wieland, H. 1922. Über den Mechanismus der Oxydationsvorgänge. *Ergeb Physiol Biol Chem Exp Pharmakol*. 20:477-518.

Wightman, B., I. Ha, and G. Ruvkun. 1993. Posttranscriptional regulation of the heterochronic gene lin-14 by lin-4 mediates temporal pattern formation in C. elegans. *Cell*. 75:855-862.

Willers, I.M., and J.M. Cuezva. 2011. Post-transcriptional regulation of the mitochondrial H(+)-ATP synthase: a key regulator of the metabolic phenotype in cancer. *Biochimica et biophysica acta*. 1807:543-551.

Wilson, R.C., A. Tambe, M.A. Kidwell, C.L. Noland, C.P. Schneider, and J.A. Doudna. 2015. Dicer-TRBP complex formation ensures accurate mammalian microRNA biogenesis. *Molecular cell*. 57:397-407.

Wroblewska, Z., and M. Olejniczak. 2016. Hfq assists small RNAs in binding to the coding sequence of ompD mRNA and in rearranging its structure. *Rna*. 22:979-994.

Wu, S., F. Zhou, Z. Zhang, and D. Xing. 2011. Mitochondrial oxidative stress causes mitochondrial fragmentation via differential modulation of mitochondrial fission-fusion proteins. *The FEBS journal*. 278:941-954.

Wu, S., S. Huang, J. Ding, Y. Zhao, L. Liang, T. Liu, R. Zhan, and X. He. 2010. Multiple microRNAs modulate p21Cip1/Waf1 expression by directly targeting its 3' untranslated region. *Oncogene*. 29:2302-2308.

Xia, M., R.E. Bumgarner, M.F. Lampe, and W.E. Stamm. 2003. Chlamydia trachomatis infection alters host cell transcription in diverse cellular pathways.

The Journal of infectious diseases. 187:424-434.

Xiao, B., Z. Liu, B.S. Li, B. Tang, W. Li, G. Guo, Y. Shi, F. Wang, Y. Wu, W.D. Tong, H. Guo, X.H. Mao, and Q.M. Zou. 2009. Induction of microRNA-155 during Helicobacter pylori infection and its negative regulatory role in the inflammatory response. *The Journal of infectious diseases*. 200:916-925.

Xie, S., Q. Wang, H. Wu, J. Cogswell, L. Lu, M. Jhanwar-Uniyal, and W. Dai. 2001. Reactive oxygen species-induced phosphorylation of p53 on serine 20 is mediated in part by polo-like kinase-3. *The Journal of biological chemistry*. 276:36194-36199.

Yamamori, T., S. Ike, T. Bo, T. Sasagawa, Y. Sakai, M. Suzuki, K. Yamamoto, M. Nagane, H. Yasui, and O. Inanami. 2015. Inhibition of the mitochondrial fission protein dynamin-related protein 1 (Drp1) impairs mitochondrial fission and mitotic catastrophe after x-irradiation. *Molecular biology of the cell*. 26:4607-4617.

Yan, L.X., X.F. Huang, Q. Shao, M.Y. Huang, L. Deng, Q.L. Wu, Y.X. Zeng, and J.Y. Shao. 2008. MicroRNA miR-21 overexpression in human breast cancer is associated with advanced clinical stage, lymph node metastasis and patient poor prognosis. *Rna*. 14:2348-2360.

Yang, J.S., M.D. Phillips, D. Betel, P. Mu, A. Ventura, A.C. Siepel, K.C. Chen, and E.C. Lai. 2011. Widespread regulatory activity of vertebrate microRNA* species. *Rna*. 17:312-326.

Yang, L., M.P. Boldin, Y. Yu, C.S. Liu, C.K. Ea, P. Ramakrishnan, K.D. Taganov, J.L. Zhao, and D. Baltimore. 2012. miR-146a controls the resolution of T cell responses in mice. *The Journal of experimental medicine*. 209:1655-1670.

Yang, X., W.W. Du, H. Li, F. Liu, A. Khorshidi, Z.J. Rutnam, and B.B. Yang. 2013. Both mature miR-17-5p and passenger strand miR-17-3p target TIMP3 and induce prostate tumor growth and invasion. *Nucleic acids research*. 41:9688-9704.

Yao, B., S. Li, S.L. Lian, M.J. Fritzler, and E.K. Chan. 2011. Mapping of Ago2-GW182 functional interactions. *Methods in molecular biology*. 725:45-62.

Yao, Y., G. Li, J. Wu, X. Zhang, and J. Wang. 2015. Inflammatory response of macrophages cultured with Helicobacter pylori strains was regulated by miR-155. *International journal of clinical and experimental pathology*. 8:4545-4554.

Yelamanchili, S.V., A.D. Chaudhuri, L.N. Chen, H. Xiong, and H.S. Fox. 2010. MicroRNA-21 dysregulates the expression of MEF2C in neurons in monkey and human SIV/HIV neurological disease. *Cell death & disease*. 1:e77.

Yeom, K.H., Y. Lee, J. Han, M.R. Suh, and V.N. Kim. 2006. Characterization of DGCR8/Pasha, the essential cofactor for Drosha in primary miRNA processing. *Nucleic acids research*. 34:4622-4629.

Yeruva, L., G.S. Myers, N. Spencer, H.H. Creasy, N.E. Adams, A.T. Maurelli, G.R. McChesney, M.A. Cleves, J. Ravel, A. Bowlin, and R.G. Rank. 2014. Early microRNA expression profile as a prognostic biomarker for the development of pelvic inflammatory disease in a mouse model of chlamydial genital infection. *mBio*. 5:e01241-01214.

Yi, R., Y. Qin, I.G. Macara, and B.R. Cullen. 2003. Exportin-5 mediates the nuclear export of pre-microRNAs and short hairpin RNAs. *Genes & development*. 17:3011-3016.

Yin, Q., J. McBride, C. Fewell, M. Lacey, X. Wang, Z. Lin, J. Cameron, and E.K. Flemington. 2008. MicroRNA-155 is an Epstein-Barr virus-induced gene that modulates Epstein-Barr virus-regulated gene expression pathways. *Journal of virology*. 82:5295-5306.

Ying, S., M. Pettengill, D.M. Ojcius, and G. Hacker. 2007. Host-Cell Survival and

Death During Chlamydia Infection. *Current immunology reviews*. 3:31-40.

Zekri, L., E. Huntzinger, S. Heimstadt, and E. Izaurralde. 2009. The silencing domain of GW182 interacts with PABPC1 to promote translational repression and degradation of microRNA targets and is required for target release. *Molecular and cellular biology*. 29:6220-6231.

Zhang, J., D.D. Jima, C. Jacobs, R. Fischer, E. Gottwein, G. Huang, P.L. Lugar, A.S. Lagoo, D.A. Rizzieri, D.R. Friedman, J.B. Weinberg, P.E. Lipsky, and S.S. Dave. 2009. Patterns of microRNA expression characterize stages of human B-cell differentiation. *Blood*. 113:4586-4594.

Zhang, Z., Z. Li, C. Gao, P. Chen, J. Chen, W. Liu, S. Xiao, and H. Lu. 2008. miR-21 plays a pivotal role in gastric cancer pathogenesis and progression. *Laboratory investigation; a journal of technical methods and pathology*. 88:1358-1366.

Zheng, F., J. Zhang, S. Luo, J. Yi, P. Wang, Q. Zheng, and Y. Wen. 2016. miR-143 is associated with proliferation and apoptosis involving ERK5 in HeLa cells. *Oncology letters*. 12:3021-3027.

Zhou, R., R. Wang, Y. Qin, J. Ji, M. Xu, W. Wu, M. Chen, D. Wu, L. Song, H. Shen, J. Sha, D. Miao, Z. Hu, Y. Xia, C. Lu, and X. Wang. 2015. Mitochondria-related miR-151a-5p reduces cellular ATP production by targeting CYTB in asthenozoospermia. *Scientific reports*. 5:17743.

Zhu, H., Z. Shen, H. Luo, W. Zhang, and X. Zhu. 2016. Chlamydia Trachomatis Infection-Associated Risk of Cervical Cancer: A Meta-Analysis. *Medicine*. 95:e3077.

Zhu, X., L. Wu, J. Yao, H. Jiang, Q. Wang, Z. Yang, and F. Wu. 2015. MicroRNA let-7c Inhibits Cell Proliferation and Induces Cell Cycle Arrest by Targeting CDC25A in Human Hepatocellular Carcinoma. *PloS one*. 10:e0124266.

Zipprich, J.T., S. Bhattacharyya, H. Mathys, and W. Filipowicz. 2009. Importance of the C-terminal domain of the human GW182 protein TNRC6C for translational repression. *Rna*. 15:781-793.

Appendix

A.1 Abbreviations

ATP	Adenosine triphosphate
C. trachomatis	*Chlamydia trachomatis*
C.tr	*Chlamydia trachomatis*
cHSP60	Chlamydial Heat Shock Protein
CLSM	Confocal Laser Scanning Microscopy
DMEM	Dulbecco's Modified Eagles Medium
DMSO	Dimethyl sulfoxide
DNA	Deoxyribonucleic acid
Drp-1	Dynamin-related protein 1
DTT	Dithiothreitol
EB	Elementary Body(s)
EDTA	Ethylenediaminetetraacetic acid
FCS	Foetal calf serum
Fig.	Figure
GFP	Green Fluorescent Protein
GTP	Guanosine triphosphate
h	Hour(s)
HFF	Human Foreskin Fibroblast
hFIMBs	Human fimbrial epithelial cells.
HUVECs	Human Umbilical Vein Endothelial Cells
IPTG	Isopropyl β-D-1-thiogalactopyranoside
kb	kilobases
kDa	Kilodalton
l	Liter
LB	Lysogeny broth
MAPK	Mitogen-activated protein kinases
Mcl-1	Induced myeloid leukemia cell differentiation protein-1
Mdm2	Mouse double minute 2 homolog
min	Minute
miR/miRNA	MicroRNA
mRFP	Monomeric Red Fluorescent Protein
NFkB	Nuclear factor kappa-light-chain-enhancer of activated B cells
nt	Nucleotide
PAGE	Polyacrylamide gel electrophoresis
PBS	Phosphate Buffered Saline
PCR	Polymerase Chain Reaction
PI3K	Phosphoinositide 3-kinase
RB	Reticulate Body(s)
RNA	Ribonucleic Acid
RNAi	RNA interference
RPMI	Roswell Park Memorial Institute medium
SD	Standard deviation
SDS	Sodium dodecyl sulfate
Ser	Serine
siRNA	Small interfering RNA
SR-SIM	Super resolution Structured illumination Microscopy
T3SS	Type 3 secretion System
TEMED	Tetramethylethylenediamine
TNFα	Tumour Necrosis Factor α

Tris	tris(hydroxymethyl)aminomethane
v/v	volume/volume
w/v	weight/volume
WHO	World Health Orgnaisation
WT	Wildtype
µ	micro

A.2 Curriculum Vitae

Name: Suvagata Roy, Chowdhury **D.O.B:** 15th of June 1987

Email: suvagata.roychowdhury@gmail.com

Correspondence address: Lehrstuhl für Mikrobiologie, University of Wuerzburg, Biozentrum, Am Hubland 97074 Würzburg Germany

Position title: Graduate Student, Department of Microbiology, University of Wuerzburg

Primary Supervisor: Prof. Dr. Thomas Rudel

Education/training :

INSTITUTION	DEGREE	START DATE MM/YYYY	END DATE MM/YYYY	FIELD OF STUDY
Institute of Genetic engineering, UoG	BSc	07/2005	08/2008	Molecular Biology
London School of Tropical Medicine	MSc	08/2008	09/2010	Medical Biotechnology
University of Wuerzburg, Department of Microbiology	PhD	04/2013	Present	Host-*Chlamydia* Interactions

Research experience:

April 2013 - Present: GSLS Fellow at the Chair of Microbiology, University of Wuerzburg; Doctoral work on the Role of miRNAs in *Chlmaydia* infection.

Thesis Committee:

- Prof. Dr. Thomas Rudel
- Dr. Ana Eulaio
- Prof. Dr. Jorg Wischhusen

Major scientific tasks: Analysis and validation of miRNA expression profile upon *Chlamydia* infection by miRNA sequencing, northern blots, modulation of miRNA expression in primary cells using miRNA mimics, sponges and inhibitors. Establishment of quantification protocols for live and fixed cell microscopy. Validation of alterations in mitochondrial motility and morphology upon *Chlamydia* infection using Python and MACRO based scripts in conjuction with confocal and super-resolution microscopy.

June 2012 - January 2013: CSIR-UGC funded Junior Research Fellow at Indian Institute of Chemical Biology, New Delhi, India (off station work in ICGEB Trieste, Italy); work involved study of regulation of cardiac miRNAs in pollutant generated cardiac hypertrophy and involvement of cardiac miRNAs in hypoxia**.**

February 2011 – February 2013: Junior Research Fellow at Molecular human Genetics Department of ICGEB, Cape Town, South Africa (off station work in The Biotechnology Centre of Oslo, Univeristy of Oslo): work involved study of Cross-talk between miRNA and Notch signaling pathways in Drosophila brain.

August 2010 – September 2010: Junior Research Fellow at Department of Bio-Physics, Molecular Biology and Bioinformatics, King's College, London, United Kingdom: work involved study of Notch mediated spinal tissue regeneration in Zebrafish.

Post Graduate Dissertation project (November 2009-July 2010): "Study Of ESBL Producing Uropathongenic E.Coli" at the Department of Medical Biotechnology and Biochemistry, The London School of Hygiene & Tropical Medicine, London, United Kingdom under guidance of Dr. Mandira Mukherjee.

Gradute Dissertation Project: "Study of Clinincal Variation in South-Asian Population of Beta Thalassemic Patients Exhibiting IVS 1-5 mutation" at the Institute of Genetic Engineering, University of Glasgow, Glasgow, United Kindgom under supervision of Dr. John Old (Oxford BRC-National Haemoglobinopathy Reference Laboratory) and Dr. Amit Chakroborty (Institue of Genetic Engineering).

Skill Set

- Analysis and validation of next generation miRNA sequencing data by informatic and wet lab techniques.
- Generation of molecular biological tools for miRNA analysis (sponge and novel 3' UTR reporter constructs).
- Cell line generation with fluorescent tags (mitochondria, ER and Actin cytoskeleton) for microscopic analysis;
- Cell line generation with shRNA and miRNA sponges; Primary cell culture, transfections and infection.
- Fixed and live cell confocal microscopy;
- Python/MACRO based scripting for mitochondrial morphological studies.
- Advanced Super-Resolution microscopy (SIM and dSTORM) and MACRO based scripting for analysis of super-resoultion imaging data.

Awards and Honors

2017	SPP5815 Best Poster Award; 2nd International Conference on Intracellular Niches of Pathogens (SPP 1580), Glashutten.
2015	FEBS Journal Best Poster prize: Mitochondria in life, death and disease 2015
2014	Eureka! 2014 Best Poster Award at the Graduate School of Life Sciences International Symposium
2013	Scholarship: The GSLS Doctoral Program Fellowships funded by the German “Excellence Initiative”
2009	Scholarship: University Grants Commission National Eligibility Test for PhD fellowship (rank 213; country-wide)
2009	Scholarship: British Council of Medical Research Fellowship (rank 116)

Certifications

- Rules of Good Scientific Practice, University of Wuerzburg
- R statistical Programming; University of Wuerzburg
- Programming with LATEX, Rechenzentrum, University of Wuerzburg
- Basic and Advanced Image processing and MACRO scripting with FIJI, Biovoxxel, University of Wuerzburg

Teaching Exprerience

- Supervision of the master thesis of Mr. Tobias Kunz, Univeristy of Wuerzburg (2017)
- Supervision of the master thesis of Ms. Heike Schrier, Univeristy of Wuerzburg (2016)
- Teaching Assistant for Advance Microbiology practical course for 5th Semester, Bachelor of Science, University ofWuerzburg, Germany (2014-2017).
- Teaching Assistant for Advance Microbiology practical course for 1st Semester, Bachelor of Science, University ofWuerzburg, Germany (2014-2015).

Languages

- English – Native proficency
- German – Elementary proficency
- Hindi – Elementary proficency
- French – Elementary proficency

Potential Referees:

Prof. Dr. Thomas Rudel
thomas.rudel@biozentrum.uni-wuerzburg.de
Lehrstuhl für Mikrobiologie
Biozentrum der Universität Wuerzburg
Am Hubland
97074 Würzburg
Germany

Dr. Ana Eulalio
ana.eulalio@uni-wuerzburg.de
Institut für Molekulare Infektionsbiologie
Josef-Schneider-Str. 2/D15
D-97080 Würzburg
Germany

Prof. Dr. Jorg Wischhusen
wischhusen_j@ukw.de
Universitatsklinikum Wuerzburg
Frauenklinik and Poliklinik
Josef-Schneider-Str. 4 · Haus C15
97080 Würzburg

Dr Vera Kozak-Pavlovic
vera.kozjak@uni-wuerzburg.de
Lehrstuhl für Mikrobiologie
Biozentrum der Universität Wuerzburg
97074 Würzburg
Germany

Place, Date Signature

A.3 Publications and Presentations

A.3.1 Publications

- **Chowdhury, S. R**., Reimer A., Sharan M., Kozjak-Pavlovic V., Eulalio A., Prusty B. K., Fraunholz M., Karunakaran K. and Rudel T. (2017). "Chlamydia preserves the mitochondrial network necessary for replication via microRNA dependent inhibition of fission." *J Cell Biol.*

- Fischer A., Harrisoz K.S., Ramirez Y., Auer D., **Chowdhury S.R.**, Prusty B. K., Sauer F., Dimond., Kisker C., Hefty S.P., Rudel T. (2017) Chlamydia containing vacuole serves as deubiquitination platform to stabilize Mcl-1 and to interfere with host defense. *eLife*

- Das B. B., Rakheja D, Lacelle C, Sedlak R. H., Gulve N, **Chowdhury S. R**., Prusty B. K. (2016) Possible Progesterone-induced Gestational Activation of ciHHV-6B and Transplacental Transmission of Activated HHV-6B. *J Heart Lung Transplant.*

A.3.2 Talks and poster presentations

2014 **Chowdhury, S. R**., Sharan M., Eulalio A., Karunakaran K. and Rudel T. Poster on "Chlamydia trachomatis alters the host miRNA profile to assist infection progression"; Eureka! 2014: **Graduate School of Life Sciences International Symposium, Wuerzburg; Best Poster Award**

2015 **Chowdhury, S. R**., Sharan M., Eulalio A., Karunakaran K. and Rudel T. Poster on "Host MicroRNA dysregulation upon Chlamydia infection"; **13th German Chlamydia Workshop, Vienna**

2015 **Chowdhury, S. R**., Reimer A., Sharan M., Kozjak-Pavlovic V., Eulalio A., Prusty B. K., Fraunholz M., Karunakaran K. and Rudel T. Poster on "The Inhibition Of Mitochondrial Fragmentation During Chlamydia trachomatis Infection"; **FEBS/EMBO Course on Mitochondria in life, death and disease, Crete; Best Poster Award**

2016 **Chowdhury, S. R**., Reimer A., Sharan M., Kozjak-Pavlovic V., Eulalio A., Prusty B. K., Fraunholz M., Karunakaran K. and Rudel T. Poster on "Chlamydia and Mitochondria: An Unfragmented Relationship"; **Eureka! 2016: Graduate School of Life Sciences International Symposium, Wuerzburg**

2017 **Chowdhury, S. R**., Reimer A., Sharan M., Kozjak-Pavlovic V., Eulalio A., Prusty B. K., Fraunholz M., Karunakaran K. and Rudel T. Talk on "Chlamydia trachomatis Prevents Mitochondrial Fragmentation Via The miR-30c-P53-Drp1 Axis"; **Microbiology and Infection 2017 – 5th Joint Conference of DGHM & VAAM, Wuerzburg**

2017 **Chowdhury, S. R**., Reimer A., Sharan M., Kozjak-Pavlovic V., Eulalio A., Prusty B. K., Fraunholz M., Karunakaran K. and Rudel T. Poster on "Chlamydia Preserves the Mitochondrial Network via a Microrna-Dependent Inhibition of Fission." **2nd International Conference on Intracellular Niches of Pathogens (SPP 1580), Glashutten; Best Poster Award**

Affidavit

I hereby confirm that my thesis entitled “The Role of miRNAs in *Chlamydia* Infection” is the result of my own work. I did not receive any help or support from commercial consultants. All sources and / or materials applied are listed and specified in the thesis.

Furthermore, I confirm that this thesis has not been submitted as a part of another examination process neither in identical nor in similar form.

Wuerzburg,
Place, Date Signature

Eidesstattliche Erklärung

Hiermit erkläre ich an Eides statt, die Thesis “Die Rolle von MicroRNA in der Chlamydien-Infeksion“ eigenständig, d.h. insbesondere selbständig und ohne Hilfe eines kommerziellen Promotionsberaters, angefertigt und keine anderen als die von mir angegebenen Quellen und Hilfsmittel verwendet zu haben.

Ich erkläre außerdem, dass die Dissertation weder in gleicher noch in ähnlicher Form bereits in einem anderen Prüfungsverfahren vorgelegen hat.

Würzburg
Place, Date Signature

Acknowledgements

"Ç'est le temps que tu a perdu pour ta rose qui fait ta rose si importante."

- ***Antoine de Saint-Exupéry***
(Le Petit Prince)

To begin thanking the scores of individuals who guided, supported and urged me on towards bringing this thesis to fruition, I simply must start with my primary supervisor, Prof. Dr. Thomas Rudel. I would like to thank him for giving me the opportunity to pursue and conduct my research at the Chair of Microbiology. My gratitude towards him, however, is reinforced not only by his guidance and input but also by the exceptional encouragement he has provided by allowing me to explore novel and uncharted territories.

I consider myself fortunate to have Dr. Ana Eulalio and Prof. Dr. Joerg Wischhusen as my supervisors. Their excellent input vastly contributed towards shaping this thesis and I am grateful to them for being a part of my Thesis Committee.
I would also like to thank Prof Dr. Thomas Dandekar for chairing the Doctoral Thesis Committee

Over the last four years, Wuerzburg and the Chair of Microbiology have been home to me and it would be hard for me to imagine calling them so without the support of the Graduate School of Life Sciences. The mix of a thriving scientific and social life that the GSLS inculcates has been paramount for my life as part of the doctoral program. I would like to thank Dr. Bulm-Ohler, Jennifer Heilig and Felizitas Berninger for their constant and unwavering support for my project and me.
I would like to thank all the members of the *Chlamydia* and Co-infection Group: Dr. Annette Fisher, Dr. Bhupesh Prusty, Dr. Karthika Karunakaran, Nitish Gulve, Maxmililan Klepsch, Nadine Vollmuth and Daniela Auer. I would like to thank Dr. Vera Kozak-Pavlovic, Dr. Martin Fraunholz and Dr. Roy Gross for their scientific inputs. I would like to thank Malvika Sharan at the Eulalio lab, IMIB, for her contribution towards the miRNA sequencing and data analysis. I would lime to express my gratitude to Prof. Dr. Marcus Sauer, Marcus Behringer, Dr. Sebastian Van de Linde and all the people at the Chair of Biotechnology & Biophysics for training me and providing unfettered access to the SIM.

Acknowledgements

There are few things that I would have ever accomplished without the upbringing and love that my Da, Late Sir George Chowdhury and my Ma, Lady Gopa Sophia Chowdhury gave me. They taught me to think, unbound by societal barriers, to strive for understanding and knowledge and I will continue doing so in whatever way possible.

My life here in Wuerzburg saw many changes but the unconditional camaraderie of DΔminik Kiser and Anna°Kries never wavered. They provided my life stability in ways that only a family can. I would also like to thank my friends The Major, Jo-Ana, Claudia, Anastasija, Franziska, Iris, Annie, Isok, Nina, Heike, Yevonne, Clara, Grit, Nicky, Eli, Scotty, Sudip, Jens, Sebastian, Nitish, Lukas, Dennis, Tobias, Philip, Yacir and Rafa for the love, laughs and encouragement over the years.

Lastly, I would like to thank all of the present and former members of the Chair of Microbiology whose journey though this department intertwined with mine. I am truly glad to have known you, learned from you, worked and laughed with you.

[l]Roy Chowdhury

(Wuerzburg, 2017)